Plate tectonics and related magmatic processes

A global perspective

Jörg A. Pfänder

V210505

Overall goal

Reconstruct the tectonic setting and geodynamic environment in which a piece (series!) of rock(s) formed in the geological past

Prerequisite: **ACTUALISM**

TECHNISCHE UNIVERSITÄT BERGAKADEMIE FREIBERG

Die Ressourcenuniversität. Seit 1765.

Tools:

Geochemistry, Petrology & Geochronology

... and more and more: Statistics, Informatics, ...

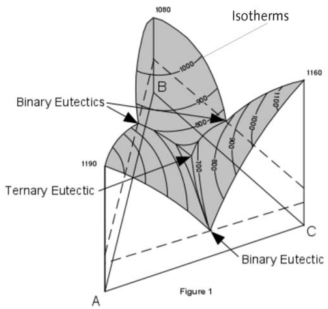

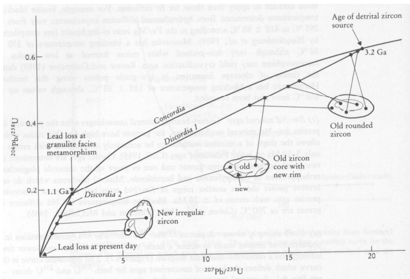

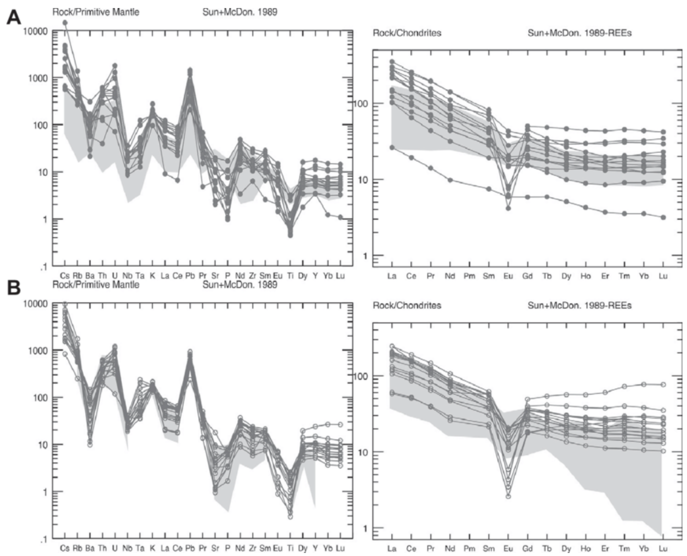

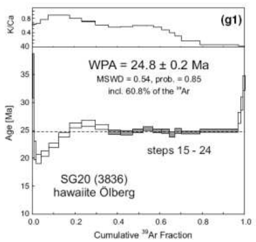

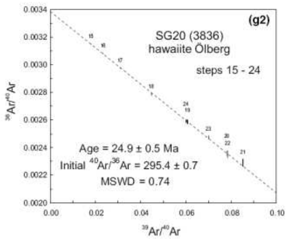

$$C(X) = \frac{1}{X}\int_0^X c(X')\,\mathrm{d}X'$$

$$c = \frac{\mathrm{d}}{\mathrm{d}X}(XC).$$

Example

MORB or OIB?

Two basalts: „BLACK ROCKS“

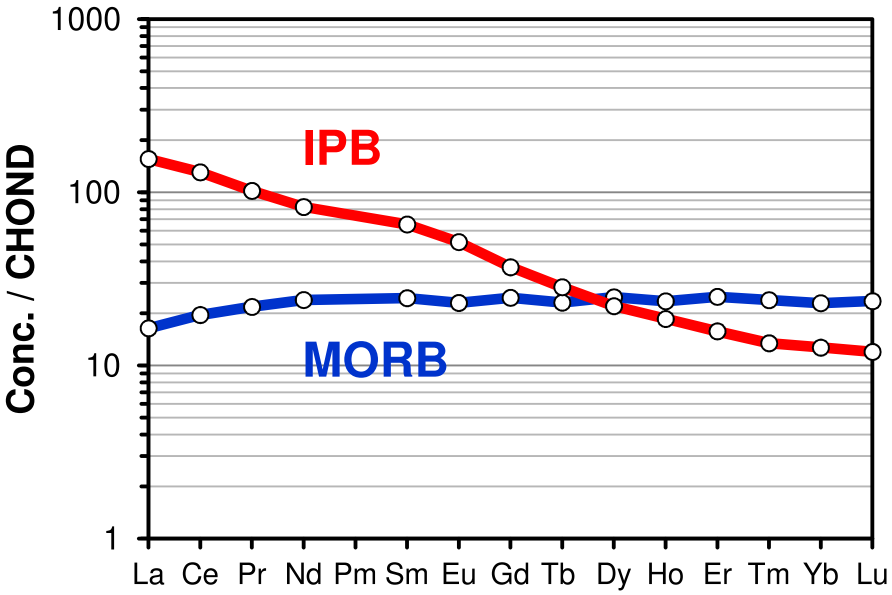

Rare Earth Element Plot of a typical Mid Ocean Ridge Basalt and a typical Intraplate Basalt

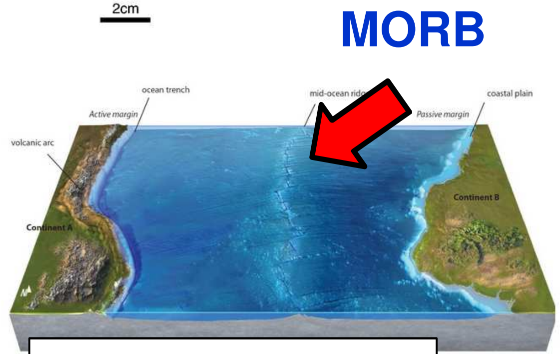

Mid Ocean Ridge Setting

Intraplate Setting (Mt. Etna, Sicily)

Tectonic settings

- Mid ocean ridges
- Oceanic island arcs
- Active continental margins
- Back-arc settings
- Oceanic intraplate settings
- Continental intraplate settings
- Convergent plate margins

} Subduction zone settings (Oceanic island arcs, Active continental margins)

} Intraplate settings (Oceanic intraplate settings, Continental intraplate settings)

Mid ocean ridge

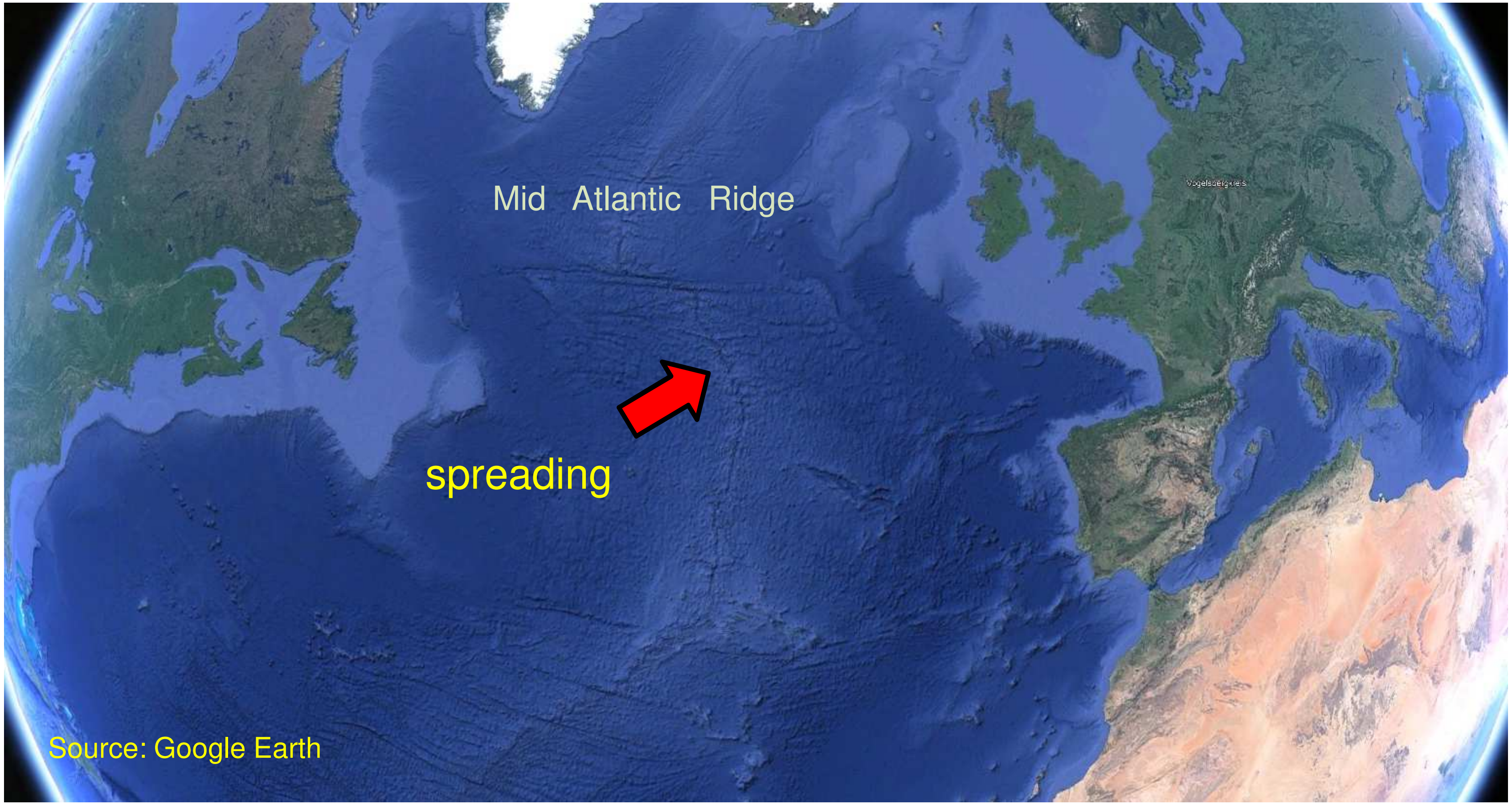

Oceanic island arc

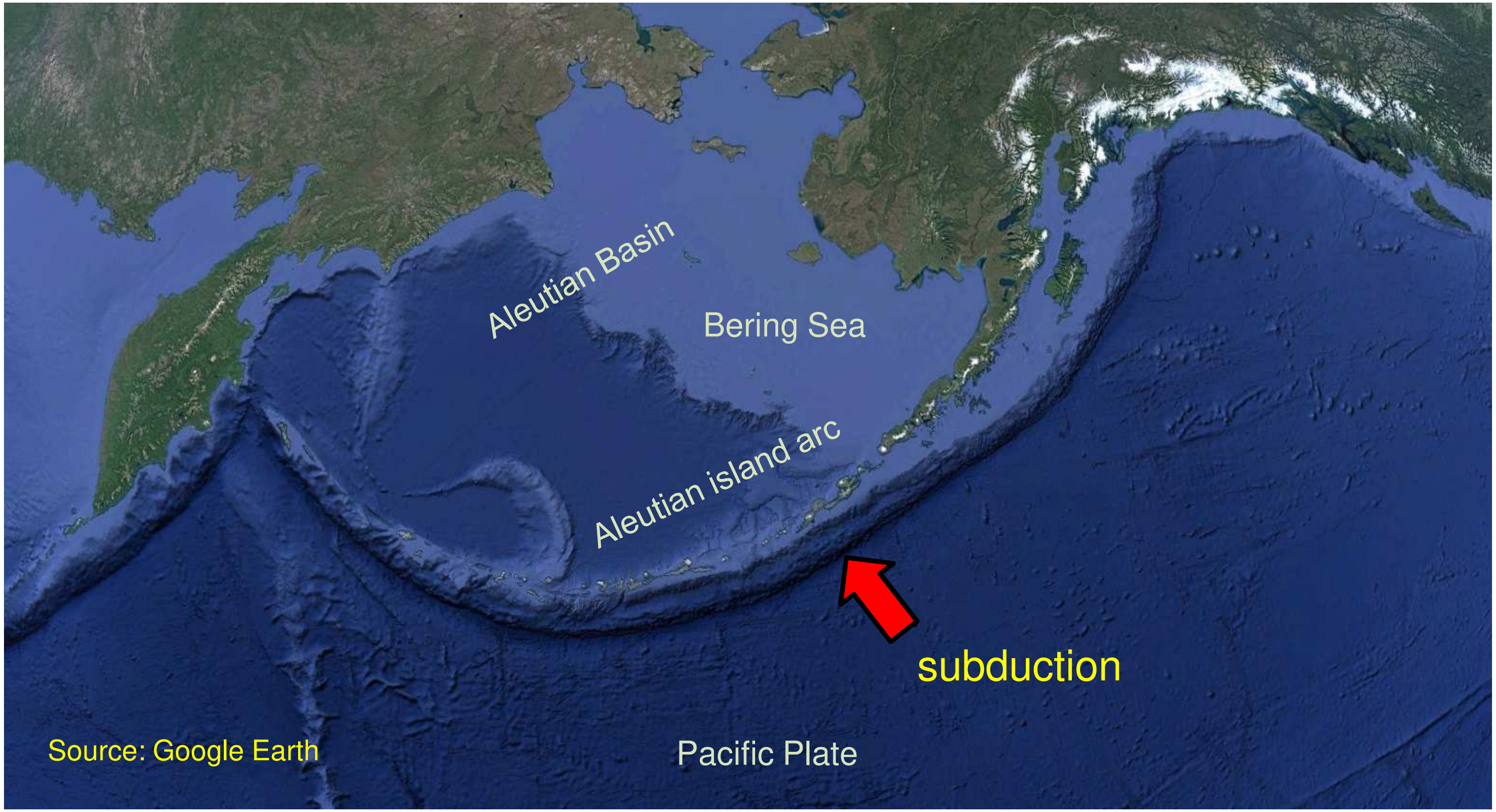

Active continental margin

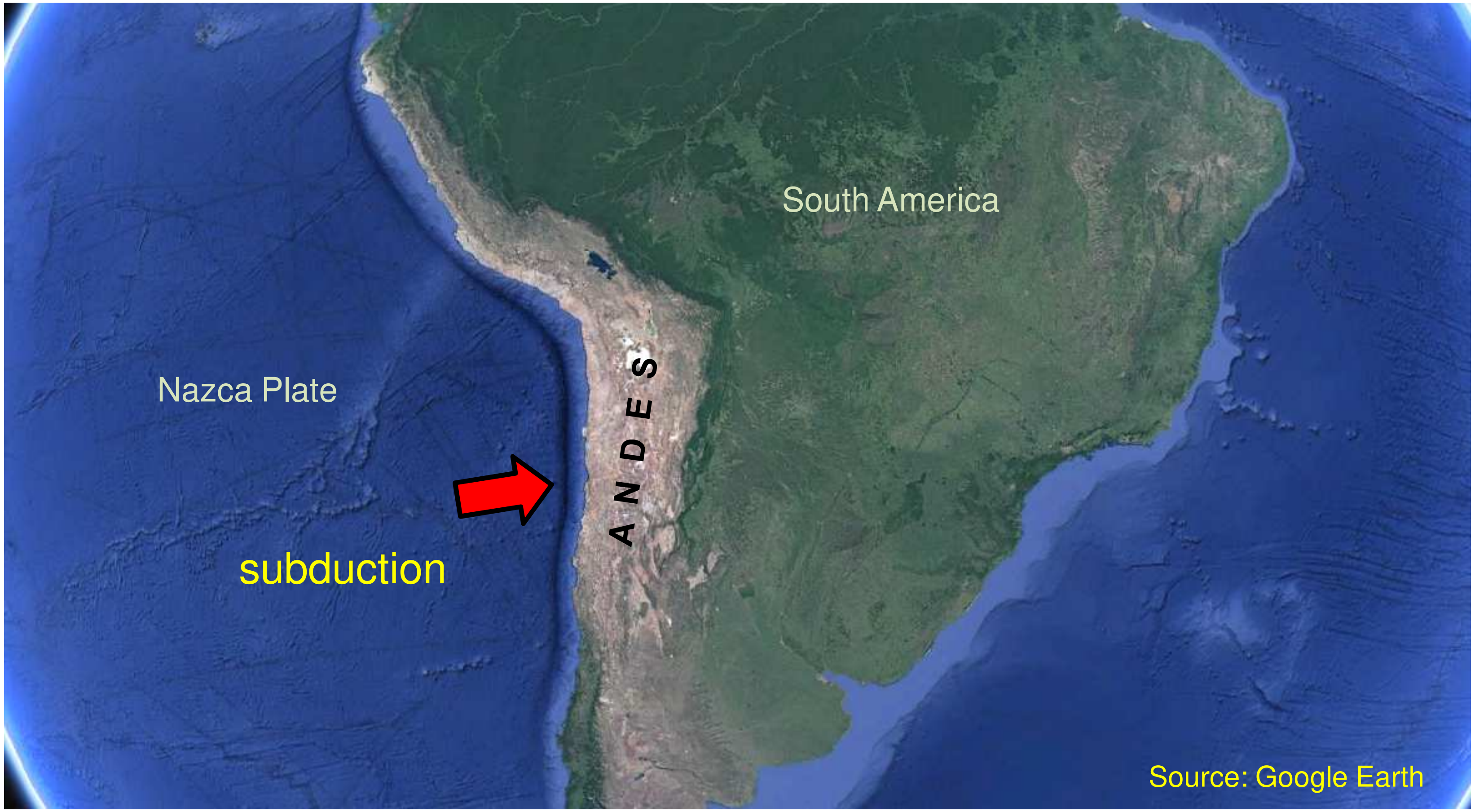

Back arc spreading

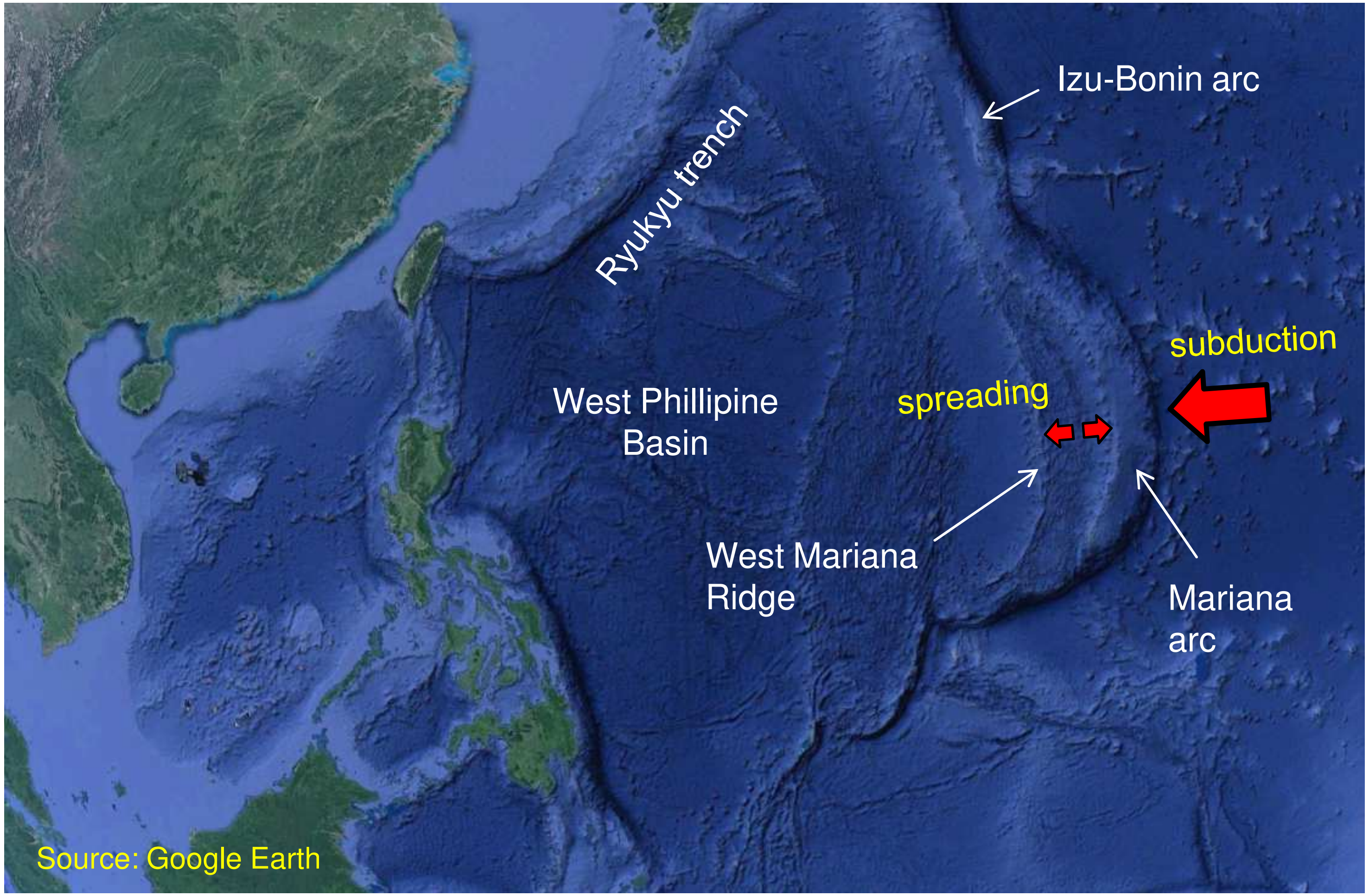

Oceanic intraplate setting

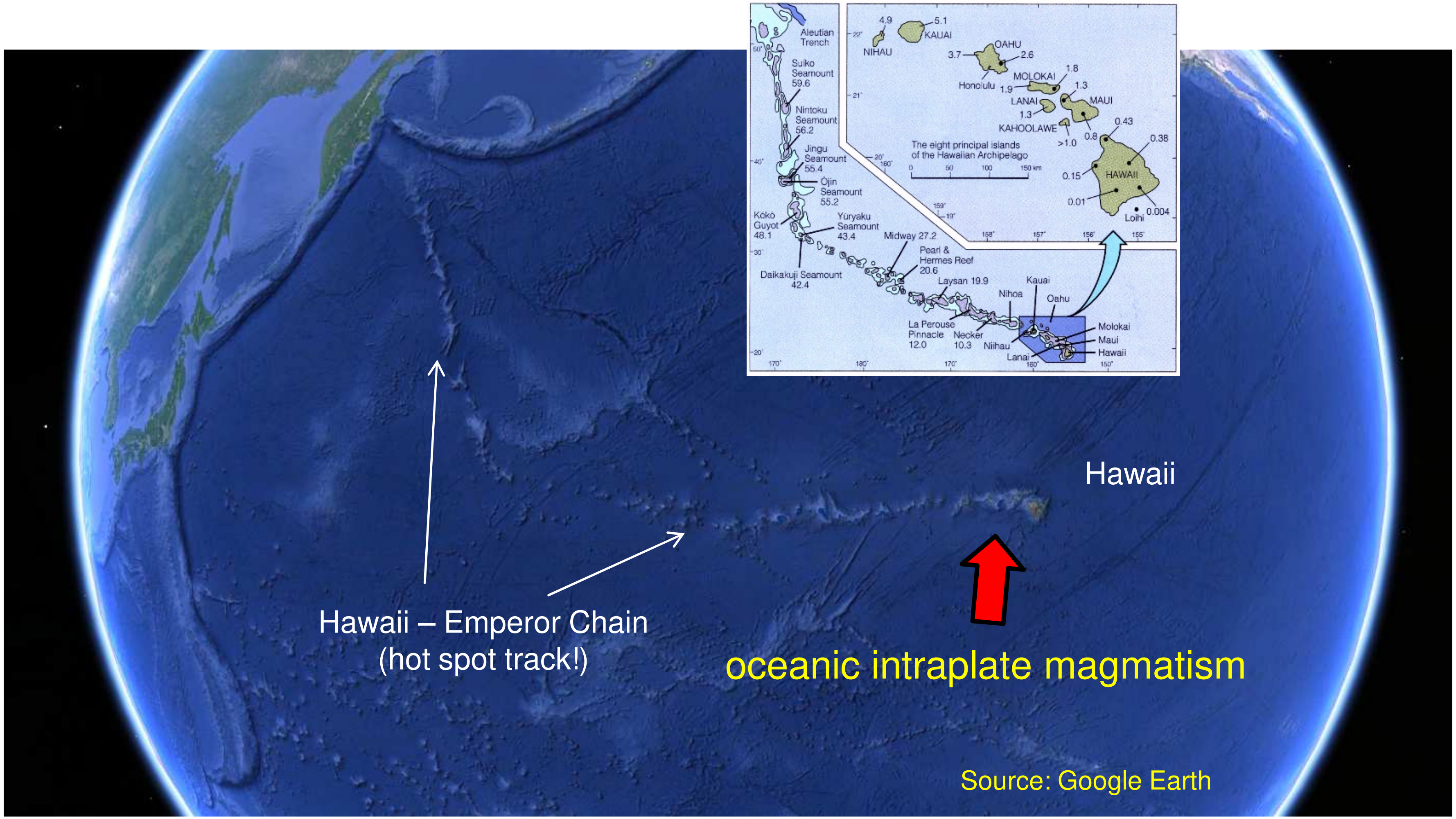

Source of inset: https://hilo.hawaii.edu/~kenhon/GEOL205/Chain/default.htm (April, 2021)

Continental intraplate setting

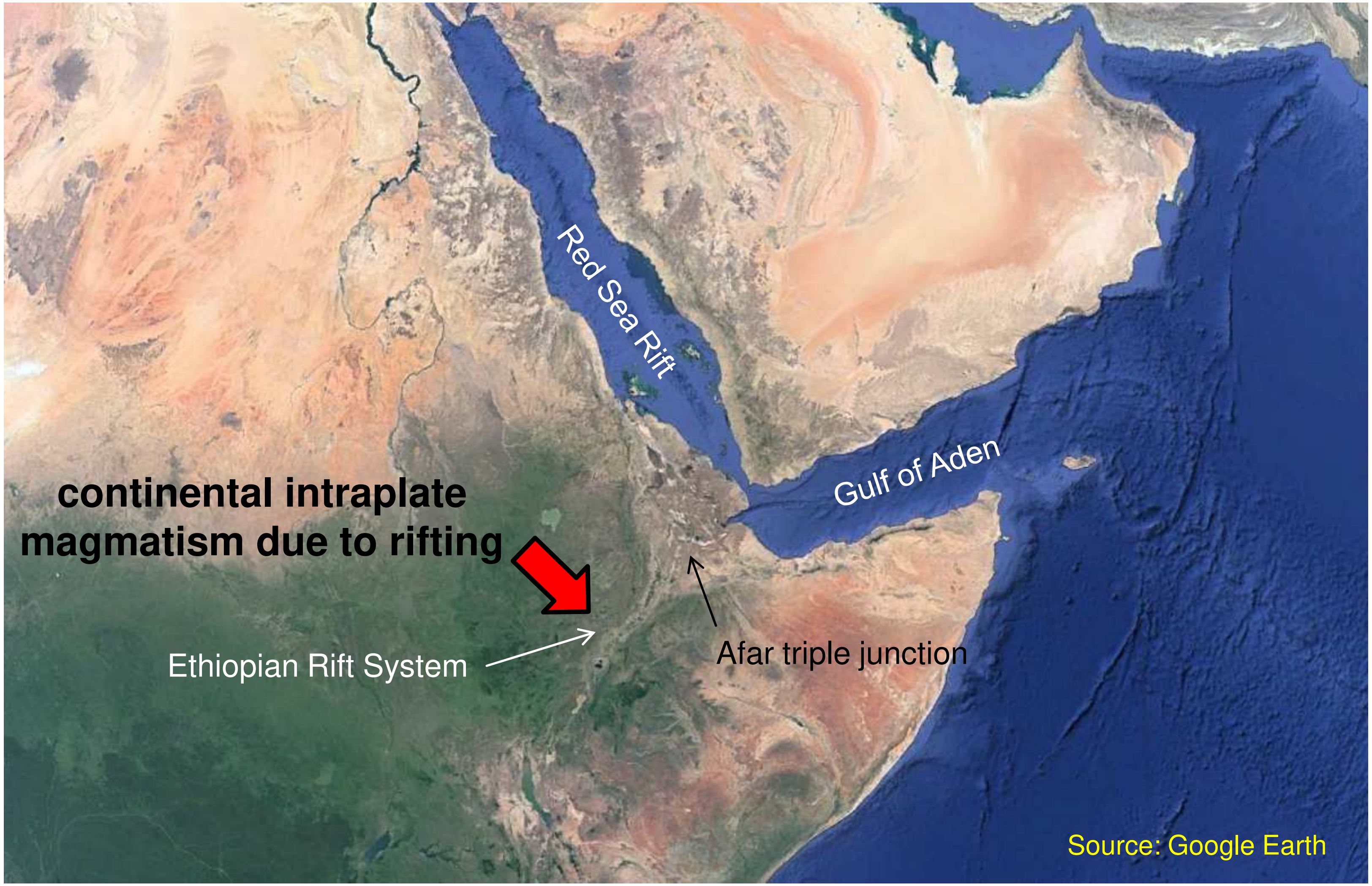

Continental intraplate setting

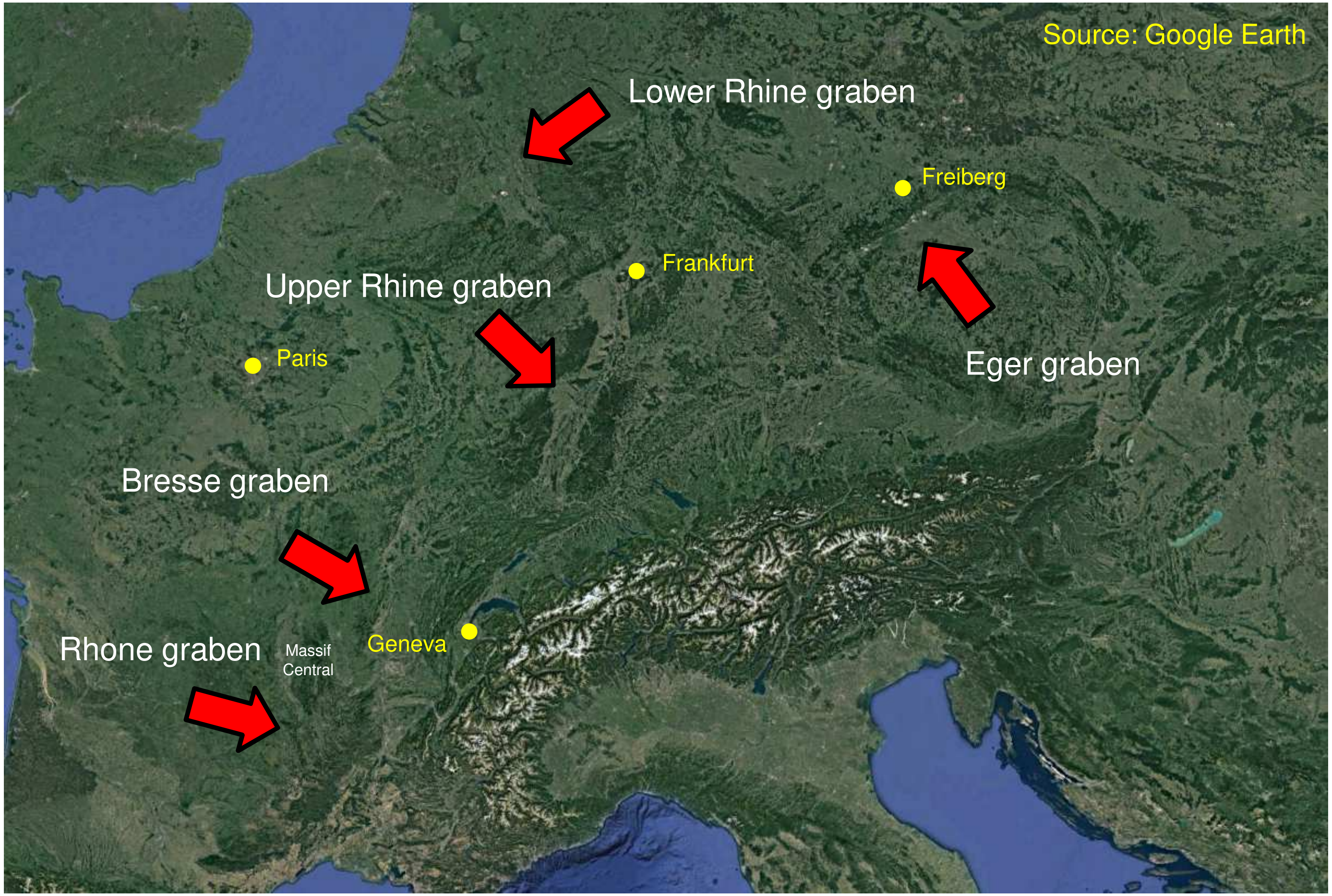

Convergent plate margins

Chapter 1

B A S I C S

$$C(X) = \frac{1}{X}\int_0^X c(X')\,\mathrm{d}X'$$

$$c = \frac{\mathrm{d}}{\mathrm{d}X}(XC).$$

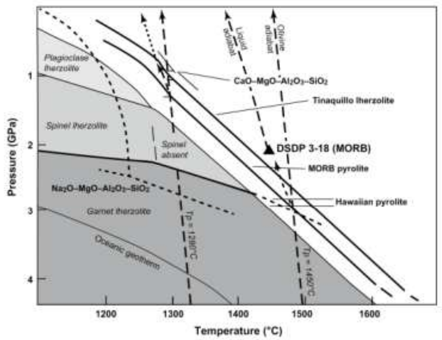

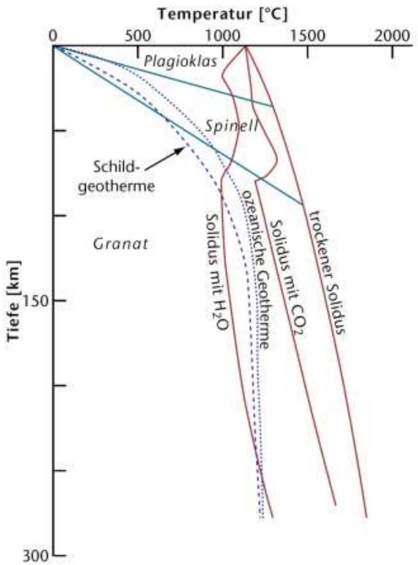

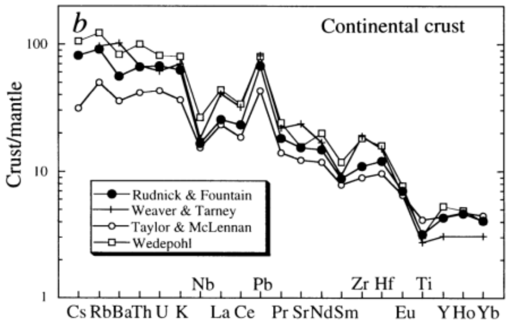

From rocks to geochemical (and geochronological) data

ROCK

Agate ball mill

or agate disc mill

ROCK POWDER

Particles <63 μm

From rocks to geochemical (and geochronological) data (very simple...)

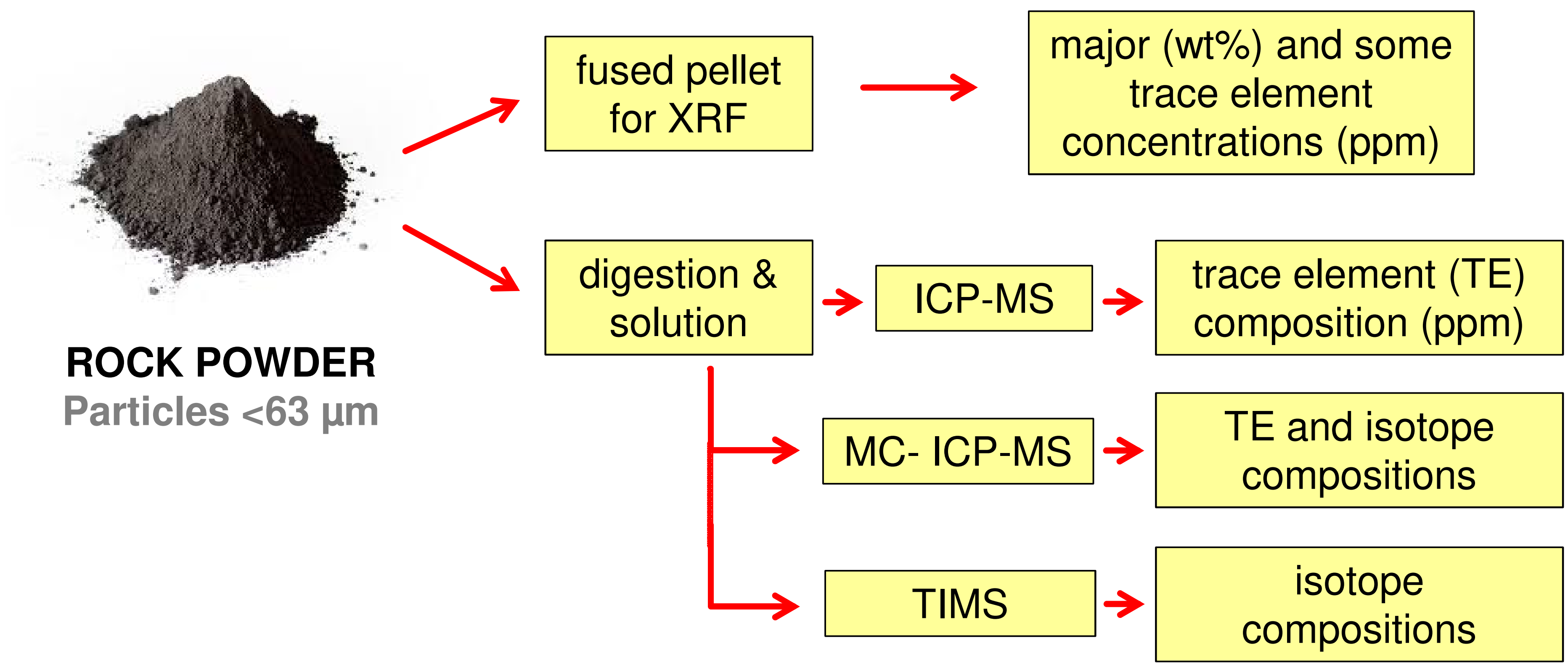

More data aquisition methods...

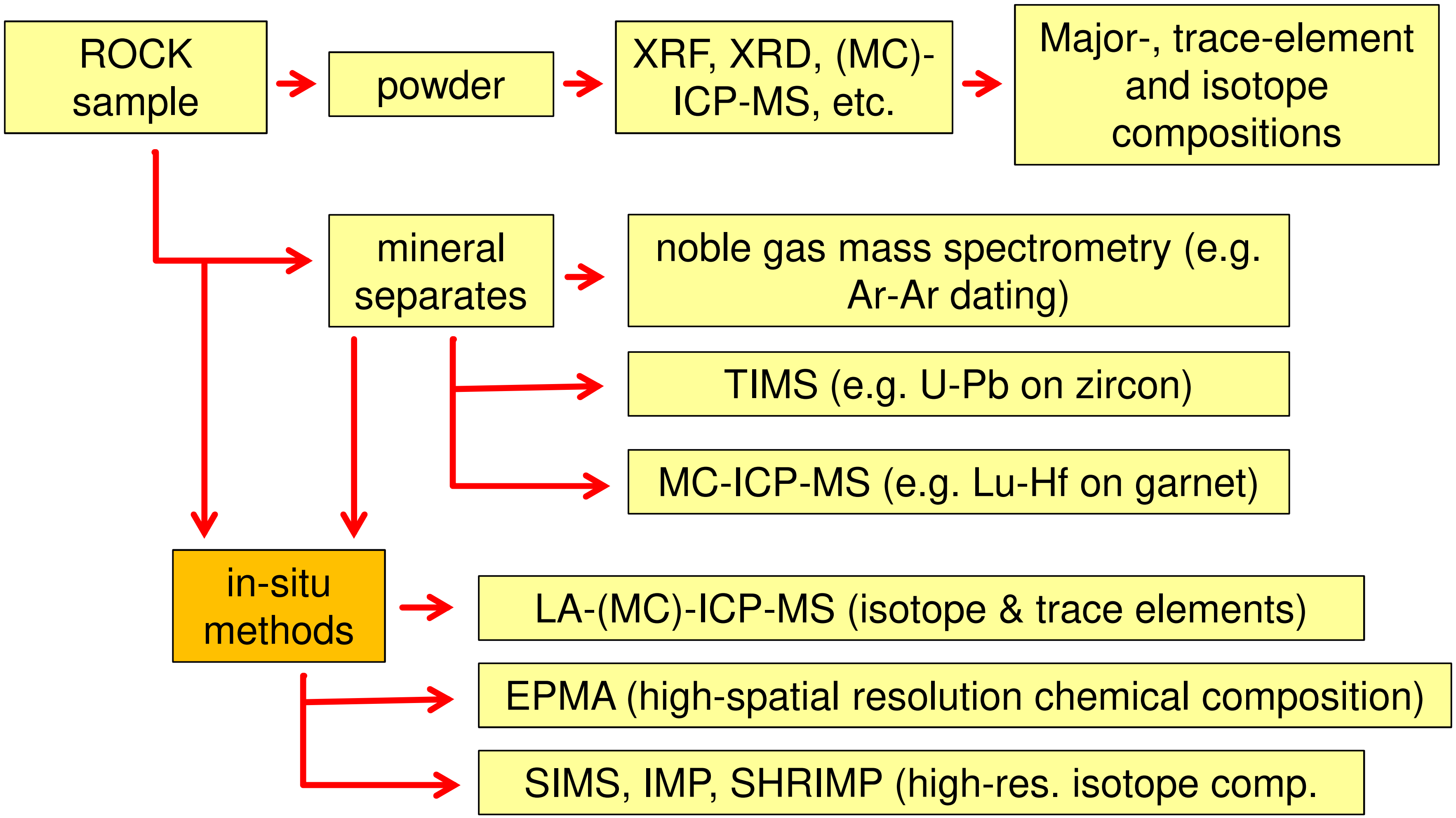

And the labs look like...

Cameca 1280 HR SIMS at GFZ Potsdam

Neptune MC-ICP-MS at Uni Cologne

Triton TIMS at WWU Münster (Inst. f. Planetologie)

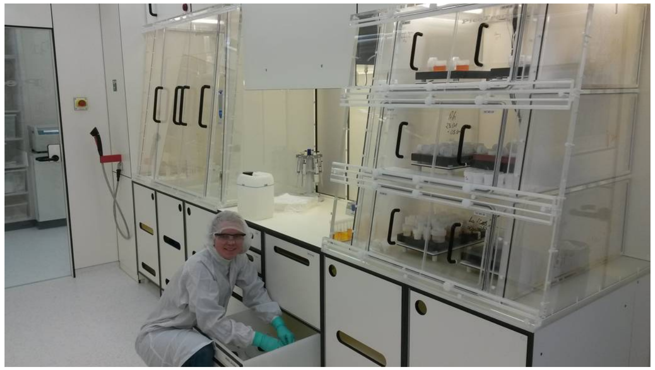

Clean-lab at Uni Cologne

Data documentation I

Table 1: Major element, trace element and isotope data of SiO_2-undersaturated rocks from the Heldburg region

Sample Rock type	Method	S097511 Mel	S097512 Mel	S097519 Mel	S107048 Mel	S107052 Mel	S097513 Neph	S097514 Neph	S097515 Neph	S107045 Neph
SiO_2	XRF	35·5	34·9	35·4	34·5	34·2	38·4	41·0	41·3	40·0
Al_2O_3	XRF	9·00	9·42	9·09	9·60	9·52	9·6	11·1	11·1	10·3
Fe_2O_3	XRF	12·9	12·2	11·8	13·4	11·6	12·0	12·6	13·1	13·3
FeO		11·6	10·9	10·6	12·0	10·4	10·8	11·4	11·8	11·9
MnO	XRF	0·20	0·18	0·17	0·18	0·17	0·17	0·20	0·20	0·20
MgO	XRF	13·3	12·8	14·0	13·3	14·1	13·6	12·3	12·6	13·7
CaO	XRF	12·0	11·6	12·5	11·6	12·7	11·2	11·8	11·3	11·9
Na_2O	XRF	3·39	3·16	3·47	3·11	3·82	2·92	4·04	3·44	3·26
K_2O	XRF	1·35	1·25	0·98	1·16	0·74	0·79	1·08	1·14	0·95
TiO_2	XRF	2·85	2·84	2·67	2·90	2·53	2·80	2·84	2·94	2·89
P_2O_5	XRF	1·00	0·99	0·84	0·76	0·82	0·61	0·82	0·77	0·86
SO_3	XRF	1·11	0·84	0·71	0·28	0·46	0·31	0·03	0·05	0·06
L·O·I	XRF	7·60	9·86	8·94	9·48	9·92	8·42	2·04	2·12	2·96
SUM	XRF	100·3	99·9	100·5	100·3	100·6	100·8	99·9	100·1	100·3
Li	ICPMS	36·9	31·6	45·2	15·5	54·6	20·0	41·5	21·1	27·2
Sc	ICPMS	20·7	20·1	22·3	21·9	26·2	21·3	21·9	24·8	24·3
V	XRF	265	265	228	272	246	262	279	281	289
Cr	XRF	494	458	409	367	539	451	476	527	643
Co	ICPMS	72·8	53·5	66·5	70·0	61·0	74·4	64·9	69·0	74·6
Ni	XRF	424	206	354	309	379	385	312	325	468
Cu	XRF	188	254	133	146	144	185	113	158	178
Zn	XRF	173	193	117	137	104	163	129	163	185
Ga	ICPMS	16·4	17·8	15·9	18·0	16·2	16·6	17·8	18·0	17·1
Rb	ICPMS	33·1	42·4	25·0	30·8	22·1	14·7	18·0	32·1	16·3
Sr	XRF	1361	1104	959	815	988	807	1105	1083	982
Y	ICPMS	29·0	30·0	23·5	23·4	23·5	21·1	27·3	26·9	25·2
Zr	XRF	321	307	266	299	225	230	264	264	286
Nb	ICPMS	106·3	117·6	91·1	96·5	99·9	72·5	97·5	91·7	92·3
Cs	ICPMS	0·677	0·485	0·392	0·302	0·299	2·50	1·32	1·06	0·976
Ba	XRF	828	778	797	2961	719	657	870	828	788
La	ICPMS	109·2	109·3	80·5	75·3	77·2	62·4	96·0	89·1	81·6
Ce	ICPMS	208	208	146	147	141	125	182	168	154
Pr	ICPMS	23·8	23·9	16·8	16·8	15·3	15·1	20·6	19·2	17·7
Nd	ICPMS	88·5	88·3	65·5	63·9	55·6	59·1	76·6	73·0	67·0
Sm	ICPMS	14·3	14·5	11·1	11·2	10·4	9·8	12·5	12·1	11·2
Eu	ICPMS	4·47	4·55	3·54	3·53	3·24	3·25	3·97	3·88	3·53
Gd	ICPMS	11·88	12·18	9·48	9·31	8·44	8·90	10·58	10·36	9·45
Tb	ICPMS	1·55	1·60	1·23	1·23	1·08	1·18	1·42	1·36	1·20

(continued)

From Pfänder et al., 2018, J. Petrol., 59, 667-694

Data documentation II

Table 1: Continued

Sample Rock type	Method	S097511 Mel	S097512 Mel	S097519 Mel	S107048 Mel	S107052 Mel	S097513 Neph	S097514 Neph	S097515 Neph	S107045 Neph
Dy	ICPMS	8·09	8·50	6·45	6·35	5·81	6·15	7·51	7·24	6·48
Ho	ICPMS	1·32	1·40	1·09	1·02	0·969	1·02	1·25	1·24	1·08
Er	ICPMS	3·09	3·31	2·54	2·48	2·35	2·36	3·11	2·98	2·63
Tm	ICPMS	0·362	0·406	0·301	0·274	0·279	0·286	0·379	0·358	0·331
Yb	ICPMS	1·73	1·89	1·48	1·40	1·54	1·32	1·84	1·78	1·67
Lu	ICPMS	0·238	0·262	0·199	0·188	0·214	0·180	0·252	0·245	0·238
Hf	ICPMS	7·11	7·17	6·18	7·03	5·46	5·62	6·10	6·06	6·44
Ta	ICPMS	5·57	5·92	4·72	5·31	4·83	4·11	4·92	4·79	5·05
Pb	ICPMS	13·36	11·99	8·72	6·73	4·89	8·20	7·75	7·93	8·77
Th	ICPMS	14·02	14·00	10·30	8·26	9·34	7·74	12·40	11·07	9·40
U	ICPMS	4·01	3·27	3·29	2·16	1·41	2·36	3·69	3·33	2·93
$(^{206}Pb/^{204}Pb)_m$		18·72	18·54	18·87	18·57	18·92	18·56	18·95	18·67	18·49
$(^{206}Pb/^{204}Pb)i$		18·61	18·45	18·73	18·47	18·82	18·47	18·77	18·55	18·41
$(^{207}Pb/^{204}Pb)_m$		15·62	15·60	15·61	15·61	15·61	15·62	15·64	15·61	15·62
$(^{207}Pb/^{204}Pb)i$		15·61	15·60	15·60	15·61	15·61	15·62	15·63	15·60	15·62
$(^{208}Pb/^{204}Pb)_m$		38·65	38·42	38·77	38·49	38·78	38·49	38·88	38·57	38·42
$(^{208}Pb/^{204}Pb)i$		38·52	38·29	38·62	38·36	38·57	38·40	38·68	38·44	38·33
$(^{176}Hf/^{177}Hf)_m$		0·282881±4	0·282879±4	0·282894±5	0·282868±5	0·282922±4	–	0·282858±7	0·282867±6	0·282917±6
$(^{176}Hf/^{177}Hf)i$		0·282878	0·282876	0·282891	0·282865	0·282919		0·282854	0·282864	0·282914
$e_{Hf(0)}$		3·9	3·8	4·3	3·4	5·3	–	3·0	3·4	5·1
$e_{Hf(i)}$		3·7	3·7	4·2	3·3	5·2		2·9	3·3	5·0
$(^{143}Nd/^{144}Nd)_m$		0·512858±7	0·512846±7	0·512866±10	0·512856±10	0·512879±8	–	0·512838±9	0·512844±8	0·512881±8
$(^{143}Nd/^{144}Nd)i$		0·512839	0·512825	0·512841	0·512834	0·512855	–	0·512813	0·512824	0·512864
$e_{Nd(0)}$		4·3	4·1	4·5	4·2	4·7	–	3·9	4·0	4·7
$e_{Nd(i)}$		4·7	4·5	4·9	4·6	5·1		4·4	4·4	5·0
$(^{87}Sr/^{86}Sr)_m$		0·705187±12	0·704482±11	0·703682±13	0·703687±13	0·703970±32	–	0·703686±11	0·703740±11	0·703517±21
$(^{87}Sr/^{86}Sr)_i$		0·70515	0·70443	0·70364	0·703637	0·703939		0·70366	0·70370	0·70350

(continued)

From Pfänder et al., 2018, J. Petrol., 59, 667-694

Data documentation III

Table 2. U–Pb analytical data of zircon from the microgranite dike at Písečný vrch, Teplice region, Czech Republic.

Sample[a]	Weight (mg)	Concentrations (ppm)		$^{206}Pb/^{204}Pb$ Measured ratios[b]	$^{232}Th/^{238}U$ (at)[c]	Radiogenic Pb (at%)[c]				Atomic ratios[c]			Apparent ages (Ma)[d]		
		U	Pb_{tot}			^{206}Pb	^{207}Pb	^{208}Pb	$^{238}U/^{204}Pb$	$^{206}Pb/^{238}U$	$^{207}Pb/^{235}U$	$^{207}Pb/^{206}Pb$	$^{206}Pb/^{238}U$	$^{207}Pb/^{235}U$	$^{207}Pb/^{206}Pb$
Abraded zircon															
1	0.067	220.6	11.90	988	0.51	82.48	4.35	13.16	29100	0.04964	0.3613	0.05279	312	313	320
2	0.103	203.2	11.65	646	0.55	81.64	4.31	14.05	14600	0.05034	0.3665	0.05281	317	317	321
3	0.033	188.0	9.97	1010	0.53	81.94	4.32	13.74	77800	0.04977	0.3614	0.05266	313	313	314
4	0.038	197.3	12.58	350	0.59	80.87	4.29	14.84	8020	0.05253	0.3845	0.05309	330	330	333
5	0.052	211.1	13.04	549	0.52	82.14	4.39	13.47	12640	0.05419	0.3997	0.05339	340	341	350
6	0.087	221.4	14.44	694	0.54	81.59	4.48	13.92	13400	0.05754	0.4360	0.05496	360	367	411
7	0.110	184.1	10.75	727	0.59	80.70	4.25	15.04	16600	0.05119	0.3720	0.05270	322	321	316
8	0.088	92.7	5.32	750	0.56	81.36	4.30	14.34	24000	0.05154	0.3752	0.05279	324	324	320
9	0.087	215.4	14.88	200	0.56	81.46	4.25	14.29	3840	0.04986	0.3587	0.05217	314	311	293
10	0.024	506.4	30.27	723	0.62	80.16	4.25	15.59	18400	0.05249	0.3837	0.05301	330	330	329
11	0.095	216.7	12.47	326	0.56	81.46	4.30	14.24	7200	0.04623	0.3365	0.05280	292	295	320
12	0.096	269	18.86	405	0.52	82.10	4.55	13.35	7100	0.05833	0.4455	0.05539	366	374	428
13	0.132	169	19.36	69.6	0.58	80.99	4.53	14.66	1030	0.05041	0.3735	0.05374	317	322	360
Weakly abraded and broken zircon															
14	0.133	125.6	18.46	52.3	0.59	80.71	4.26	15.04	680	0.05082	0.3697	0.02753	320	319	318
15	0.128	131.3	41.4	29.95	0.68	79.18	4.03	16.79	240	0.0494	0.347	0.0509	311	302	236
16	0.121	182.2	13.35	172	0.59	80.88	4.27	14.85	3200	0.05017	0.3650	0.05277	316	316	319
Non-abraded zircon															
17															
18	0.146	277.3	17.25	184	0.70	77.99	4.95	17.06	4030	0.04221	0.3695	0.06350	267	319	725
19	0.222	953	123.9	54.0	0.58	81.09	4.22	14.69	778	0.04619	0.3315	0.05204	291	291	287
20	0.222	180.3	10.2	199	0.61	79.61	5.04	15.35	4660	0.03984	0.3476	0.06327	252	303	717
21	0.154	356.8	30.95	87.3	0.54	81.79	4.37	13.84	1570	0.04434	0.3268	0.05344	280	287	348
22	0.445	232.5	14.04	226	0.66	78.75	4.99	16.26	4860	0.04335	0.3785	0.06332	274	326	719

[a] Zircon concentrates were cleaned in warm 7N HNO_3 and H_2O before dissolution in concentrated HF in teflon-lined autoclaves at 210 °C for 4 days. A mixed ^{205}Pb-^{235}U tracer was added before sample dissolution. Lead and U were separated using ion-exchange chromatographic p rocedures (e.g., Romer et al. 1996; Schmid et al. 2003). Lead and U were loaded together on single Re-filaments using a silica-gel emitter and H_3PO_4 (Gerstenberger & Haase 1997) and measured at 1200°–1260 °C and 1350–1400 °C, respectively, on a Finnigan MAT262 multicollector mass-spectrometer (modified with an ion source by Spectromat) using Faraday collectors and ion counting.
[b] Lead isotope ratios corrected for fractionation (0.1 % / a.m.u.).
[c] Lead corrected for fractionation, blank, tracer contribution, and initial lead ($^{206}Pb/^{204}Pb = 18.1 \pm 0.1$, $^{207}Pb/^{204}Pb = 15.60 \pm 0.02$, $^{208}Pb/^{204}Pb = 38.2 \pm 0.2$). During the measurement period, total blanks were < 15 pg for lead and < 1 pg for uranium. $^{232}Th/^{238}U$ ratios calculated for an age of 320 Ma from $^{208}Pb_{rad}/^{206}Pb_{rad}$.
[d] Apparent ages were calculated using the constants recommended by IUGS (Steiger & Jäger 1977).

From Romer et al., 2010, N. Jb. Miner. Abr., 187, 289-305

Databases

Large datasets need an adequate infrastructure: DATABASES

Available geochemical databases are:

EarthChem (PetDB, SedDB, Geochron,...)
https://earthchem.org

GEOROC (Geochemistry of Rocks of the Oceans and Continents): http://georoc.mpch-mainz.gwdg.de/georoc/

GERM (**G**eochemical **E**arth **R**eference **M**odel)
https://earthref.org/GERM/

Exercise !!

How can we use geochemical data?

- Rock classification !!
- Process identification !
- Reconstruct ancient Tectonic Settings... !(?) ... sometimes

Common types of magmatic rocks

Exercise !!

- Classification of the most common rock types by chemistry

TAS classification of volcanic rocks

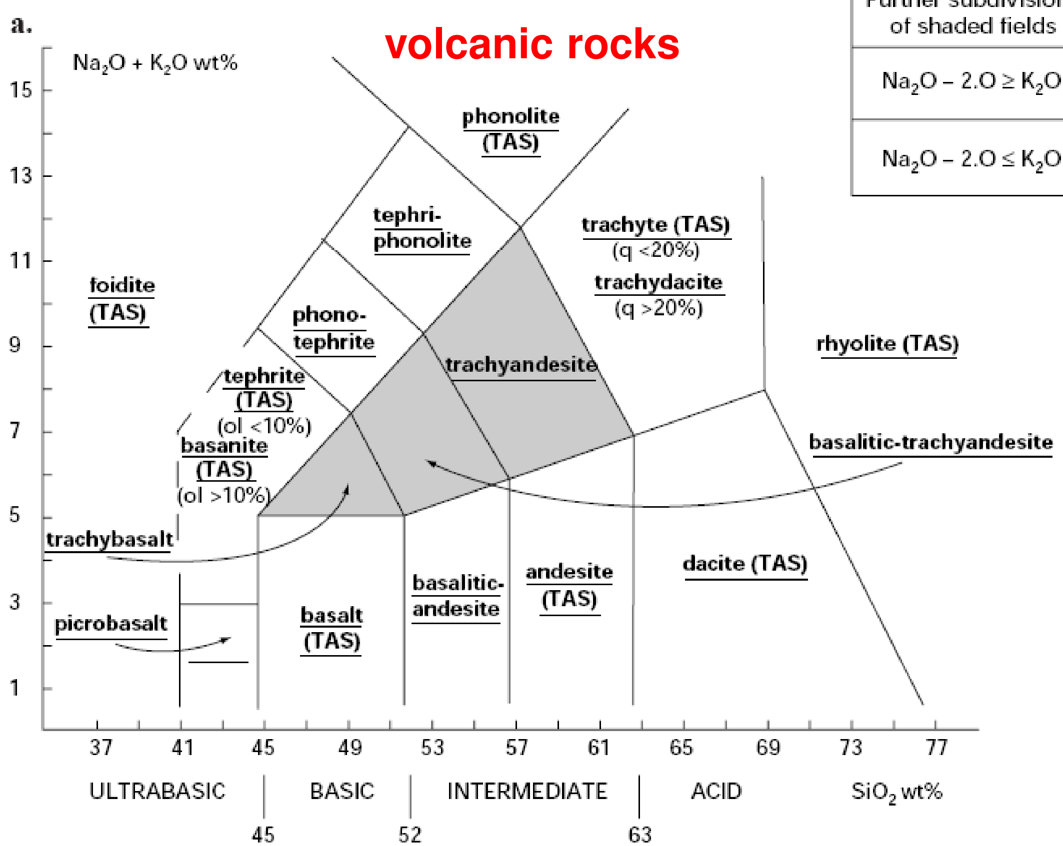

Further subdivisions of shaded fields	trachybasalt	basaltic-trachyandesite	trachyandesite
$Na_2O - 2.0 \geq K_2O$	hawaiite	mugearite	benmoreite
$Na_2O - 2.0 \leq K_2O$	potassic-trachybasalt	shoshonite	latite (TAS)

Note that trachybasalts, basaltic-trachyandesites and trachyandesites are further subdivided based on their **Na**/**K** **ratio** [f(p)]

From: Gillespie & Styles, BGS (British Geological Survey) Rock Classification – Vol 1 – Classification of igneous rocks

Common types of magmatic rocks

- Classification of the most common rock types by chemistry

TAS classification **for volcanic and plutonic rocks**

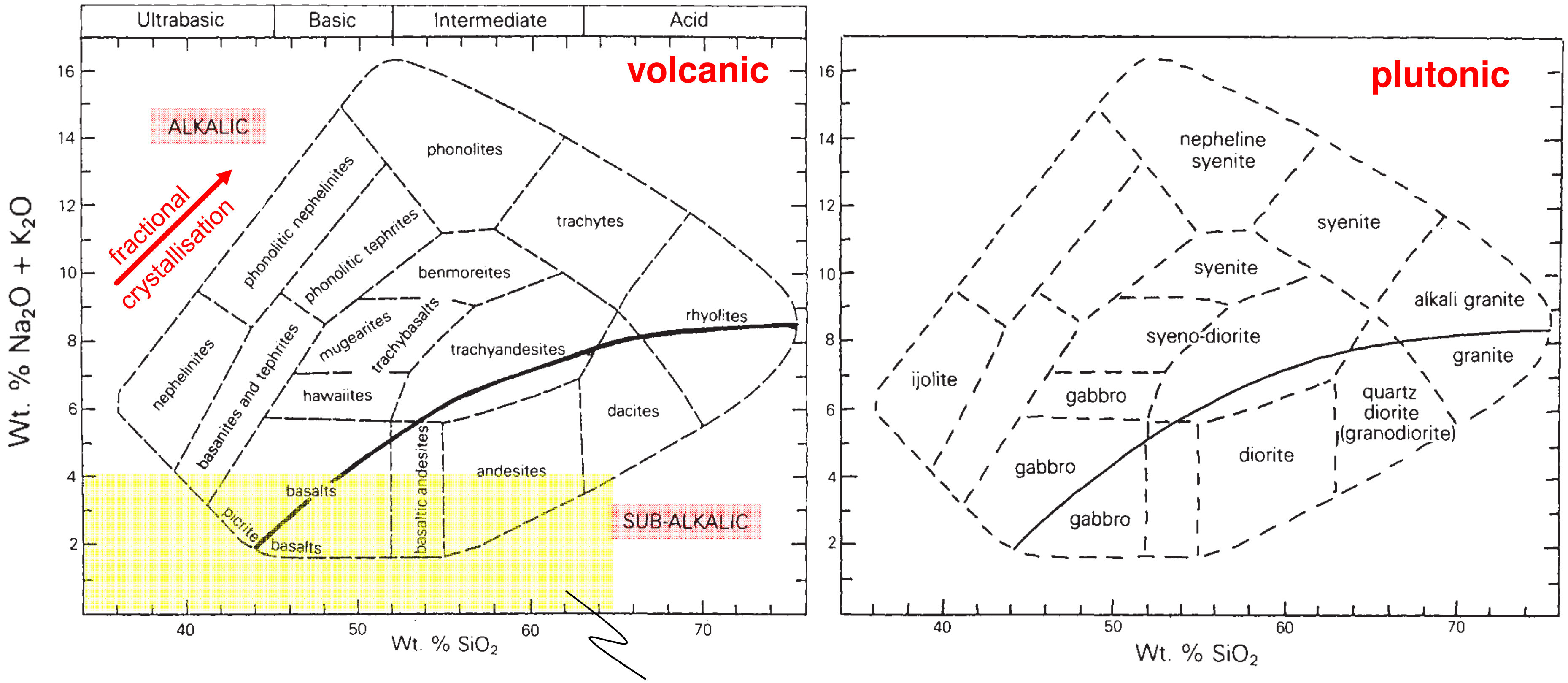

range shown in next slide....

From: Wilson, M.: Igneous Petrogenesis, Springer.

Common types of magmatic rocks

- Classification of the most common rock types by chemistry

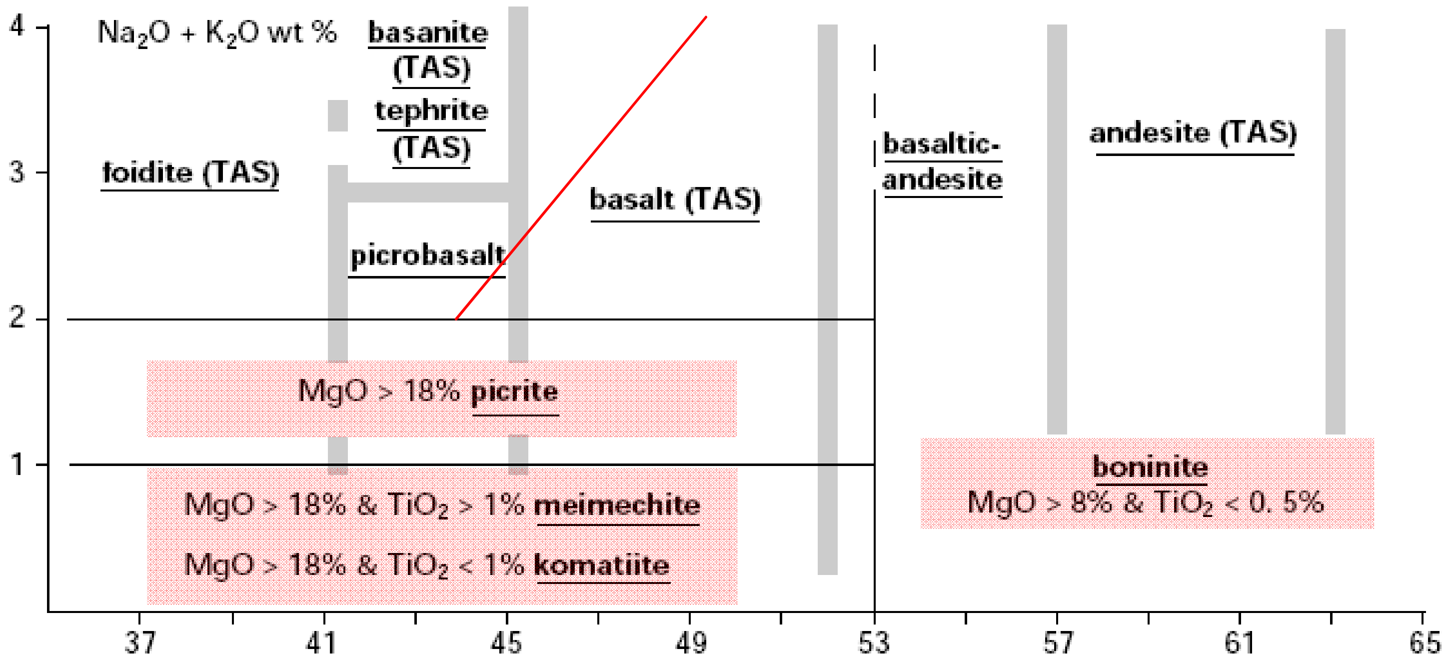

From: Gillespie & Styles, BGS (British Geological Survey)
Rock Classification – Vol 1 – Classification of igneous rocks

Picrites, Meimechites, **Komatiites** and **Boninites** are defined by combining the TAS nomenclature with MgO and TiO_2 contents

Common types of magmatic rocks

- Classification of the most common rock types by chemistry

From: Gillespie & Styles, BGS Rock Classification, Vol 1 (originally from Le Maitre et al. 1981)

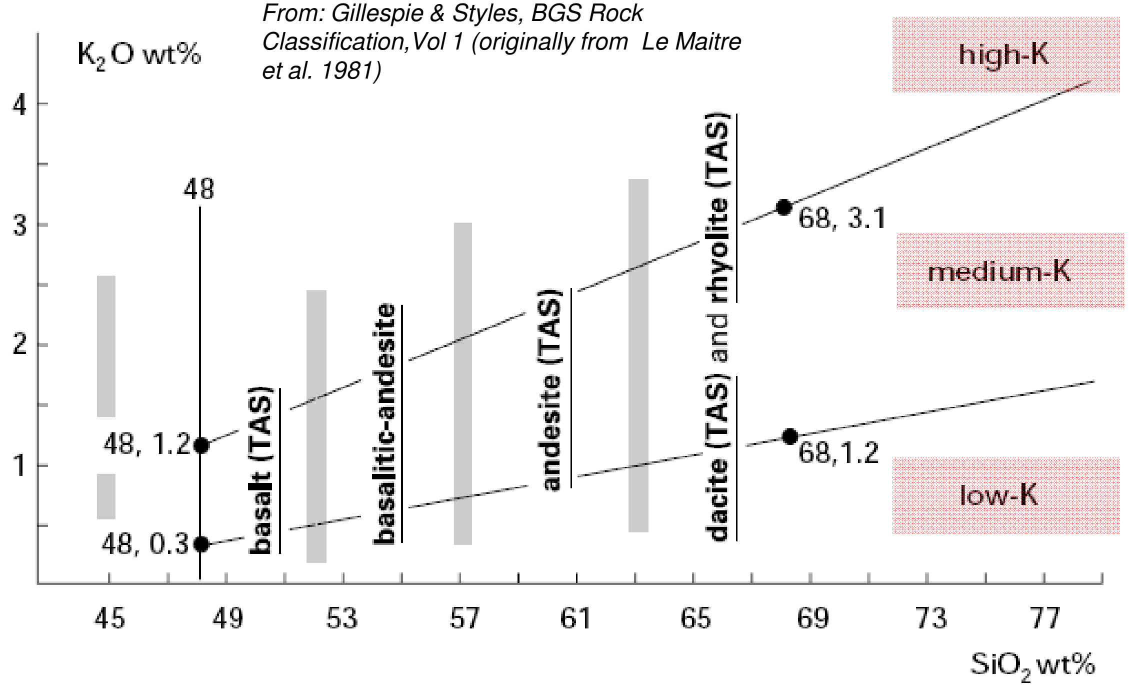

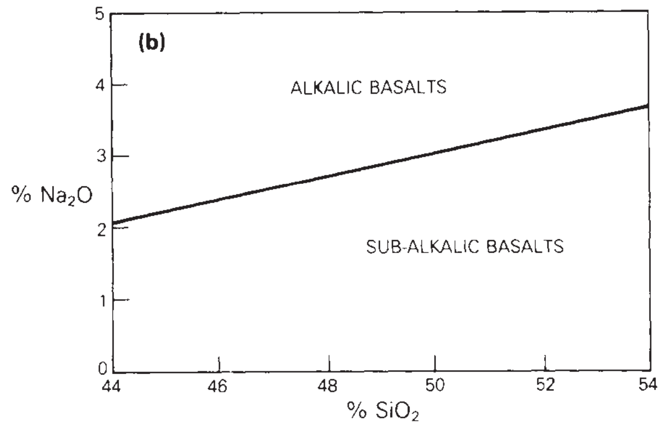

Subdivision of basalts in alkalic and subalkalic

Refinement of the TAS classification by using the K_2O (and Na_2O) contents

From: Wilson, M.: Igneous Petrogenesis, Springer.

Process identification

- Fractional crystallisation

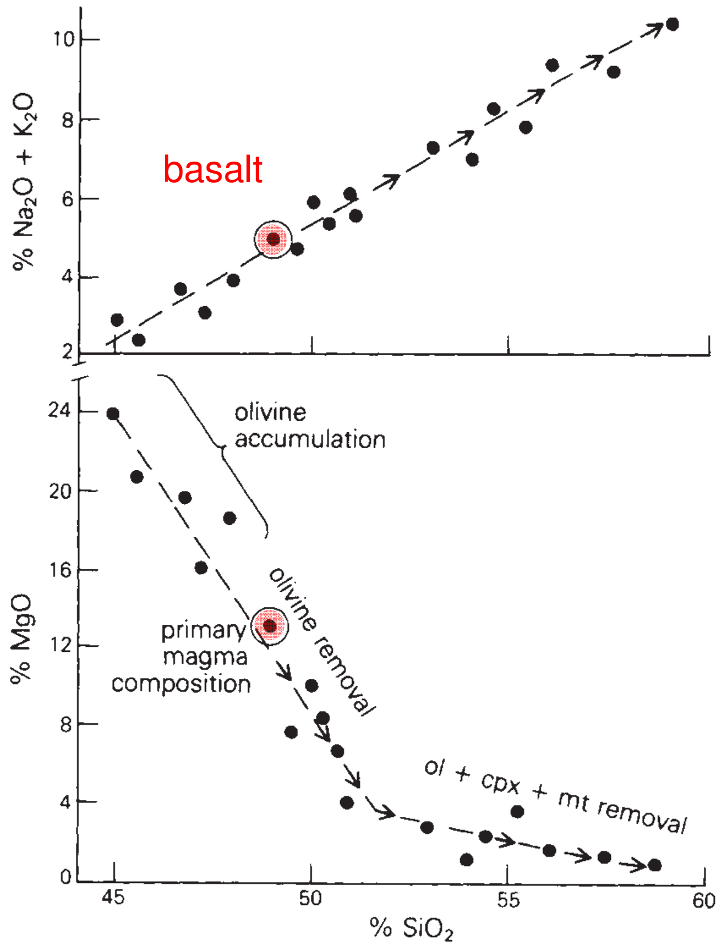

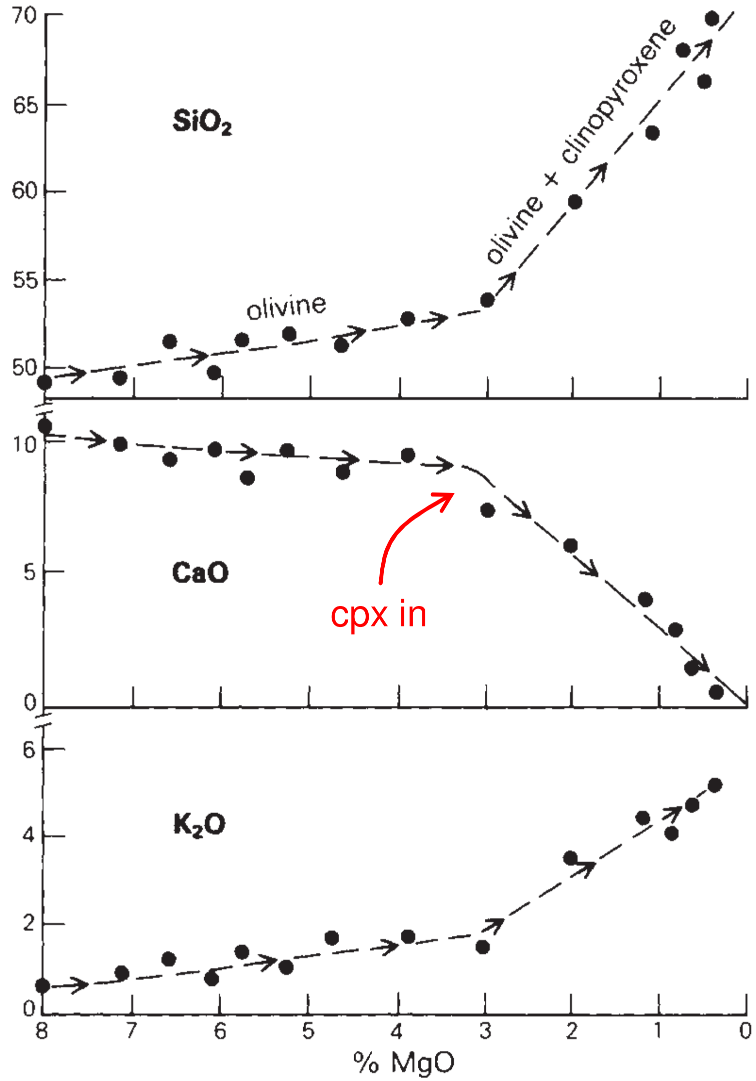

Process identification

- Fractional crystallisation
  (and partial melting)

Exercise !!

How do REEs behave upon **fractional crystallisation** and **partial melting**?

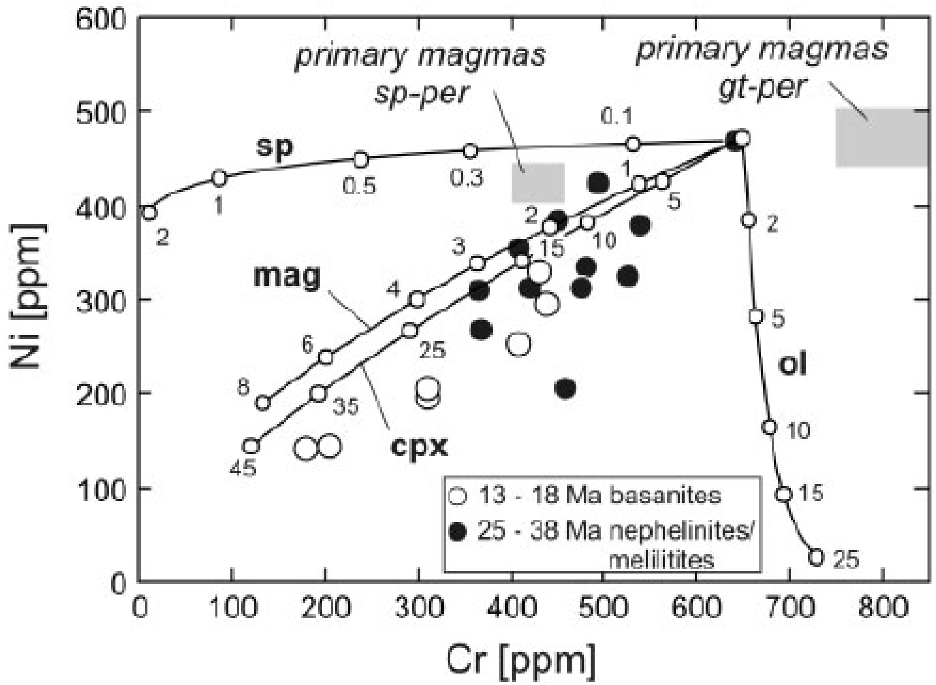

From Pfänder et al., 2018

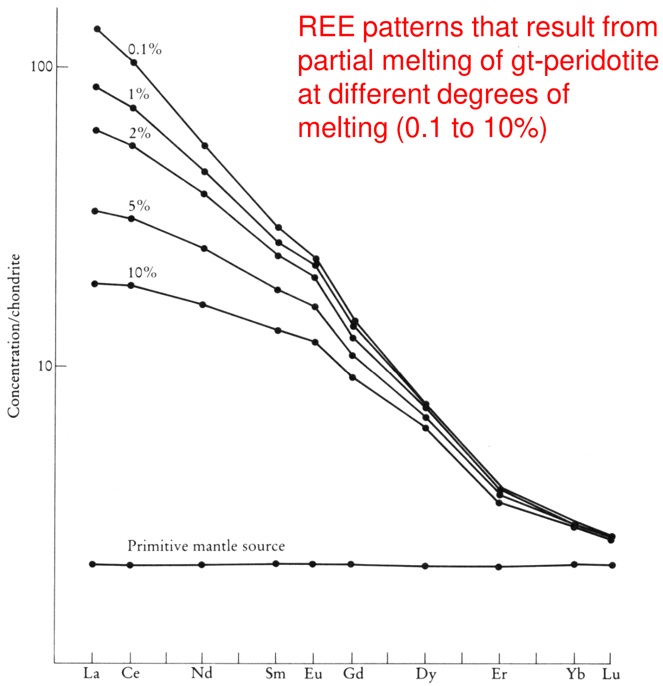

From Rollinson, Using geochemical data

Process identification

- Crustal assimilation of mantle derived primary magmas

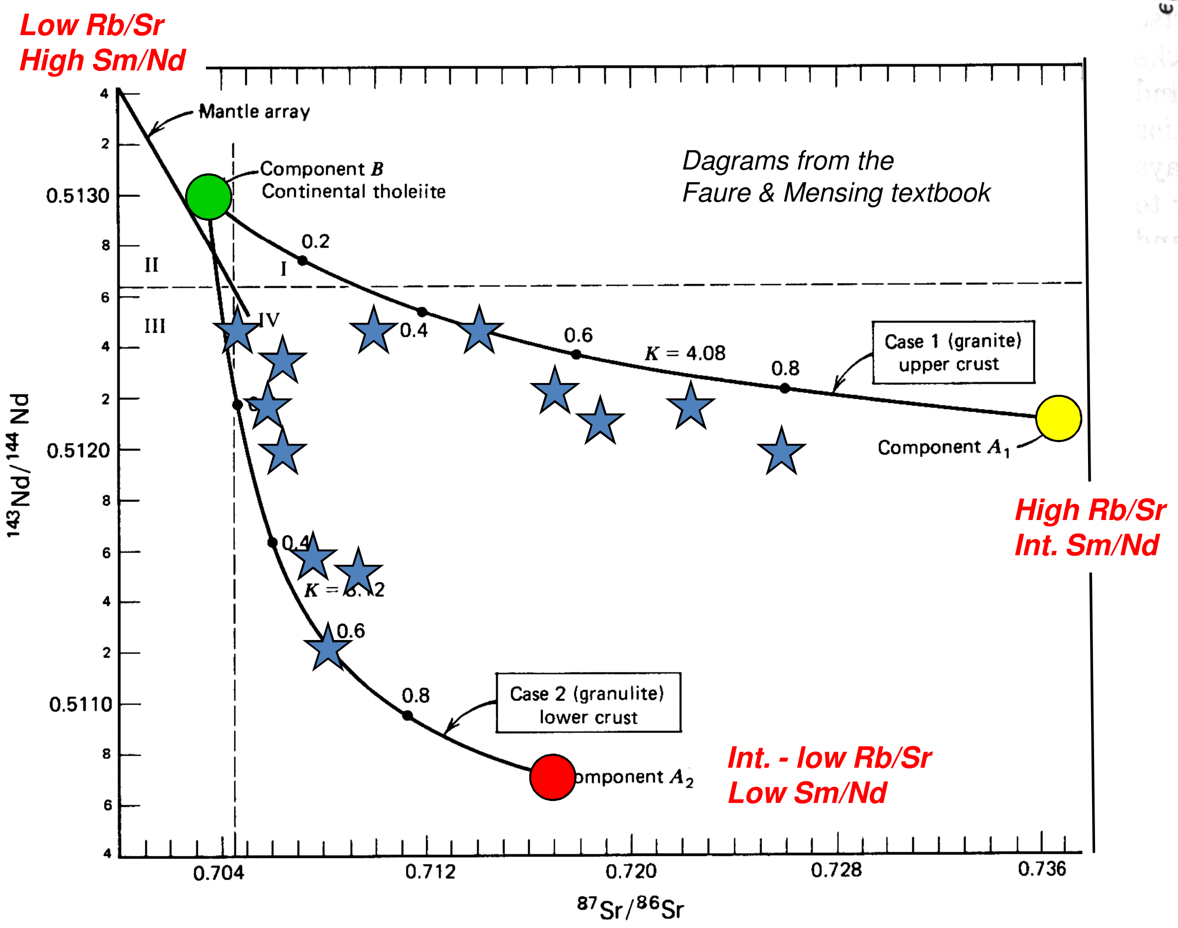

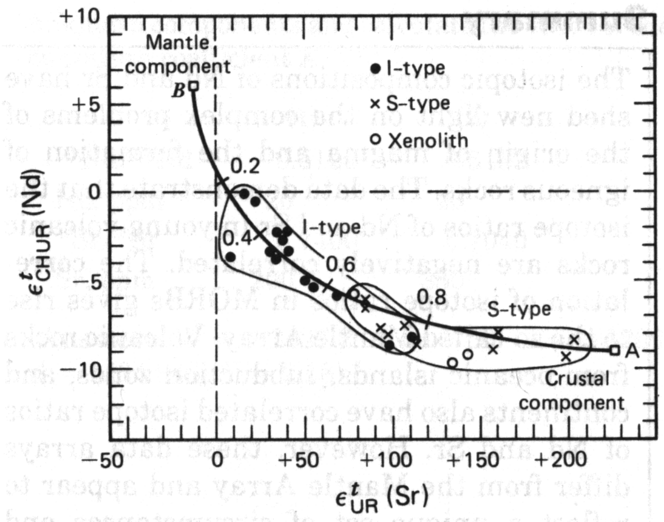

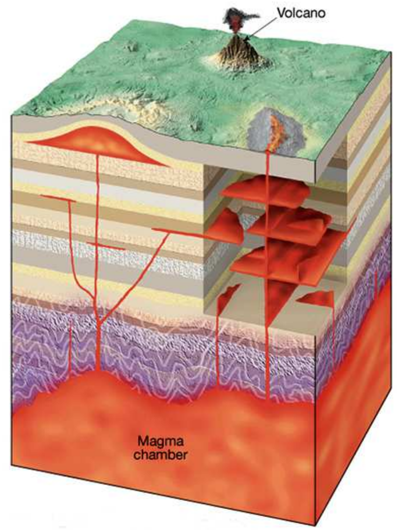

Tectonic setting

Fe/Mg ratio and crystallisation trends in the ternary plot
FeO – MgO – Na_2O+K_2O

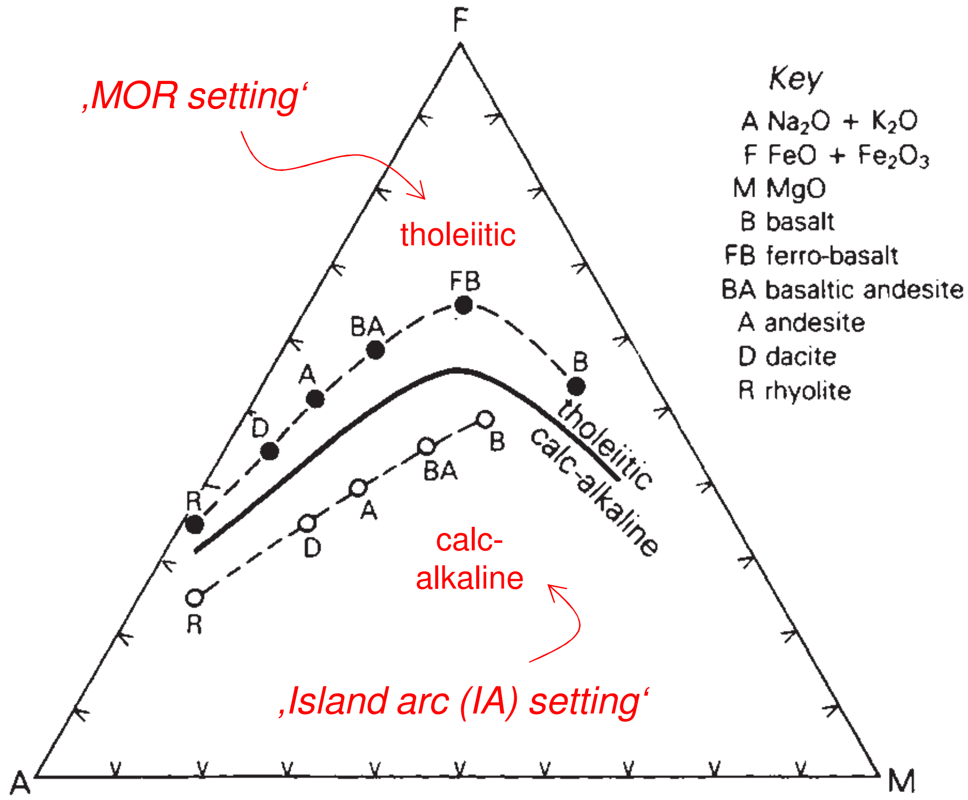

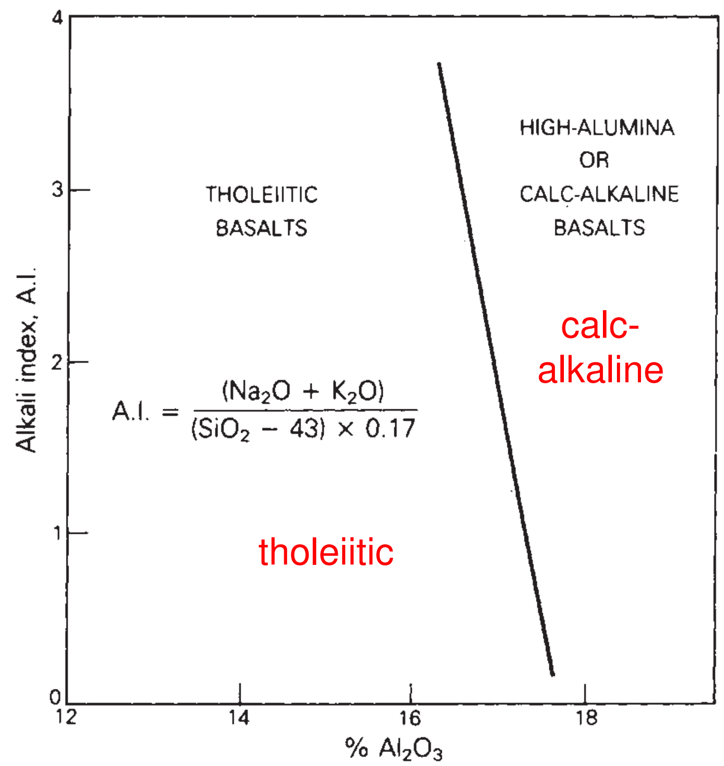

Both taken from: Wilson, M.: Igneous Petrogenesis, Springer. A.I. vs. Al2O3 from Middlemost 1975)

Tectonic setting

- Magma series and their first-order tectonic affinity

Table 1.3 Characteristic magma series associated with specific tectonic settings.

	Plate margin		Within plate	
Tectonic setting	Convergent (destructive)	Divergent (constructive)	Intra-oceanic	Intra-continental
volcanic feature	island arcs, active continental margins	mid-oceanic ridges back-arc spreading centres	oceanic islands	continental rift zones continental flood-basalt provinces
characteristic magma series	tholeiitic calc-alkaline alkaline	tholeiitic — —	tholeiitic — alkaline	tholeiitic — alkaline
SiO_2 range	basalts and differentiates	basalts	basalts and differentiates	basalts and differentiates

From: Wilson, M.: Igneous Petrogenesis, Springer.

... not really helpful ...

How else can we use geochemical data?

And how we should not?

Or why we should better not use the ‚classical‘ tectono-magmatic discrimination diagrams

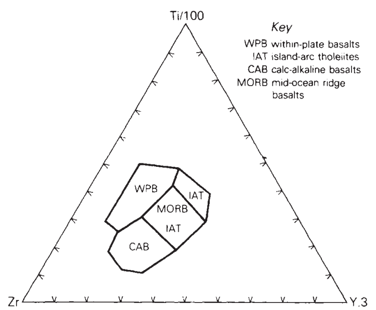

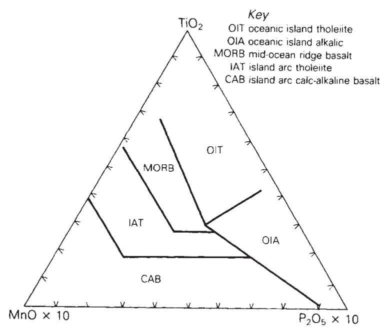

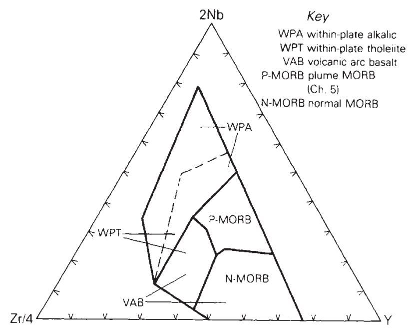

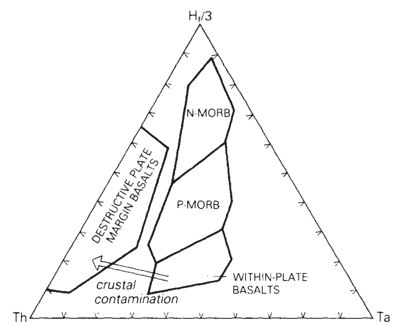

Rationale behind the ‚classical' tectonomagmatic discrimination diagrams

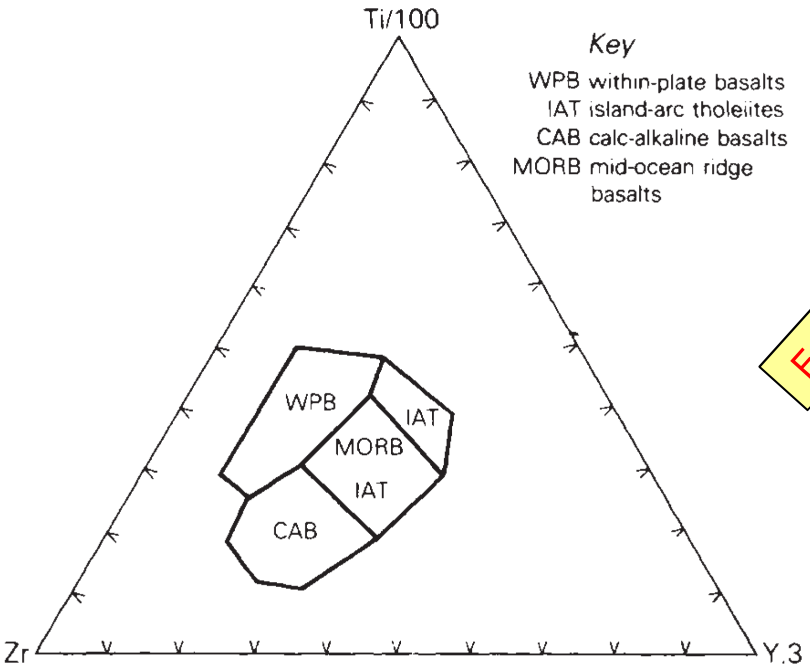

Pearce & Cann (1973)

For basalts only !!!!!!!!

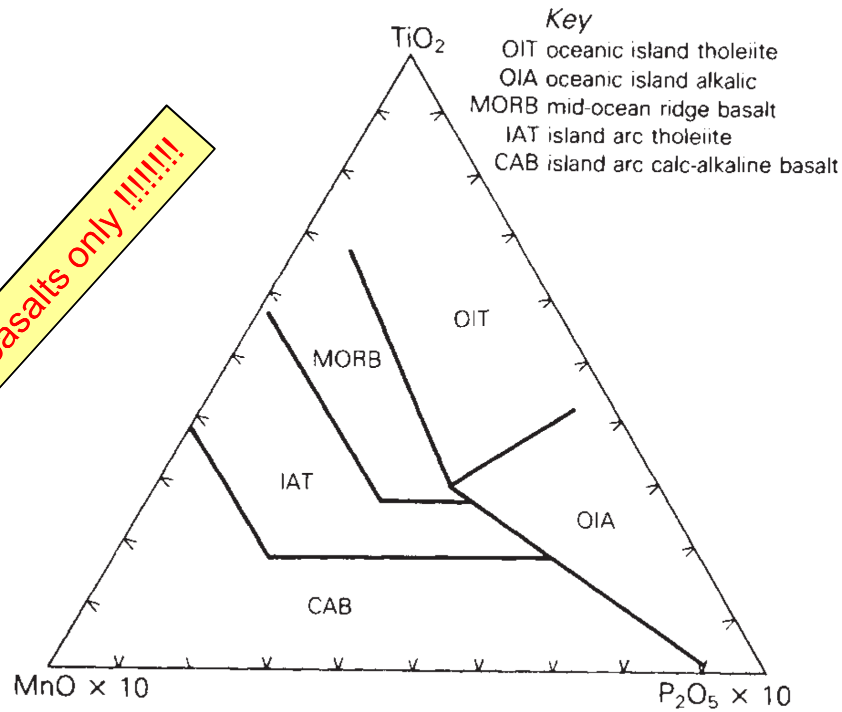

Mullen (1983)

EASY TO USE: No detailled process understanding required (simply measure, plot, read the result). All elements are easy to determine (XRF, INAA).

Rationale behind the ‚classical' tectonomagmatic discrimination diagrams

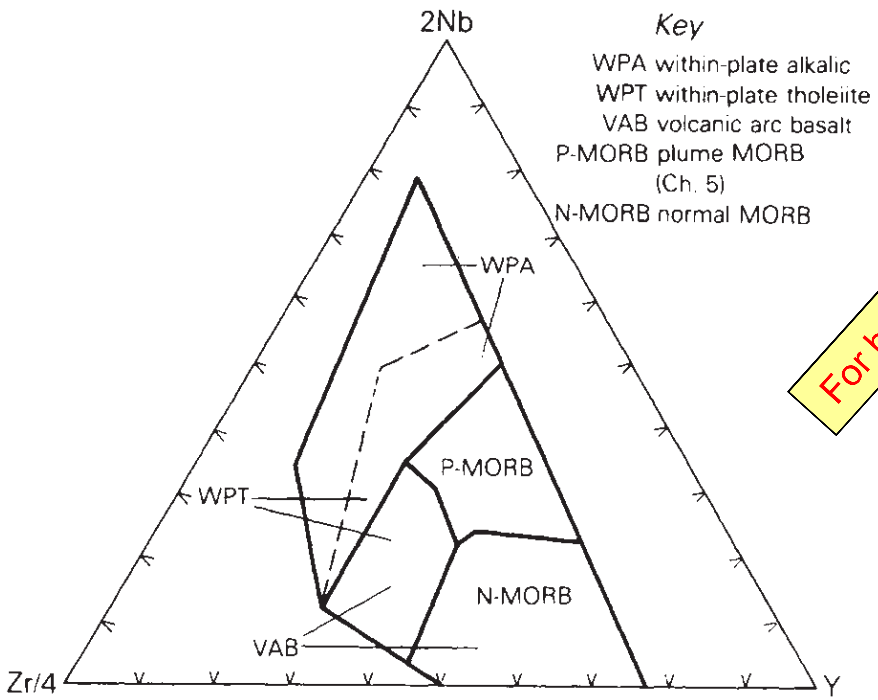

Meschede (1986)

For basalts only !!!!!!!!

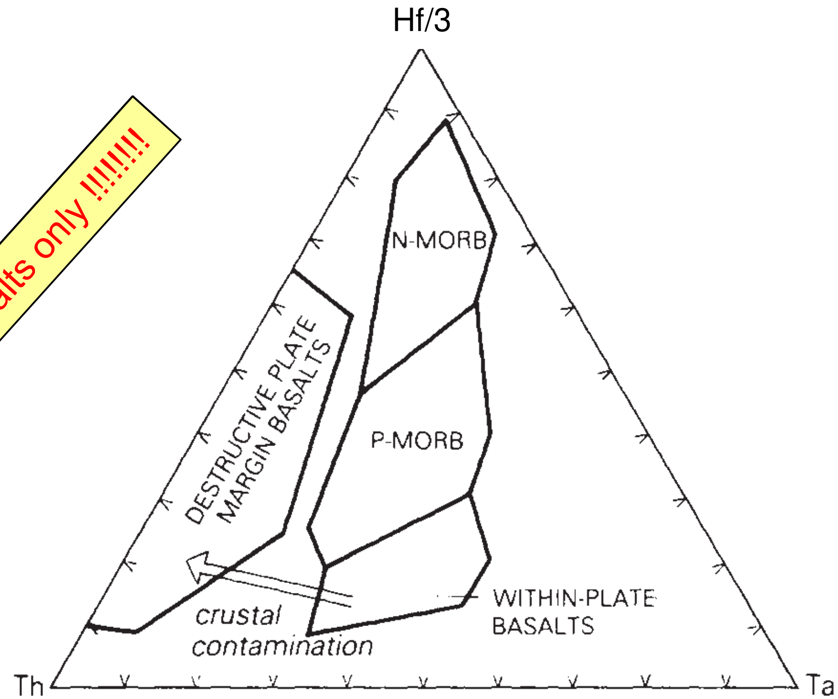

Wood et al. (1979)

EASY TO USE, no detailled process understanding required (simply measure, plot, read the result). All elements are easy to determine (XRF, INAA).

Use and abuse of geochemical data – tectonic indiscrimination

Lithos 232 (2015) 76–83

Contents lists available at ScienceDirect

Lithos

journal homepage: www.elsevier.com/locate/lithos

Trace element indiscrimination diagrams

Chusi Li [a,b,*], Nicholas T. Arndt [c], Qingyan Tang [d], Edward M. Ripley [b]

[a] State Key Laboratory of Geological Processes and Mineral Resources, China University of Geosciences, Beijing 100083, China
[b] Department of Geological Sciences, Indiana University, Bloomington, IN 47405, USA
[c] ISTerre, Université Joseph Fourier, 38400 St Martin d'Hères, France
[d] School of Earth Sciences and Key Laboratory of Mineral Resources in Western China Guansu Province, Lanzhou University, Lanzhou 730000, China

ARTICLE INFO

Article history:
Received 12 February 2015
Accepted 29 June 2015
Available online 3 July 2015

Keywords:
Basalts
Trace elements
Tectonic discrimination
Petrological database utilization

ABSTRACT

We tested the accuracy of trace element discrimination diagrams for basalts using new datasets from two petrological databases, PetDB and GEOROC. Both binary and ternary diagrams using Zr, Ti, V, Y, Th, Hf, Nb, Ta, Sm, and Sc do a poor job of discriminating between basalts generated in various tectonic environments (continental flood basalt, mid-ocean ridge basalt, ocean island basalt, oceanic plateau basalt, back-arc basin basalt, and various types of arc basalt). The overlaps between the different types of basalt are too large for the confident application of such diagrams when used in the absence of geological and petrological constraints. None of the diagrams we tested can clearly discriminate between back-arc basin basalt and mid-ocean ridge basalt, between continental flood basalt and oceanic plateau basalt, and between different types of arc basalt (intra-oceanic, island and continental arcs). Only ocean island basalt and some mid-ocean ridge basalt are generally distinguishable in the diagrams, and even in this case, mantle-normalized trace element patterns offer a better solution for discriminating between the two types of basalt.

Tectonic indiscrimination...

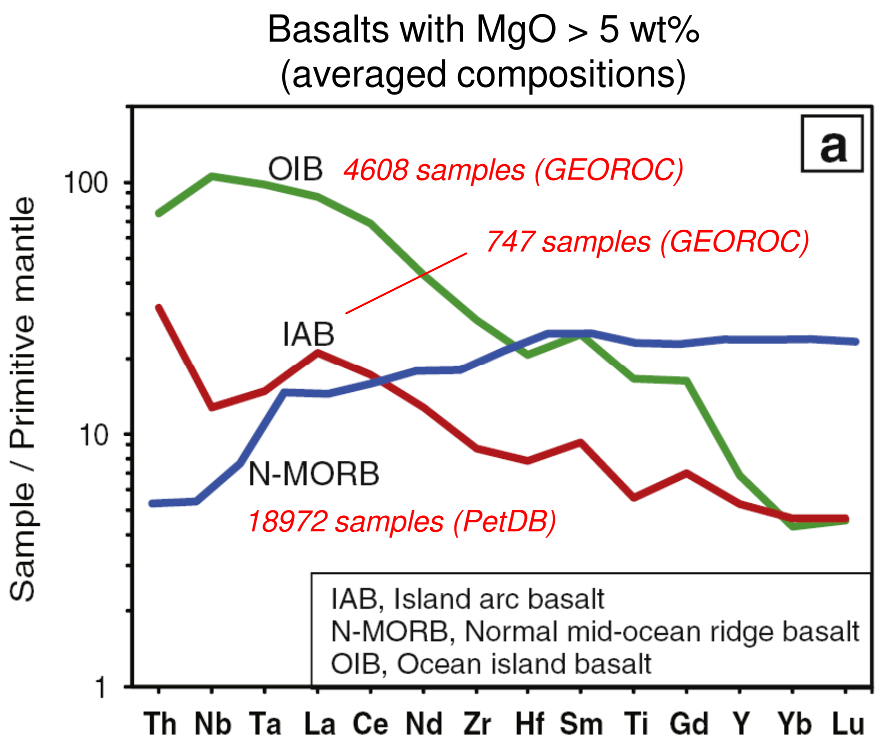

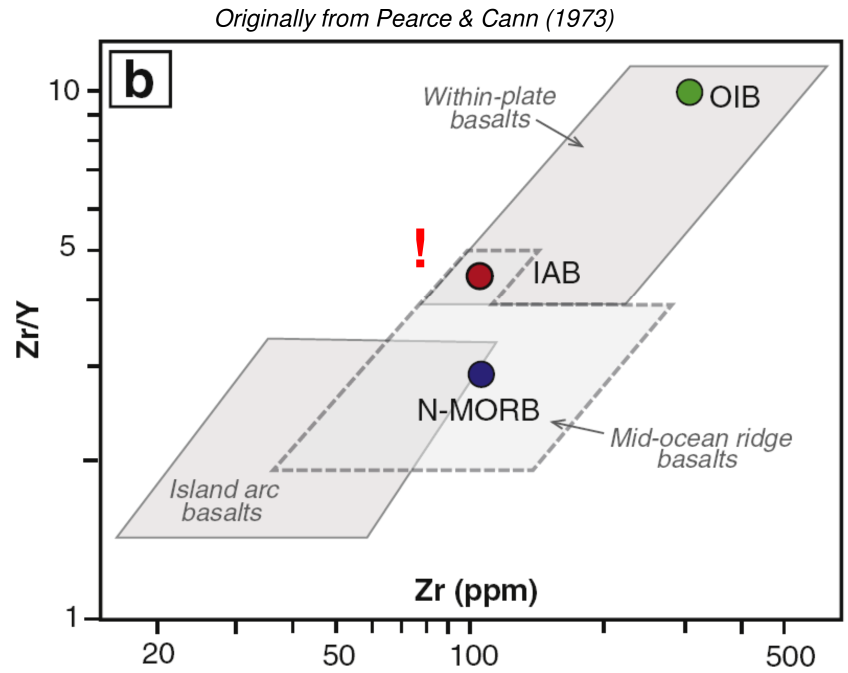

Li et al. (2015)

The **averaged** compositions of **OIB** and **MORB** fit relatively well into the fields proposed by Pearce & Cann (1973), but the **IAB** composition is completely off.

Tectonic indiscrimination...

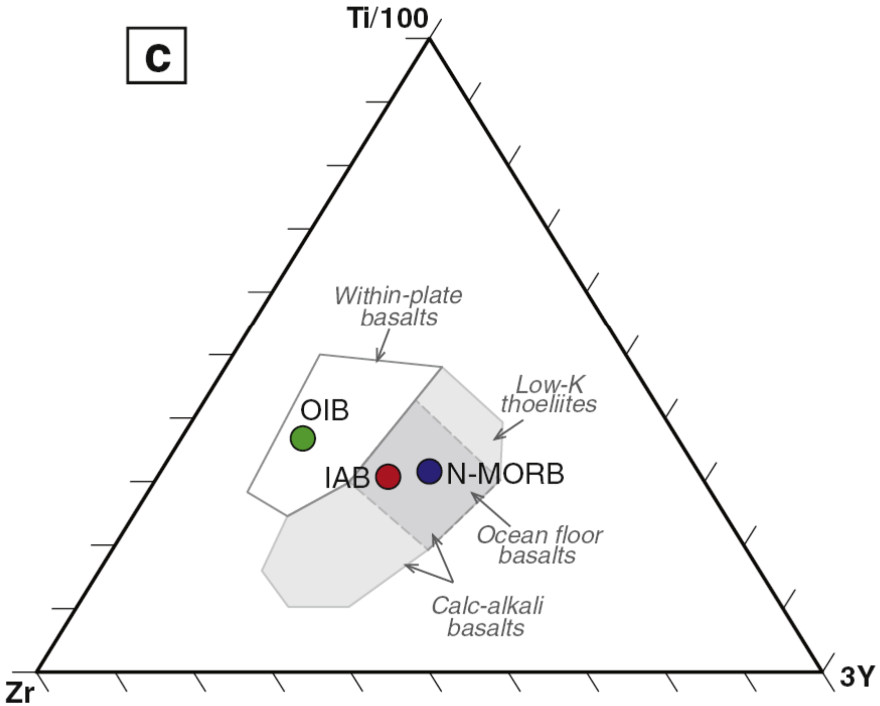

Originally from Pearce & Norry (1979)

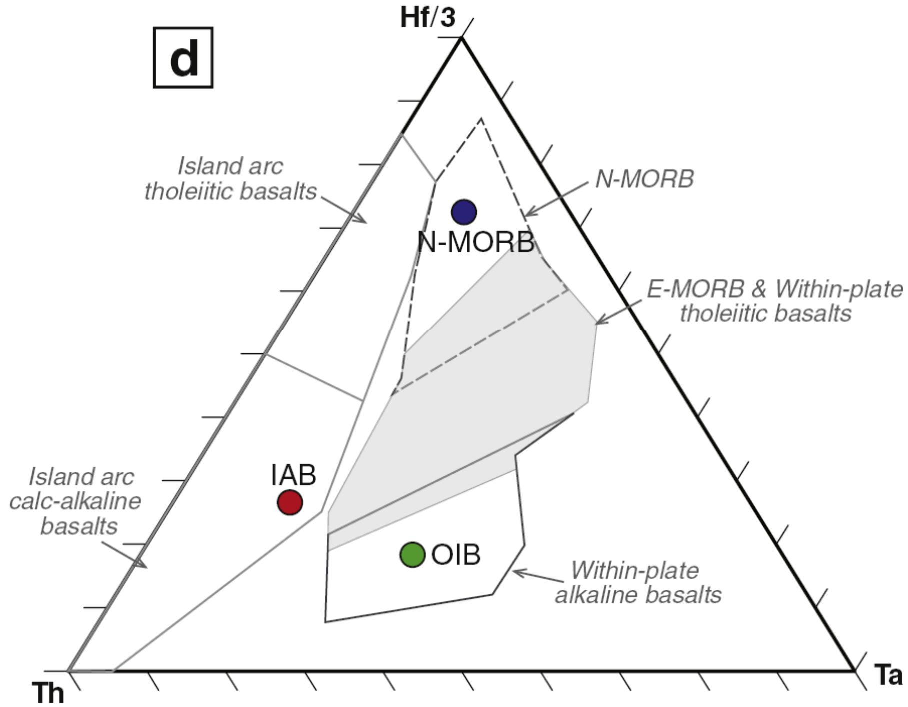

Originally from Wood (1980)

The **averaged** compositions of **OIB**, **IAB** and **MORB** fit into the fields proposed by Pearce & Norry (1979), but are very close to each other. By contrast, the settings are well discriminated by the fields defined by Wood (1980)

Tectonic indiscrimination... a closer look

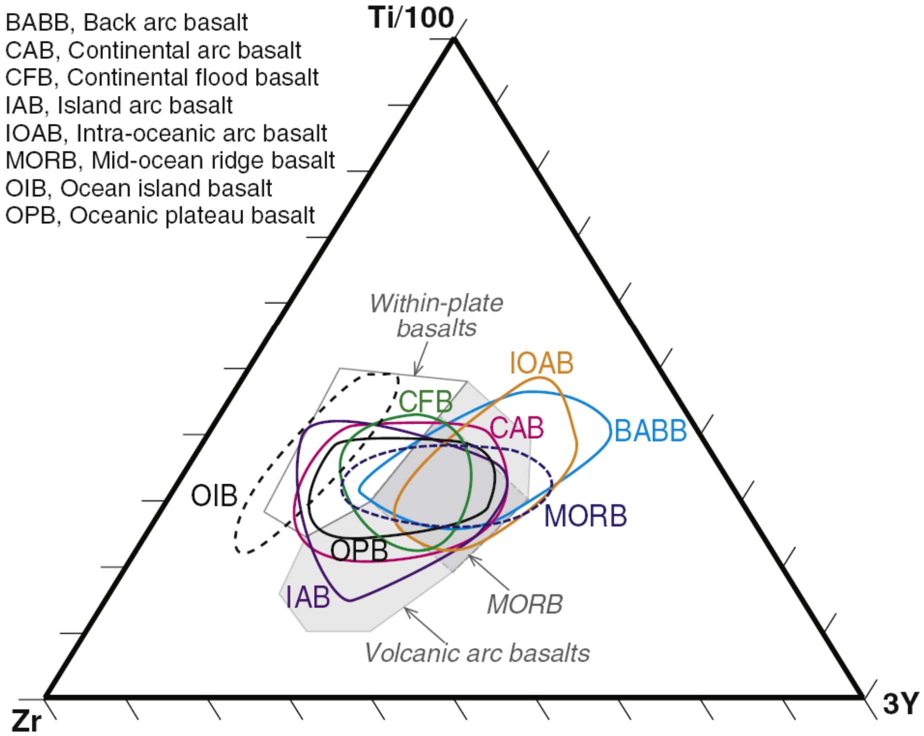

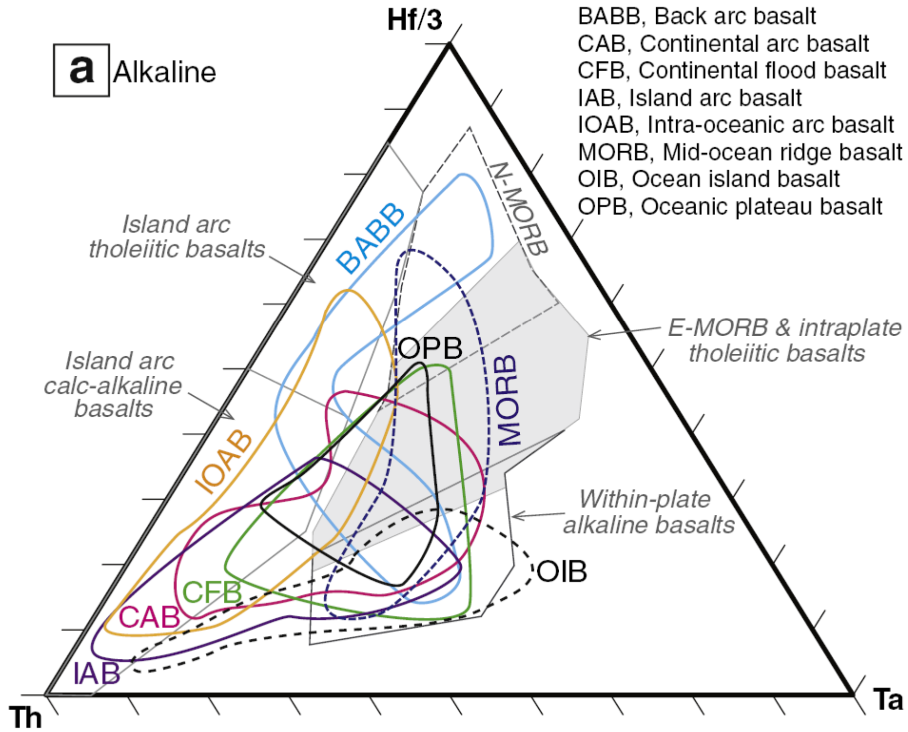

Using a very **large dataset**, the classical discrimination diagrams fail to discriminate different types of basalt from different tectonic settings (MORB, BABB, IOAB, IAB, CAB, OPB, CFB), only **OIBs** are slightly offset!

Tectonic indiscrimination... a closer look

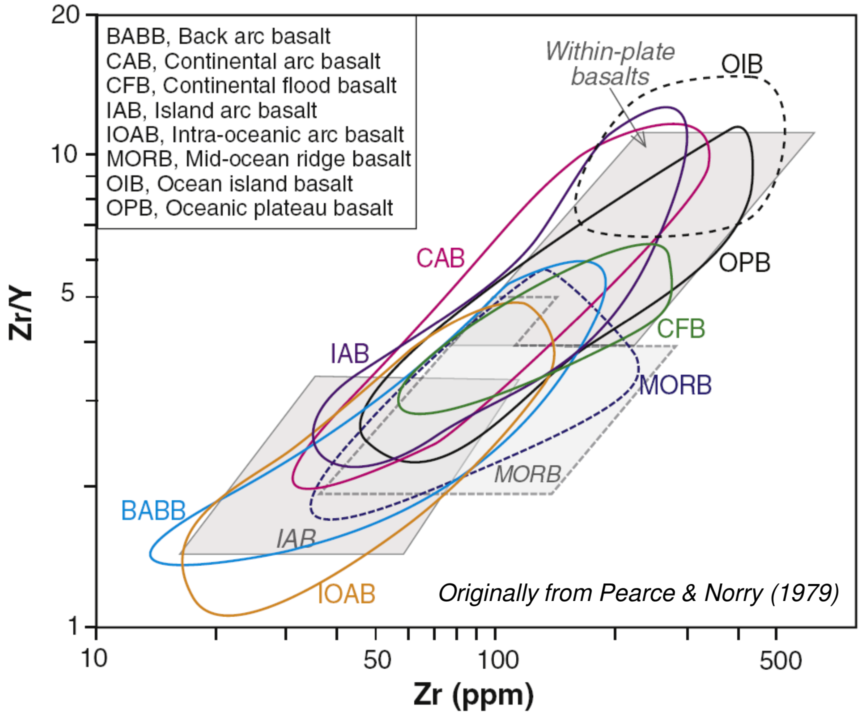

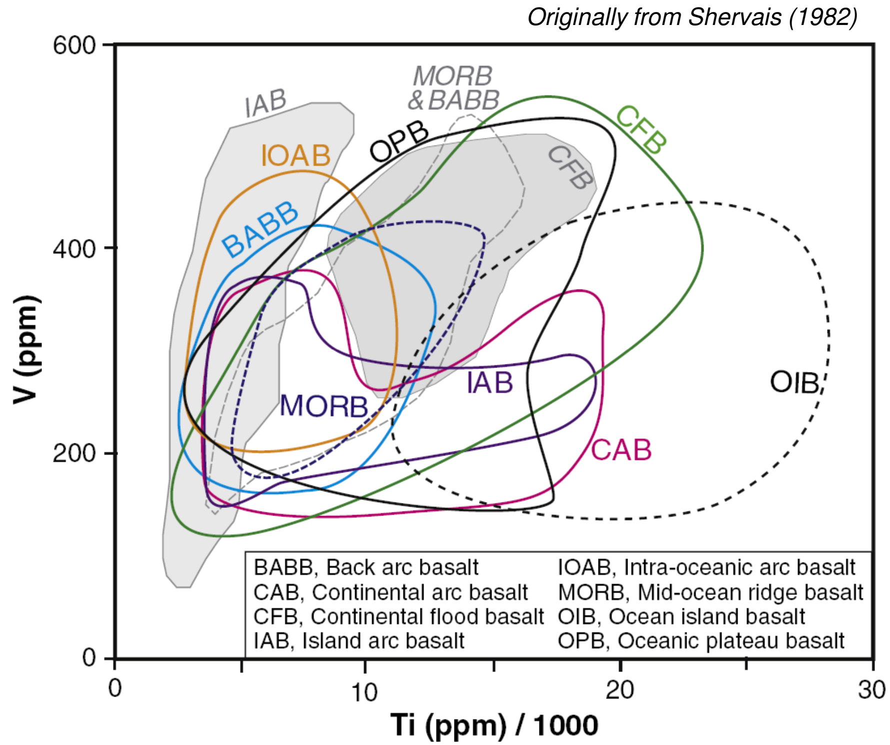

This valids for any other of the classical discrimination diagrams, without any exception! Therefore... more sophisticated appoaches are recommended!

Tectonic indiscrimination... what to do?

Multi-element concentration diagrams (normalized to the „primitive mantle“ composition) do a better job

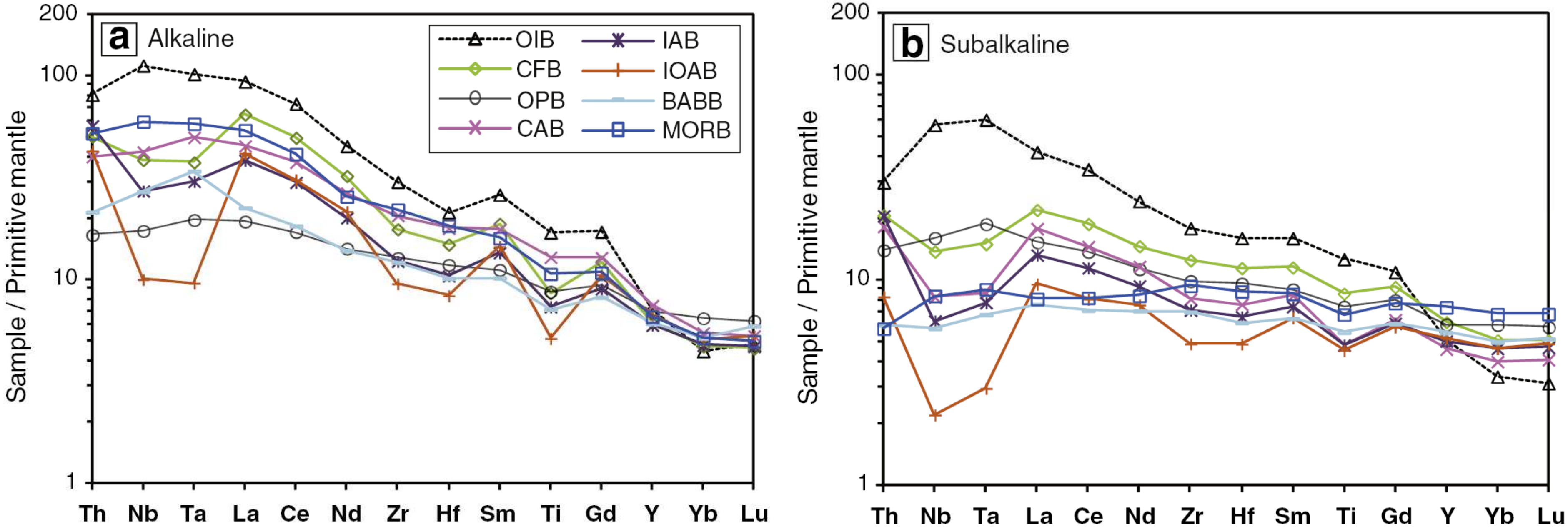

Including more elements improves the **resolution**! Alkaline and subalkaline series have **similar patterns**, but distinctly **different concentrations**.

BUT – NEVER IGNORE THE GEOLOGICAL CONTEXT!

Chapter 2

Mid ocean ridges

What is the composition of primary basalts generated at mid-ocean ridges?

What are the degrees of melting?

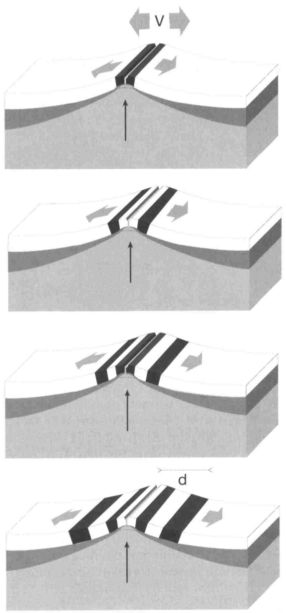

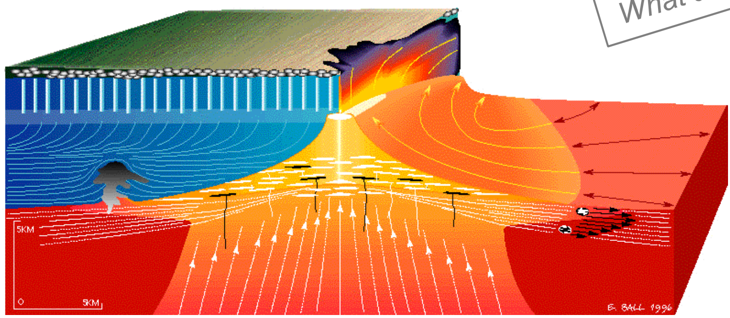

Melting at a mid-ocean ridge (from A. Nicolas)

What is the composition of the asthenospheric mantle source?

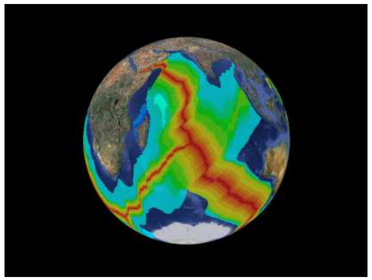

What is the thermal state of the oceanic mantle?

What are the spreading rates, do they correlate to melt production rates and ridge topography??

Very Simple profile through the oceanic lithosphere

Temperature, water depth and lithosphere thickness as a function of lithosphere age (simplified estimate!)

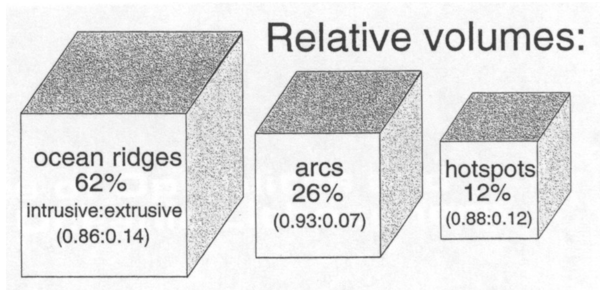

Mapfre Team at the Volvo Ocean Race in the South Pacific ;)

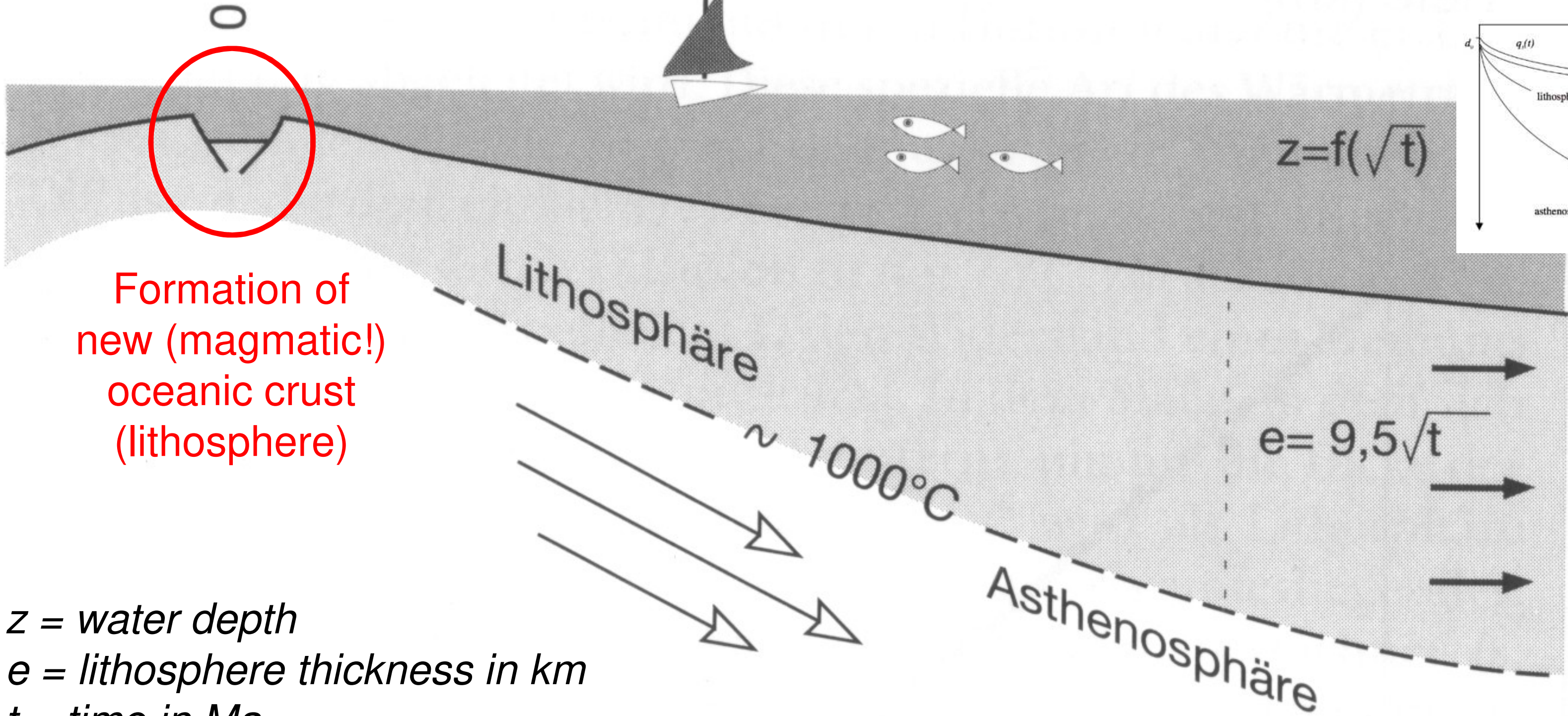

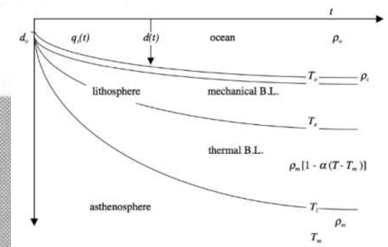

1 Ma ~9.5 km

10 Ma ~30 km

100 Ma ~95 km

crust makes ~7-8 km of each

z = water depth
e = lithosphere thickness in km
t = time in Ma

Schematic profile across an ocean ridge...

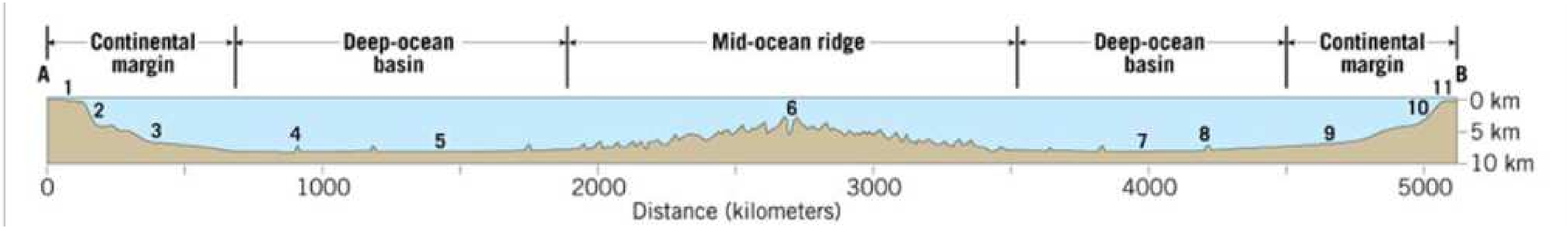

...and simplified age distribution of the ocean floor

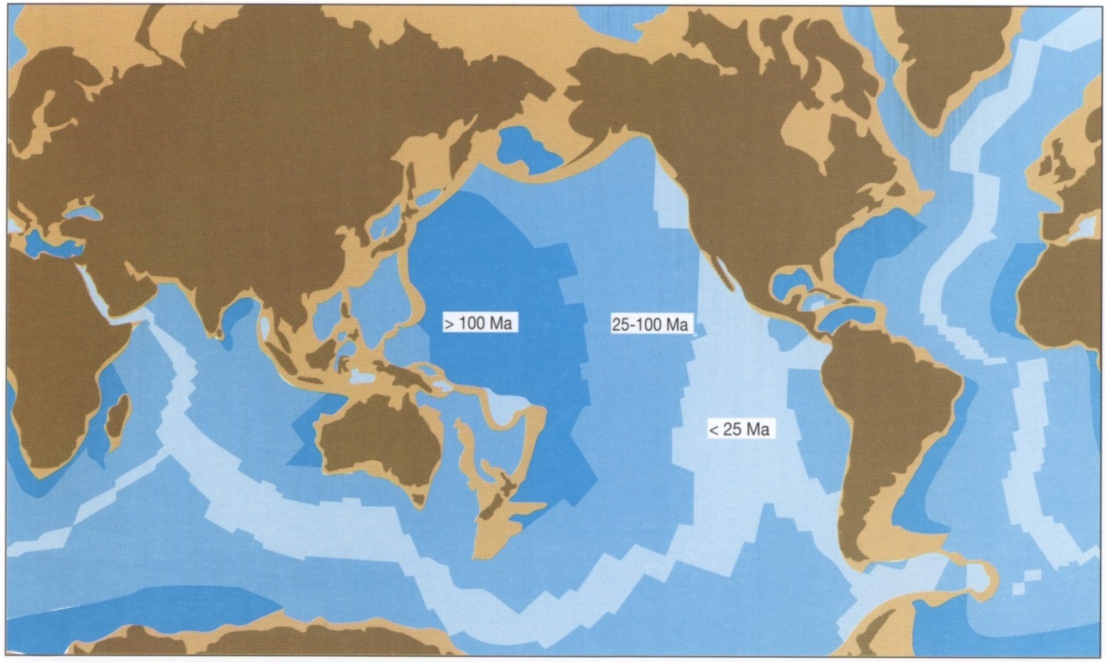

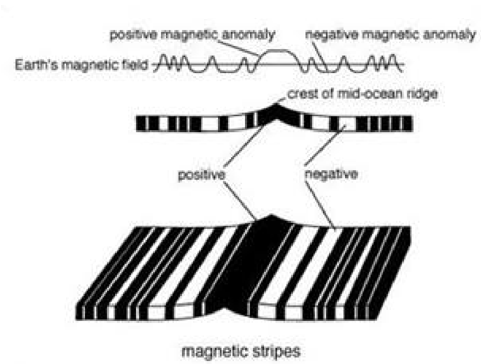

Magnetic structure of the basaltic ocean floor preserves the **magnetic field reversals**

This is due to the **remanent magnetisation** of Fe-bearing phases (Ti-magnetite, etc.) upon cooling

Lithology of the oceanic lithosphere as deduced from ophiolites

Ophiolite example: OMAN

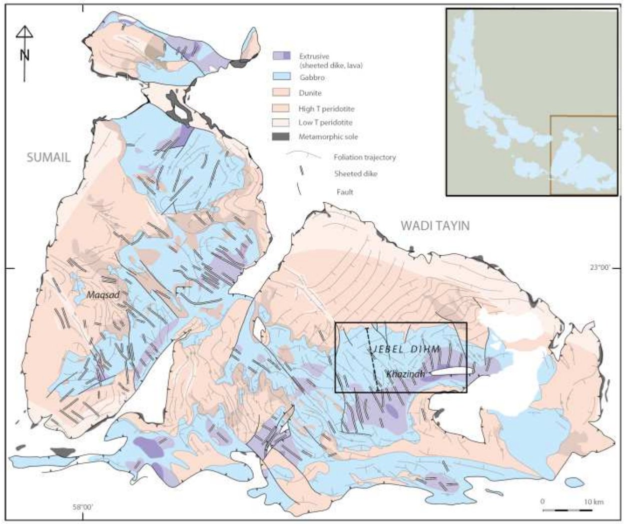

Nicolas & Boudier, 2015

OMAN

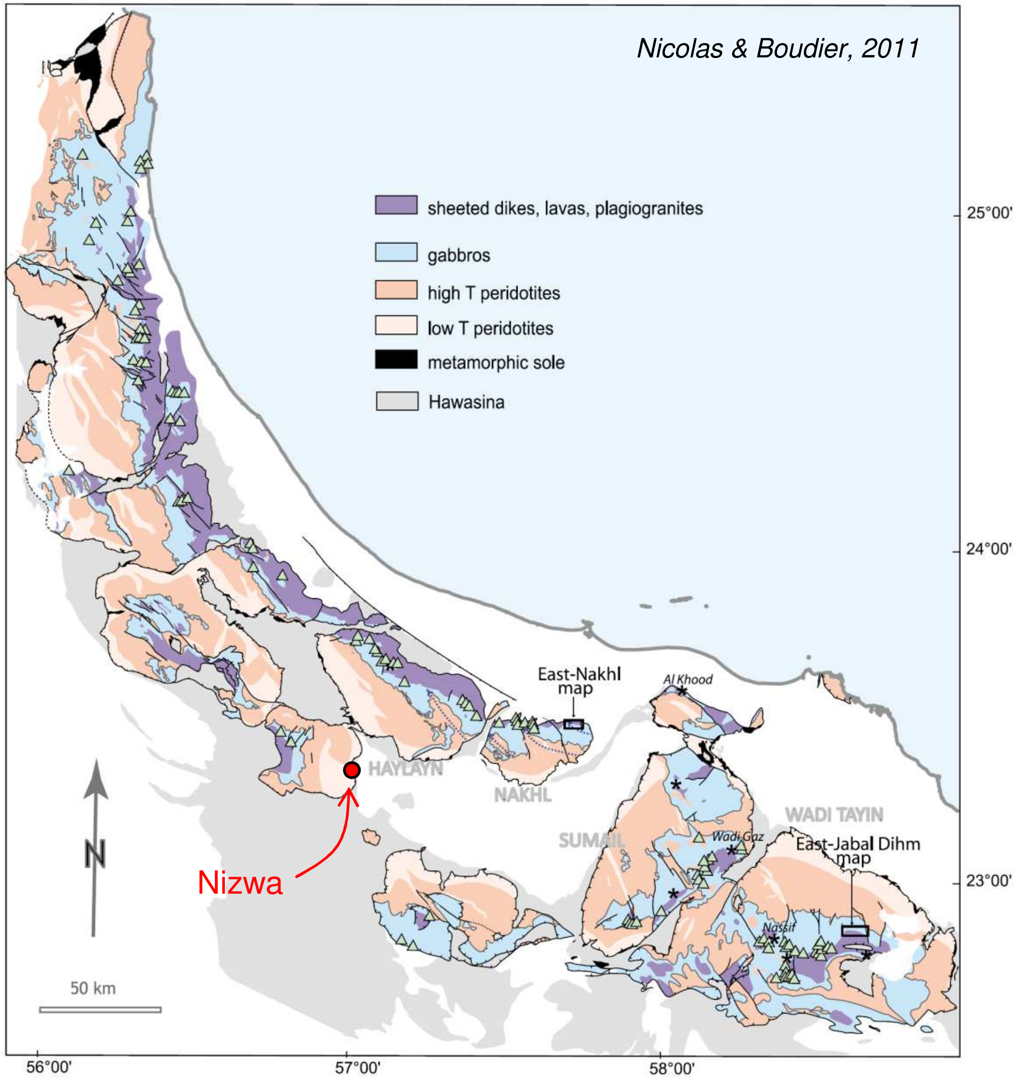

Nicolas & Boudier, 2011

Lithology of the oceanic lithosphere as deduced from ophiolites (here: Oman)

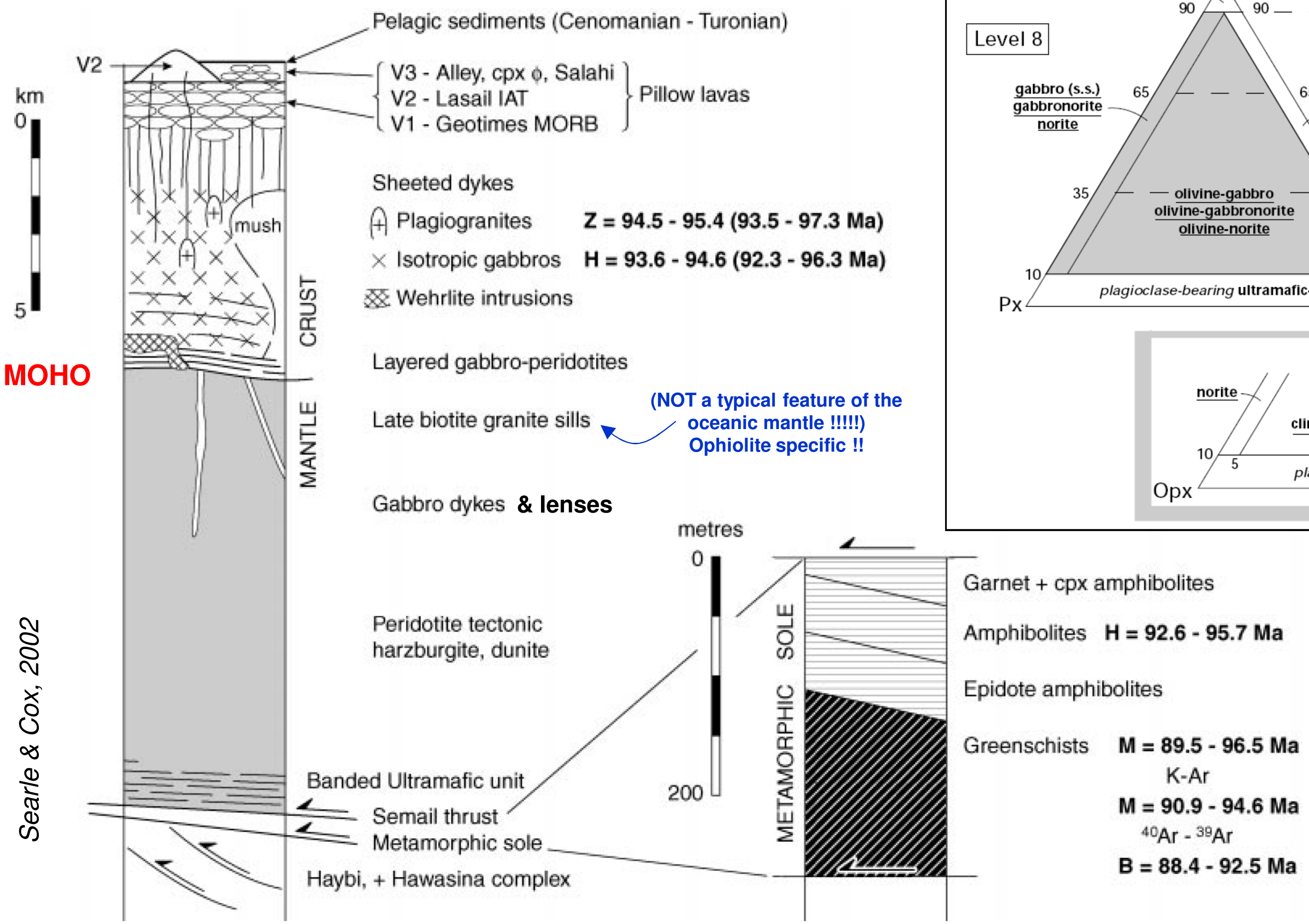

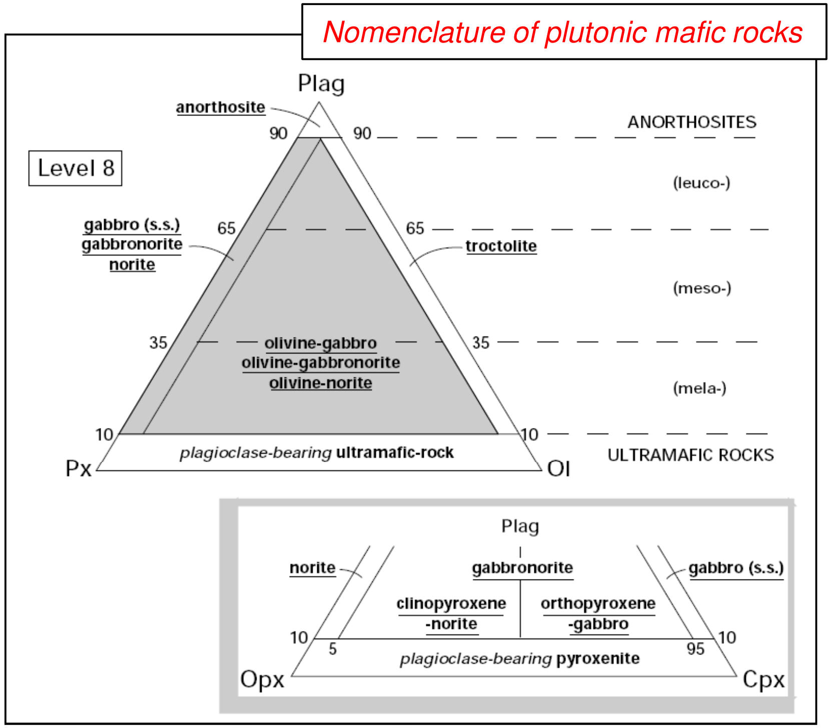

Seismic structure of the oceanic crust...

... and its lithological interpretation

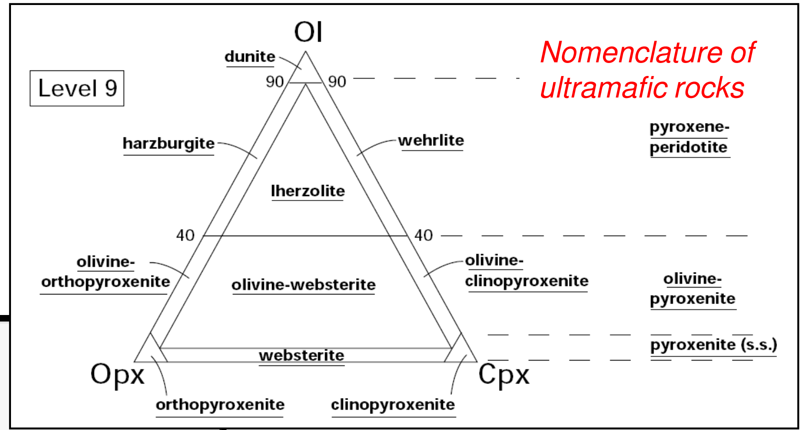

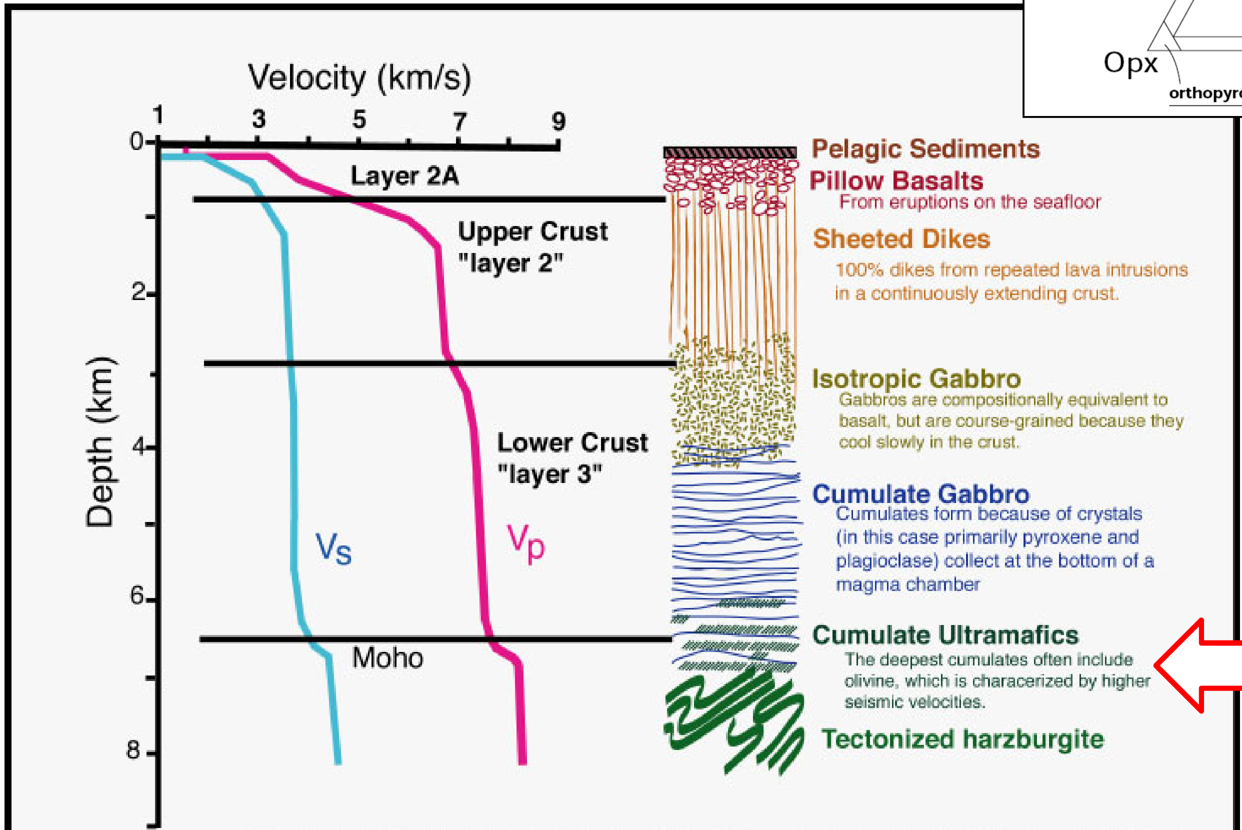

The ocean crust, combining the seismic structure (from seismic experiments) with the lithology of ophiolites. Modfied from McClain (2002).

„off axis profile“

(no melt lens/magma chamber!)

These ‚ultramafic cumulates‘ are sometimes **wehrlites**, but mostly **residual** dunites.

But note, that these ‚ultramafic cumulates‘ are often NO cumulates but **residual rocks** or **olivine mush** dragged by basaltic melt!

2D seismic profile across the Eeast Pacific Rise (EPR)

Velocitiy contours perpendicular to the ridge axis

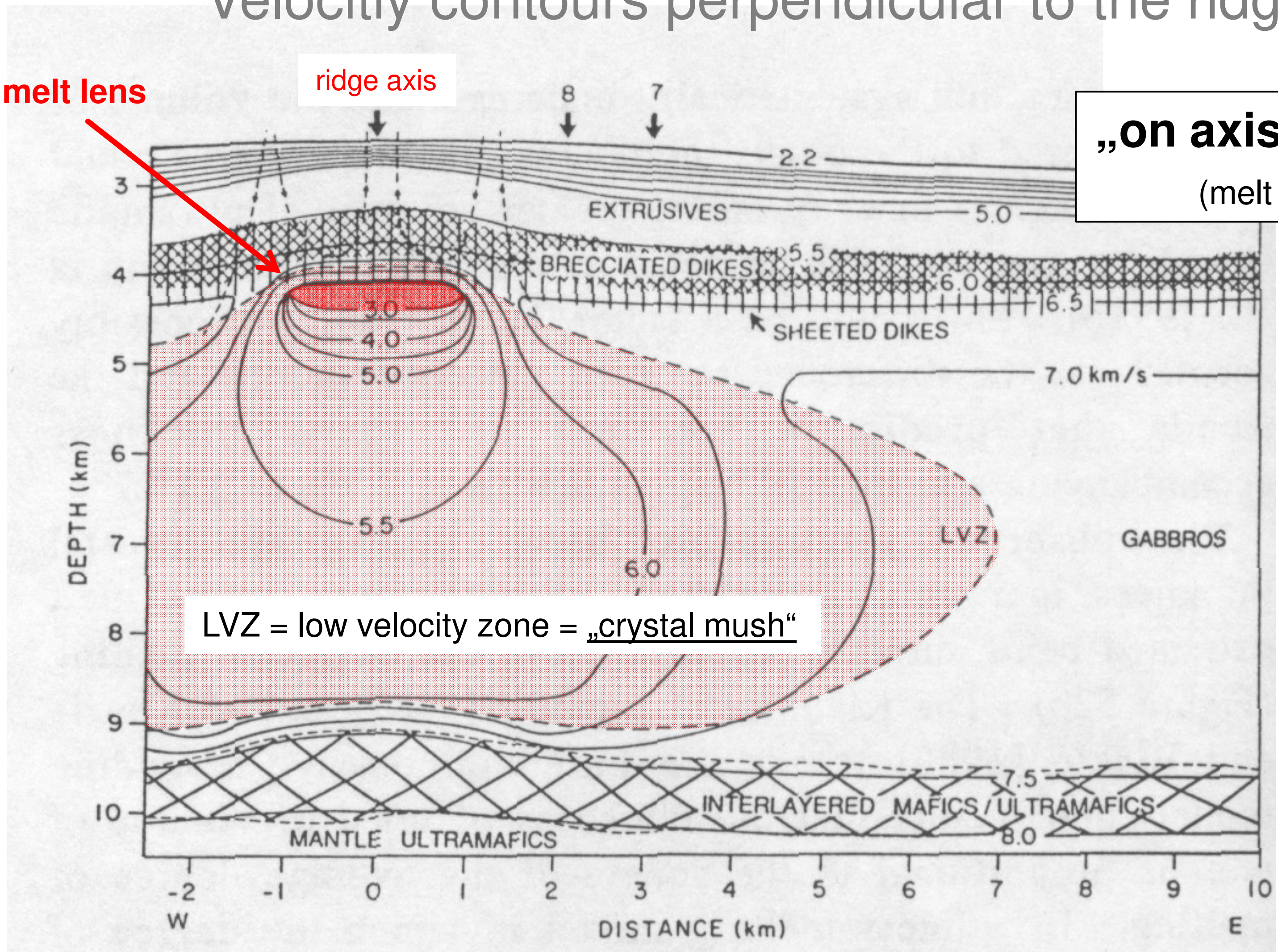

„on axis profile"

(melt lens!)

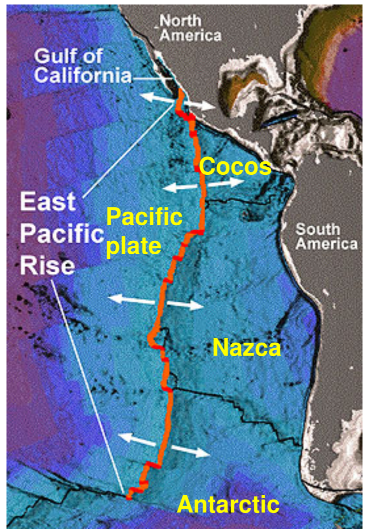

EPR is a fast spreading ridge

Temperature within the Earth‘ mantle ...

There is magma production in the interior of our planet:

1) What is the temperature distribution in the Earth‘s mantle?
2) What are the conditions that cause partial melting there?

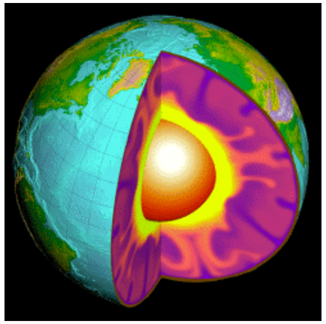

Mantle convection model

The ‚potential temperature‘ T_p ...

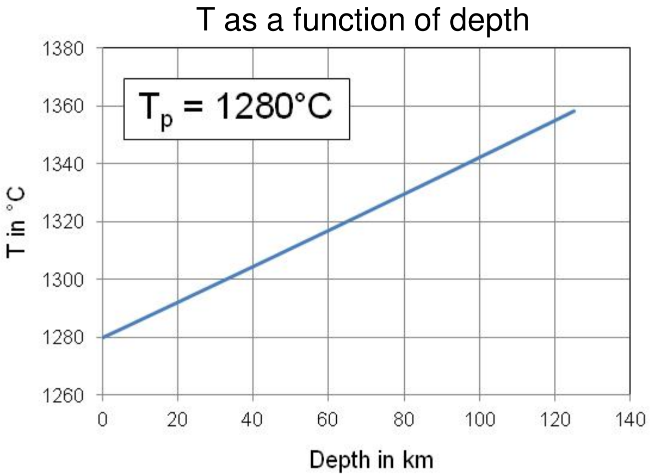

$$T_P = T \exp\left(-\frac{g\alpha z}{C_P}\right)$$

$$\left(\frac{\partial T}{\partial z}\right)_S = \frac{g\alpha_f T}{C_P}$$

adiabatic temperature gradient due to the work of volume

$$\left(\frac{\partial T}{\partial z}\right)_S \simeq 1\,°\mathrm{C\,km^{-1}}$$

For a basaltic melt!

... is the temperature within the Earth corrected for the **work of volume**. T_p therefore does not change during **adiabatic decompression**.

But clearly there are (strong) temperature variations within the mantle!!!

g = acceleration due to gravity
α = thermal expansion coefficient
z = depth
C_p = specific heat,
T = absolute temperature
T_p = potential temperature

Thermal state of the (oceanic) lithosphere and underlying asthenosphere

„plumes“

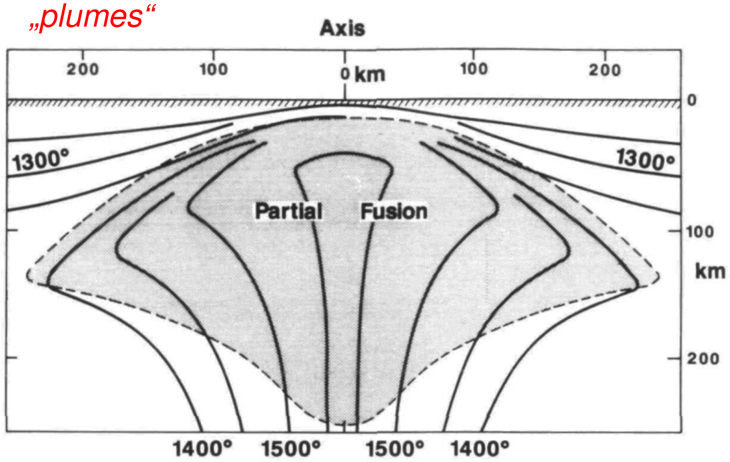

„ridges“

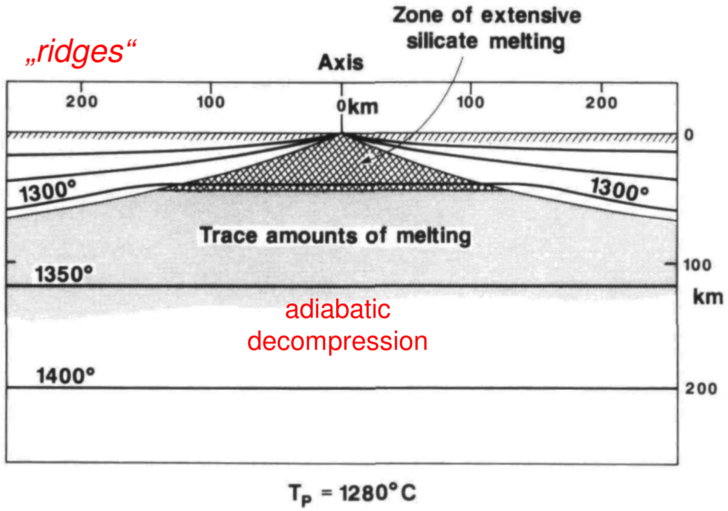

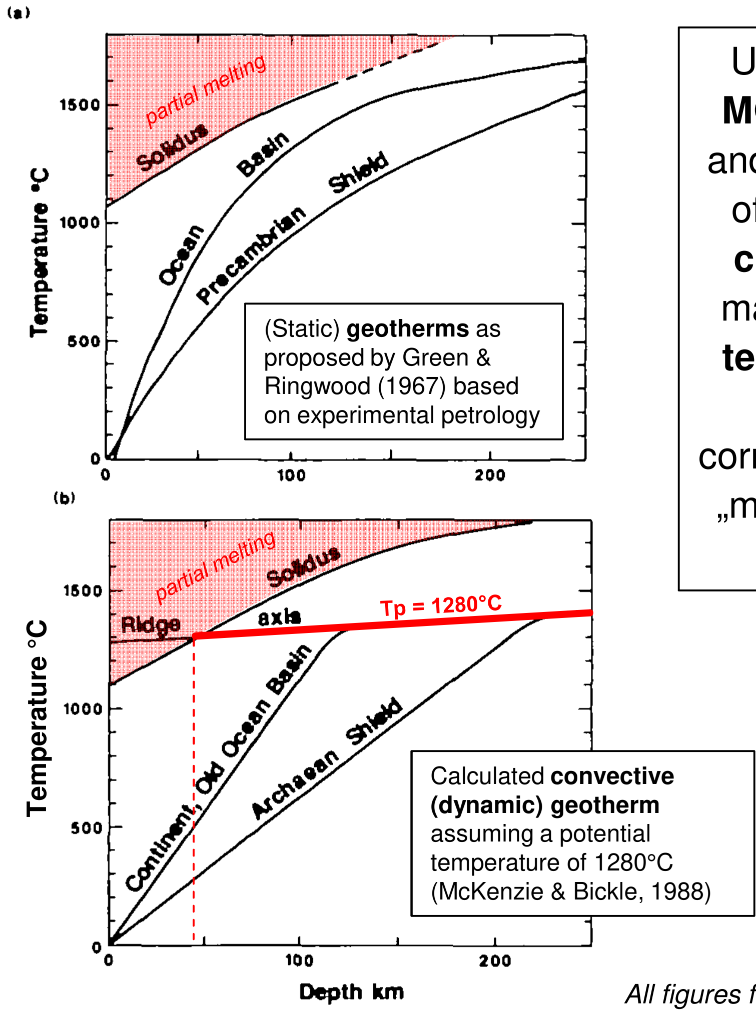

Using primitive **MORB glasses** and the thickness of the **oceanic crust**, yields a mantle potential **temperature of ~1280°C**, corresponding to a „melt thickness“ of **7 km**

All figures from: McKenzie & Bickle, 1988. J. Petrol., 29, 625-679

Thermal state of the (oceanic) lithosphere and underlying asthenosphere

TBL: isotopic **homogeneous** (i.e. convecting)

MBL: isotopic **heterogeneous** (i.e. non-convecting)

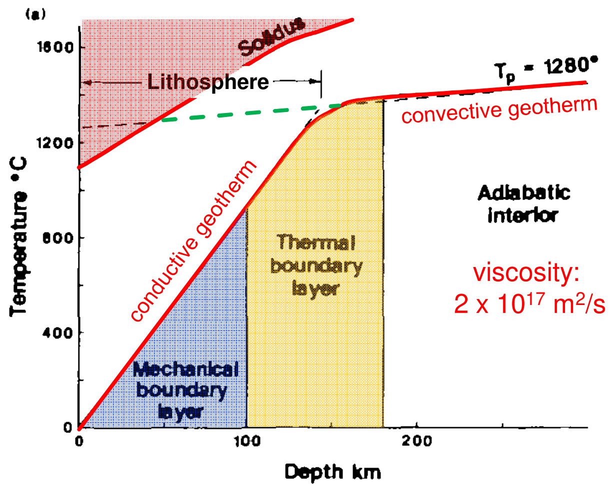

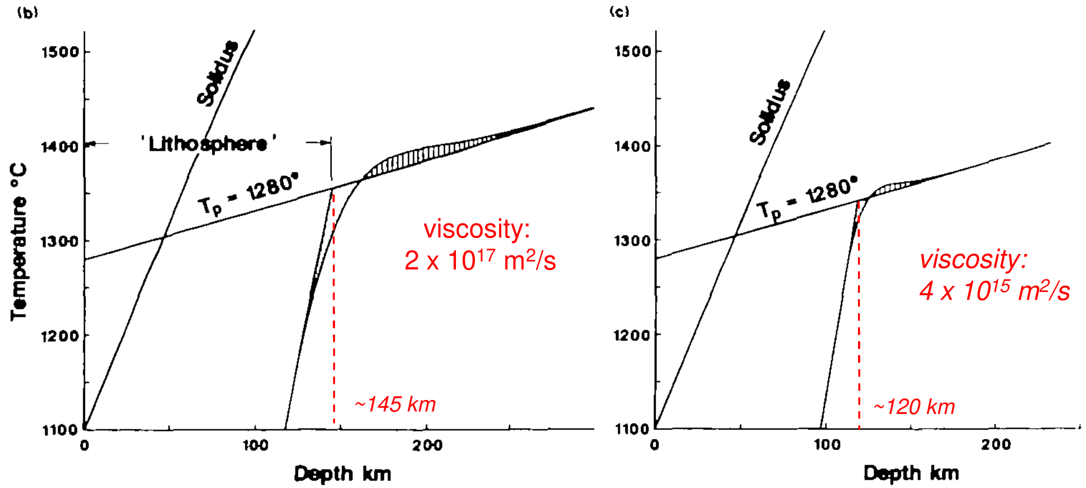

From: McKenzie & Bickle, 1988. J. Petrol., 29, 625-679

Melting the mantle?
Temperature is, what matters!

But if the solidus is located **within** the non-convecting lithospheric mantle (within the MBL, think about thick cratonic lithosphere!), then **no partial melting** will occur!

Therefore, (1) the potential temperature and (2) the thickness of the lithosphere will control the **volume of magma** that is produced!

In other words, T_p will control the depth where **melting starts**, and the thickness of the lithosphere will control the depth where **melting ends** > *see next overhead!*

Adiabatic decompression melting and melt volume as a function of T_p

T as a function of depth

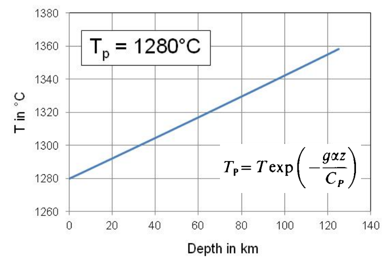

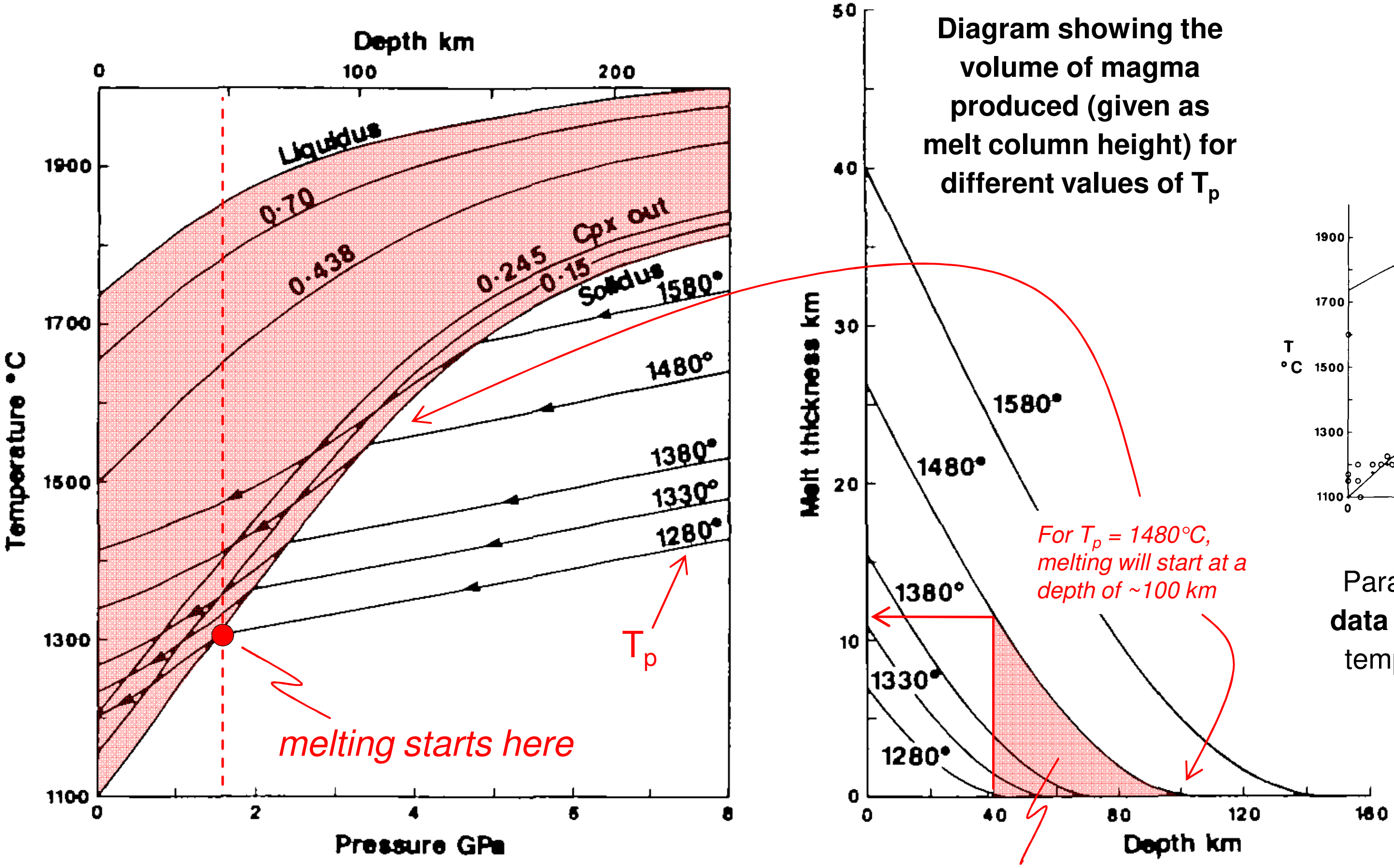

Diagram showing the volume of magma produced (given as melt column height) for different values of T_p

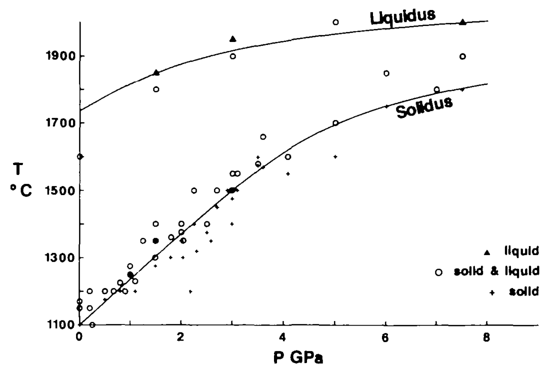

Parameterization of **experimental data** to obtain **solidus** and **liquidus** temperatures for mantle peridotite

Example: If melting starts at ~100 km depth (this is the case for T_p = 1480°C), and ends at ~40 km depth, this produces a melt column of about 12 km thickness

From: McKenzie & Bickle, 1988. J. Petrol., 29, 625-679

Oceanic asthenosphere: Melting in „diapirs“

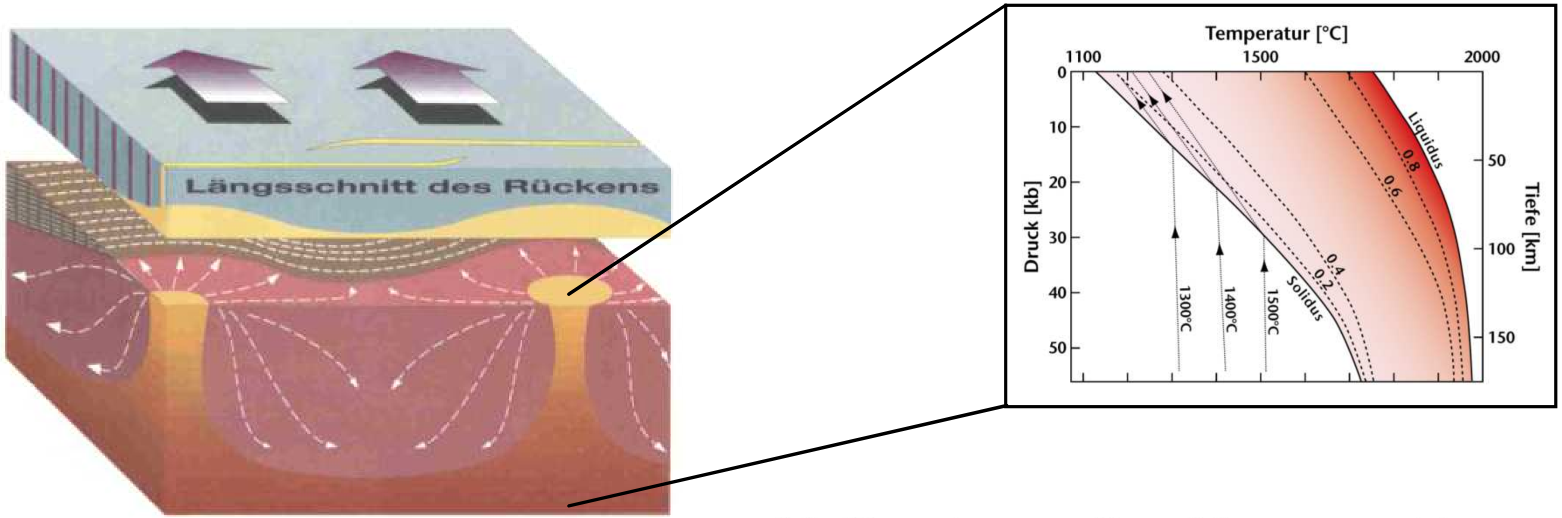

Melting beneath mid-ocean ridges

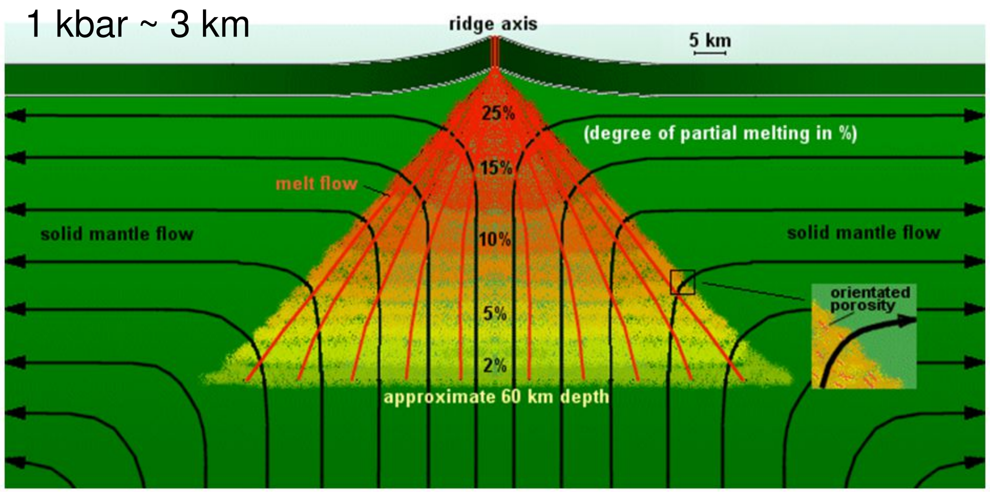

Upwelling and **decompression melting** likely does occur in **„diapirs“**, not along linear structures

Melting occurs in up-welling „diapirs“

Mantle diapir and **propagating ridge segment** (structural reconstruction, Oman ophiolite)

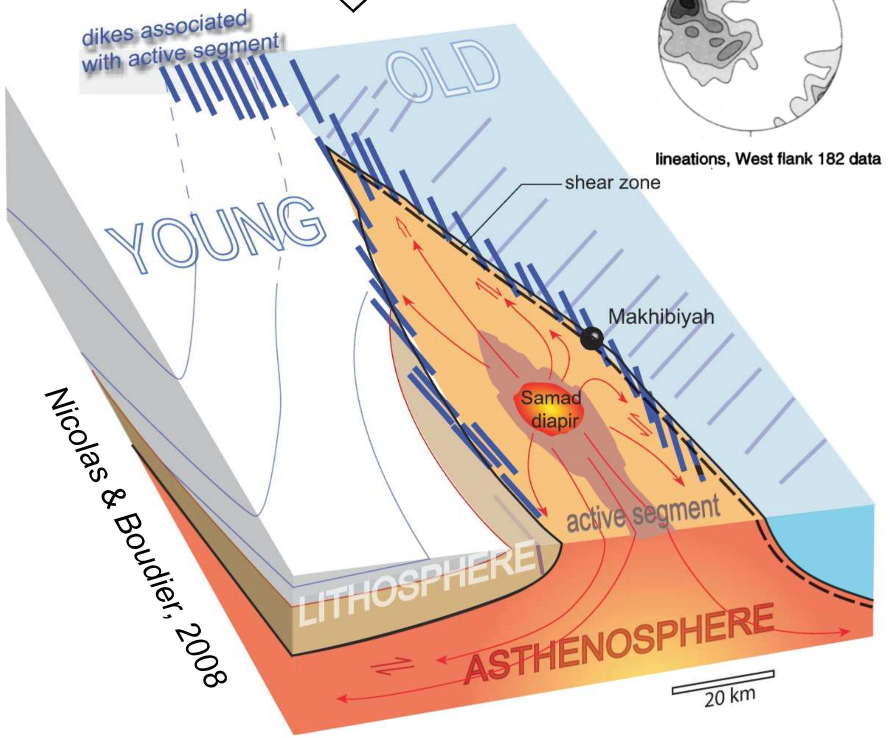

Nicolas & Boudier, 2008

Jousselin et al., 1998

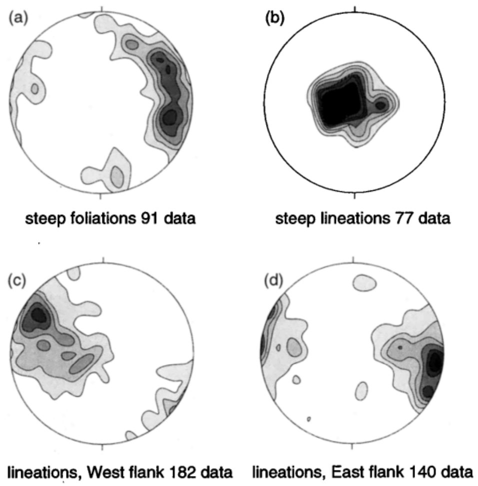

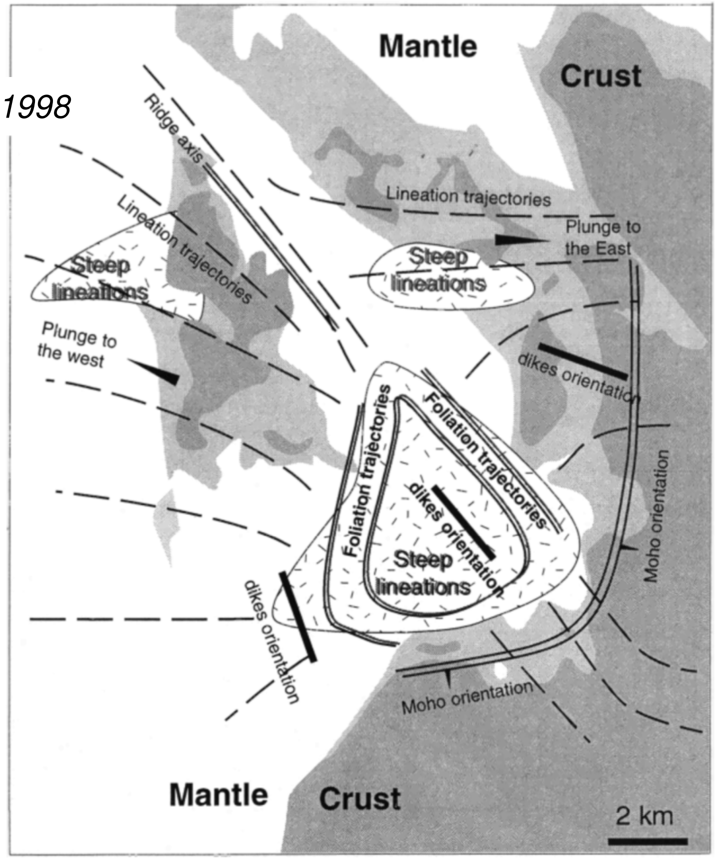

Maqusad mantle diapir and inferred **ridge axis** (Oman ophiolite) as reconstructed from **structural data** (foliation planes and lineations in **mantle peridotite** and **lower gabbros**)

How does the melt leave the source (mantle)?

Porous flow vs. hydraulic fracturing

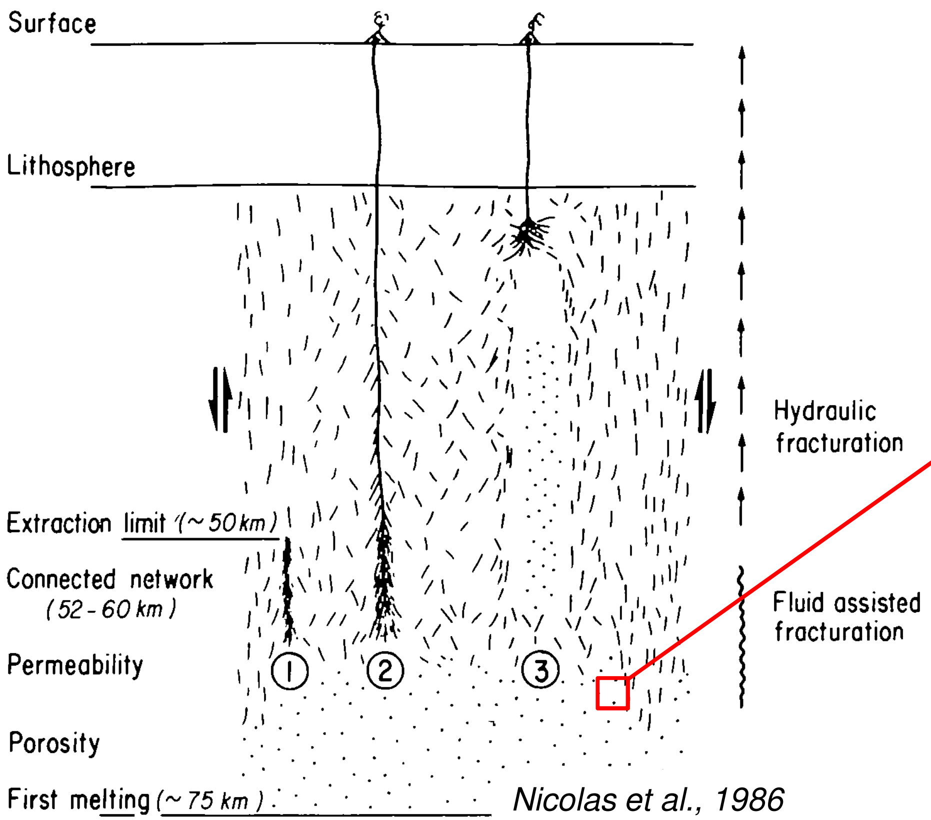

Nicolas et al., 1986

Three stages of melt extraction: 1) Formation of a connected melt network, 2) melt overpressure and hydrofracturing, 3) dying conduit

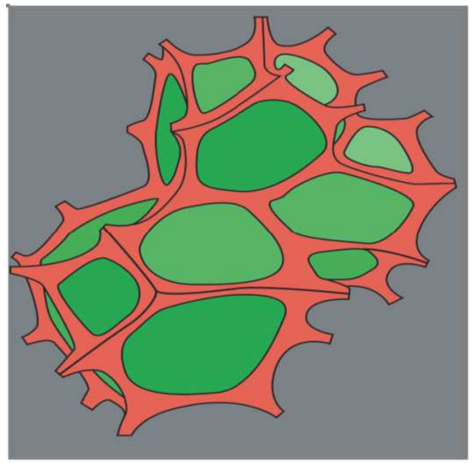

Schematic drawing of an interconnected melt-network

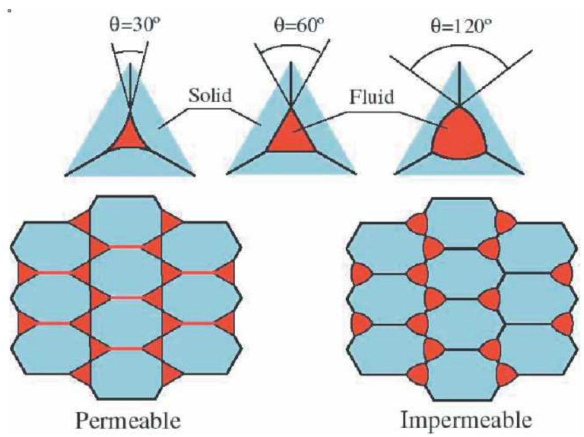

How does the melt leave the source (mantle)?

Reactive porous flow – Oman ophiolite

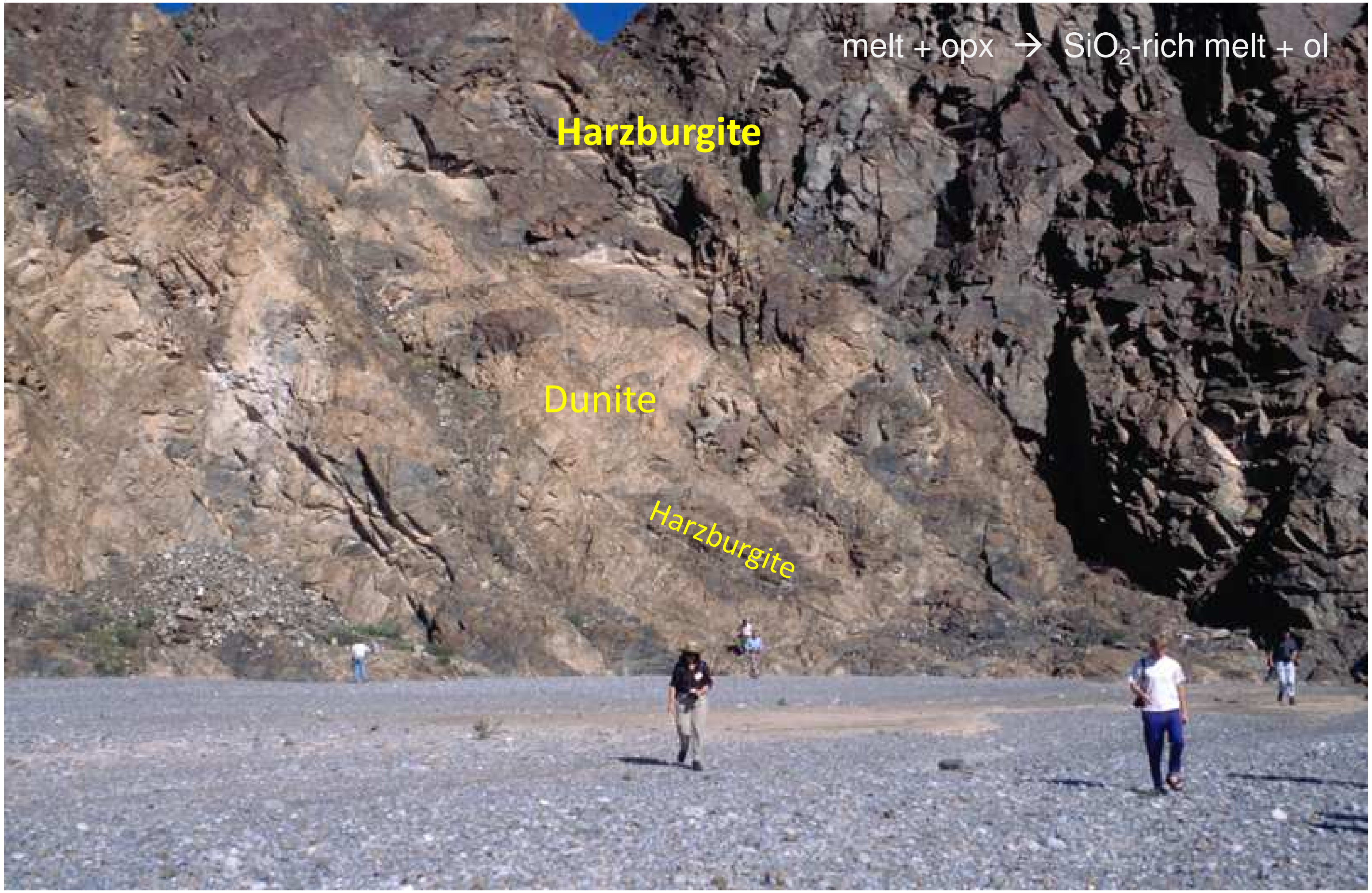

How does the melt leave the source (mantle)?

Residual dunite – Oman ophiolite

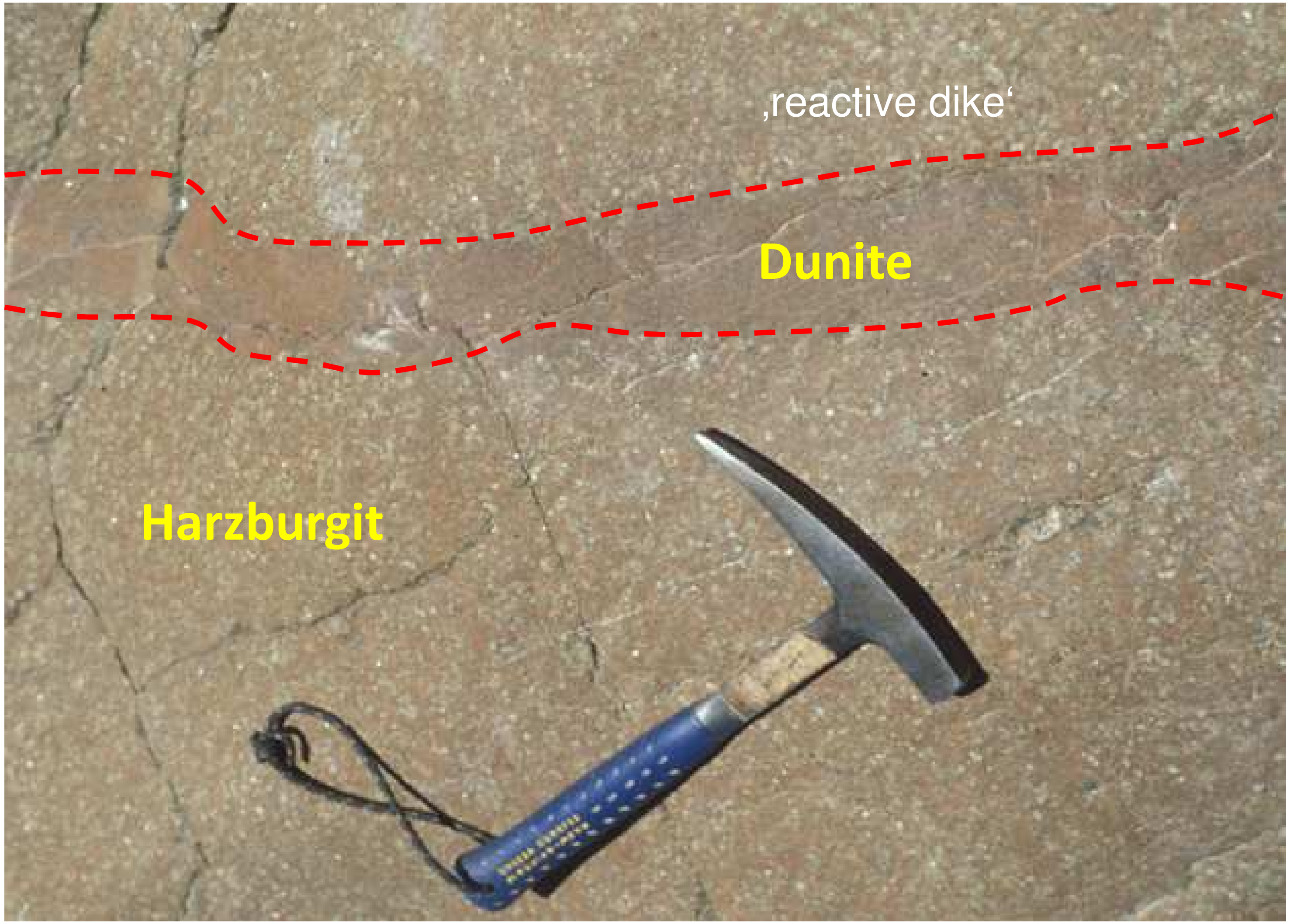

How does the melt leave the source (mantle)?

Transition to hydraulic fracturing – Oman ophiolite

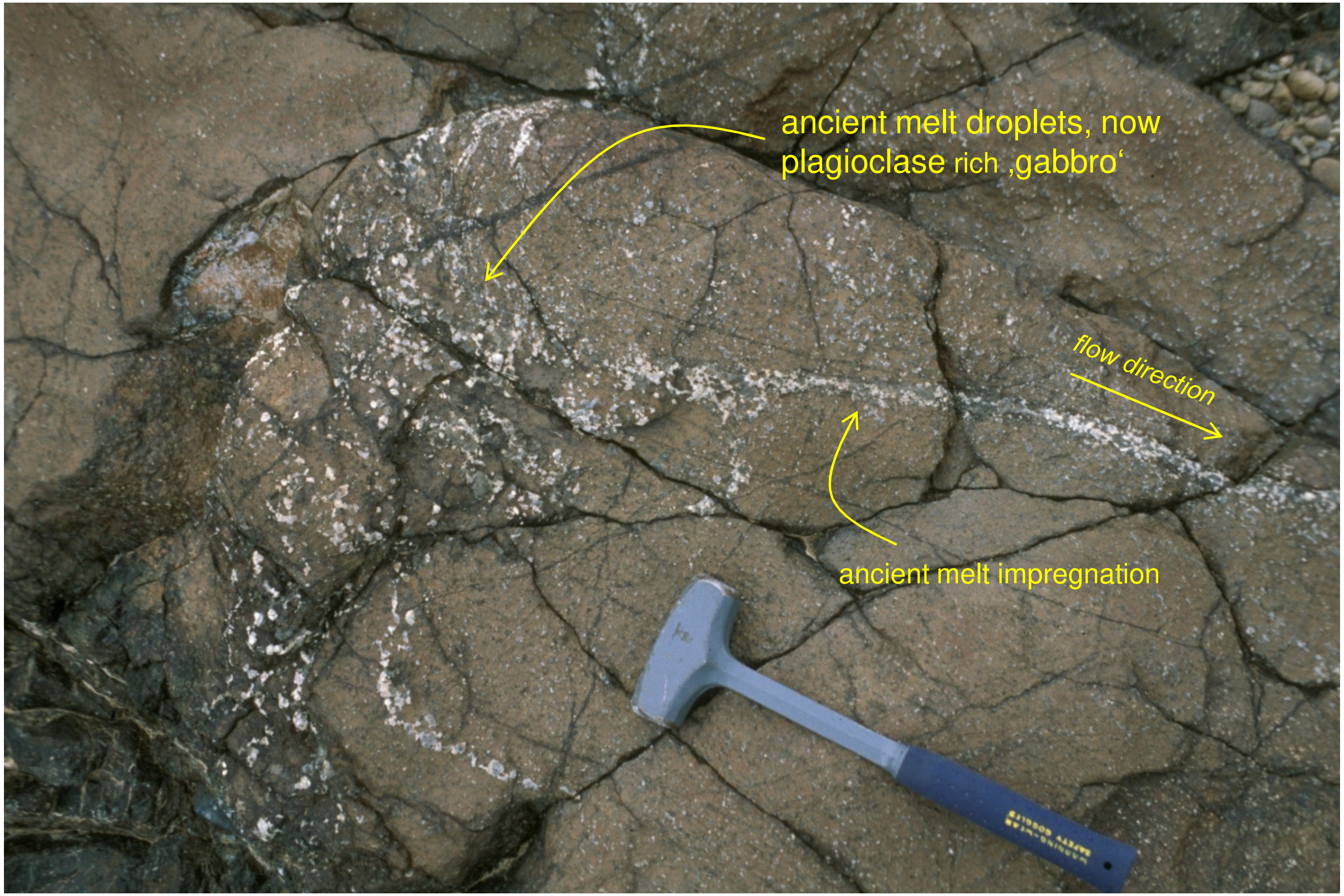

Melt compositions at mid ocean ridges - Major elements

Table 4. Primitive MORB compositions.

	Iceland[1]	Global Range[2]
SiO_2	48.72	47.2 – 51.4
TiO_2	0.93	0.50 – 1.29
Al_2O_3	15.99	15.0 – 17.58
FeO	8.96	7.21 – 8.97
MnO	0.16	0.06 – 0.21
MgO	10.56	8.39 – 10.90
CaO	14.01	11.56 – 13.35
Na_2O	1.72	1.62 – 2.49
K_2O	0.05	0.00 – 0.28

[1] Most magnesian published Icelandic glass (Breddam, 2002).
[2] 39 primitive MORB glasses from Atlantic and Pacific Oceans (Presnall and Hoover, 1987).

39 samples

Presnall et al., 2002

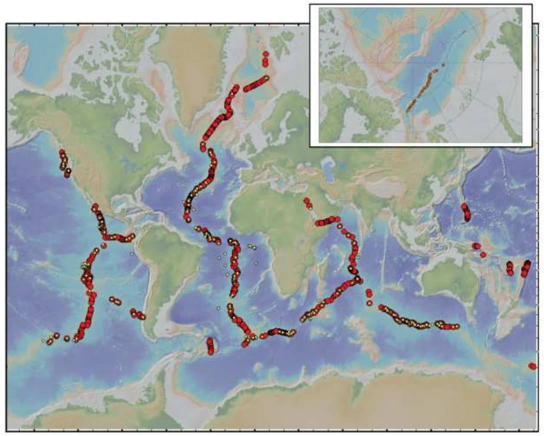

430 samples

Table 1. The Composition of ALL MORB[a]

	n	ALL MORB Mean[b]	± (95% conf)	ALL MORB Log-Normal Mean[c]	± (95% conf)	Upper Bound	Lower Bound
MgO	430	**7.58**	0.12	7.69	0.08	9.04	6.21
SiO_2	430	**50.47**	0.08	50.41	0.08	51.75	49.22
FeO	430	**10.43**	0.21	10.07	0.14	13.48	8.12
CaO	430	**11.39**	0.09	11.35	0.07	12.49	10.15
Na_2O	430	**2.79**	0.03	2.76	0.04	3.69	2.06
Al_2O_3	430	**14.70**	0.12	14.95	0.10	16.74	13.25
TiO_2	430	**1.68**	0.05	1.54	0.03	2.32	1.06
K_2O	430	**0.160**	0.014	0.144	0.011	0.558	0.045
P_2O_5	409	**0.184**	0.012	0.169	0.008	0.400	0.082
MnO	379	**0.184**	0.005	0.173	0.004	0.231	0.105

Gale et al., 2013, The mean composition of ocean ridge basalts. Geochemistry, Geophysics, Geosystems.

>> This publication also provides **trace-element** and **isotope** data!

Melt compositions at mid ocean ridges

Experimental constraints on p-T conditions

Melting at MOR's is basically **dry** and at relativeley **low pressure** (thin lithosphere!)

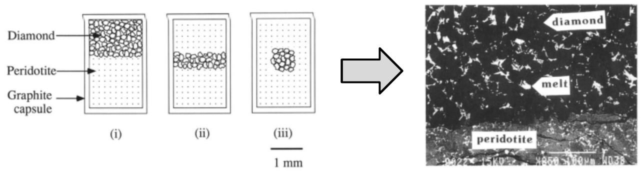

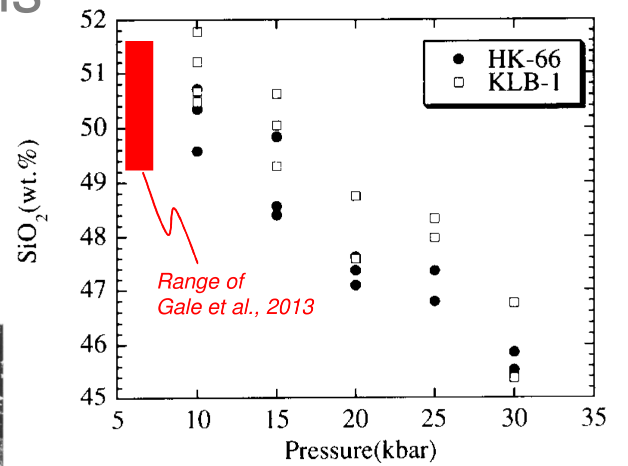

Modal composition of KLB-1 (wt%):
ol: 58, opx: 25, cpx: 15, sp: 2

	KLB-1	HK-66
SiO_2	44.48	48.02
TiO_2	0.16	0.22
Al_2O_3	3.59	4.88
FeO*	8.10	9.90
MnO	0.12	0.14
MgO	39.22	32.35
CaO	3.44	2.97
Na_2O	0.30	0.66
K_2O	0.02	0.07
P_2O_5	0.03	0.07
Cr_2O_3	0.31	0.25
NiO	0.25	n.d.
Total	100.02	99.53

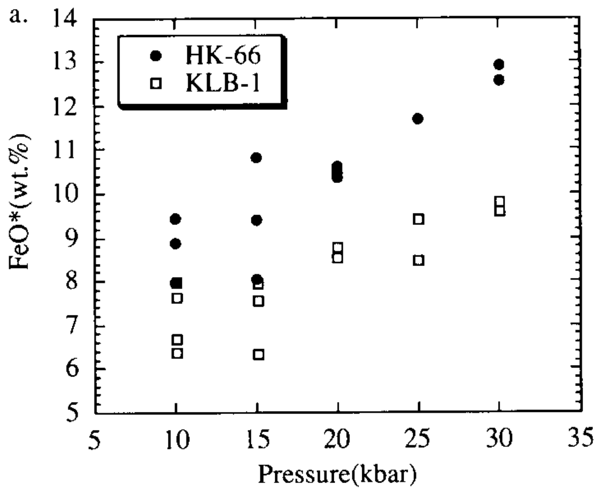

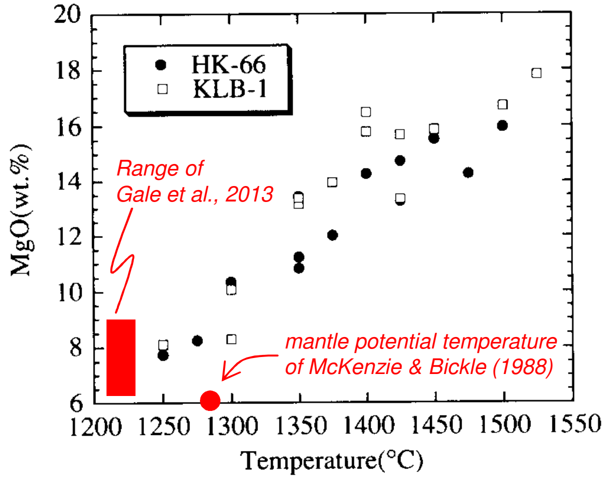

Figures & tables from Hirose & Kushiro (1993), Eath. Planet. Sci. Lett., 114, 477-489

Melt compositions at mid ocean ridges

Trace element compositions, early work, principal implications

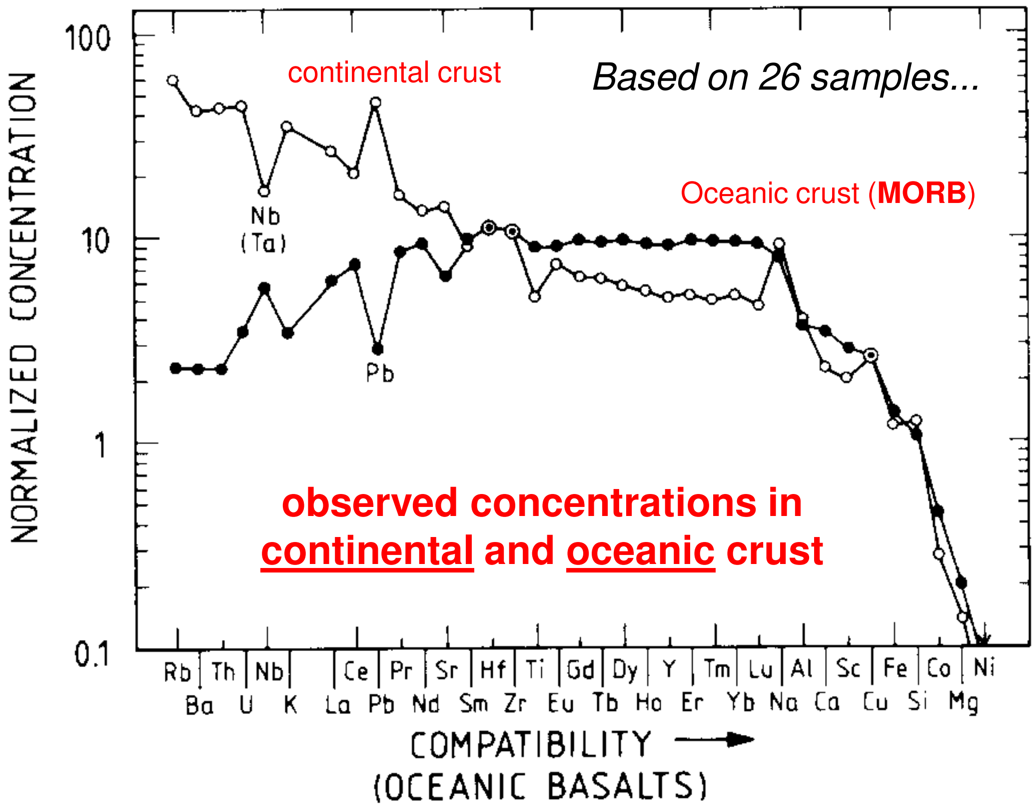

Hofmann, 1988: Chemical differentiation of the Earth: the relationship between mantle, continental crust, and oceanic crust. Earth Planet. Sci. Lett., 90, 297-314.

Explained by the extraction of **1.5% melt** from **PRIMA** to form the **CC**, and subsequent **8-10% melt** from **DM** to form the **OC**

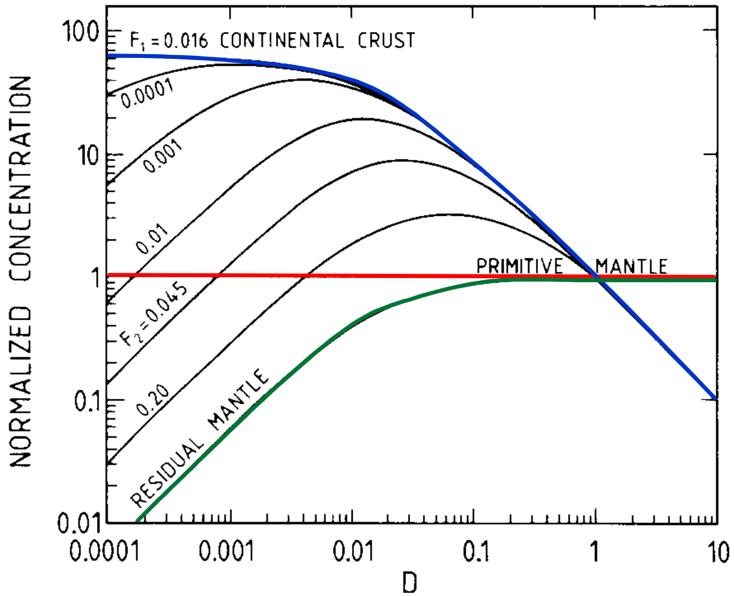

Melt compositions at mid ocean ridges

Trace element compositions

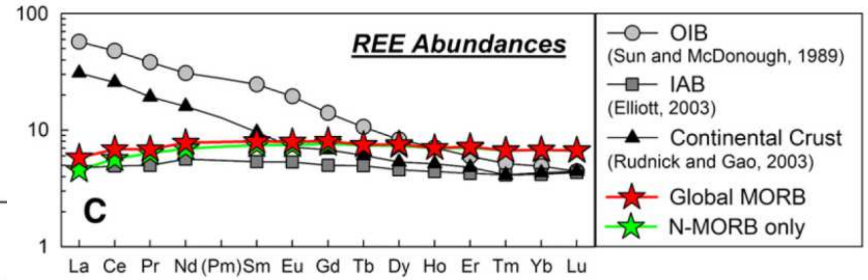

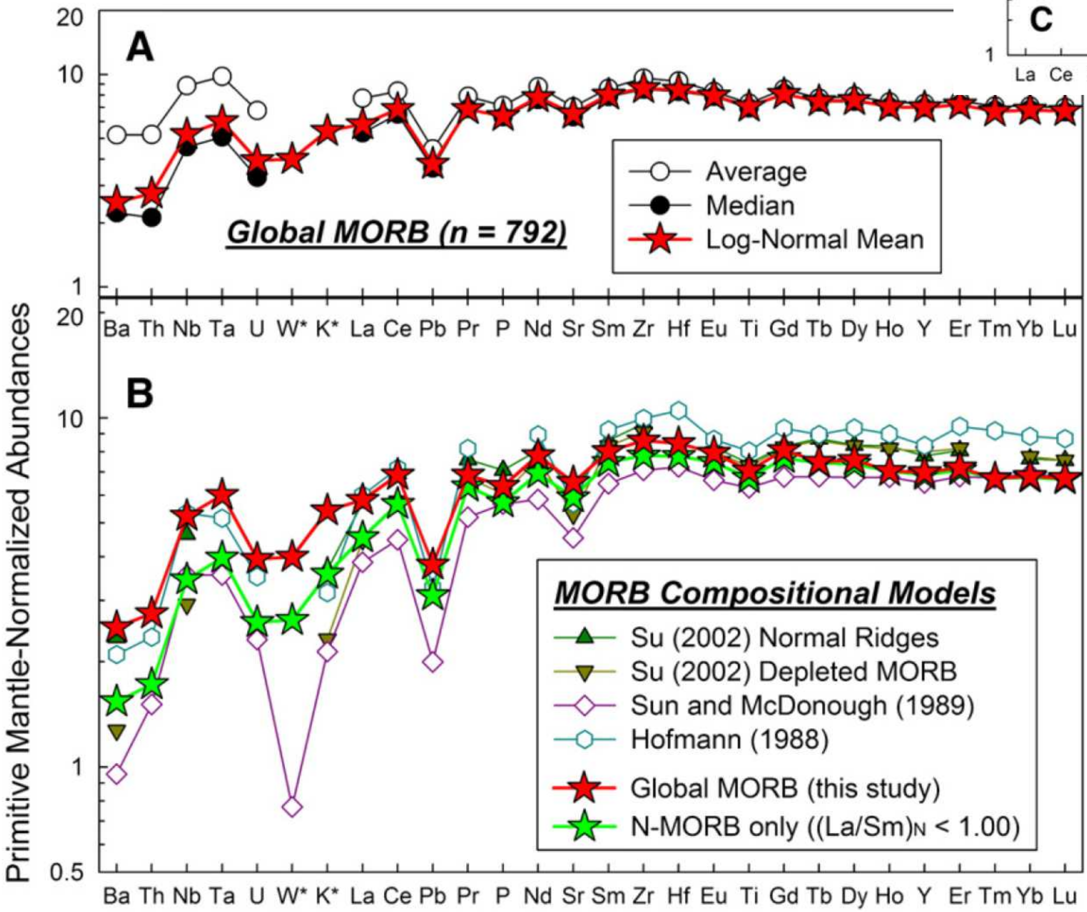

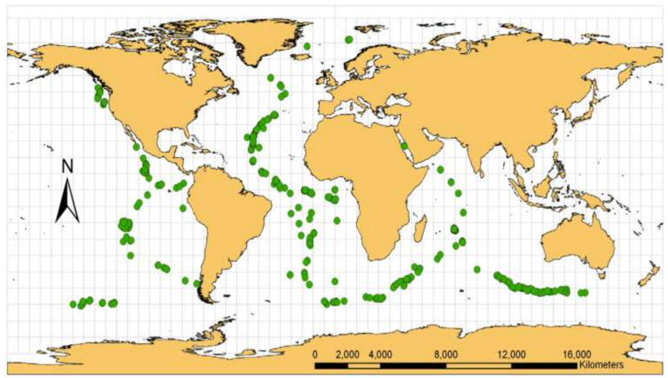

Locations of MORB samples evaluated by Arevalo & McDonough (2010)

Melt compositions at mid ocean ridges

Trace element compositions

„Constancy“ of distinct ratios

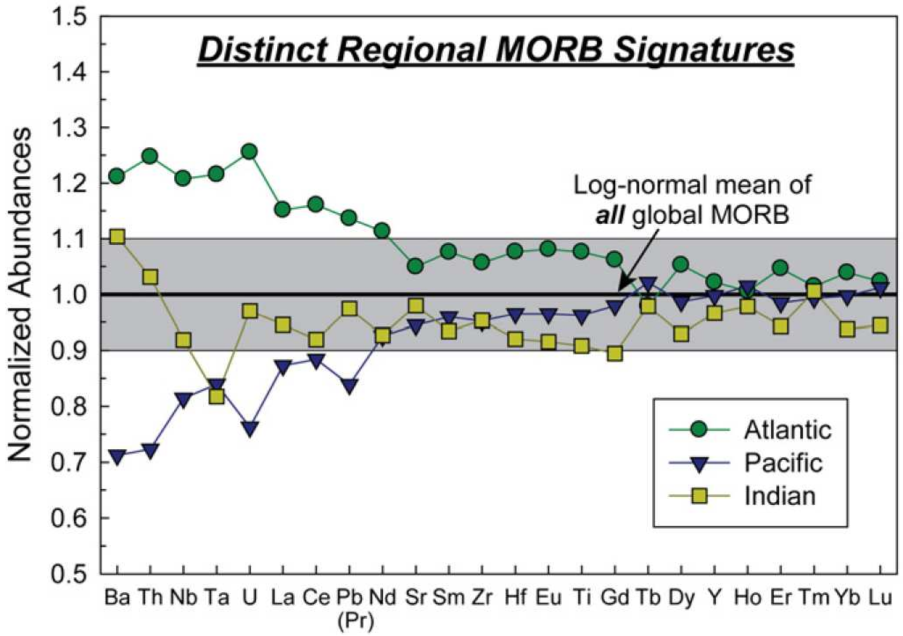

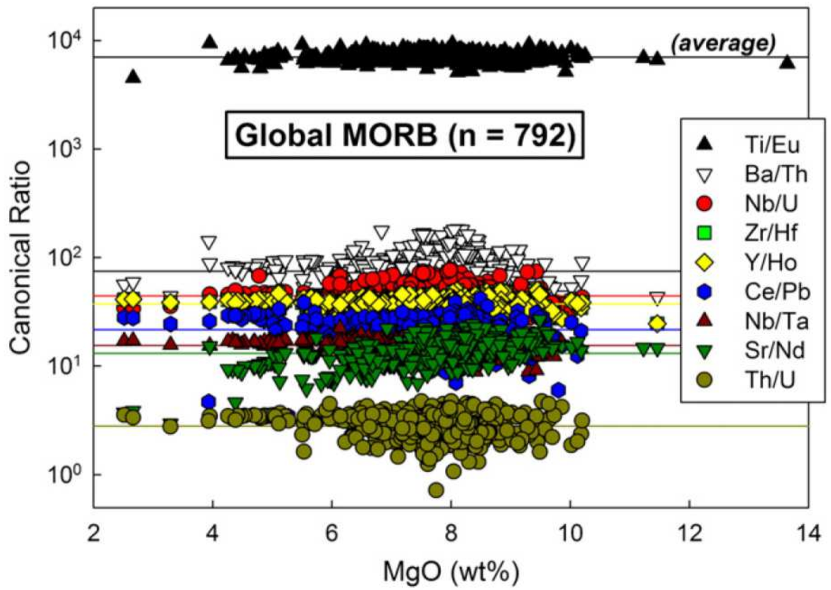

▲ Differences between Atlantic, Pacific and Indian MORB

Slopes of **unity** in bivariate concentration plots indicate identical D-values (i.e. identical behaviour) ►

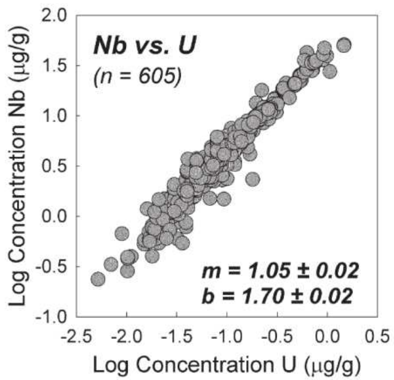

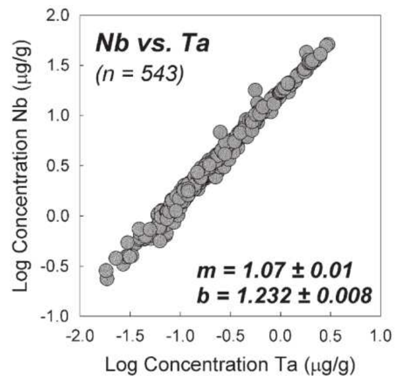

All figures from Arevalo & McDonough (2010)

Melt compositions at mid ocean ridges

Trace element compositions

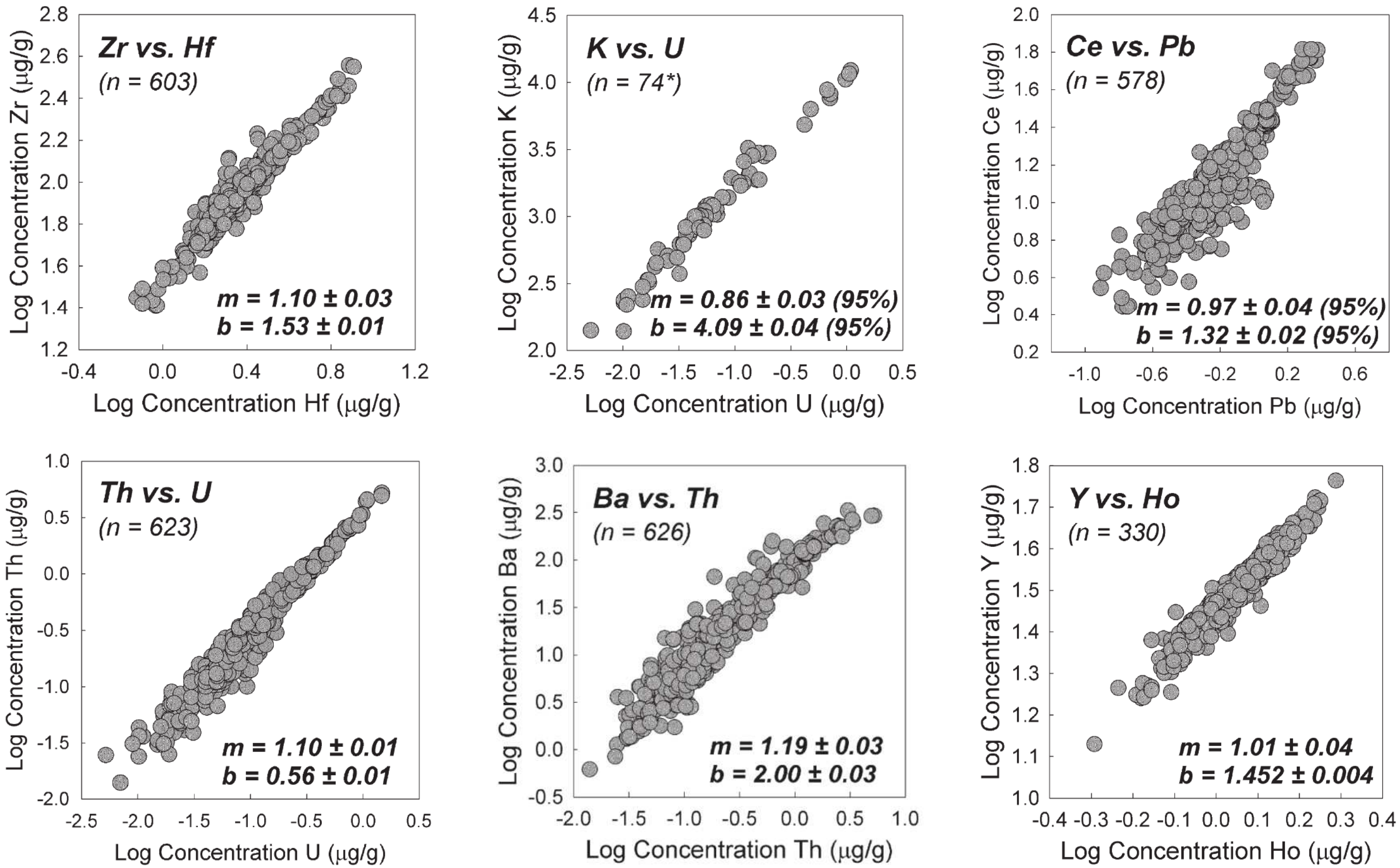

All figures from Arevalo & McDonough (2010)

Melt compositions at mid ocean ridges

Isotope compositions

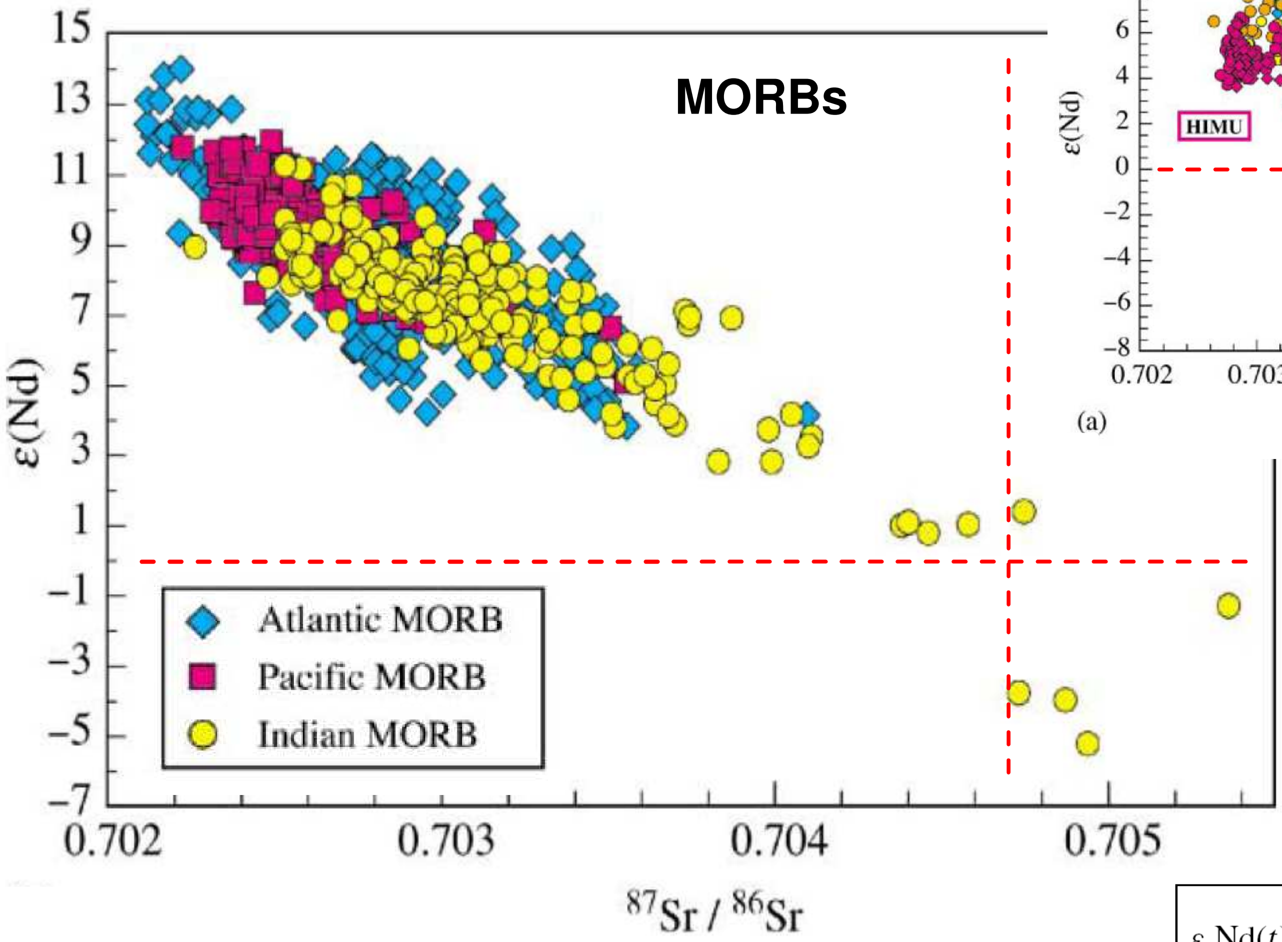

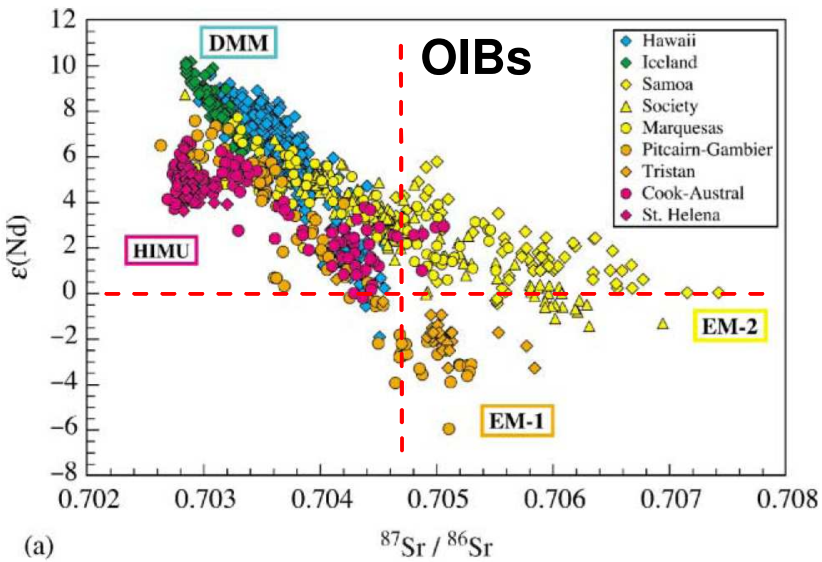

^{87}Rb (48.8 Ga) ^{87}Sr

^{147}Sm (106 Ga) ^{143}Nd

$$\varepsilon\,\mathrm{Nd}(t) = \left(\frac{(^{143}\mathrm{Nd}/^{144}\mathrm{Nd})_{\mathrm{sample}}(t)}{(^{143}\mathrm{Nd}/^{144}\mathrm{Nd})_{\mathrm{CHUR}}(t)} - 1\right) \times 10^4$$

Hofmann (2003), Treatise on Geochemistry

Melt compositions at mid ocean ridges

Isotope compositions

^{238}U (4.47 Ga) ^{206}Pb

^{235}U (0.738 Ga) ^{207}Pb

^{232}Th (14.0 Ga) ^{208}Pb

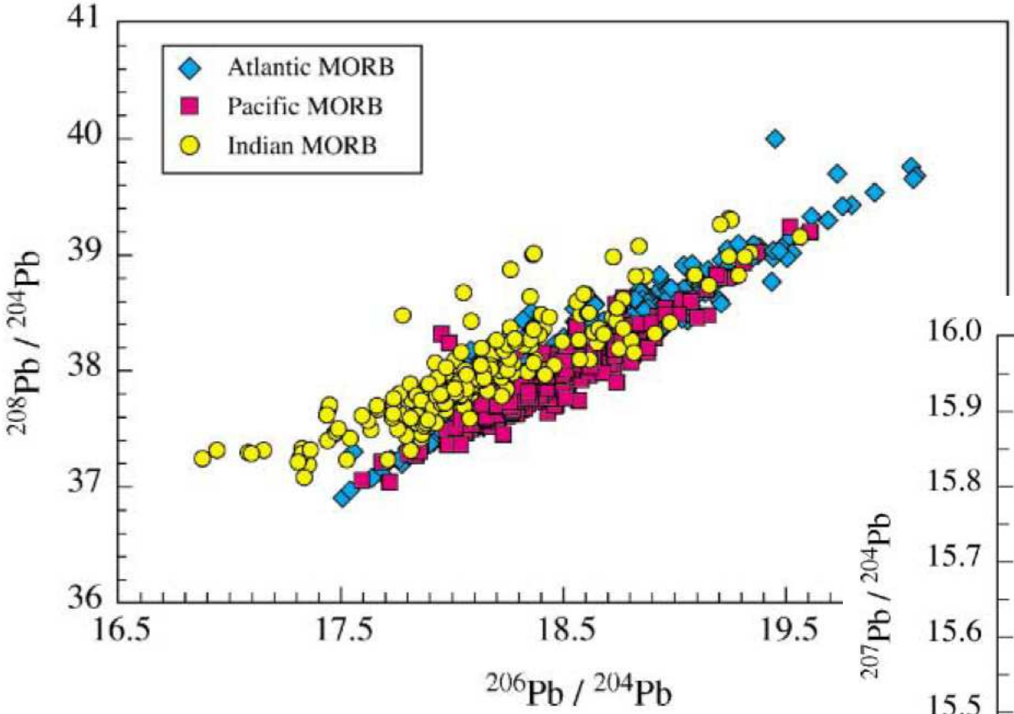

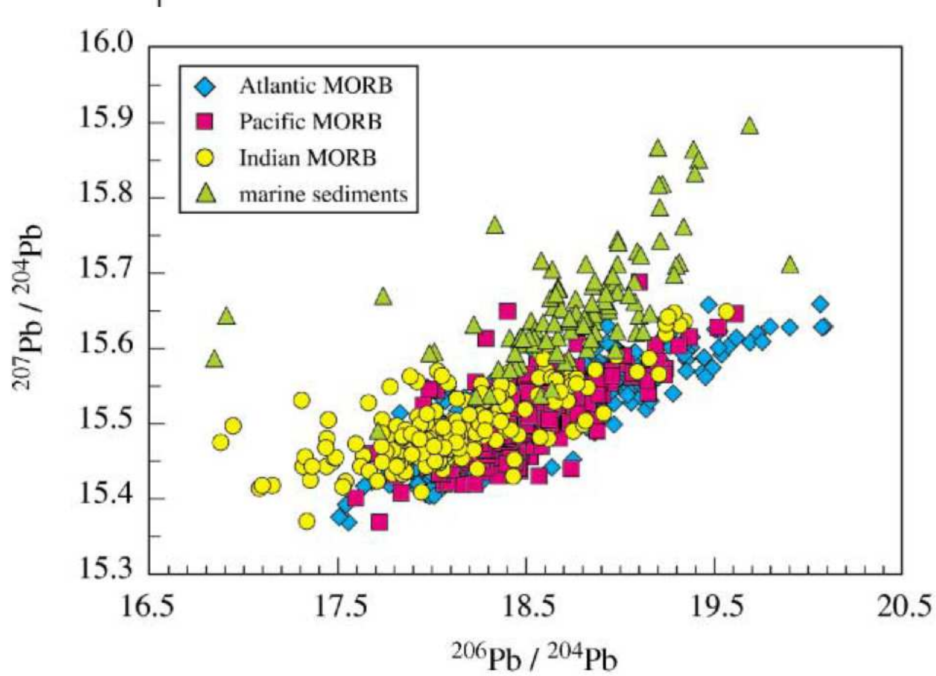

No distinct differences exist, but Indian MORB seems to be slighlty enriched in ^{208}Pb

Hofmann (2003), Treatise on Geochemistry

Melt compositions at mid ocean ridges

Hf-Nd isotope compositions

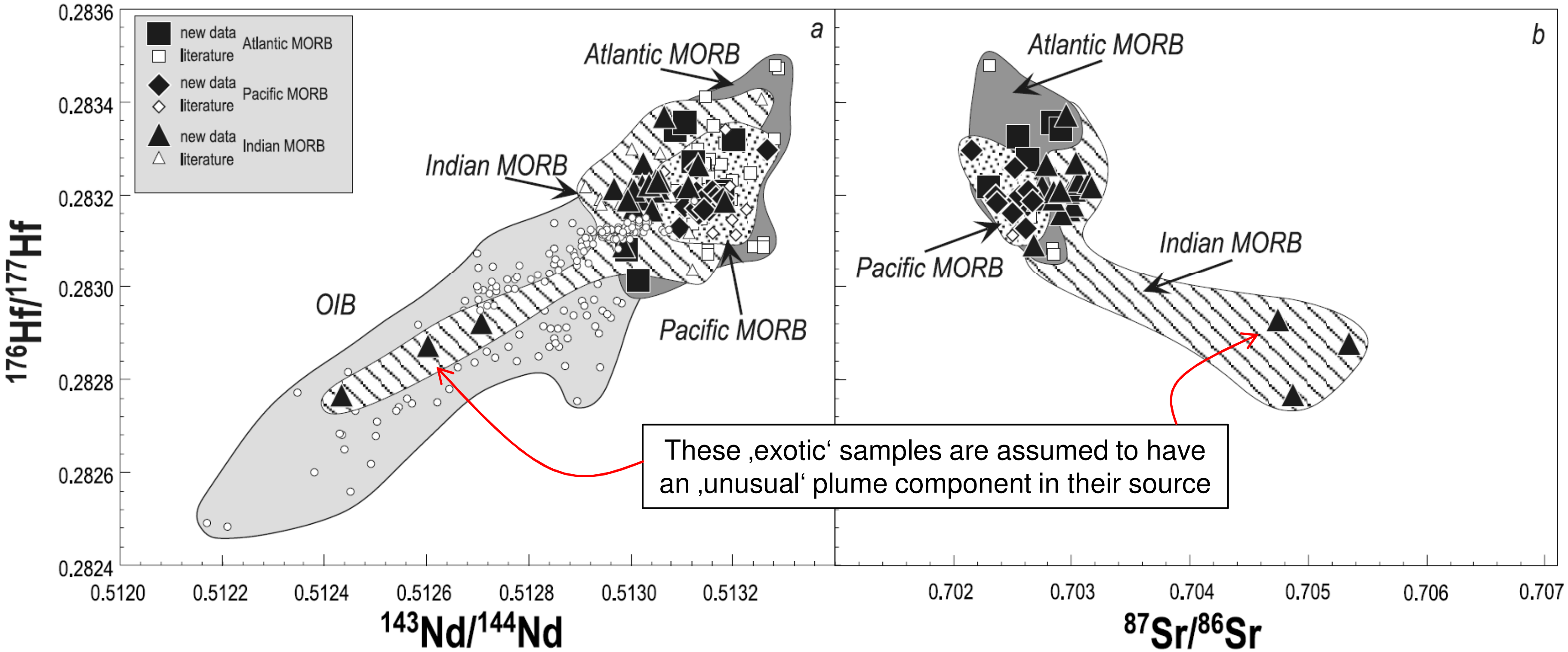

^{87}Rb (48.8 Ga) ^{87}Sr

^{176}Lu (35.7 Ga) ^{176}Hf

^{147}Sm (106 Ga) ^{143}Nd

Chauvel & Blichert-Toft (2001)

Melt compositions at mid ocean ridges

Causes of observed isotope compositions

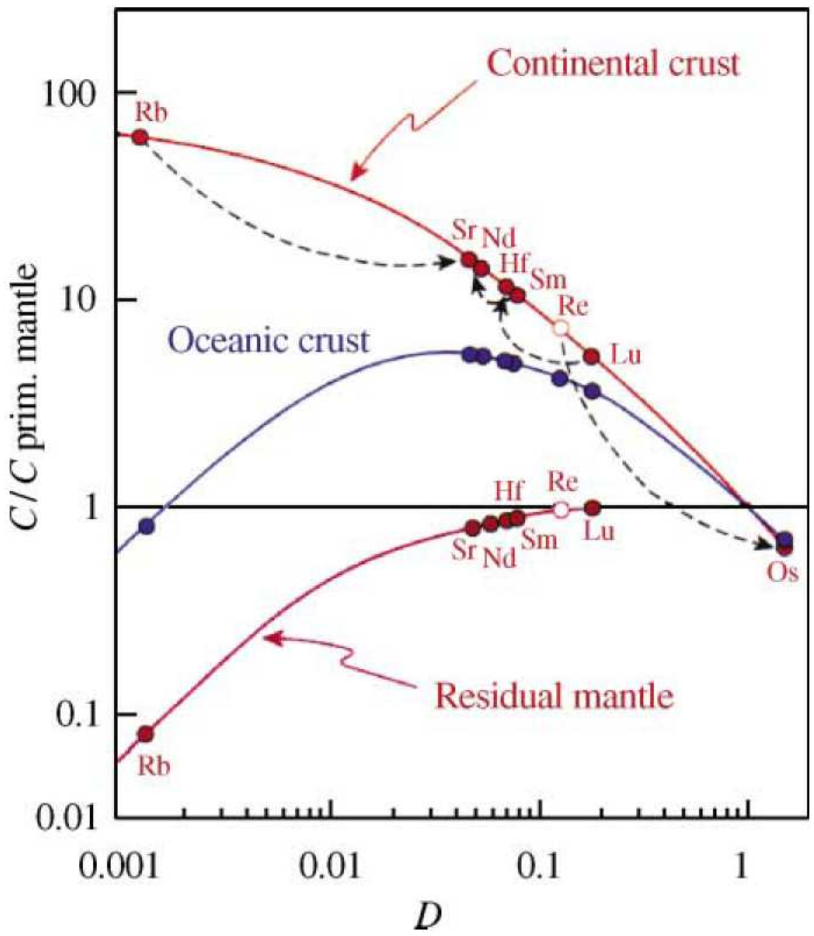

Hofmann, 2003, Treatise on Geochemistry

Ratio	DM	CC
Rb/Sr	low	high
Re/Os	low	high
U/Pb	low	high
Th/Pb	low	high
Sm/Nd	high	low
Lu/Hf	high	low

Due to this, and given enough **time**, different geochemical **reservoirs** develop **different radiogenic isotope signatures**

Melt compositions at mid ocean ridges

How to explain the observed isotope compositions

(here $^{143}Nd/^{144}Nd$) – valids basically also for other radiogenic isotope ratios

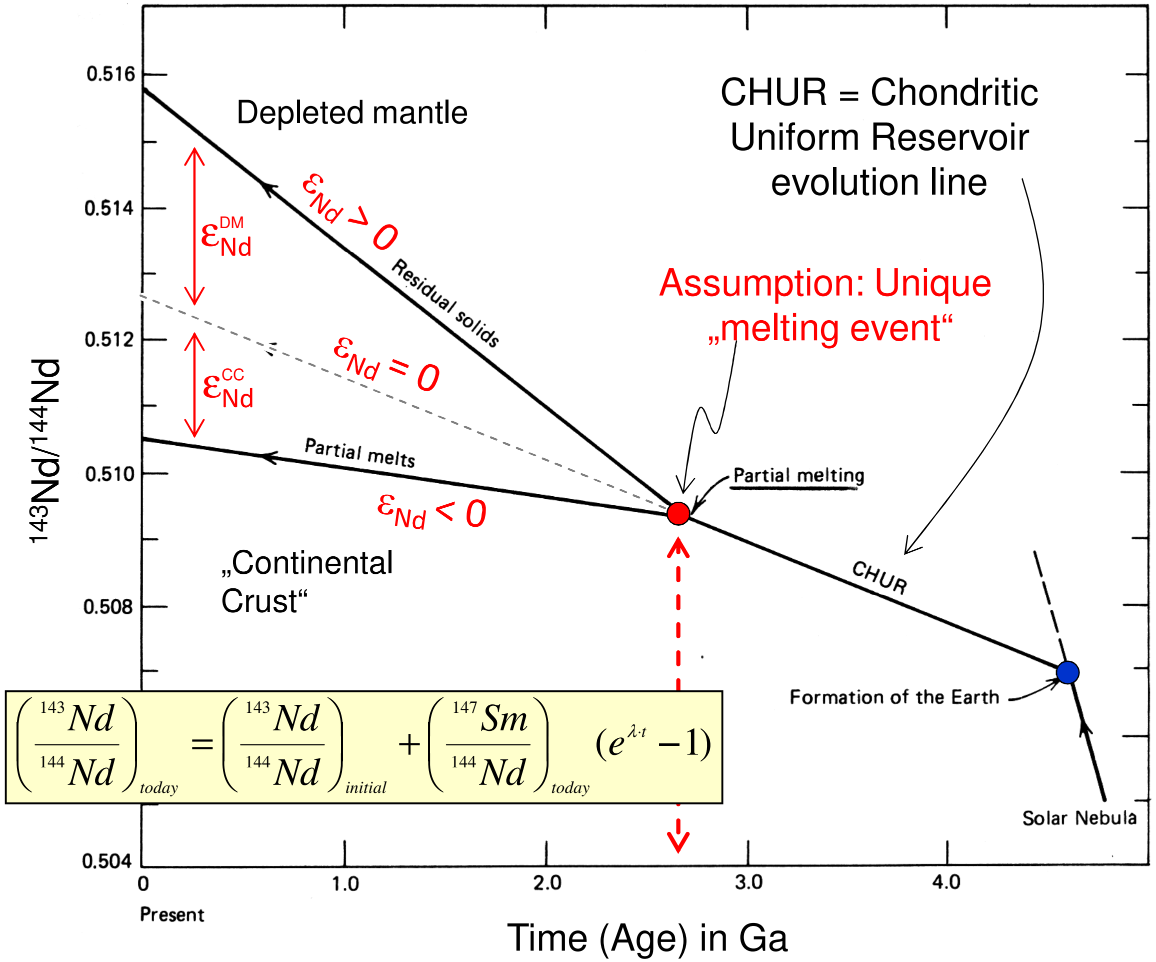

$$\left(\frac{^{143}Nd}{^{144}Nd}\right)_{today} = \left(\frac{^{143}Nd}{^{144}Nd}\right)_{initial} + \left(\frac{^{147}Sm}{^{144}Nd}\right)_{today} (e^{\lambda \cdot t} - 1)$$

Data base:

$(^{147}Sm/^{144}Nd)_{DM} = 0.2395$

$(^{143}Nd/^{144}Nd)_{DM} = 0.513110$

$(^{147}Sm/^{144}Nd)_{CHUR} = 0.1960$

$(^{143}Nd/^{144}Nd)_{CHUR} = 0.512630$

DM estimate from Salters & Stracke (2004), $^{147}Sm/^{144}Nd$ calculated from concentrations in DM and using natural isotope abundances. Values for CHUR from Bouvier et al. (2008).

Decay const. $^{147}Sm = 6.54 \times 10^{-12}$ 1/a

Melt compositions at mid ocean ridges

How to explain the observed isotope compositions

(here $^{143}Nd/^{144}Nd$) – valids basically also for other radiogenic isotope ratios

Isotope evolution of CHUR over time:

$$\left(\frac{^{143}Nd}{^{144}Nd}\right)_0^{CHUR} = \left(\frac{^{143}Nd}{^{144}Nd}\right)_i^{CHUR} + \left(\frac{^{147}Sm}{^{144}Nd}\right)_0^{CHUR} (e^{\lambda \cdot t} - 1)$$

Isotope evolution of DM over time:

$$\left(\frac{^{143}Nd}{^{144}Nd}\right)_0^{DM} = \left(\frac{^{143}Nd}{^{144}Nd}\right)_i^{DM} + \left(\frac{^{147}Sm}{^{144}Nd}\right)_0^{DM} (e^{\lambda \cdot t} - 1)$$

At the time of the **single melting event** (red point in the previous diagram), the **initial values** of DM and CHUR are equal! This allows to calculate the „age“ of this event.

$^{143}Nd/^{144}Nd$ values can be expressed as **deviation** relative to CHUR for any time **t** in the past:

$$\varepsilon_{Nd}^{sample}(t) = \left[\frac{(^{143}Nd/^{144}Nd)_t^{sample}}{(^{143}Nd/^{144}Nd)_t^{CHUR}} - 1\right] \times 10^4$$

„sample“ means any reservoir (DM, CC, ...) or any individual sample, t is time

Data:

$(^{147}Sm/^{144}Nd)_{DM} = 0.2395$

$(^{143}Nd/^{144}Nd)_{DM} = 0.513110$

$(^{147}Sm/^{144}Nd)_{CHUR} = 0.1960$

$(^{143}Nd/^{144}Nd)_{CHUR} = 0.512630$

DM estimate from Salters & Stracke (2004), $^{147}Sm/^{144}Nd$ calculated from concentrations in DM and using natural isotope abundances. Values for CHUR from Bouvier et al. (2008).

Decay const. $^{147}Sm = 6.54 \times 10^{-12}$ 1/a

Melt compositions at mid ocean ridges

Noble gas systematics – mantle degassing

Sources of terrestrial noble gases

- **Inherited** (from the solar nebula)
- **Nucleogenic** (products of nuclear reactions)
- **Cosmogenic**

Noble gas elemental ratios in chondrites and the terrestrial atmosphere

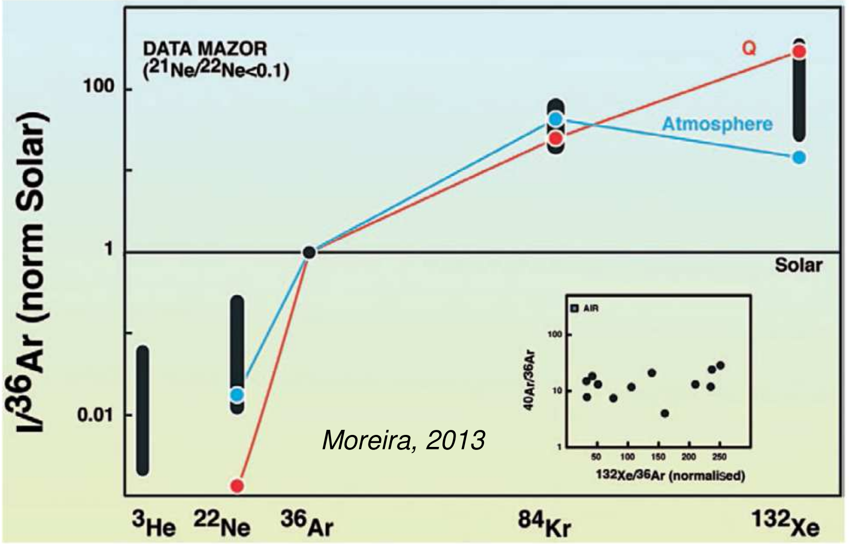

Table 3 Some nuclear reactions producing noble gases.

Reaction	*Upper crust production ratios*[a]
$^{6}Li(n,\alpha)^{3}H(\beta-)^{3}He$	$^{3}He/^{4}He = 1 \times 10^{-8}$
$^{17}O(\alpha,n)^{20}Ne$	$^{20}Ne/^{4}He = 4.4 \times 10^{-9}$
$^{18}O(\alpha,n)^{21}Ne$	$^{21}Ne/^{4}He = 4.5 \times 10^{-8}$
$^{24}Mg(n,\alpha)^{21}Ne$	$^{21}Ne/^{4}He = 1 \times 10^{-10}$
$^{25}Mg(n,\alpha)^{22}Ne$	Combined crustal production:
$^{19}F(\alpha,n)^{22}Na(\beta+)^{22}Ne$	$^{22}Ne/^{4}He = 9.1 \times 10^{-8}$
$^{35}Cl(n,\gamma)^{36}Cl(\beta-)^{36}Ar$	$^{40}Ar/^{36}Ar = 1.5 \times 10^{7}$

Source: Porcelli *et al*. (2002).
[a] See Ballentine and Burnard (2002) for details and production rates in different compositions.

Hilton & Porcelli (2003), Treatise on Geochemistry

Melt compositions at mid ocean ridges

Noble gas systematics – mantle degassing

Table 1 Solar system isotopic compositions of He, Ne, and Ar.

Reservoir	*$^{3}He/^{4}He$* ($\times 10^{-6}$)	*R/R_A*[a]	*$^{20}Ne/^{22}Ne$*	*$^{21}Ne/^{22}Ne$*	*$^{38}Ar/^{36}Ar$*	*$^{40}Ar/^{36}Ar$*
Solar	457	326	13.8	0.0328	0.1825	$\sim 3\times 10^{-4}$
Planetary	143	102	8.2	0.024	0.188	$\sim 3\times 10^{-4}$
Earth atmosphere	1.4	1	9.8	0.0290	0.1880	295.5

After McDougall and Honda (1998).
[a] $R/R_A = (^3He/^4He)_{observed}/(^3He/^4He)_{air}$, where air $^3He/^4He = 1.4\times 10^{-6}$.

Table 2 Half-lives of parent nuclides for noble gases.

Nuclide	*Half-life*	*Daughter*	*Yield* (atoms/decay)	*Comments*
^{3}H	12.26 yr	^{3}He	1	Continuously produced in atm
^{238}U	4.468 Gyr	^{4}He	8	
		^{136}Xe	3.6×10^{-8} $(4.4\pm 0.1)\times 10^{-8}$	Spontaneous fission
^{235}U	0.7038 Gyr	^{4}He	7	$^{238}U/^{235}U = 137.88$
^{232}Th	14.01 Gyr	^{4}He	6	Th/U = 3.8 in bulk Earth
		^{136}Xe	$<4.2\times 10^{-11}$	No significant production in Earth
^{40}K	1.251 Gyr	^{40}Ar	0.1048	$^{40}K = 0.01167\%$ total K
^{244}Pu	80.0 Myr	^{136}Xe	7.00×10^{-5}	$^{244}Pu/^{238}U = 6.8\times 10^{-3}$ at 4.56 Ga
^{129}I	15.7 Myr	^{129}Xe	1	$^{129}I/^{127}I = 1.1\times 10^{-4}$ at 4.56 Ga

Source: Porcelli *et al*. (2002).

From Hilton & Porcelli (2003), Treatise on Geochemistry

Melt compositions at mid ocean ridges

Noble gas systematics – is there primordial He in the mantle?

^{3}He excess in seawater above the East Pacific Rise

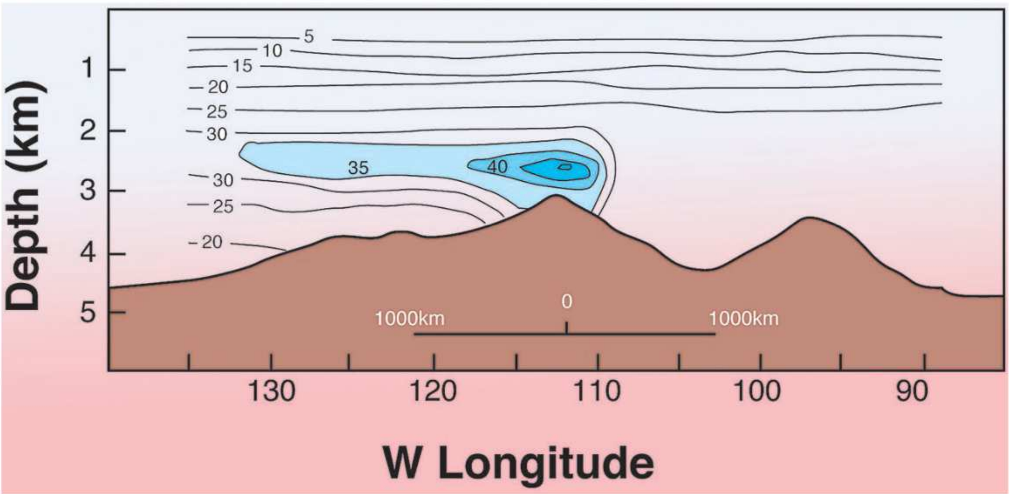

Excluding nucleogenic sources for ^{3}He, the **elevated ^{3}He/^{4}He ratios** relative to air (i.e., $R/R_A > 1$) in **MORB** and **submarine hydrothermal fluids** suggest that the Earth's mantle is **not** completely degassed (i.e., comprises primordial Helium)

^{3}He/^{4}He relative to air along the Mid Atlantic Ride

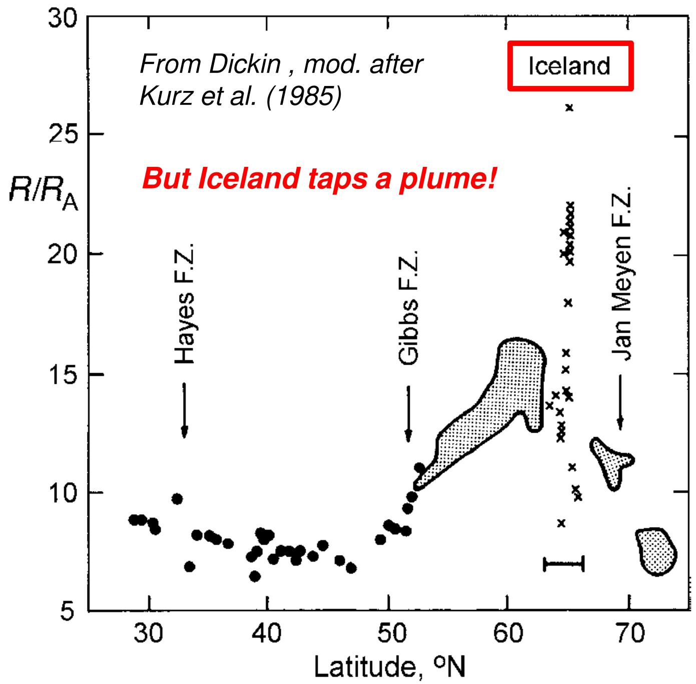

Moreira (2013), Geochemical perspective letters

Melt compositions at mid ocean ridges ... and elsewhere ;)

Noble gas systematics – is there primordial He in the mantle?

He isotope composition of basalts from different settings

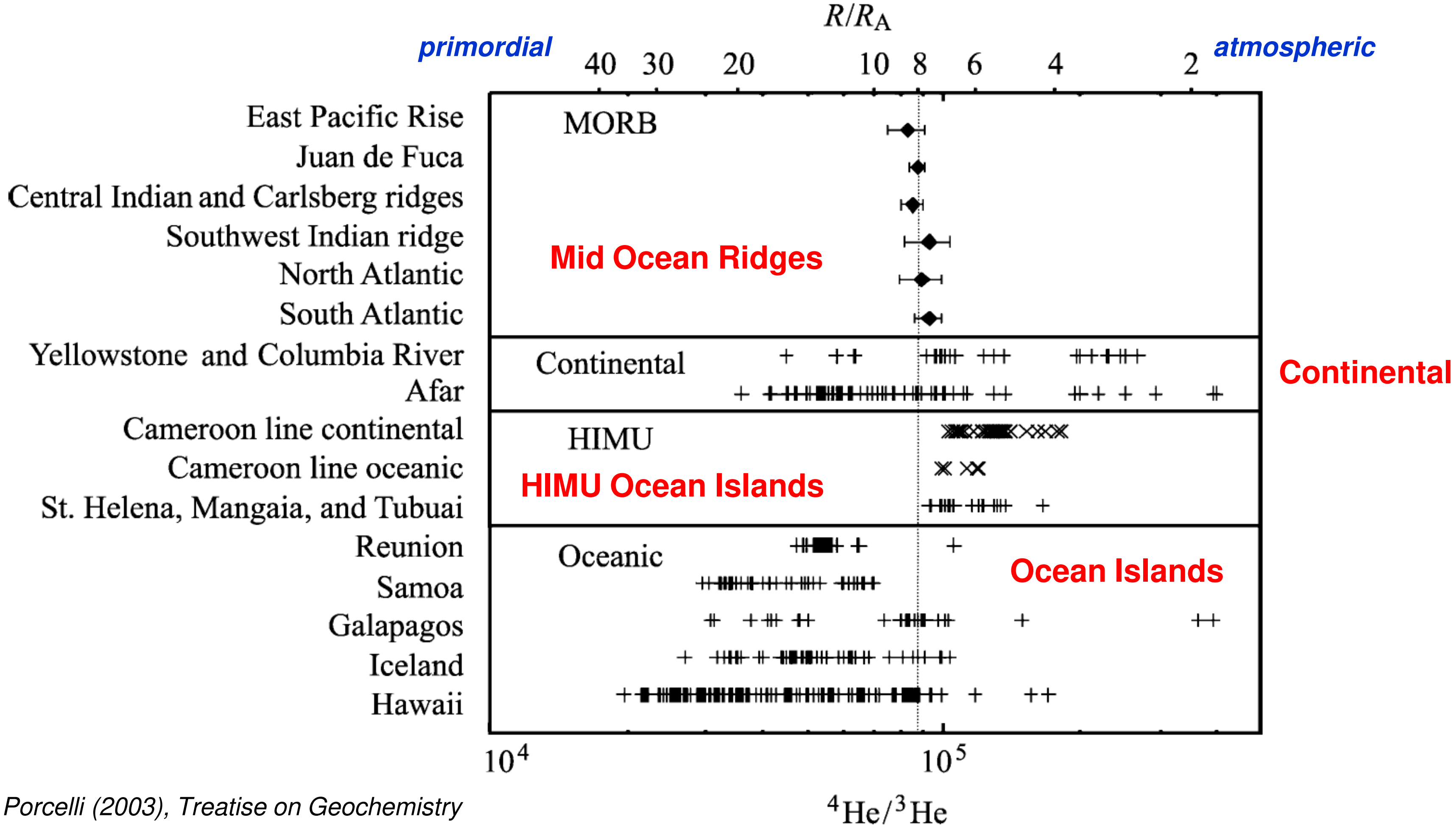

Hilton & Porcelli (2003), Treatise on Geochemistry

Melt compositions at mid ocean ridges ... and elsewhere ;)

Partial melting in the mantle is a fundamental process that determines the **primary** composition of basalts, but the final composition of MORB is controlled by **fractional crystallisation!**

During this process, *primary basalt* differentiates to form **cumulate rocks** (e.g. wehrlites, gabbros) on the one hand, and **differentiated basalts** on the other.

In the oceanic crust, mostly differentiated basalt forms the upper gabbros along with the extrusives (sheeted dikes, pillow lavas, lava flows & sills)

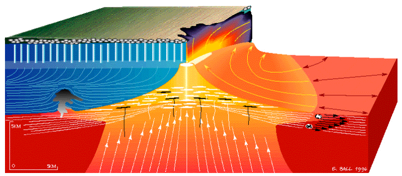

Melt compositions at mid ocean ridges

Low-pressure fractional crystallisation of MORB (very briefly!)

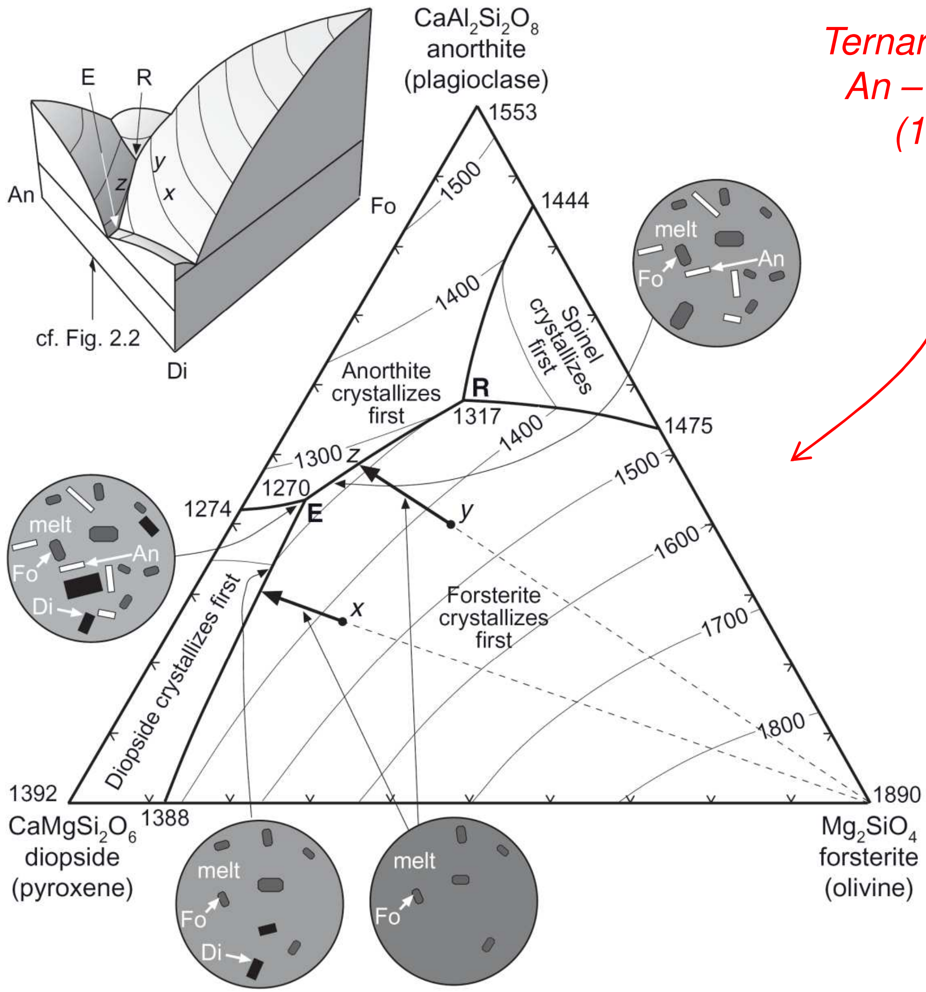

Ternary system An – Di – Fo (1 bar)

Ternary system An – Di – Fo at low and high pressure

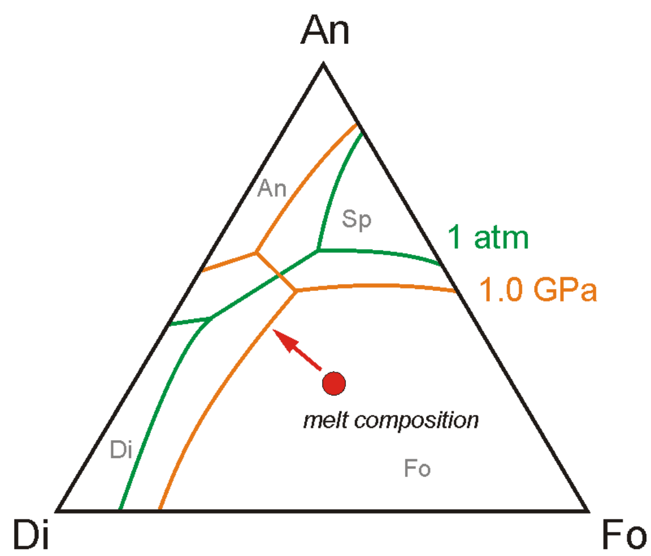

Melt compositions at mid ocean ridges

Low-pressure fractional crystallisation of MORB (very briefly!)

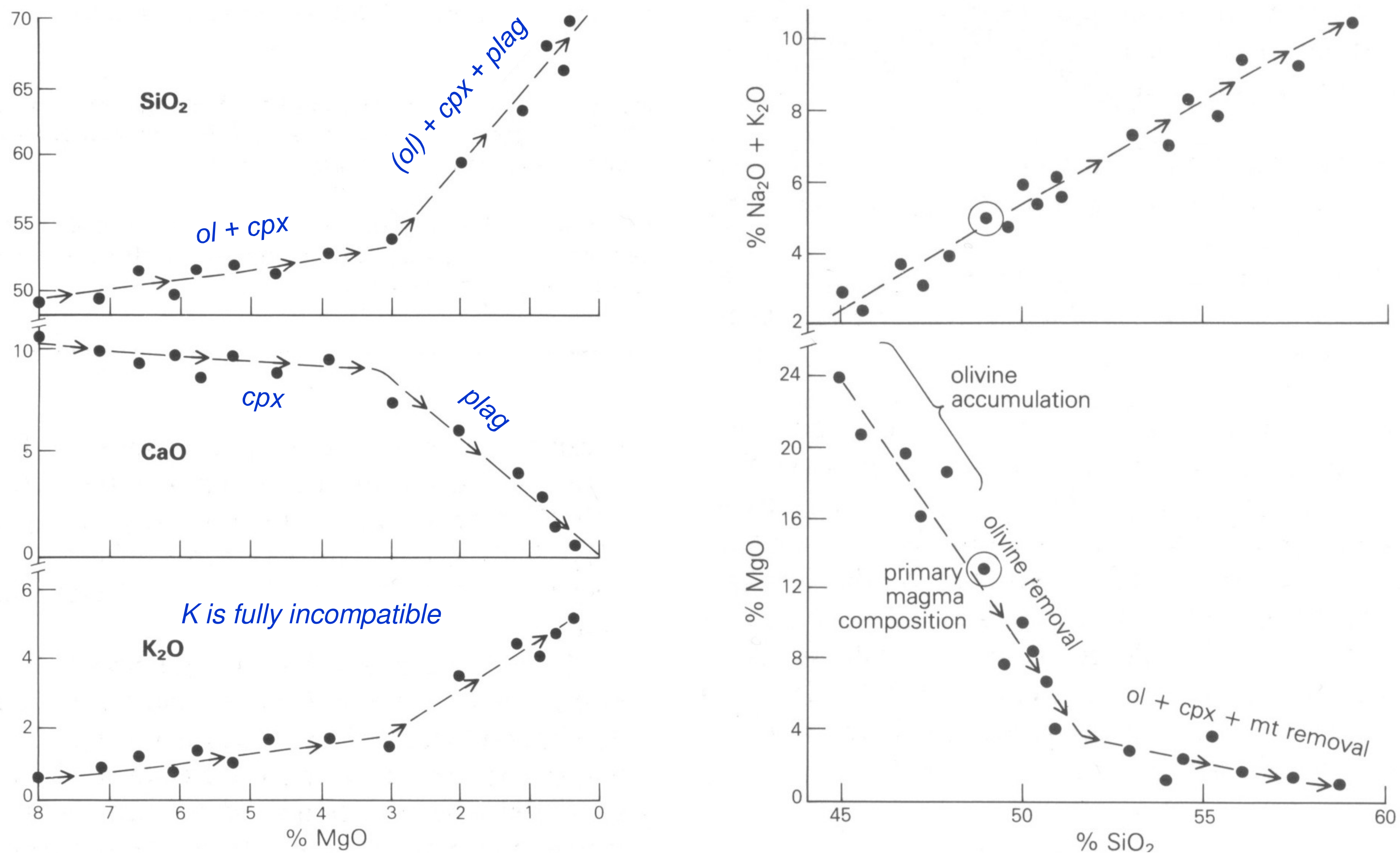

Melt compositions at mid ocean ridges

Low-pressure fractional crystallisation of MORB (very briefly!)

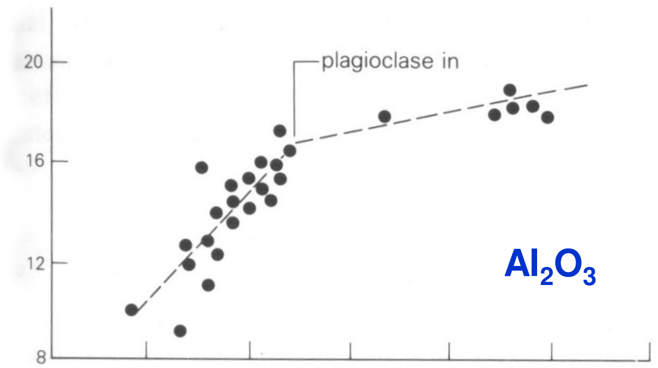

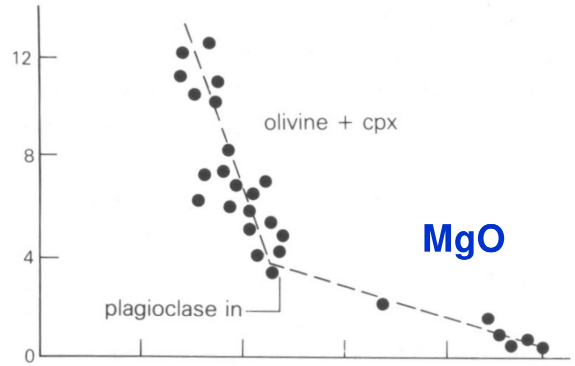

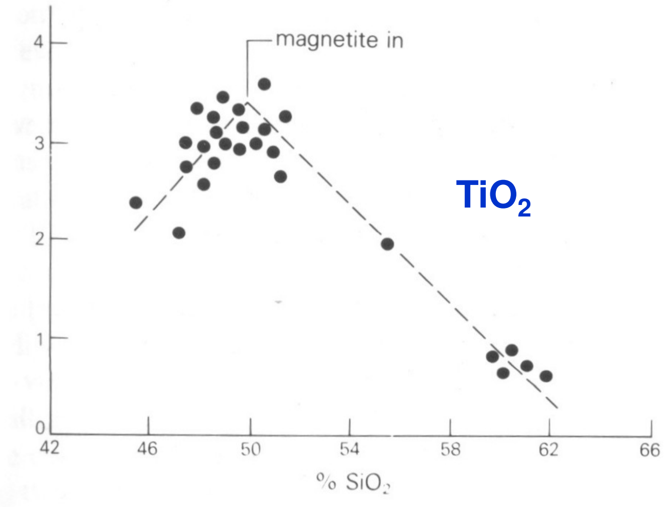

These fractional crystallisation processes predominantly occur during magma ascend and in the melt lenses located at the base of the sheeted dike complex

Synthesis

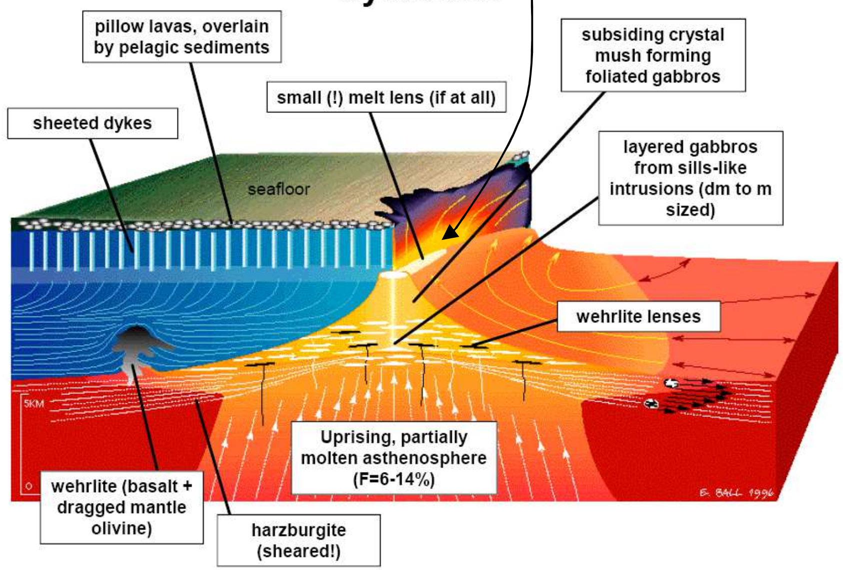

Hydrothermal processes at mid ocean ridges

Seawater infiltrates the oceanic crust along fractures

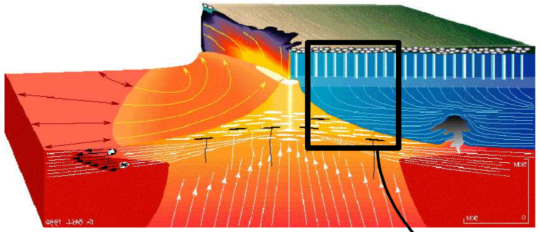

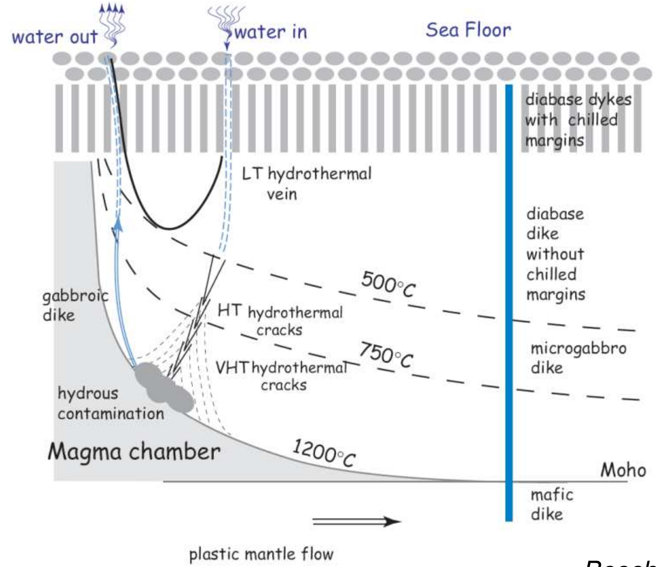

Bosch et al. (2004)

Seawater infiltration causes **hydratisation** reactions, leading to the formation of **water bearing mineral phases**. These are in **basalt/gabbro** *(oceanic crust)* for example:

- **lawsonite, amphibole,**
- **chlorite, epidote**

and in **harzburgite/peridotite** *(oceanic lithospheric mantle)*:

- **serpentine, talc,**
- **chlorite, amphibole**

oxygen isotope composition of **hydrous phases** in gabbros from the Oman ophiolite reveal **exchange with seawater** at temperatures up to **~975°C (!)**

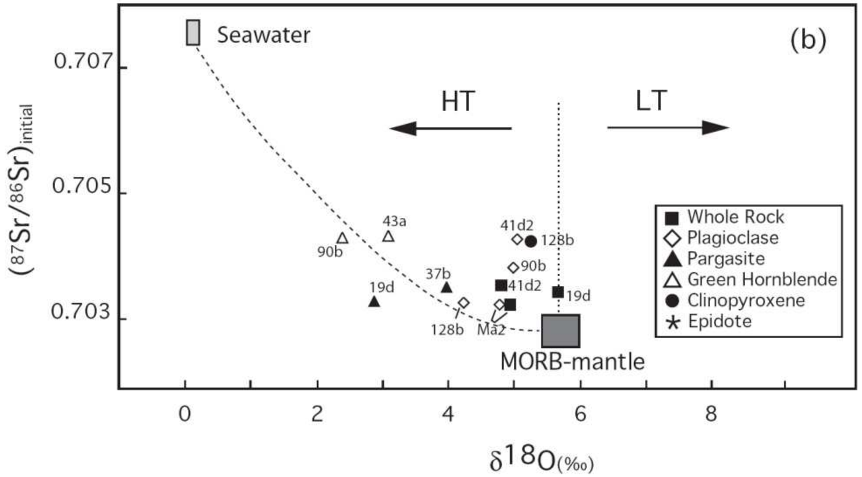

Hydrothermal processes at mid ocean ridges

Convective hydrothermal systems and VMS deposits

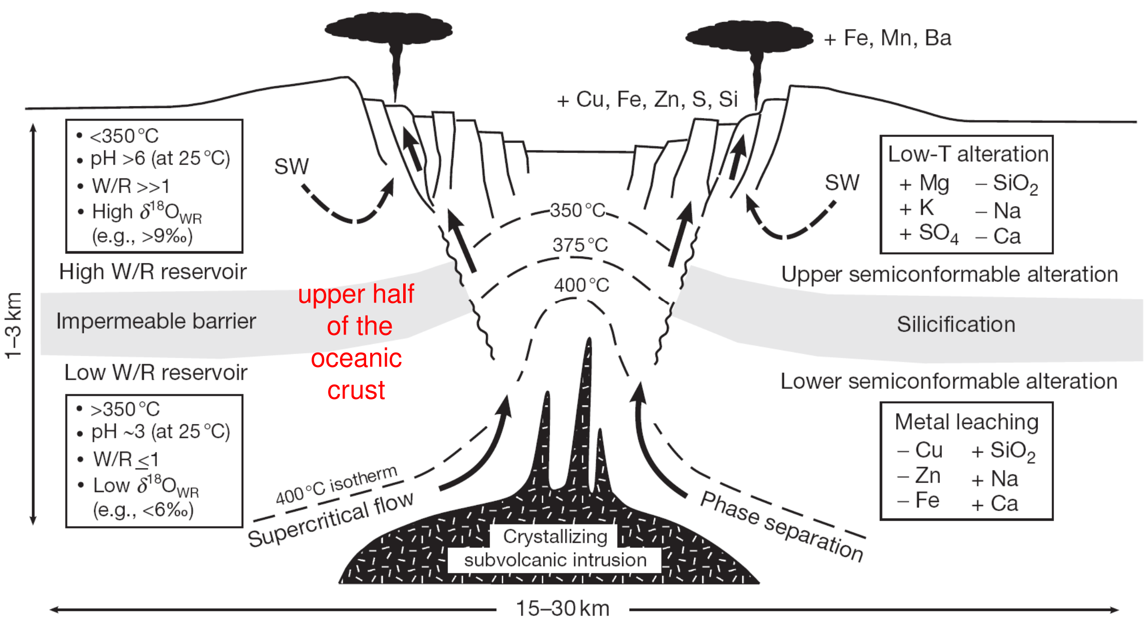

LT and HT **hydrothermal circulation** systems and **mass fluxes** to and out of the **oceanic crust (lithosphere)**. Metals such as **Cu, Zn, and Fe**, but also Ca, Si and S are **leached out**, whereas Mg, **K** and SO_4^{2-} were **added** to the oceanic (crust) lithosphere.

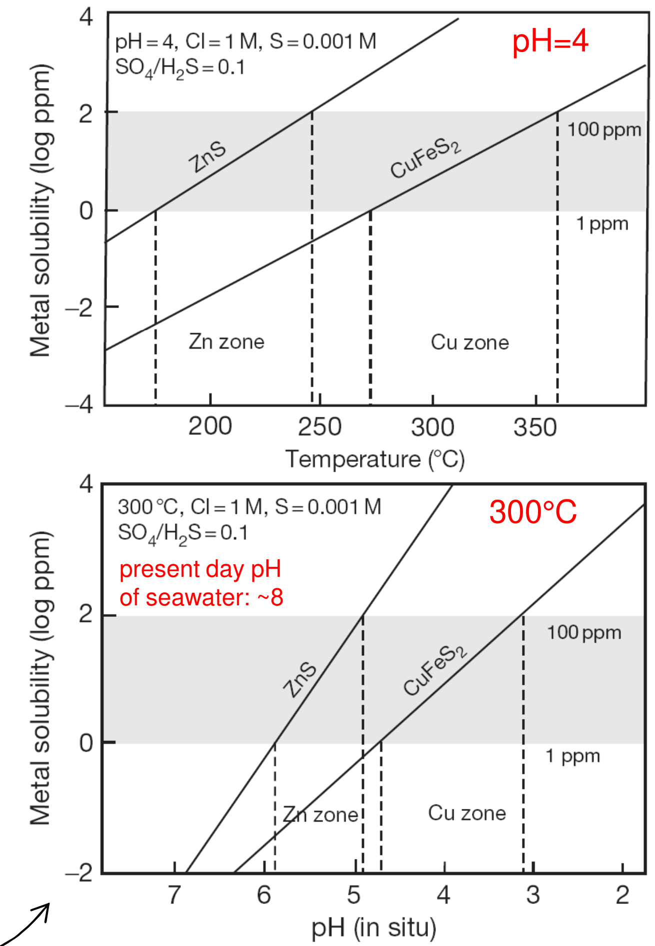

Solubility of **chalcopyrite** and **sphalerite** (in ppm) in **hydrothermal fluids** dependent on **temperature** and **pH value**.

Hannington, 2014, Treatise on geochemistry

Mid ocean ridges – magmatic processes

SYNTHESIS - ABSTRACT

- MORB‘s provide information about the **(upper) mantle** of the Earth
- They form by **decompression partial melting** of predominantly **spinel-peridotie (lherzolite)**, melting degrees (F) are in the order of **8-10%**
- MORB‘s have overall **depleted trace-element patterns**, and SiO_2 and MgO contents of undifferentiated magmas are **comparatively uniform** (~50 wt% and ~8-10 wt%, respectively)
- **Ni** and **Cr** contents of **undifferentiated (primary) magmas** in equilibrium with mantle peridotite are ~**400 ppm Ni** and ~**500-600 ppm Cr**
- Low-pressure **fractional crystallisation** of **Ol + Plag + Cpx** lowers MgO, CaO, Al_2O_3, Ni and Cr contents, but increases SiO_2
- **Radiogenic Nd - Hf** and **unradiogenic Sr** isotope compositions of MORB indicate that the **depletion of the upper portion of the mantle** started **early in Earth‘s history** (evidence for this also comes from short-lived ^{146}Sm (103 Ma) ^{142}Nd)

Chapter 3

(Oceanic) Island Arcs

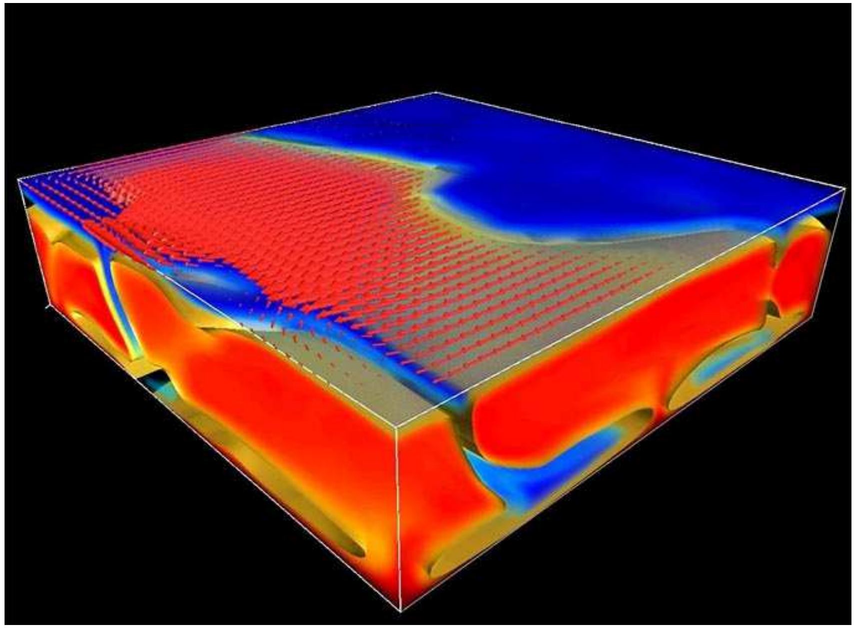

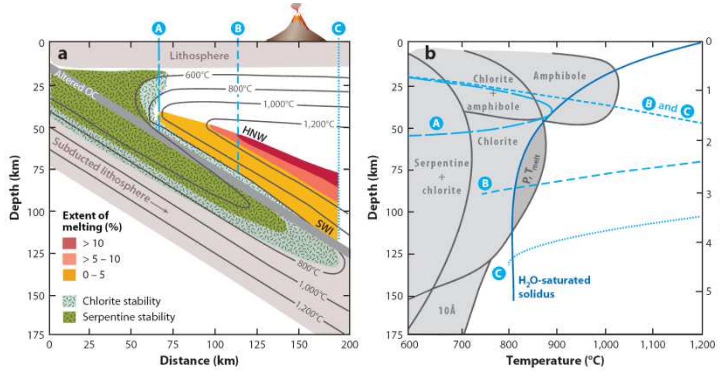

Grove et al., 2012

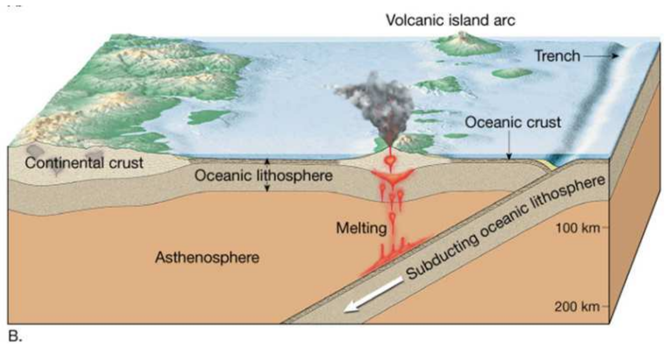

Arc magmatism: Introduction – Terms - Rocks

Three selected terms relevant in the context of arc magmatic rocks

Adakite: An andesite or dacite with very high LRRE at low HREE (La/Yb>9, very high Sr/Y, e.g. >50) (from Adak Island)

Boninite: Andesites and basaltic andesites with very low TiO_2 (< 0.5 wt%) but very high MgO (from Bonin Island)

Calc-alkaline: Magmas with higher Na+K and SiO_2 at given Mg# than in tholeiites

From: Kelemen, 2003, Treatise on Geochemistry

Arc magmatism is caused by subduction zone processes: What happens during subduction?

Dehydration of subducting oceanic lithosphere is **not** a single, but a **continuous event** from near surface down to ~**200 km** or more!

Primitive arc magma with an initial water content of ~1.7 wt%

Hydrated oceanic crust with ~5-6 wt% H_2O

Nevertheless, the **volcanic front** is a relatively **narrow** zone!

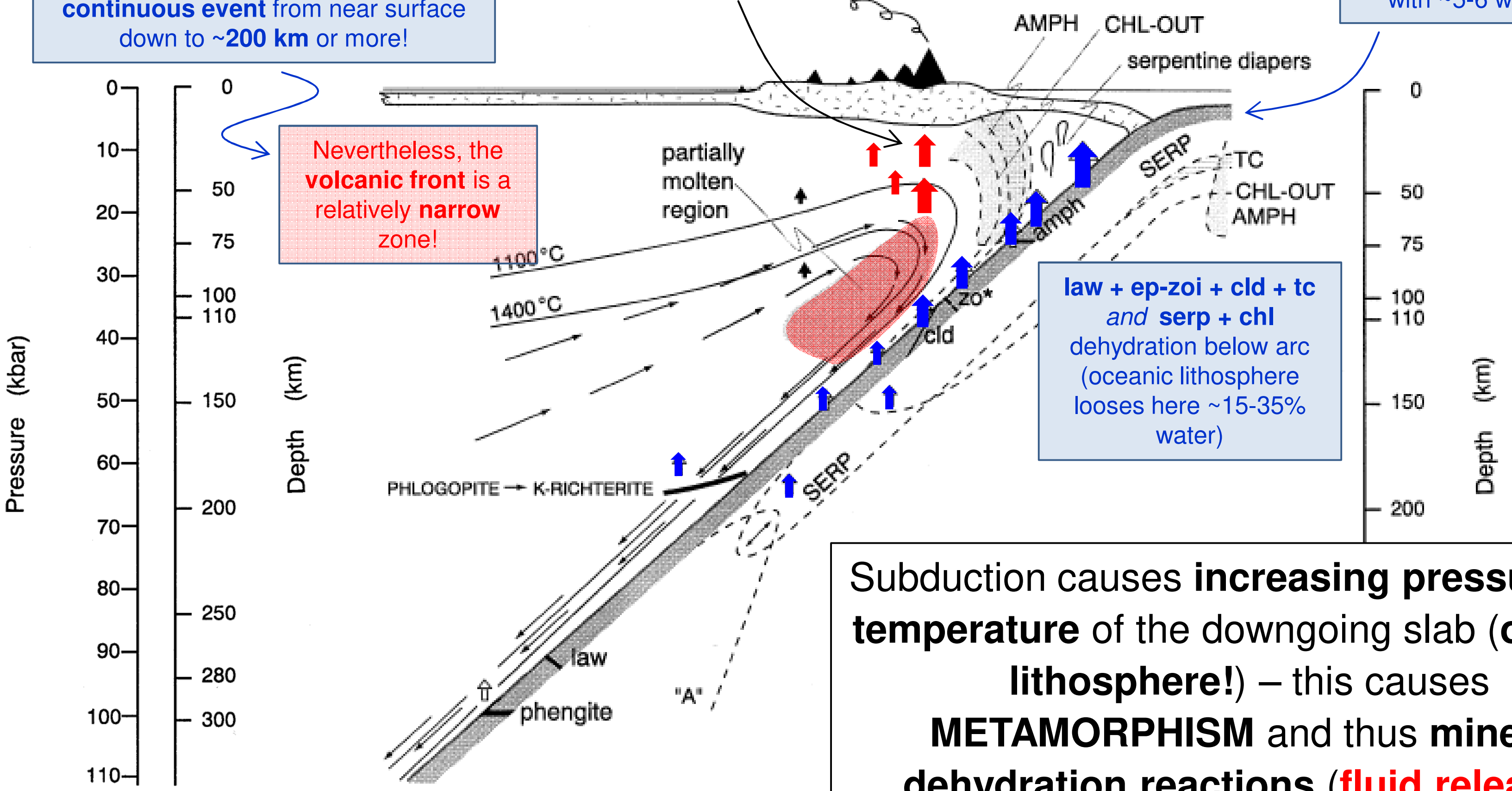

law + ep-zoi + cld + tc *and* **serp + chl** dehydration below arc (oceanic lithosphere looses here ~15-35% water)

From: Schmidt & Poli, 1998

Subduction causes **increasing pressure and temperature** of the downgoing slab (**oceanic lithosphere!**) – this causes **METAMORPHISM** and thus **mineral dehydration reactions** (**fluid release!**)

What happens during subduction?

Water bearing phases in hydrous basalt and peridotite

Phases stable in hydrous basalt (numbers in parentheses give H_2O content in wt%)

Chlorite (~12%)	$(Fe,Mg,Al)_6(Si,Al)_4O_{10}(OH)_8$
Lawsonite (~11.3%)	$CaAl_2Si_2O_7(OH)_2 \cdot H_2O$
Epidote (~1.9%)	$Ca_2Fe^{3+}Al_2(Si_2O_7)(SiO_4)O(OH)$
Zoisite (~1.9%)	$Ca_2Al_3(Si_2O_7)(SiO_4)O(OH)$
Amph (e.g. Glaukophane, ~2.1%)	$Na_2(Mg,Fe^{2+})_3Al_2Si_8O_{22}(OH)_2$
Paragonite (~6.1%)	$NaAl_2(Si_3Al)O_{10}(OH)_2$
Chloritoid (~7.4%)	$(Fe^{2+},Mg,Mn)_2Al_4Si_2O_{10}(OH)_4$
Phengite (~2.5%)	$KAl_2(Si_4O_{10})(OH,F)_2$

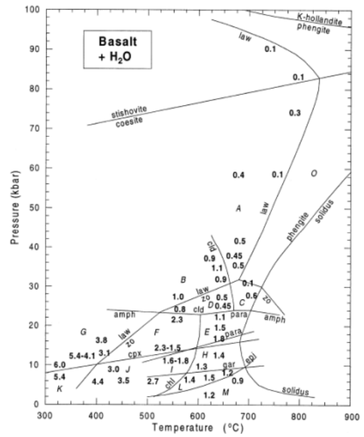

Phases stable in hydrous peridotite (numbers in parentheses give H_2O content in wt%)

Serpentine (e.g. Chrysotil, ~13%)	$Mg_3Si_2O_5(OH)_4$
Talc (~4.7%)	$Mg_3Si_4O_{10}(OH)_2$
Chlorite (~10.8%)	$(Fe,Mg,Al)_6(Si,Al)_4O_{10}(OH)_8$
Amphibole (e.g. Aktinolite, ~2.3%)	$Ca_2(Mg,Fe^{2+})_5Si_8O_{22}(OH)_2$
Phase A (~11.8%)	$Mg_7Si_2O_8(OH)_6$

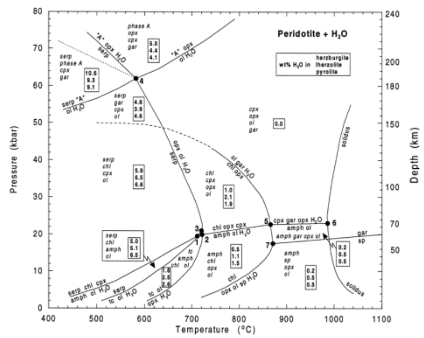

What happens during subduction?

Dehydration phase relations in hydrous basalt and peridotite

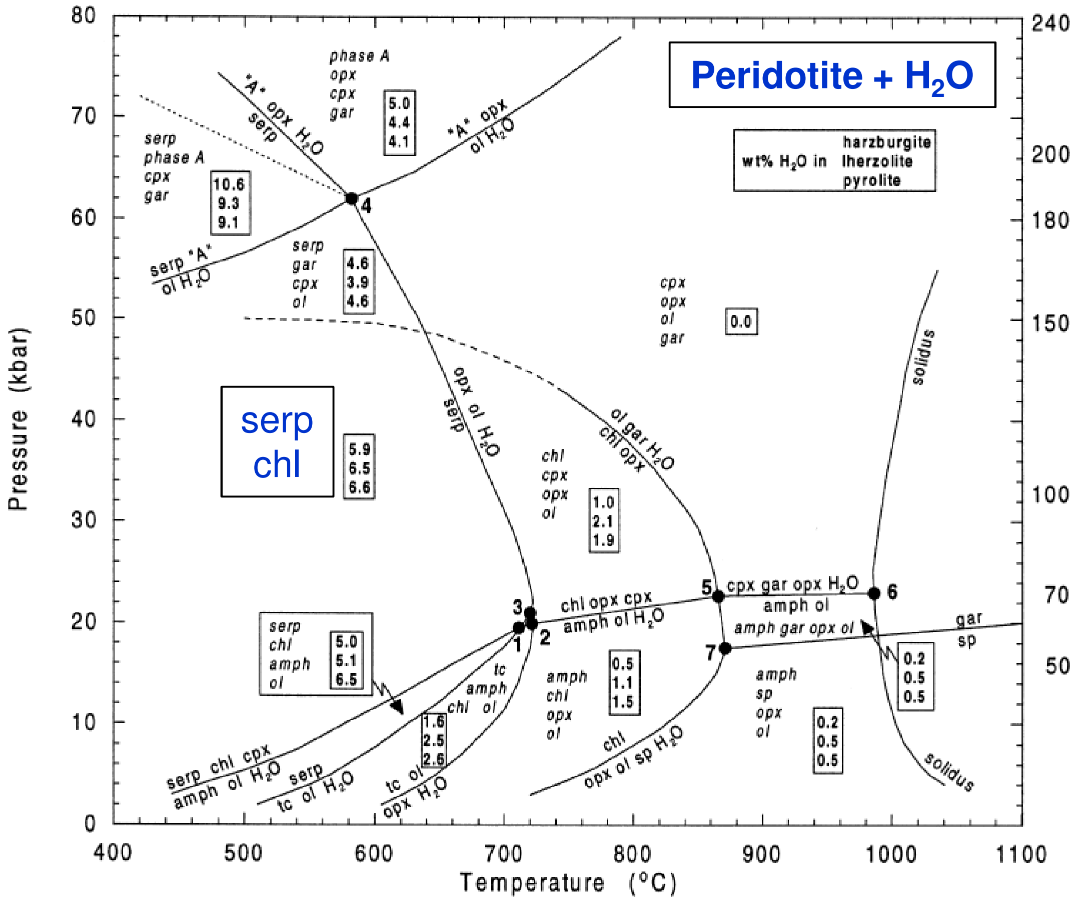

Numbers denote max. water contents!

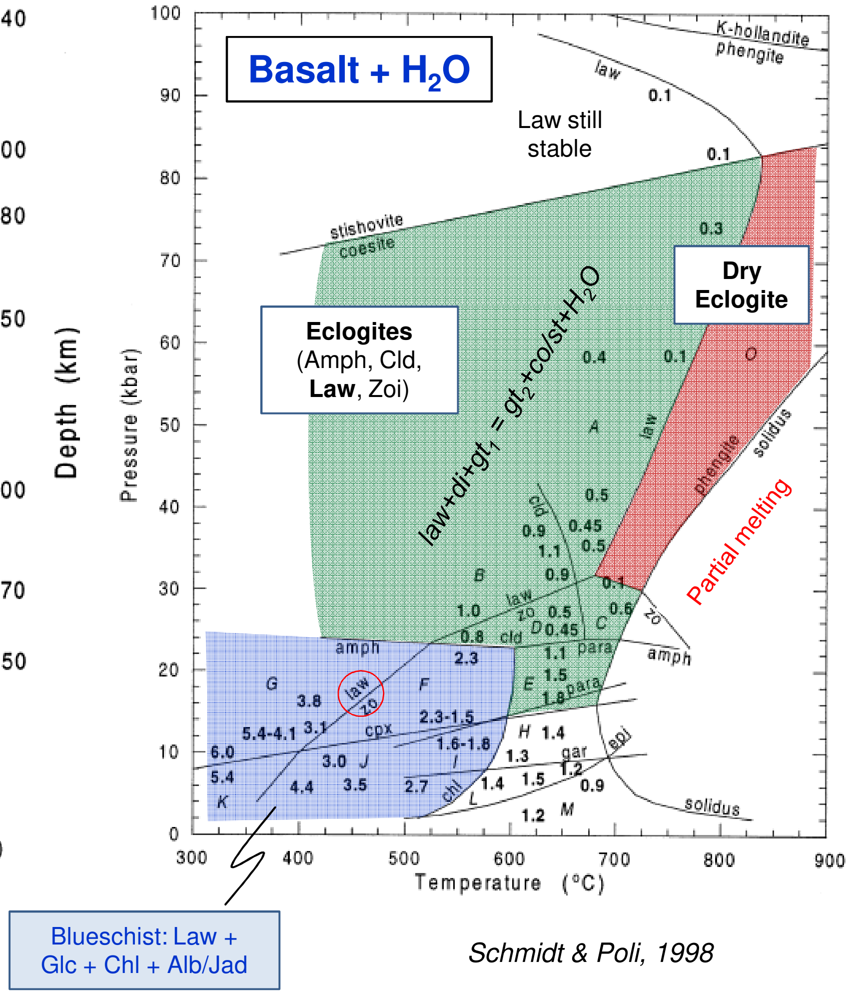

1 GPa = 10 kbar ~ 30 km depth

Schmidt & Poli, 1998

What happens during subduction?

Thermal structure within a subduction zone

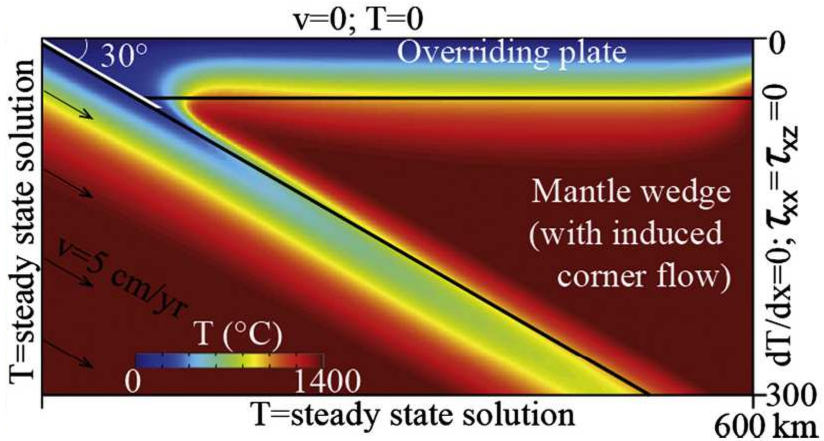

Builhol et al., 2015

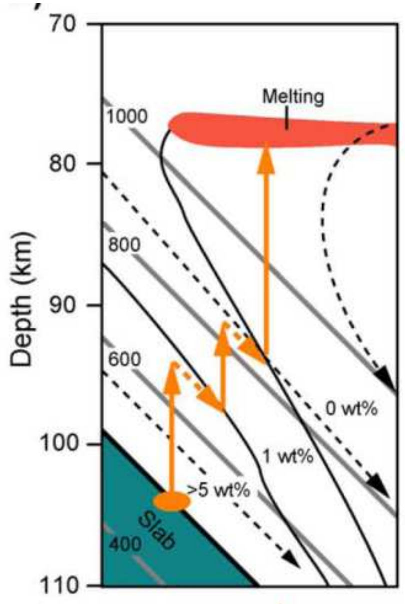

Manning, 2004

Thermal structure within a subduction zone and **flow path of fluids**

Kogiso et al., 2009

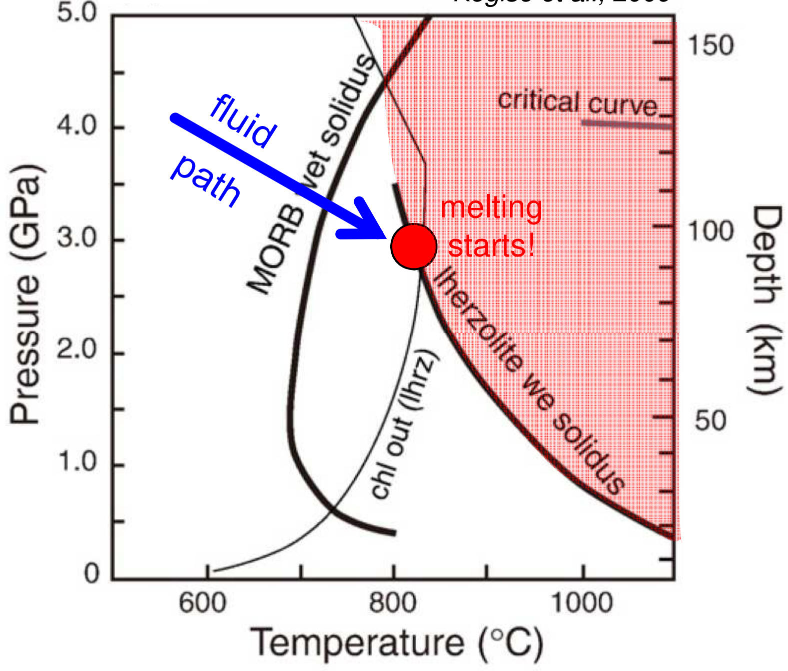

Fluid rises **upwards** towards **higher** temperatures until the solidus of **wet lherzolite** is reached !!!!

What happens during subduction?

Solidi and dissociation curves in subduction zone lithologies

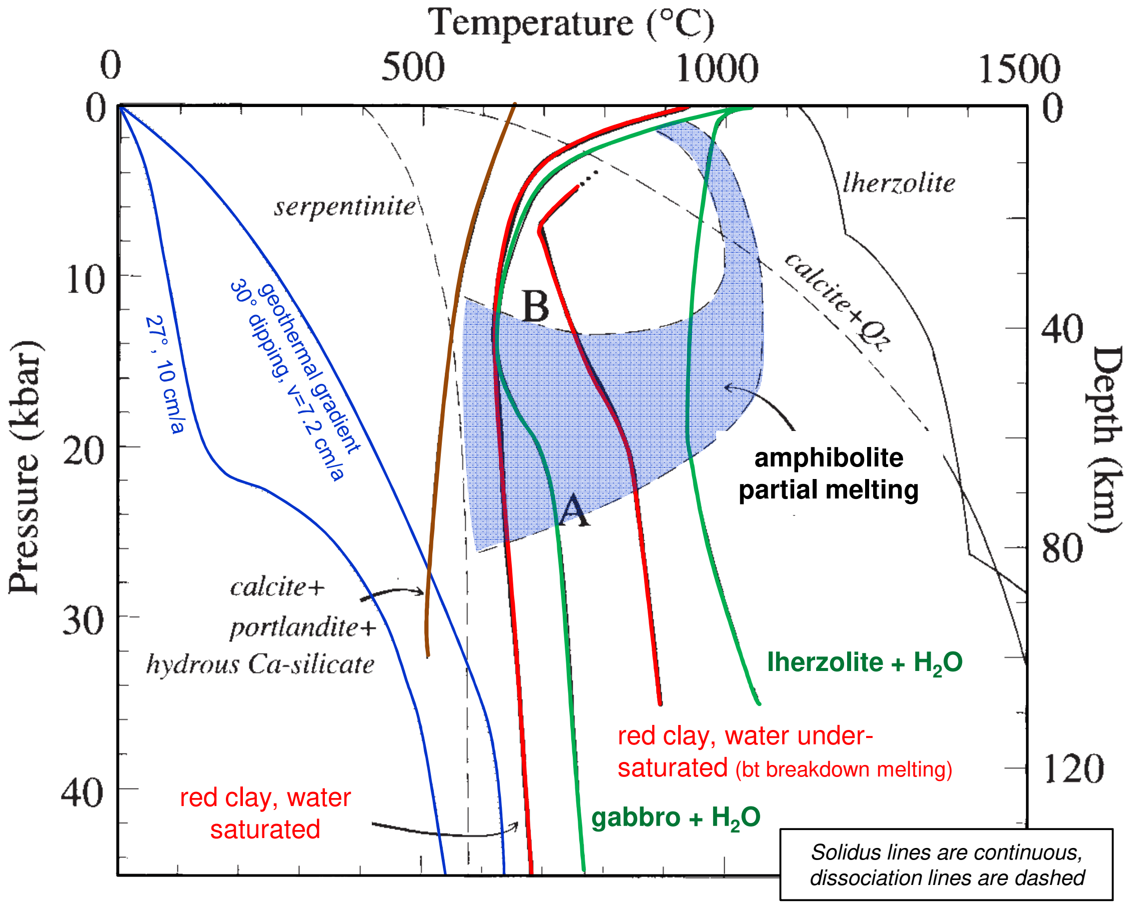

Nichols et al., 1994, Nature

Melting of subduction zone lithologies (oceanic crust, oceanic mantle lithosphere & subducted sediments) requires **slow subduction (<5-6 cm/a)**

But, if melting does occur, the melting order might be as follows:
Carbonates > clay + H_2O > gabbro + H_2O > clay (us) > lherz. + H_2O

1 GPa = 10 kbar ~ 30 km depth

What happens during subduction?

Temperature distrubution – real estimates

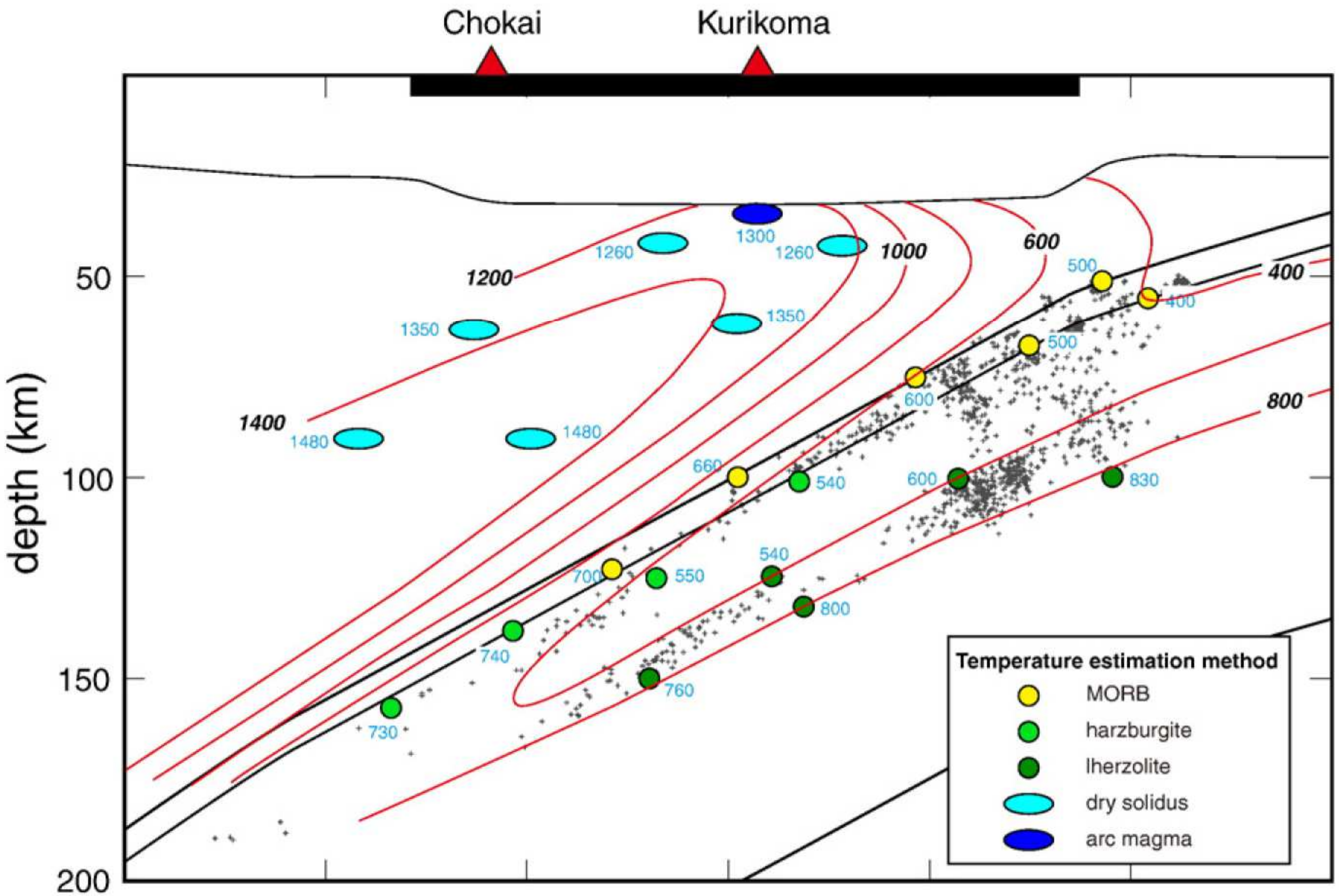

Kogiso et al., 2009

Estimated **temperature distribution** beneath NE Japan.

Note the distribution of **intraslab earthquakes**, which are assumed to be caused by **dehydration reactions** (‚dehydration embrittlement‘)

1 GPa = 10 kbar ~ 30 km depth

What happens during subduction?

Phase relations and **solidi** in (hydrated) pelagic sediments

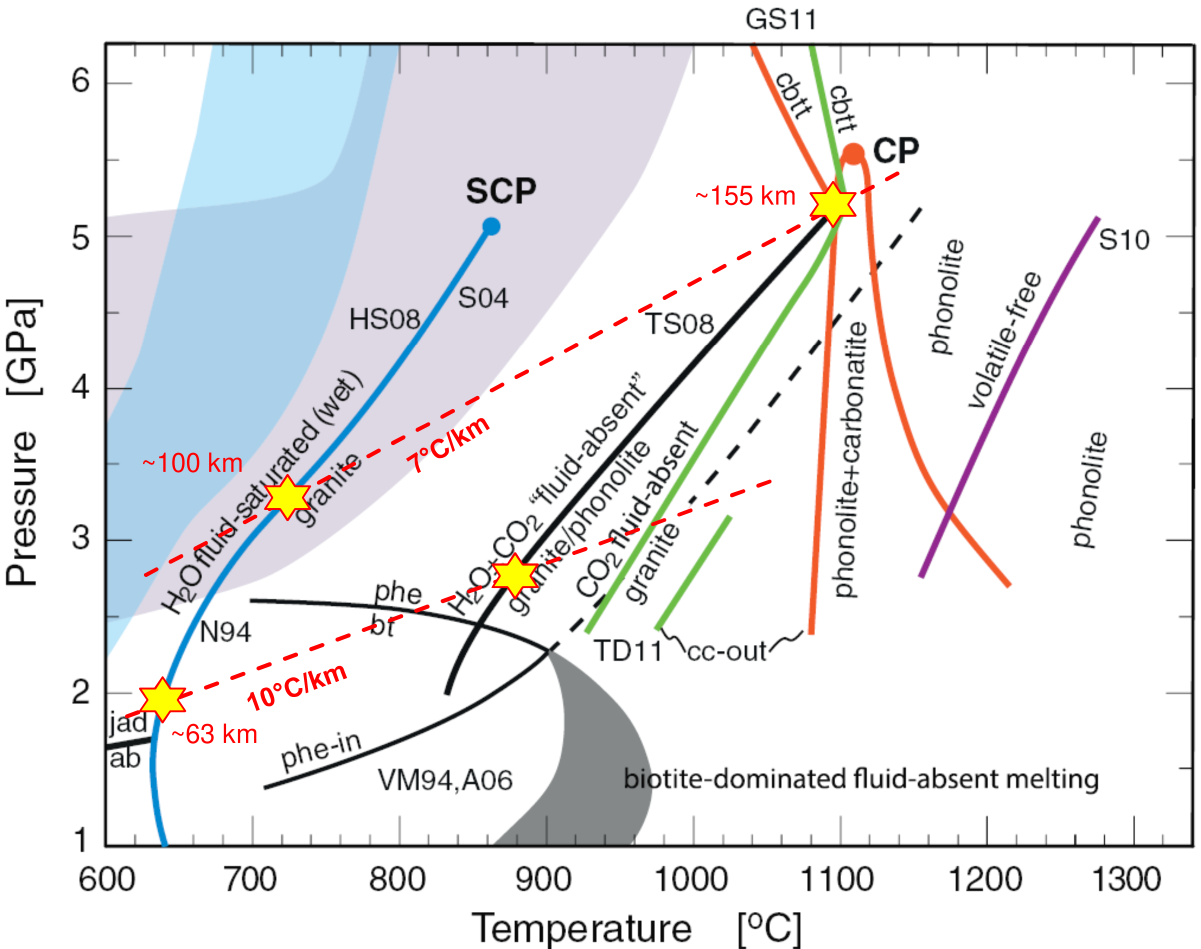

Mann & Schmidt, 2015

Pelites and **greywackes** make up to **~10%** of the uppermost oceanic crust. Their **water contribution** is small, but they host high contents of **LILE** (Cs, Rb, Ba, K, Sr) and **^{10}Be** (and **^{207}Pb**)

At higher temperature gradients, dragged **sediments** will start melting! Melts will have a hydrous granodioritic to granitic composition.

1 GPa = 10 kbar ~ 30 km depth

What happens during subduction?

Will the downgoing magmatic lithosphere melt?

Hydrous peridotite

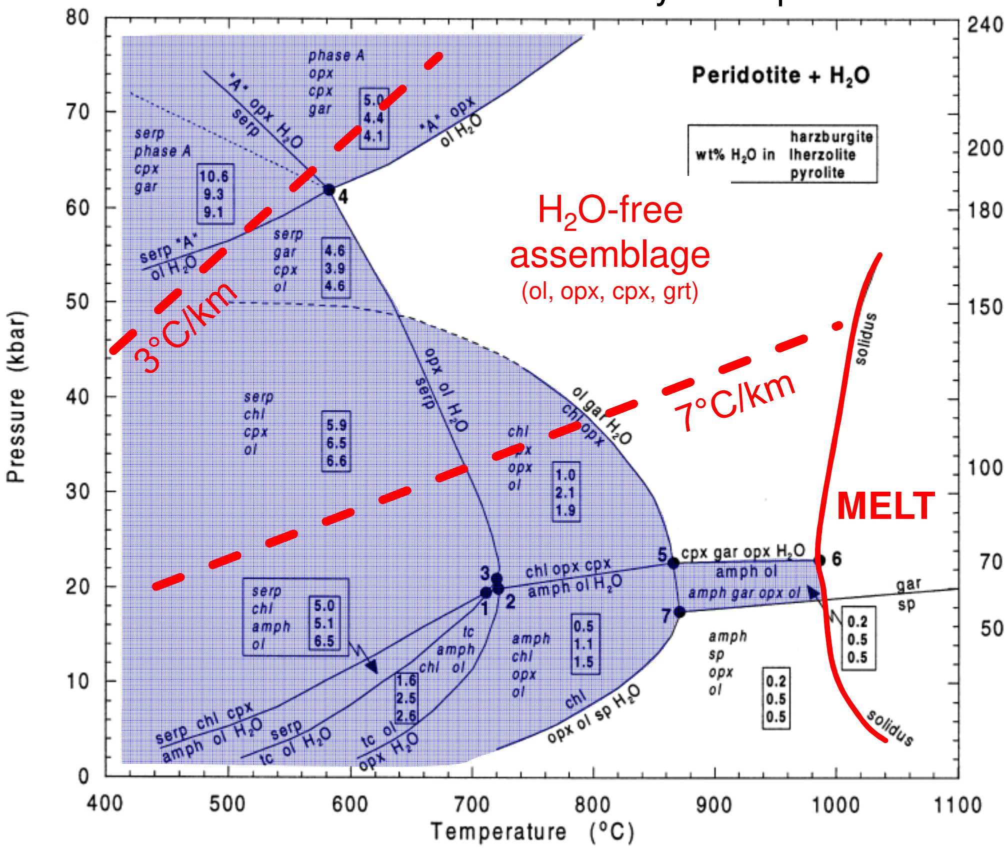

Hydrous basalt

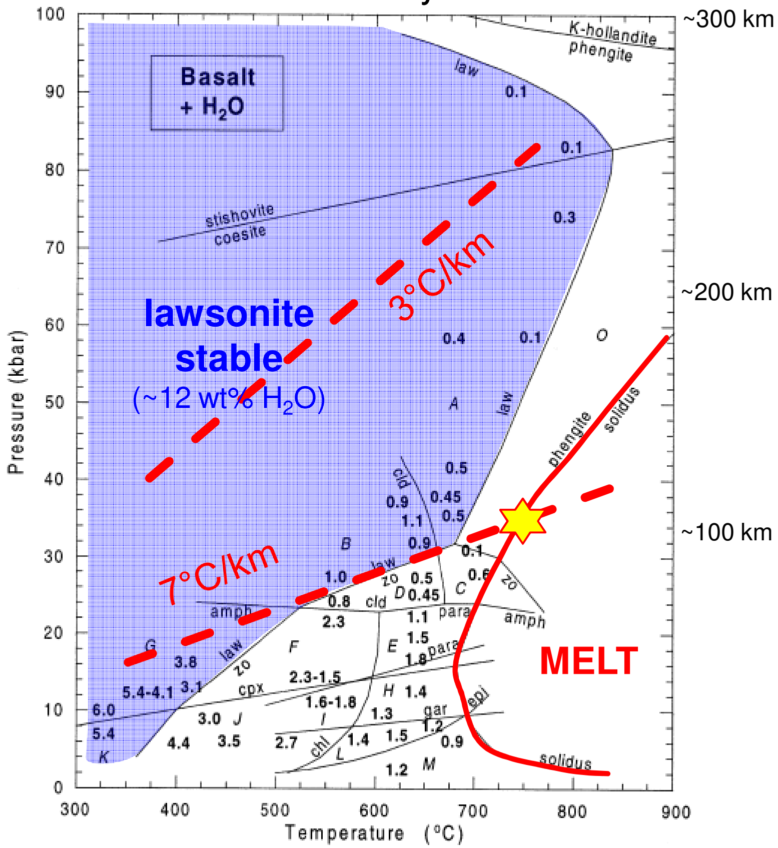

Schmidt & Poli, 1998

1 GPa = 10 kbar ~ 30 km depth

Chemical signatures in island arc magmas

Major element characteristics

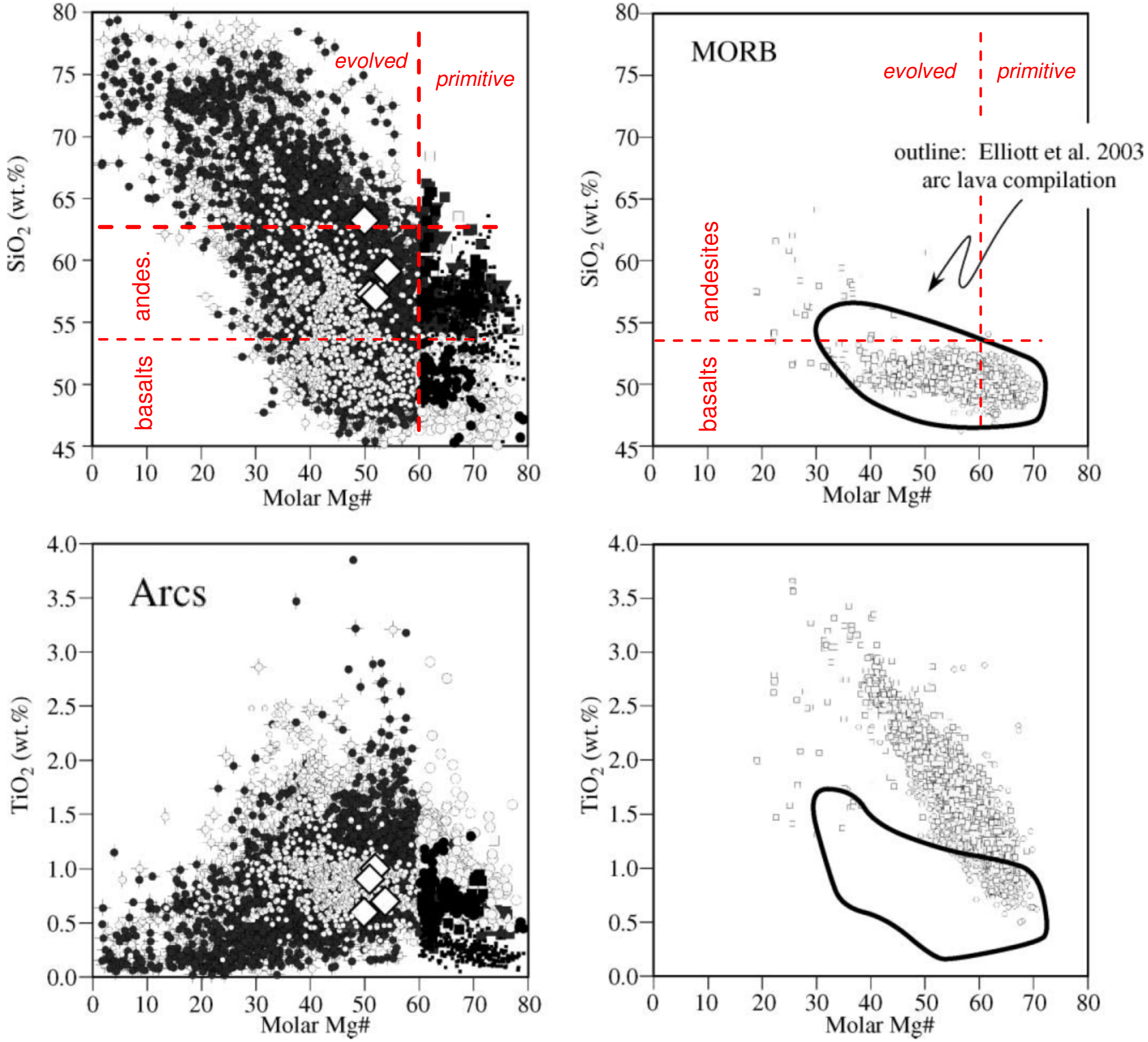

Primitive island arc magmas have SiO_2 up to **~63 wt%**, TiO_2 is **lower** than in MORB. These are **primary features**! Decrease of TiO_2 from Mg#~50 marks onset of Fe-Ti-oxide crystallisation.

$$Mg\#=100\times molar\left[\frac{MgO}{MgO+FeO}\right]$$

From: Kelemen et al., 2003, Treatise on Geochemistry

Chemical signatures in island arc magmas

Major element characteristics

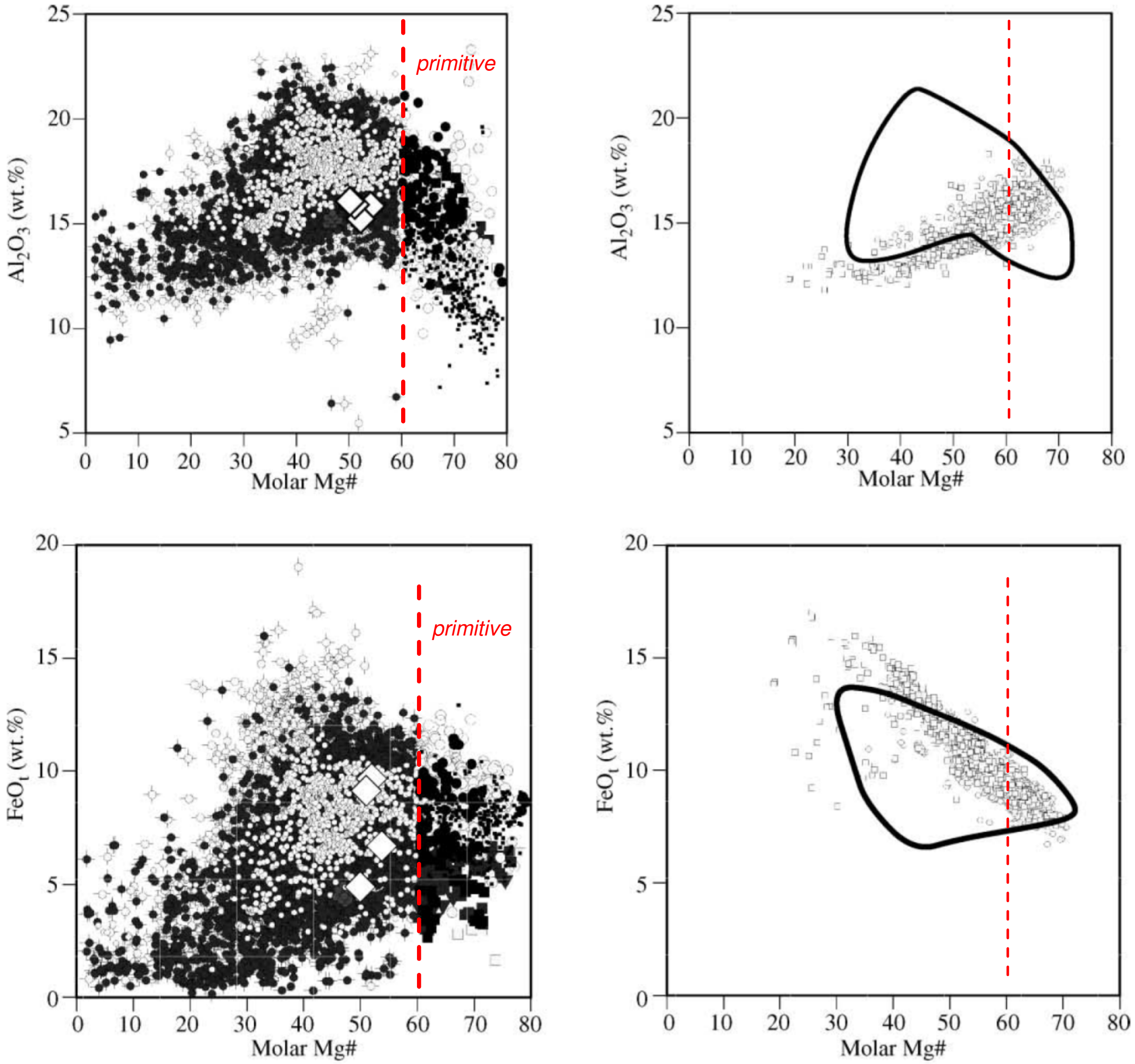

Al_2O_3 tends to be **similar** or higher as in MORB, with firstly increasing, then decreasing values from **Mg#~45** (onset of **plag** fractionation).

Primary arc magmas predominantly crystallise **ol + cpx** (±opx) to form <u>wehrlite</u>, <u>(ol)-clinopyrox-enite</u>, <u>websterite</u>. **Hornblende** is unstable if liquidus temperatures are >1100°C

From: Kelemen et al., 2003, Treatise on Geochemistry

Chemical signatures in island arc magmas

Major element characteristics

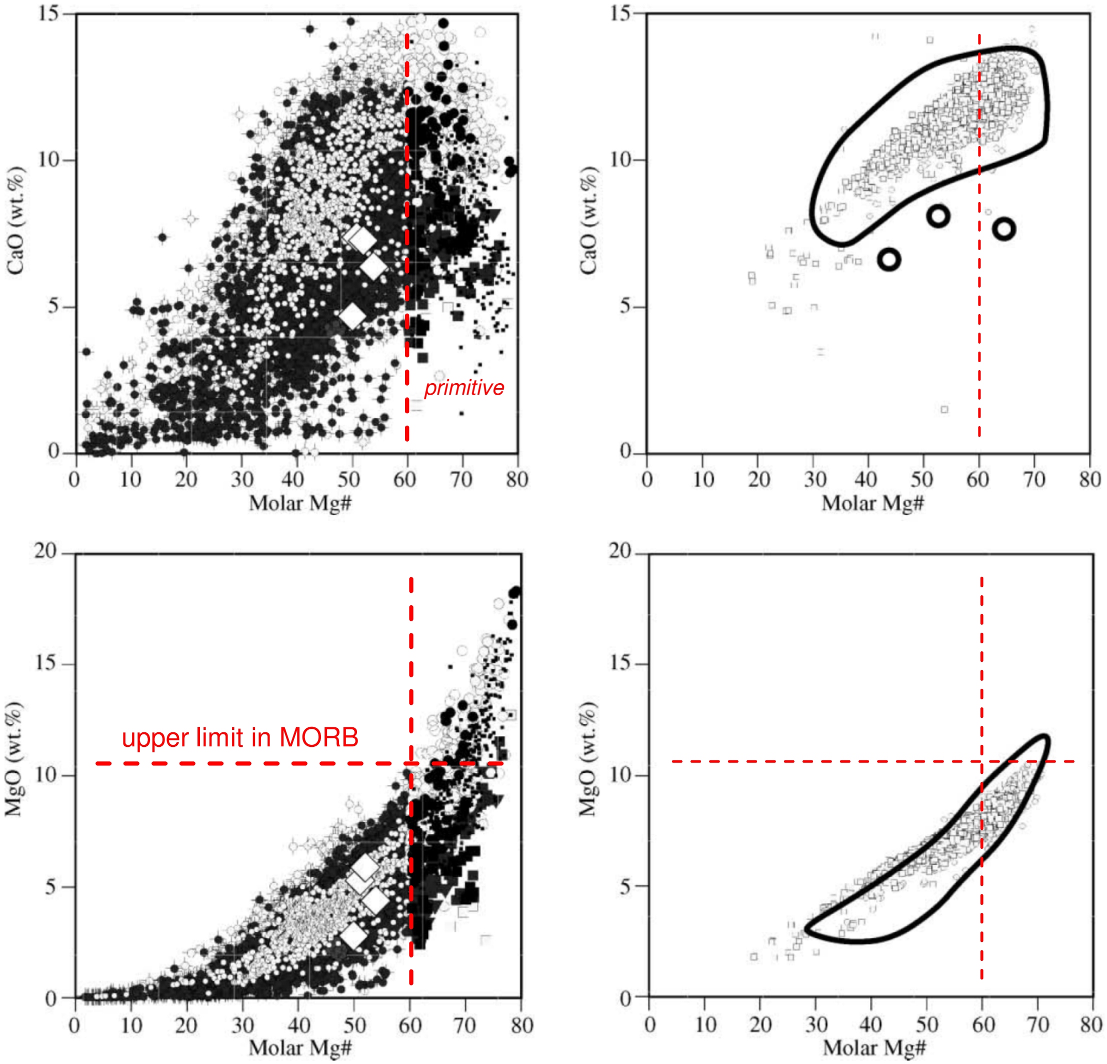

CaO in primitive arc lavas is similar or mostly **lower** than in MORB. Evolved series have much lower CaO than evolved MORB. *The term calc-alkaline series for arc magmas is therefore **misleading**!!*

MgO values **exeed** those observed in the most **primitive MORB** lavas, but also decrease to much **lower** values

From: Kelemen et al., 2003, Treatise on Geochemistry

Chemical signatures in island arc magmas

Major element characteristics

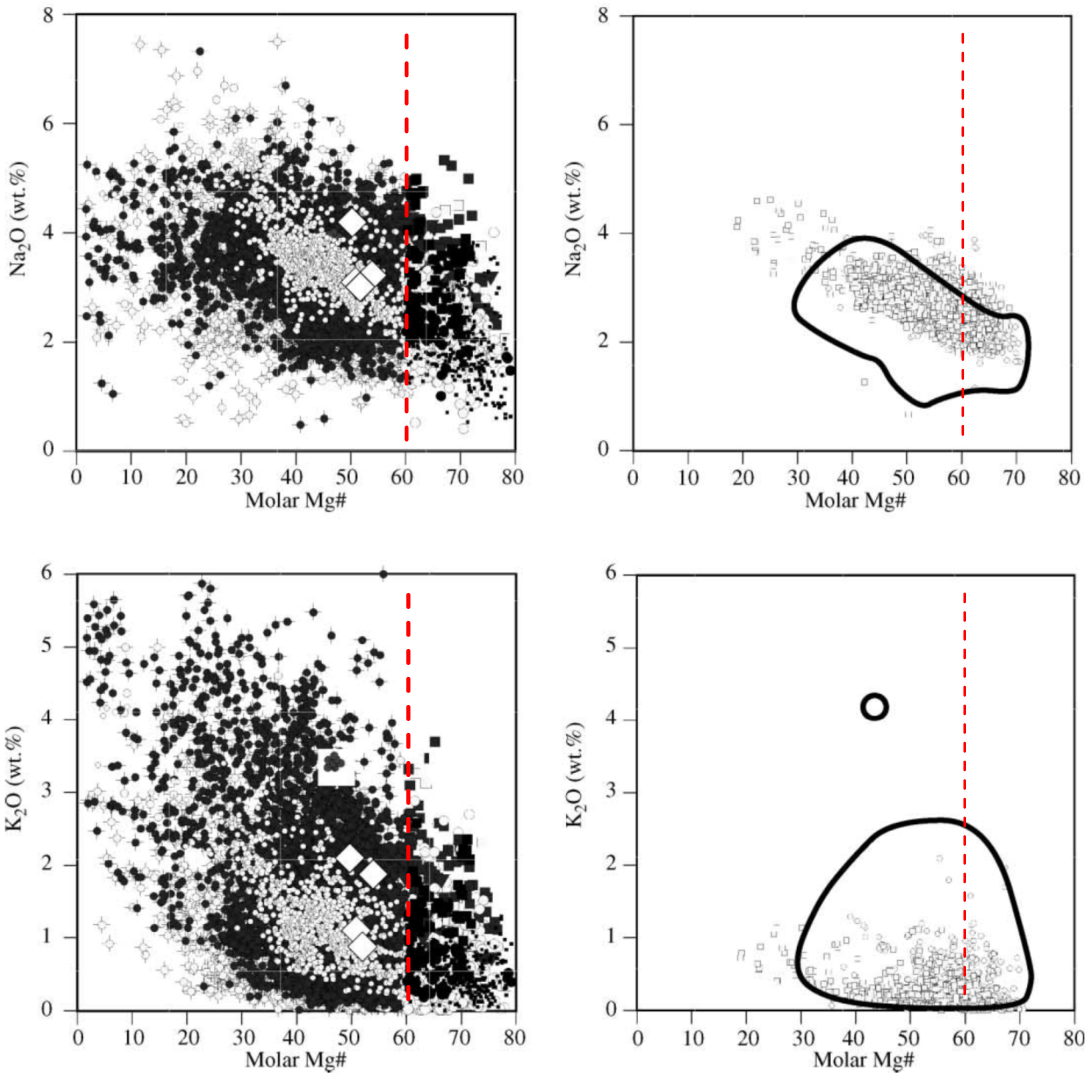

Na_2O and **K_2O** in primitive arc magmas can be both, **lower and higher** than in primitive MORB. This variation is a **primary feature,** reflecting the involvement of more **different chemical endmembers** (sub-arc mantle, subducted lithosphere, fluids & sediments) during arc magma generation than during MORB formation (i.e., not simply fractionation!)

From: Kelemen et al., 2003, Treatise on Geochemistry

Chemical signatures in island arc magmas

Primary & derivative arc magmas - summary

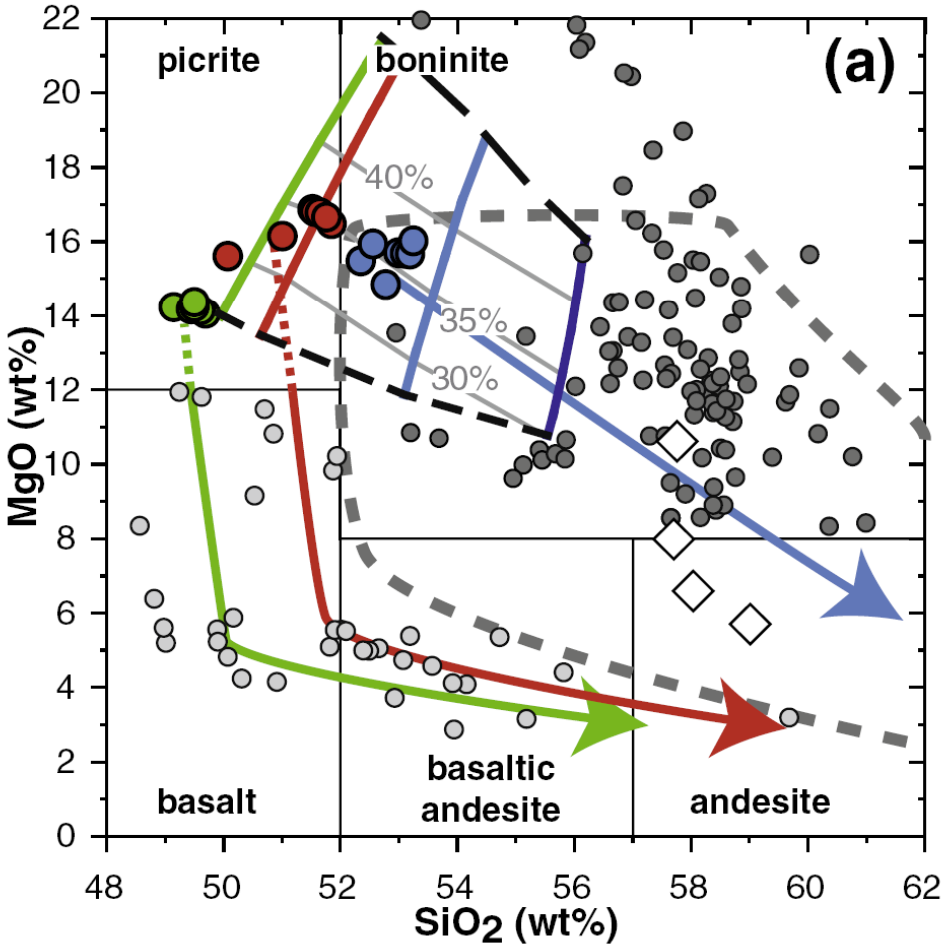

Red, green and blue dots are (SiO_2-rich) **picrites** and Ca-rich **boninites** from Bismarck and Kamchatka arcs. These rocks represent **near primay magmas** from a **silica-enriched refractory mantle wedge** (high modal opx, very little cpx, normal ol). Whether the primary magmas are more picritic or boninitic depends on the **water content of the mantle wedge** and melting pressure.

The source of SiO_2 in the wedge are likely slab derived fluids!

From: Benard et al. 2017

Chemical signatures in island arc magmas

Primary & derivative arc magmas - summary

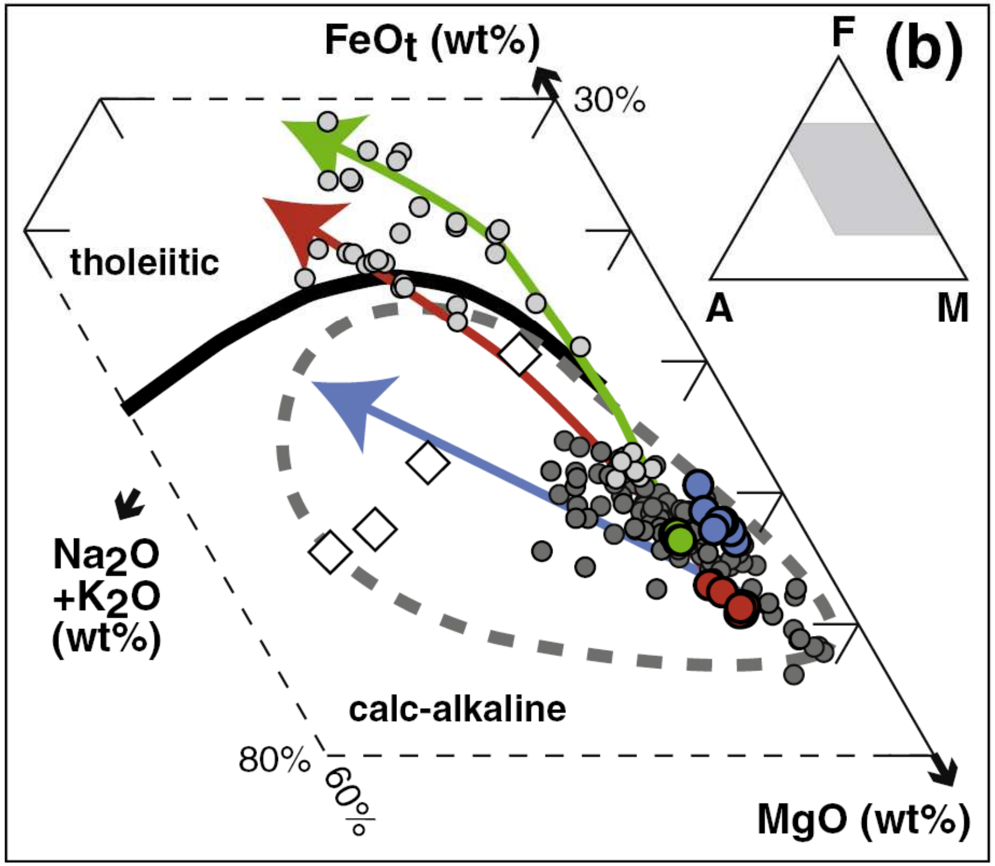

...... this is text ....

From: Benard et al. 2017

Chemical signatures in island arc magmas

Trace element characteristics

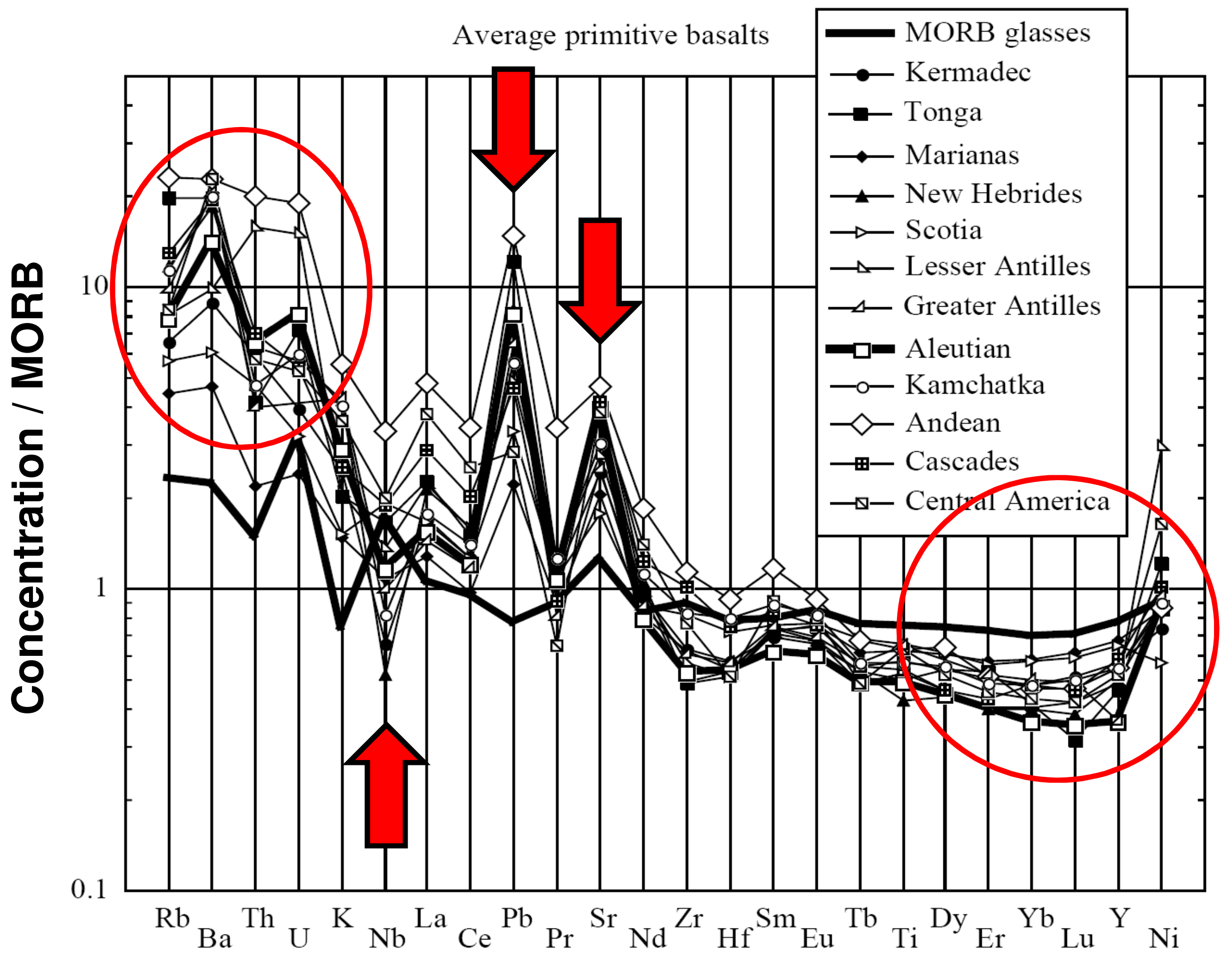

Kelemen et al., 2003, Treatise on Geochemistry

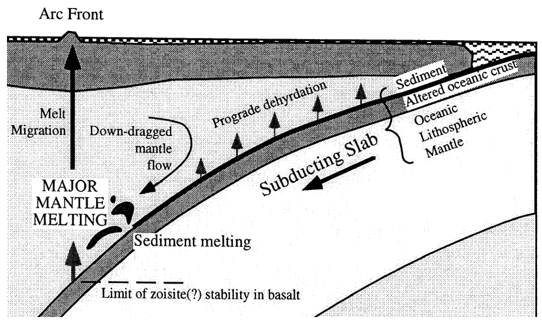

Elliott et al., 1997

Trace element characteristics of **primitive** island arc magmas <u>relative to MORB</u>:

- Enrichment in LILE
- Depletion in Nb and Ta
- Pos. Pb + Sr anomalies
- Depletion in HREE

Chemical signatures in island arc magmas

Causes of specific anomalies

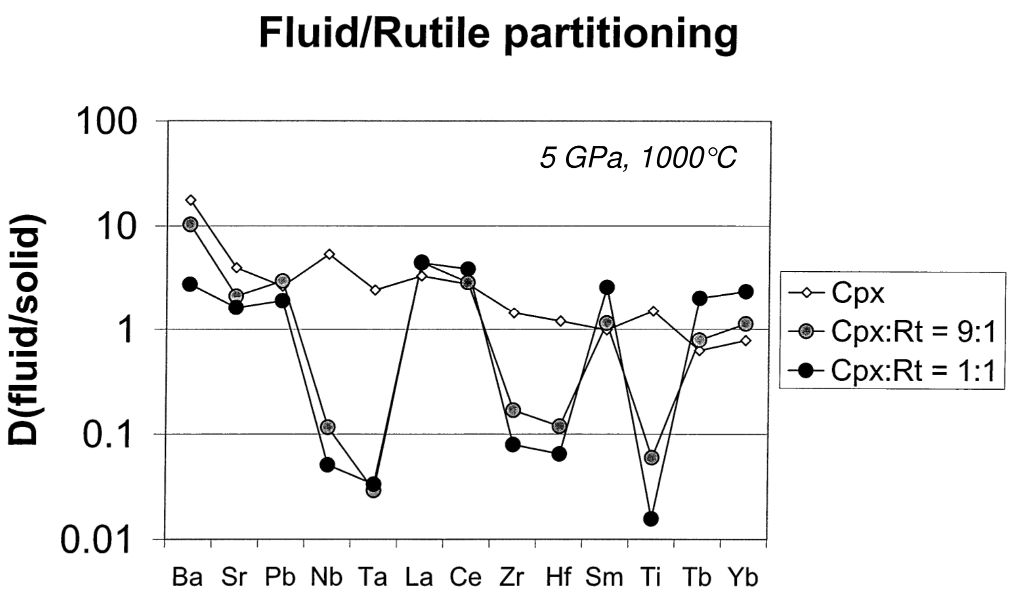

Partitioning of trace-elements between **fluid** and **cpx/rutile** at **5 GPa** (~150 km) and 1000°C. Note that all **HFSE** (Nb, Ta, Zr, Hf, Ti) **retain** in the residue as long as **rutile** is present

From: Stalder et al., 1998

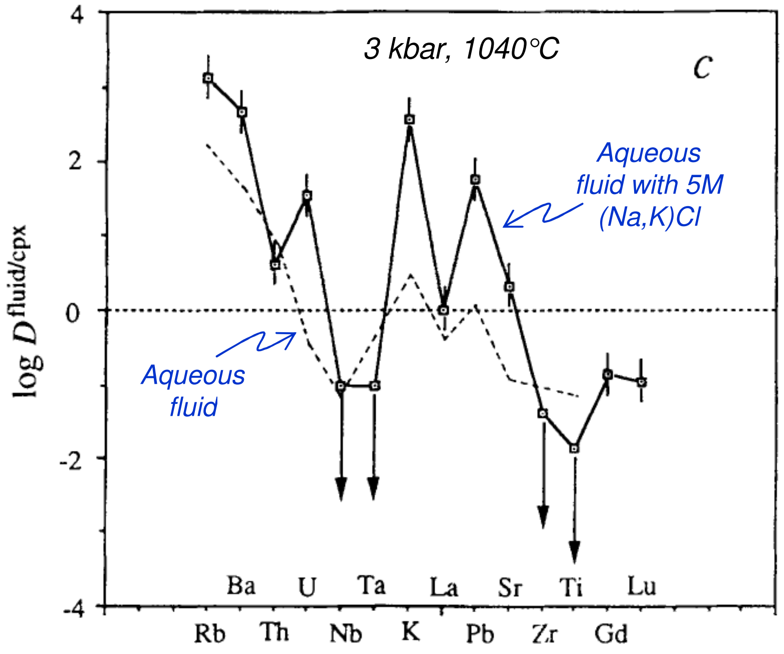

Partitioning of trace-elements between **fluid** and **clinopyroxene** at 3 kbar (~10 km) and 1040°C. **LILE, U, K, Pb** and ±Th but not Sr were **enriched in the fluid**, **HFSE** (and **HREE**) remain in the **solid phase**

From Keppler, 1996, Nature

Chemical signatures in island arc magmas

Causes of specific anomalies – rutile solubility in aqueous fluids

Rutile solubility only little depends on pressure!

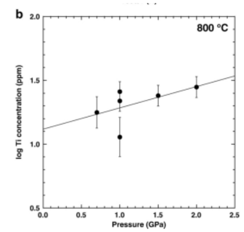

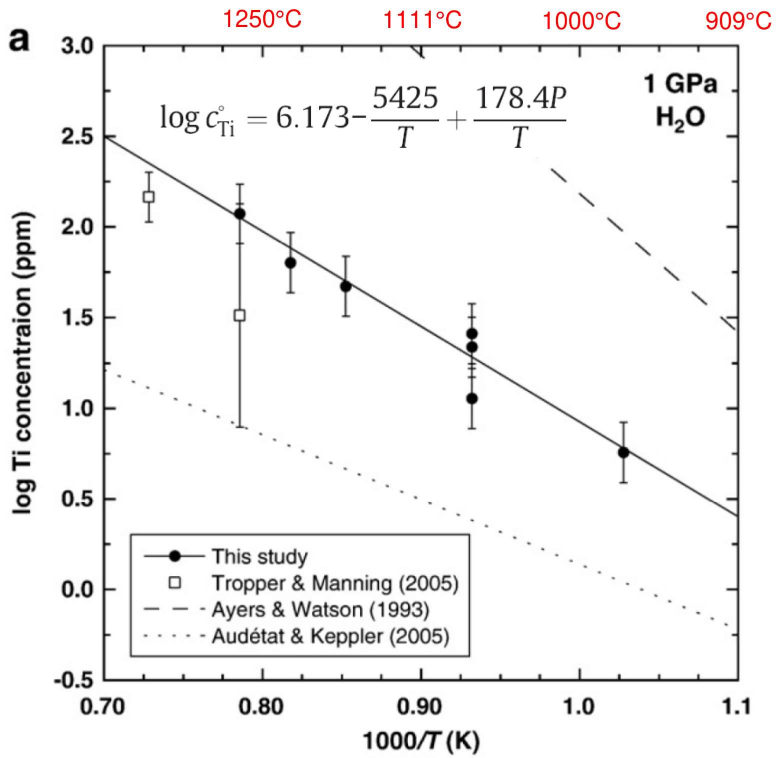

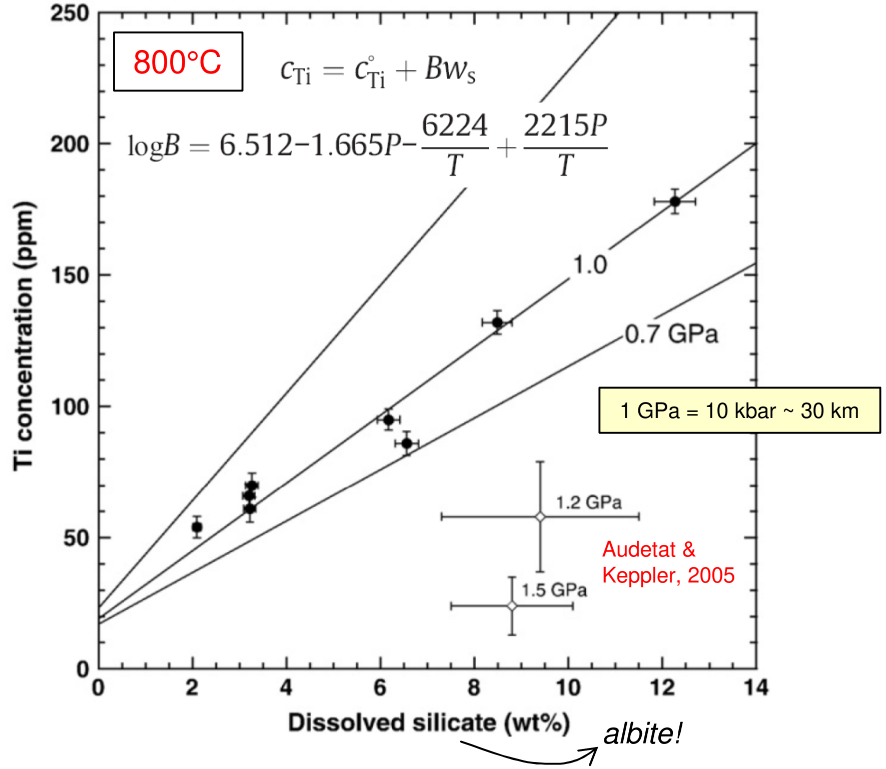

Solubility of **rutile** in **aqueous fluids** dependent on temperature, pressure and amount of **dissolved silicate** – **SOLUBILITY IS LOW !**

From Antignano & Manning, 2008, Chemical Geology

Chemical signatures in island arc magmas

Causes of specific anomalies – rutile saturation in silicate melts (during eclogite melting)

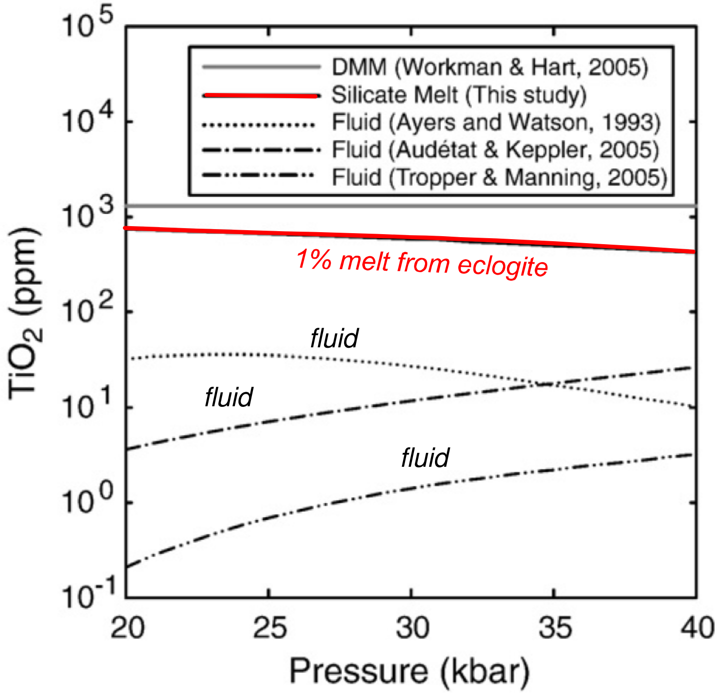

TiO_2 concentration in a melt produced by **1% partial melting** of a MORB-type **eclogite** at <u>H_2O saturated</u> conditions

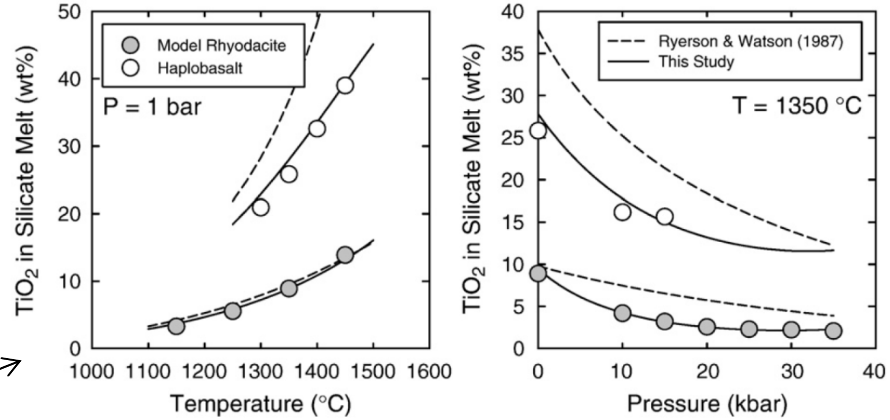

Rutile saturation in model **rhyodacite** and **basalt** as a function of pressure and temperature

Gaetani et al., 2008, EPSL

1 GPa = 10 kbar ~ 30 km

These experiments lead to this result and to this conclusion:

The **low** TiO_2 saturation concentration in melts formed <u>potentially</u> during **eclogite melting** during **slow subduction** suggests that **rutile will remain stable in the downgoing slab** !

Chemical signatures in island arc magmas

More experiments.... at ~ 5-6 GPa the solubility of most elements increases drastically

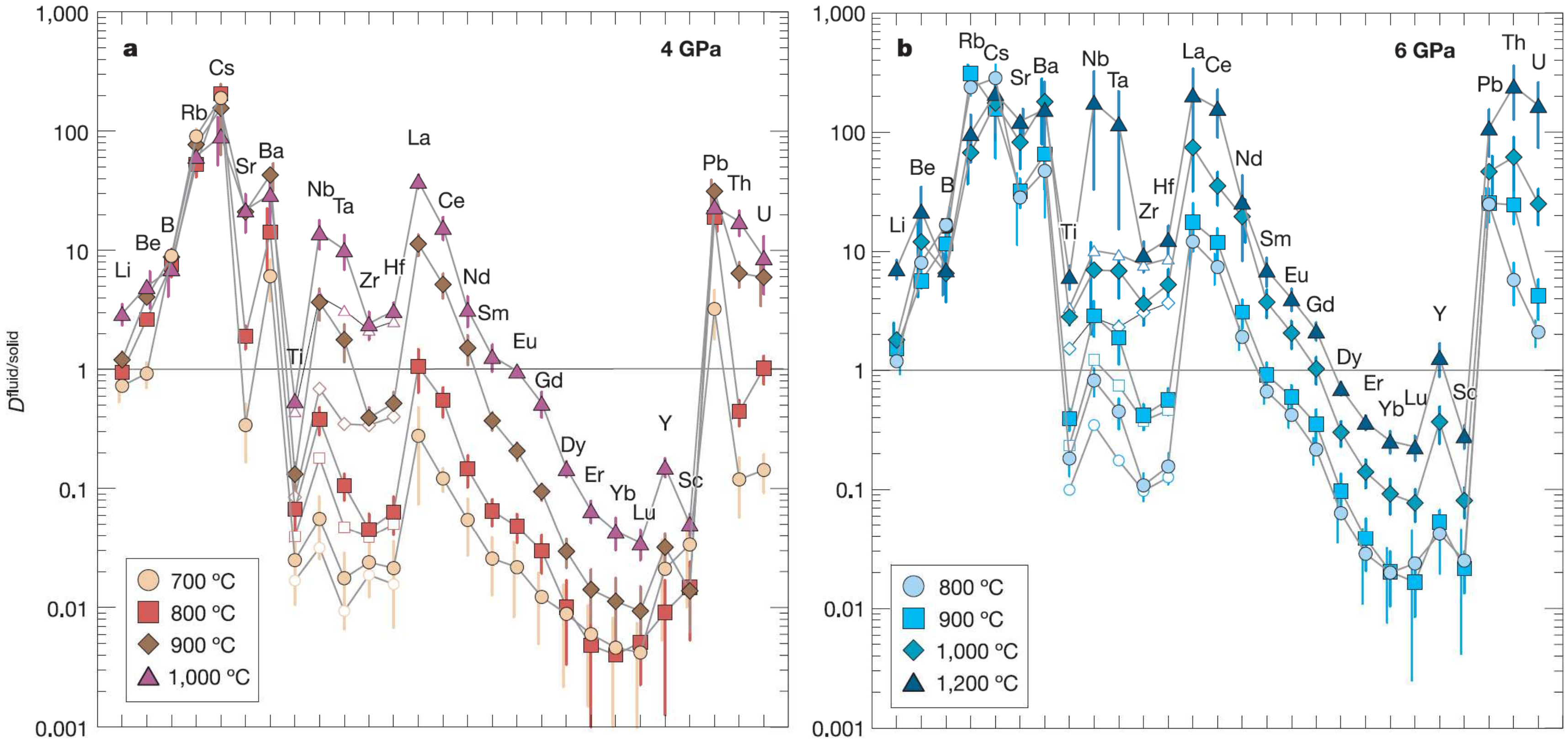

Partitioning of trace-elements between **fluids/supercritical liquids** and **residual eclogite** at 4 and 6 GPa (~120 and ~180 km)

From Kessel et al., 2005, Nature

Chemical signatures in island arc magmas

Speciation exemplary shown by Y-H_2O-Cl-F complexes

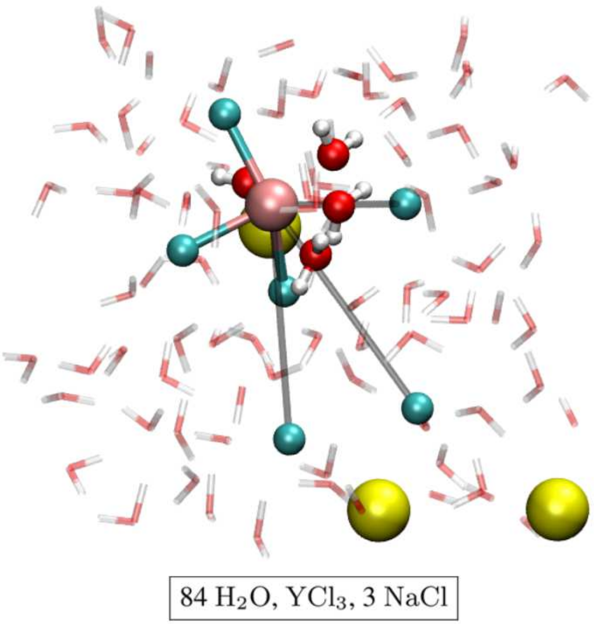

Stefanski & Jahn, 2020

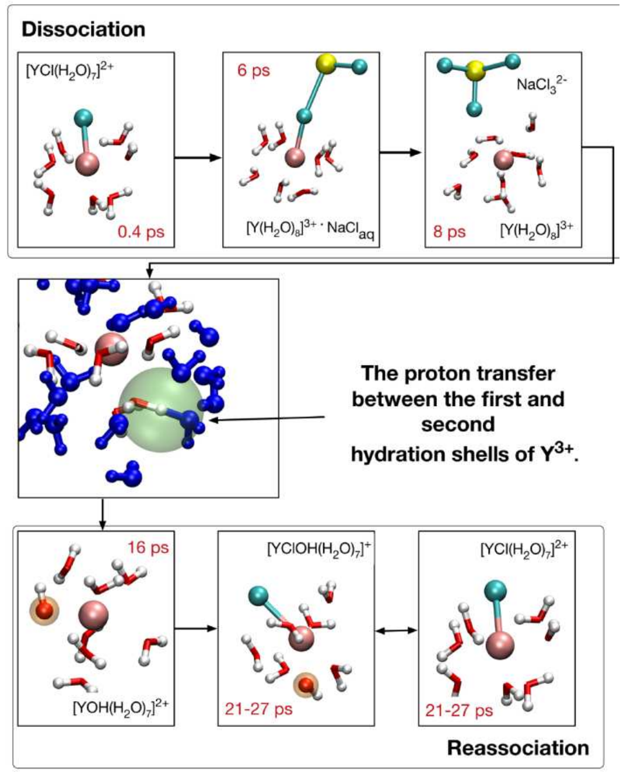

Partitioning of trace-elements between **fluids/supercritical liquids** and **residual eclogite** at 4 and 6 GPa (~120 and ~180 km)

Chemical signatures in island arc magmas

Sediment vs. fluid signature in arc magmas

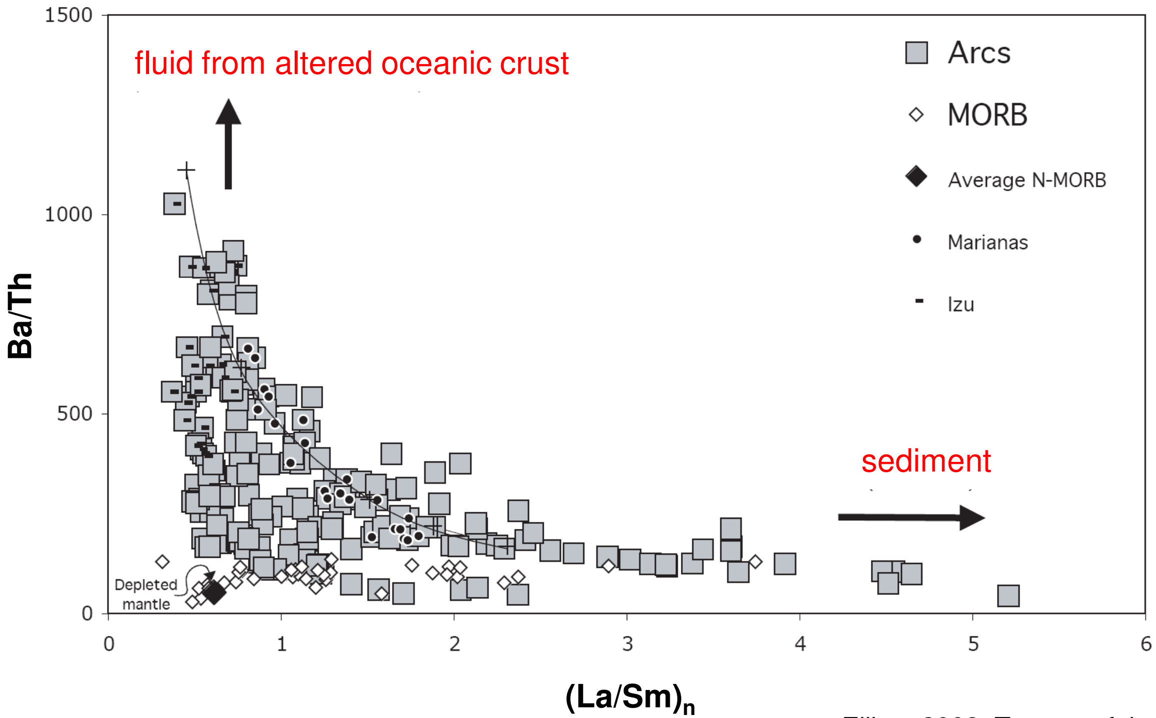

Elliott, 2003, Tracers of the slab

Barium is fluid mobile, Th is not, but **Th is enriched in sediments** over Ba. **La/Sm** in **fluids** from altered mafic crust is **low** (i.e., mostly unfractionated relative to MORB), but **high** in **continent derived** pelagic sediments (clay)

Chemical signatures in island arc magmas

Sediment vs. fluid signature in arc magmas

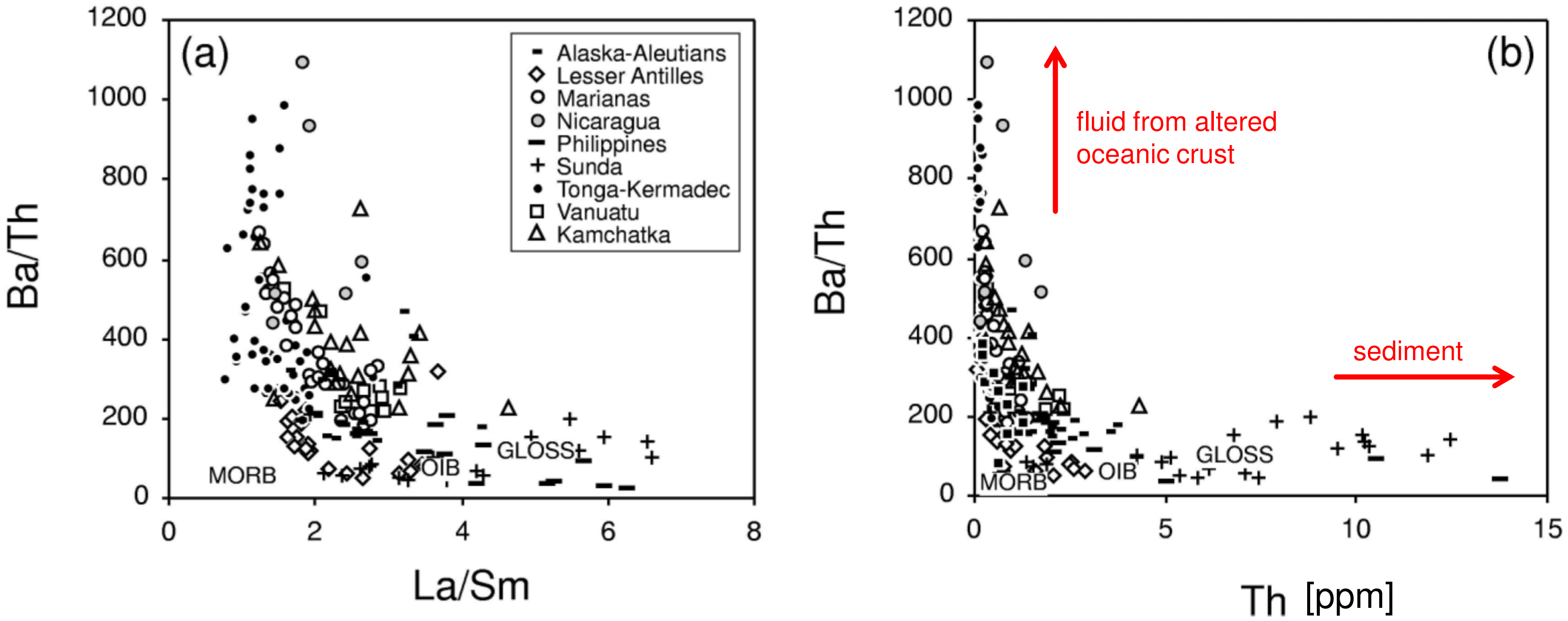

Ba/Th vs. La/Sm and Ba/Th vs. Th concentration in a number of island arcs. As La/Sm, **Th concentrations in pelagic sediments are high!**

Turner et al., 2003

Chemical signatures in island arc magmas

Sediment vs. fluid signature in arc magmas ... where does the fluid come from?

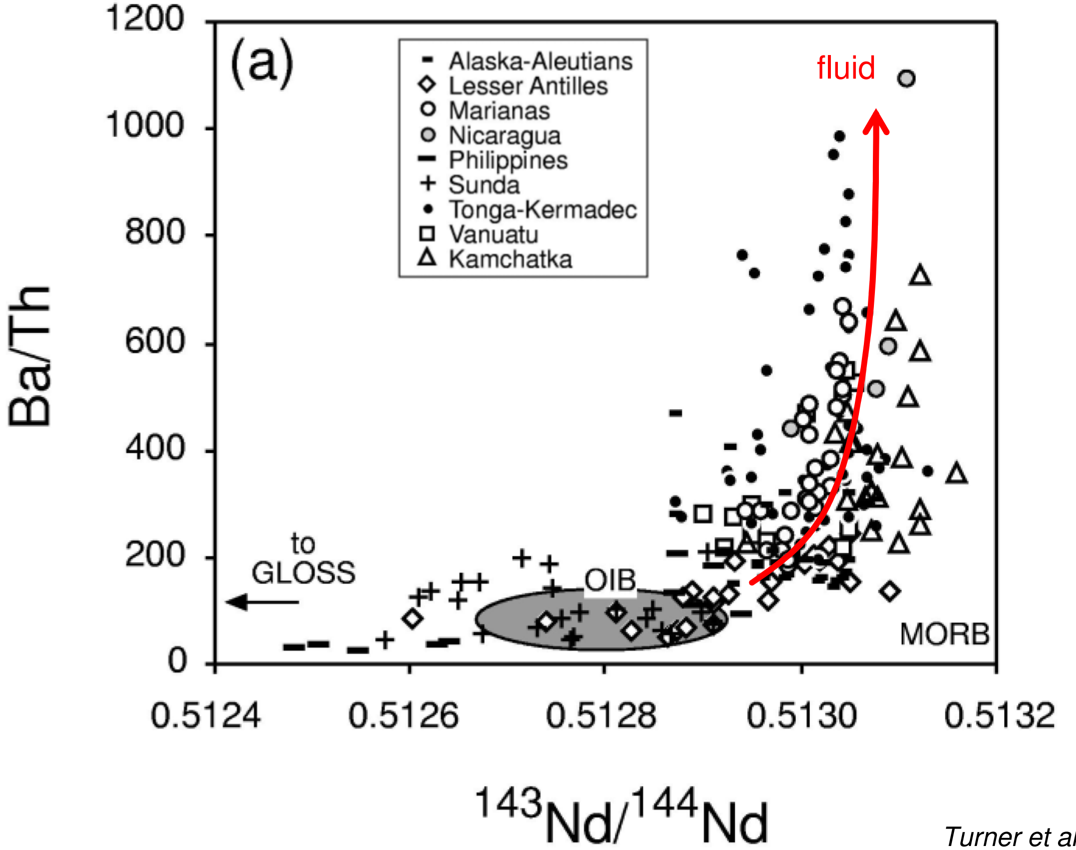

Turner et al., 2003

Radiogenic Nd-isotope ratios, i.e. **high $^{143}Nd/^{144}Nd$** in samples with **high Ba/Th** indicate that the fluid component is predominantly derived from the **altered oceanic lithosphere**, not from the subducted sediment. It also implies that **Nd is moderately mobile** during slab dehydration.

Chemical signatures in island arc magmas

(Time) constraints from B, ^{10}Be and U-Th disequilibrium

Formation of ^{10}Be in the atmosphere caused by cosmic rays

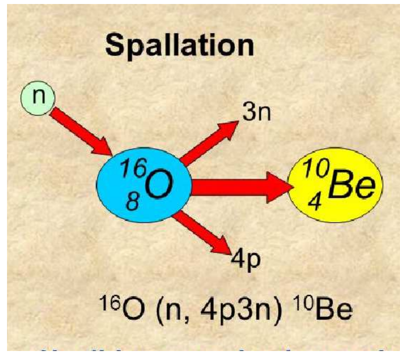

Half life of ^{10}Be: ~1.5 Ma

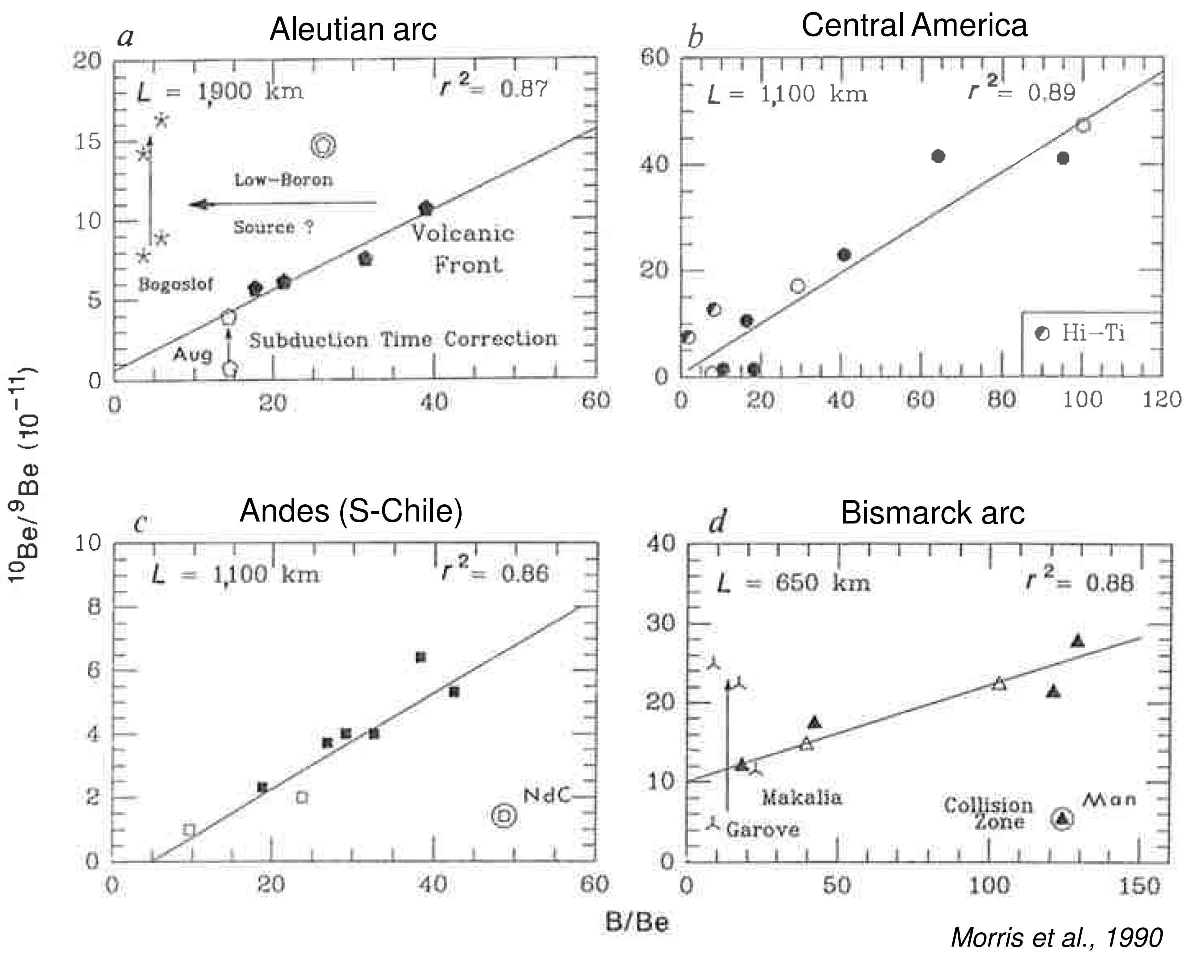

Morris et al., 1990

^{10}Be/^{9}Be and B/Be ratios in **arc lavas** from four different settings.

Note the overall linear correlations at **different slopes** and the **variable ranges in B/Be**

Chemical signatures in island arc magmas

(Time) constraints from B, ^{10}Be and U-Th disequilibrium

Formation of ^{10}Be in the atmosphere caused by cosmic rays

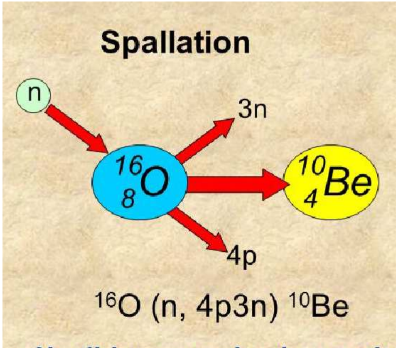

Half life of ^{10}Be: ~1.5 Ma

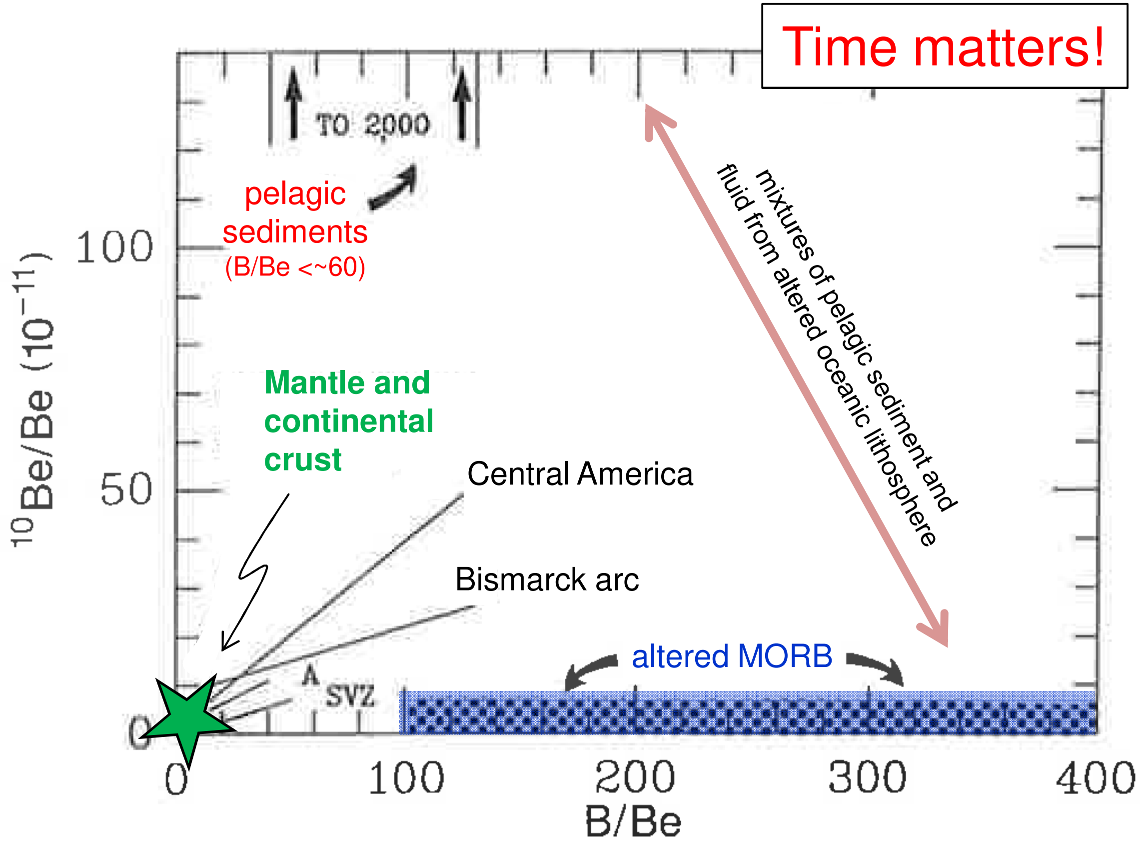

Morris et al., 1990

$^{10}Be/^{9}Be$ and B/Be ratios of **different components** (altered mafic crust, sediments & sub-arc mantle) contributing to the formation of **island arc magmas**.

Boron in sea water: ~5 ppm
Boron in sediments: ~50-150 ppm
B in MORB and OIB: ~1-3 ppm
B in altered oceanic crust: ~10-300 ppm
^{9}Be is quite uniform in all reservoirs!

Chemical signatures in island arc magmas

More time constraints from U-Th disequilibrium

$$\left(\frac{^{230}\mathrm{Th}}{^{232}\mathrm{Th}}\right)_P = \left(\frac{^{230}\mathrm{Th}}{^{232}\mathrm{Th}}\right)_I e^{-\lambda_{230}t} + \frac{^{238}\mathrm{U}}{^{232}\mathrm{Th}}\left(1 - e^{-\lambda_{230}t}\right)$$

measured — *„initial"=f(t)* — *„ingrowth"=f(t)*

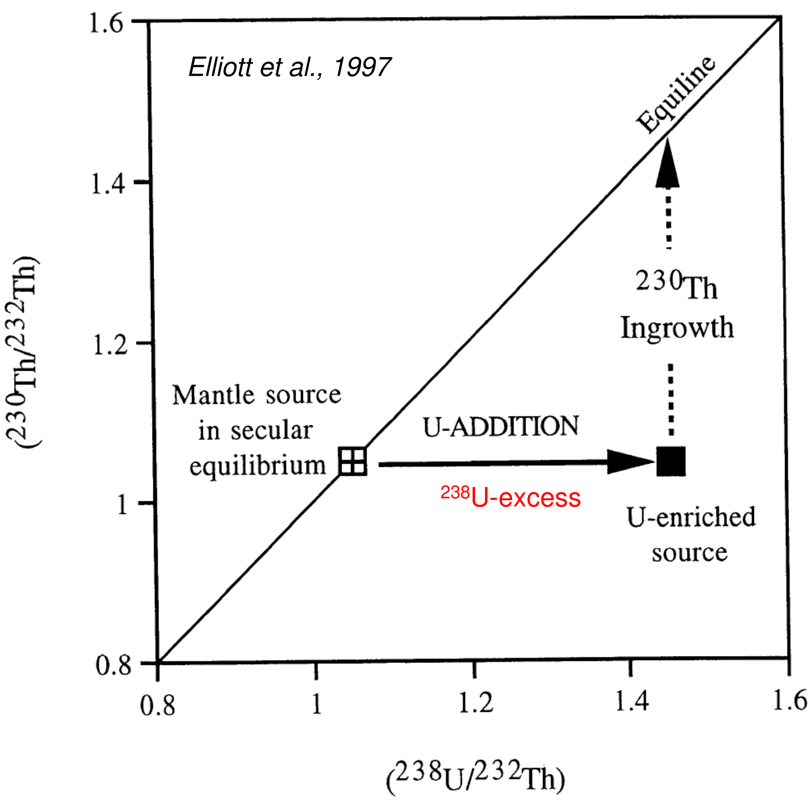

Equiline diagram. Samples in **secular equilibrium** with respect to ^{238}U and ^{230}Th [i.e. A(^{238}U) = A(^{230}Th)] plot along the **equiline**.

Any elemental fractionation between U and Th moves a point (sample) **away from the equiline**, either to the right (**U-addition**), or to the left (**Th-addition**)

Half life of ^{230}Th: ~75 ka

Chemical signatures in island arc magmas

U-Th disequilibrium in Mariana arc lavas

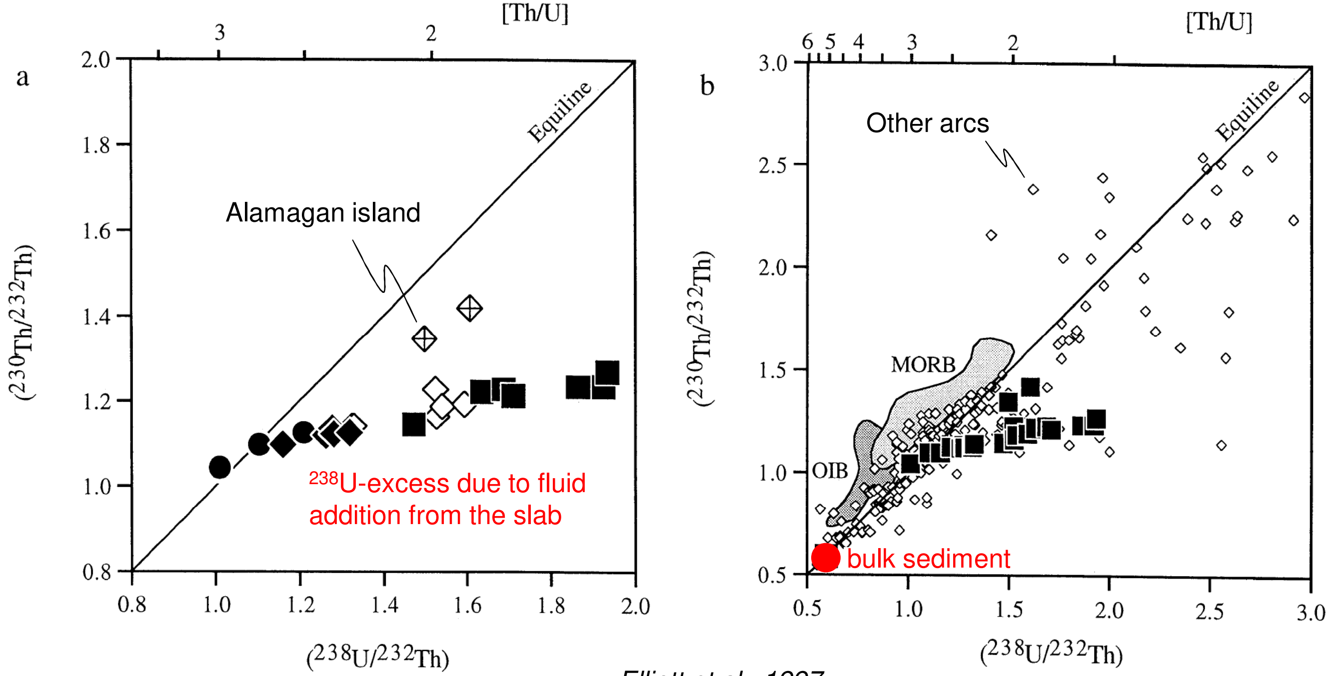

Elliott et al., 1997

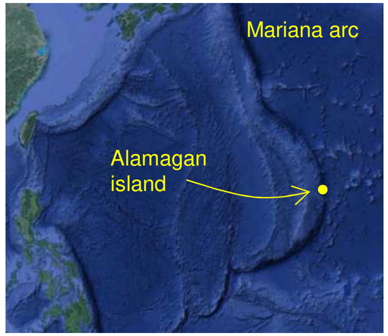

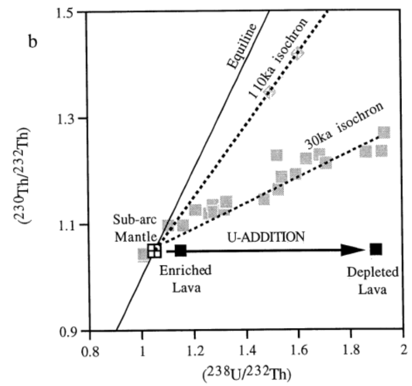

Mariana arc samples plot distinctly **off** the equiline, indicating that **fluid-controlled U-transfer**, **melting**, **melt migration** and **eruption** of Mariana arc lavas are „fast" processes!

Secular disequilibrium is a **unique feature** observed in **island arc lavas** (note the slight offset of MORB and OIB due to Th/U fractionation during partial melting)

Assuming variably enriched and depleted sources with constant Th/U (or variable amounts of U-addition), secular disequilibrium was imprinted ~30 ka ago

Chemical signatures in island arc magmas

U-Th disequilibrium in arc lavas

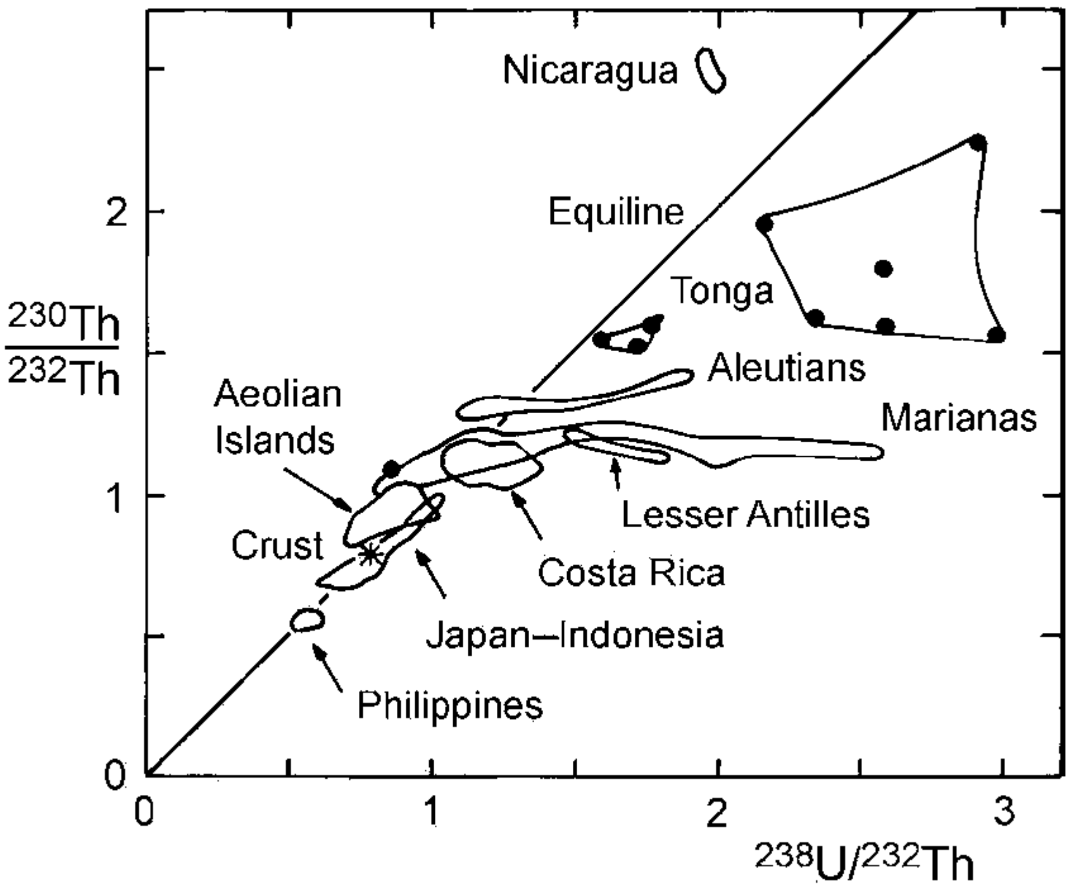

From Dickin (2005), after Hawkesworth et al. (1991)

U-Th disequilibrium in island arc magmas from different locations

The **degree of dis-equilibrium** is caused by different amounts of U added from the slab, or by **differing times** between mantle source metasomatism and lava eruption at the surface

Chemical signatures in island arc magmas

U-Th disequilibrium in island arc magmas

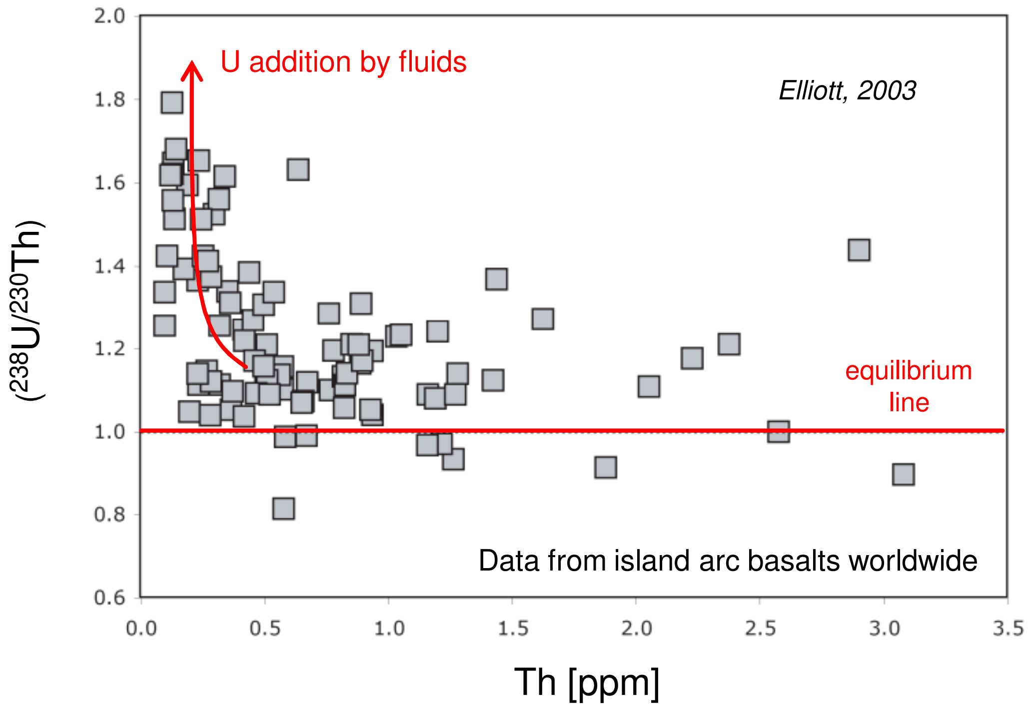

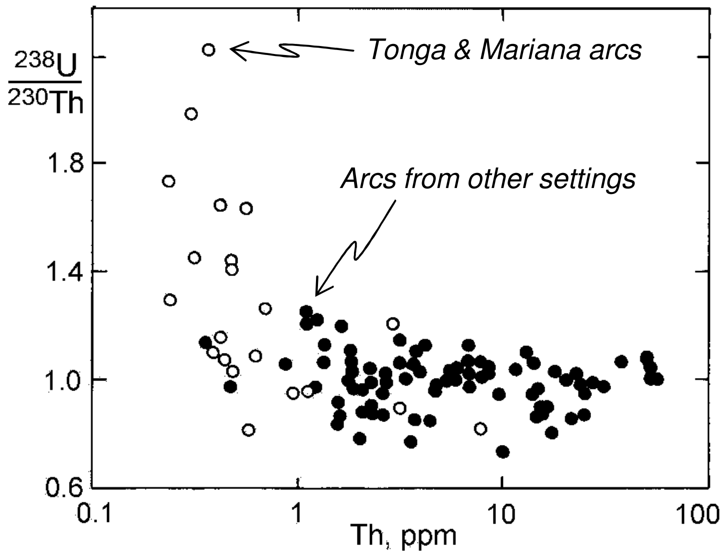

From Dickin (2005), after McDermott & Hawkesworth (1991)

Secular disequilibrium between ^{238}U and ^{230}Th is **strongest** in island arc lavas with **low Th contents**. This confirms that **U addition** is predominantly by **fluids** released from the downgoing oceanic lithosphere

Chemical signatures in island arc magmas

Overall radiogenic isotope signatures

Kelemen et al., 2003, Treatise on Geochemistry

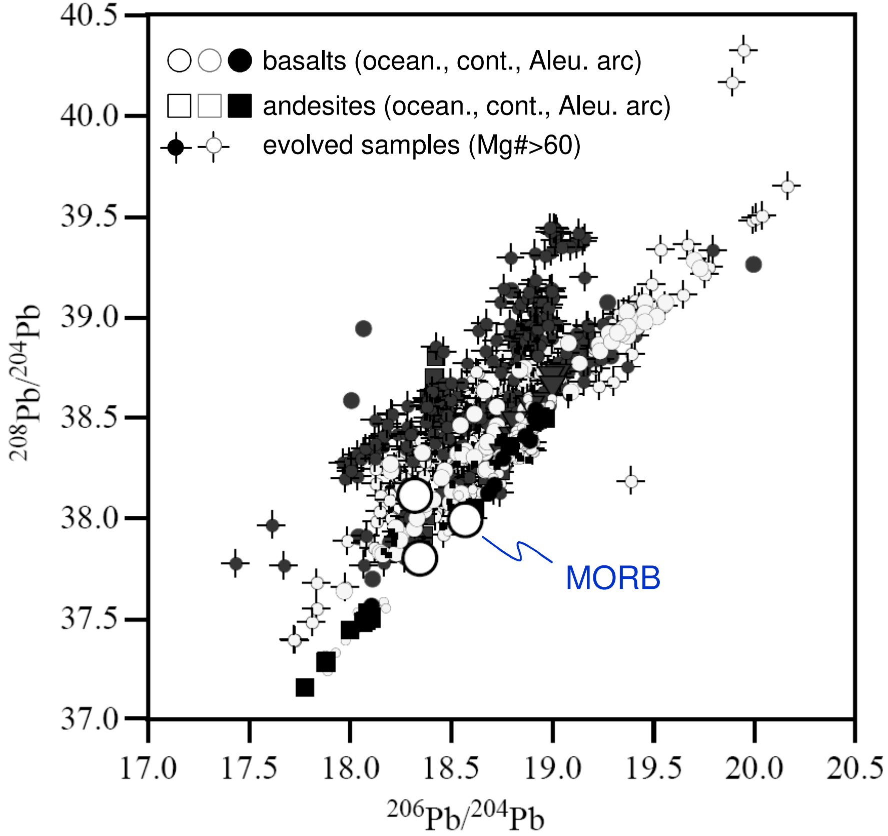

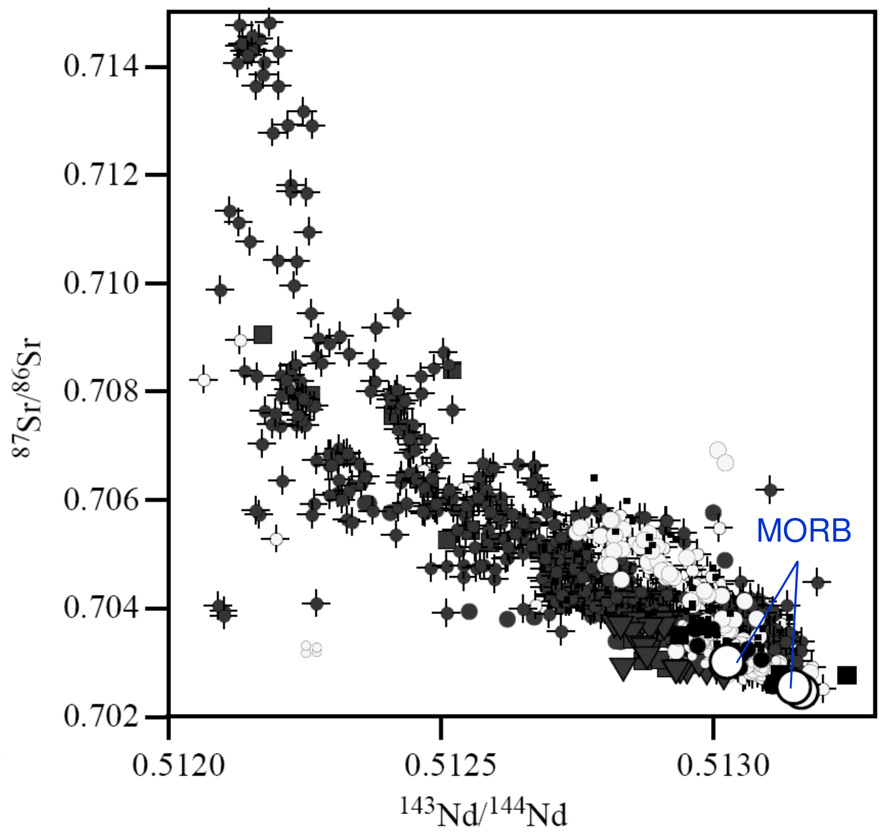

Pb-isotopes are mostly <u>enriched</u> relativ to MORB, with distinctly higher ^{208}Pb at given ^{206}Pb, indicating a long-term **high Th/U** in the source of most arc lavas. The **Nd-Sr isotope array** reflects the aforementioned involvement of subducted **continental sediments** during magma genesis

Chemical signatures in island arc magmas

Liquid lines of descent in calc-alkaline magas

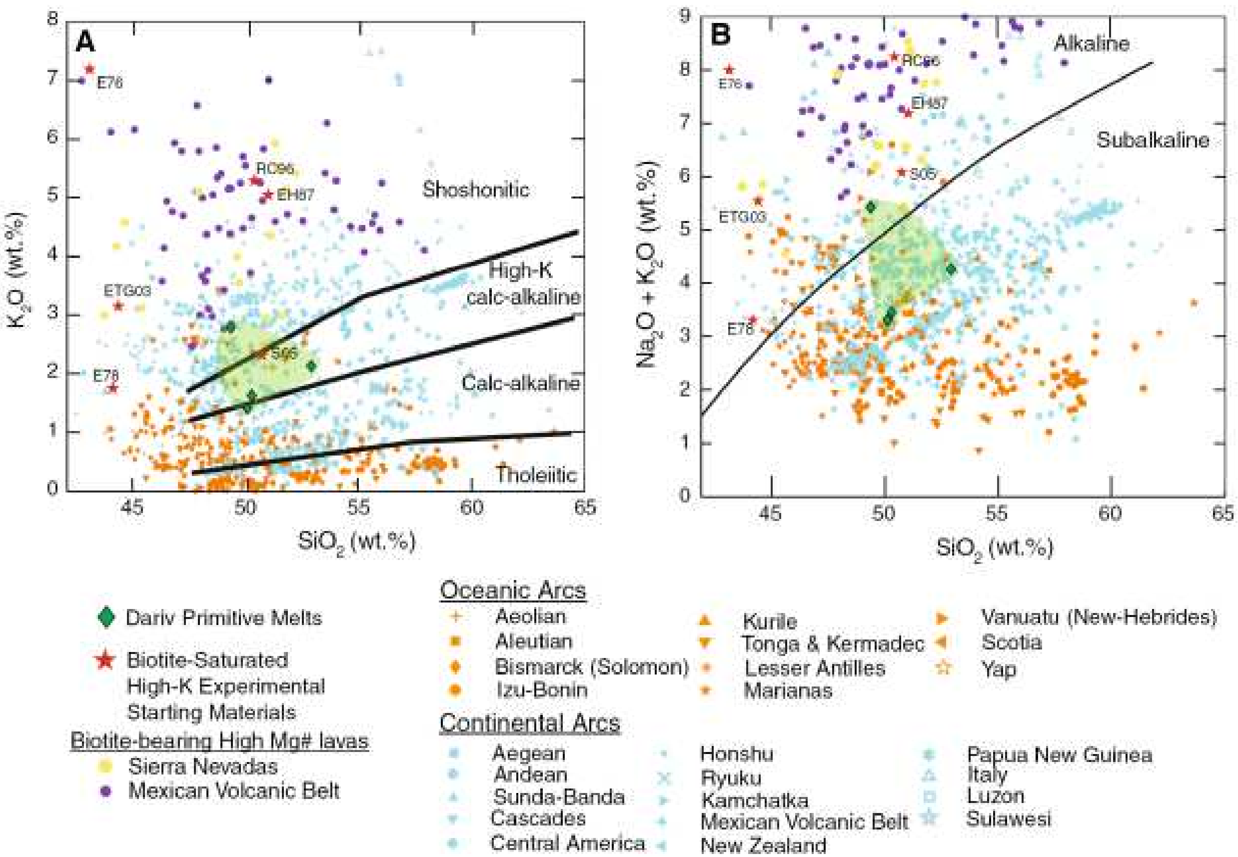

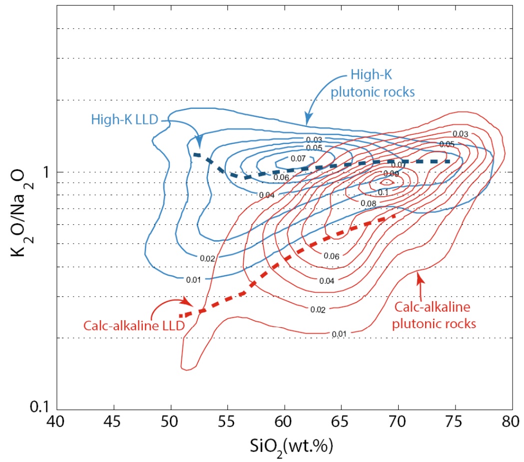

Bucholz et al., 2014b

Chapter 4

Ocean islands *in brief...*

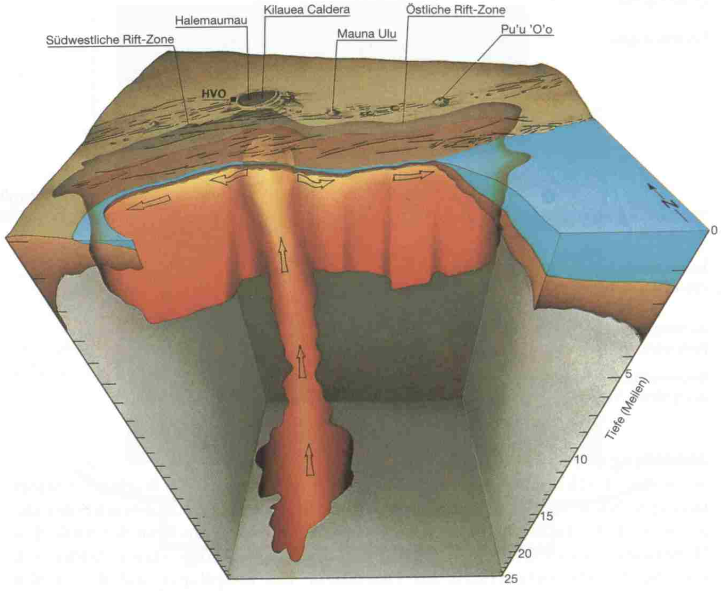

Hawaii

Ocean Island Basalts = OIB

Ocean island basalts = <u>oceanic</u> intraplate basalts

Continental basalts = <u>continental</u> intraplate basalts

Ocean islands

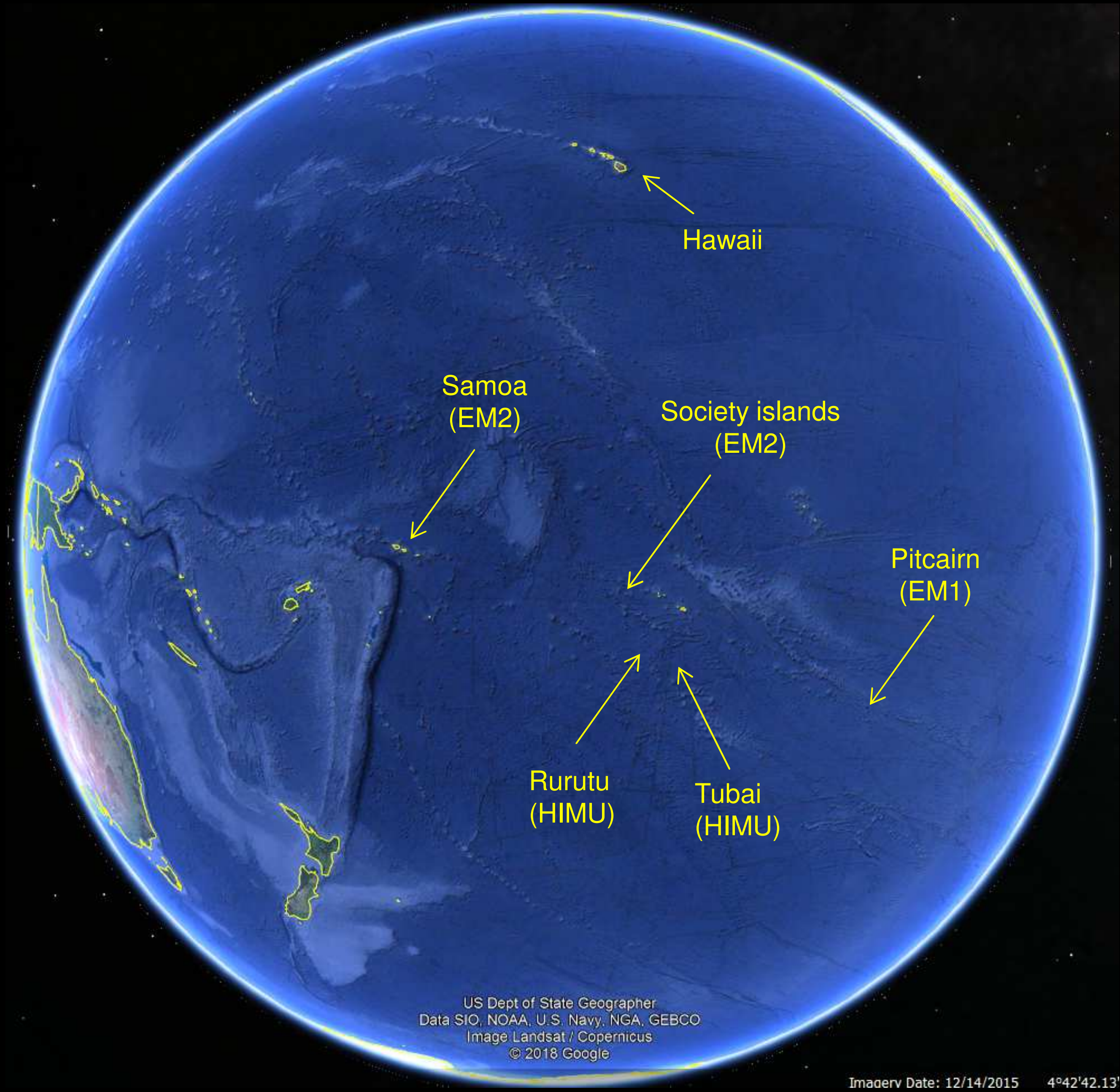

Ocean islands

Ocean islands

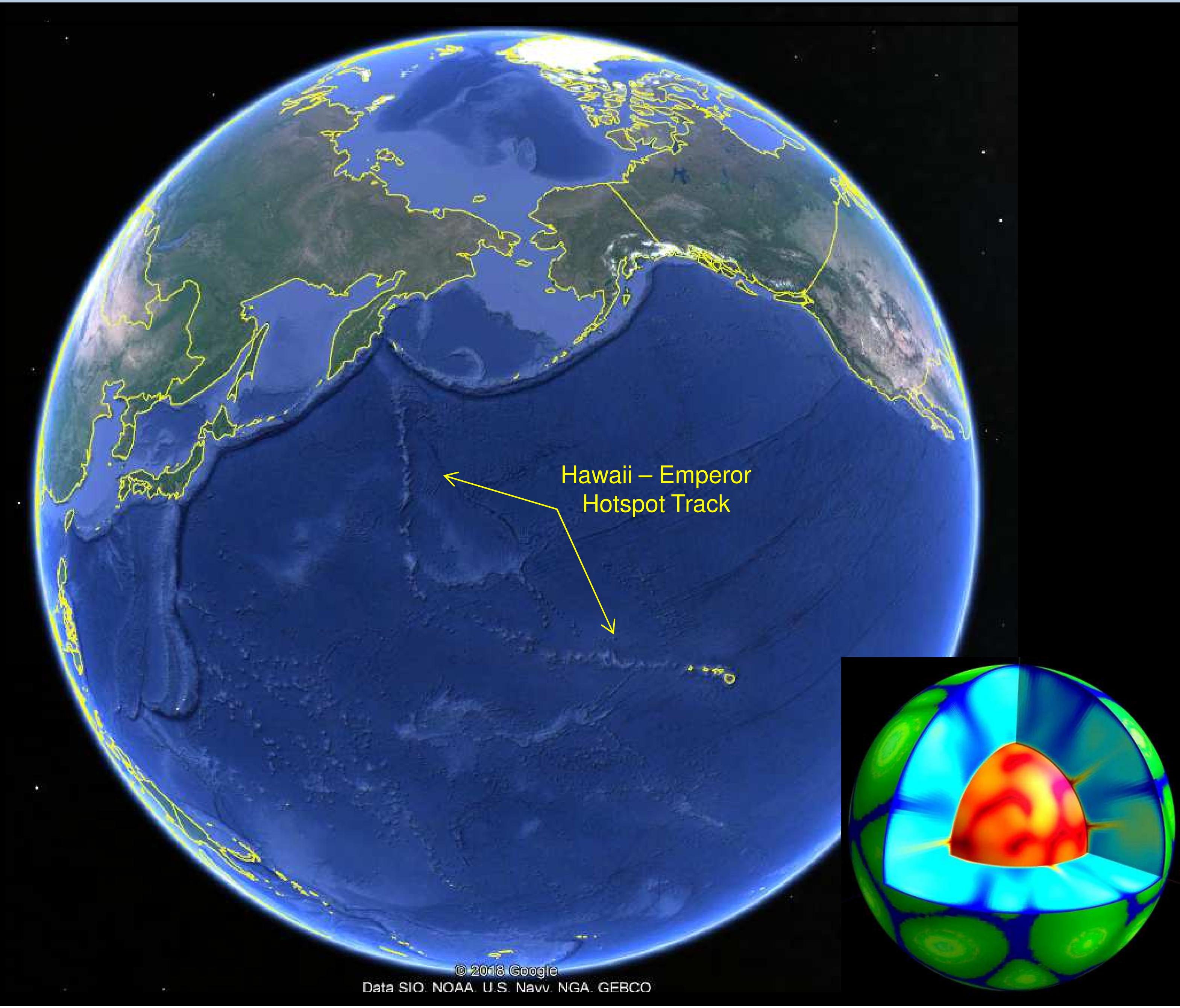

Composition of ocean island basalts

Radiogenic isotope features

Hofmann, 2003, Treatise on Geochemistry

As firstly outlined in 1964 by **Gast, Tilton & Hedge**, the strongly different isotope signatures in OIB if compared to MORB cannot be explained by different melting depths.

Instead the OIB mantle source must be <u>chemically different</u>, and in some respect been isolated from the MORB mantle source for millions to billions of years!

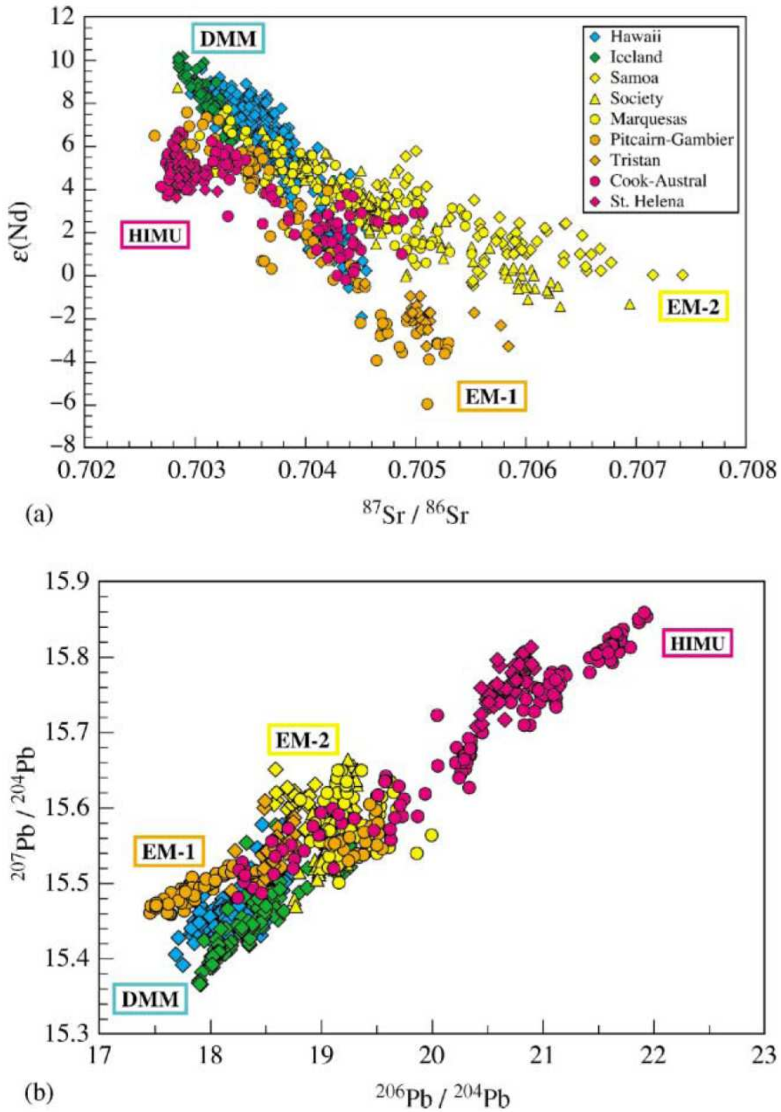

Composition of ocean island basalts

Radiogenic isotope features

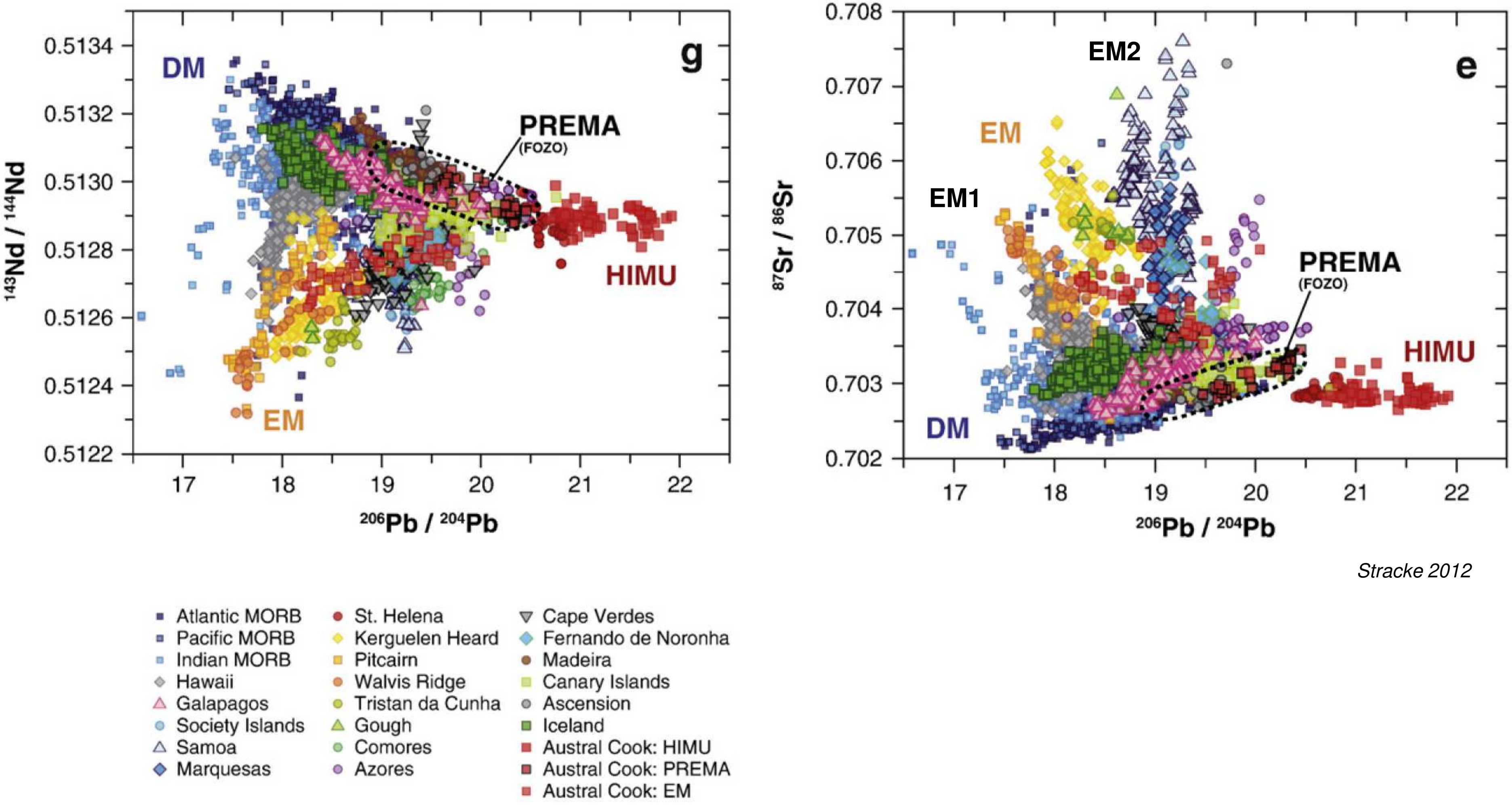

Stracke 2012

Composition of ocean island basalts

Radiogenic isotope features

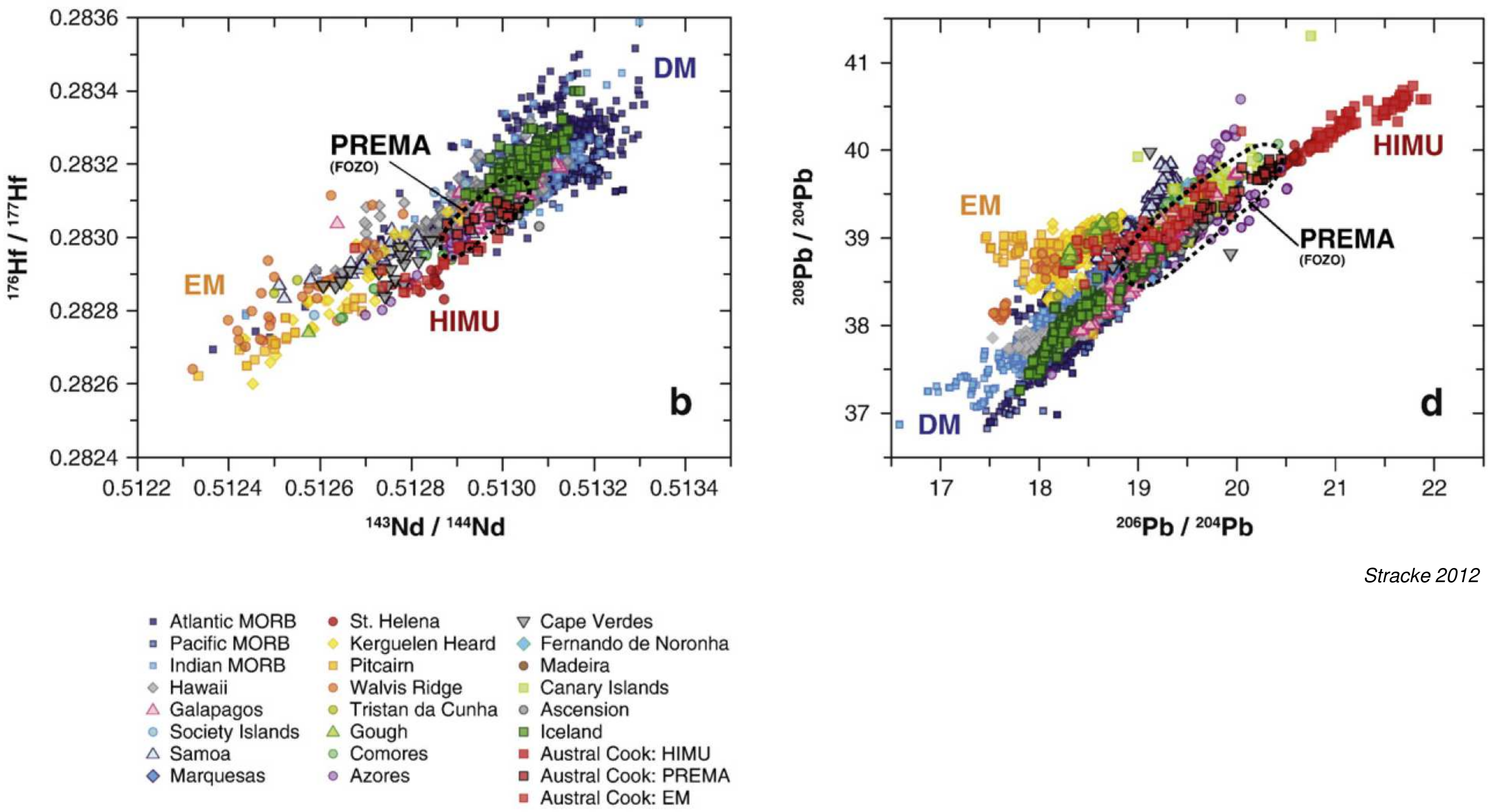

Stracke 2012

Composition of ocean island basalts

Trace element features

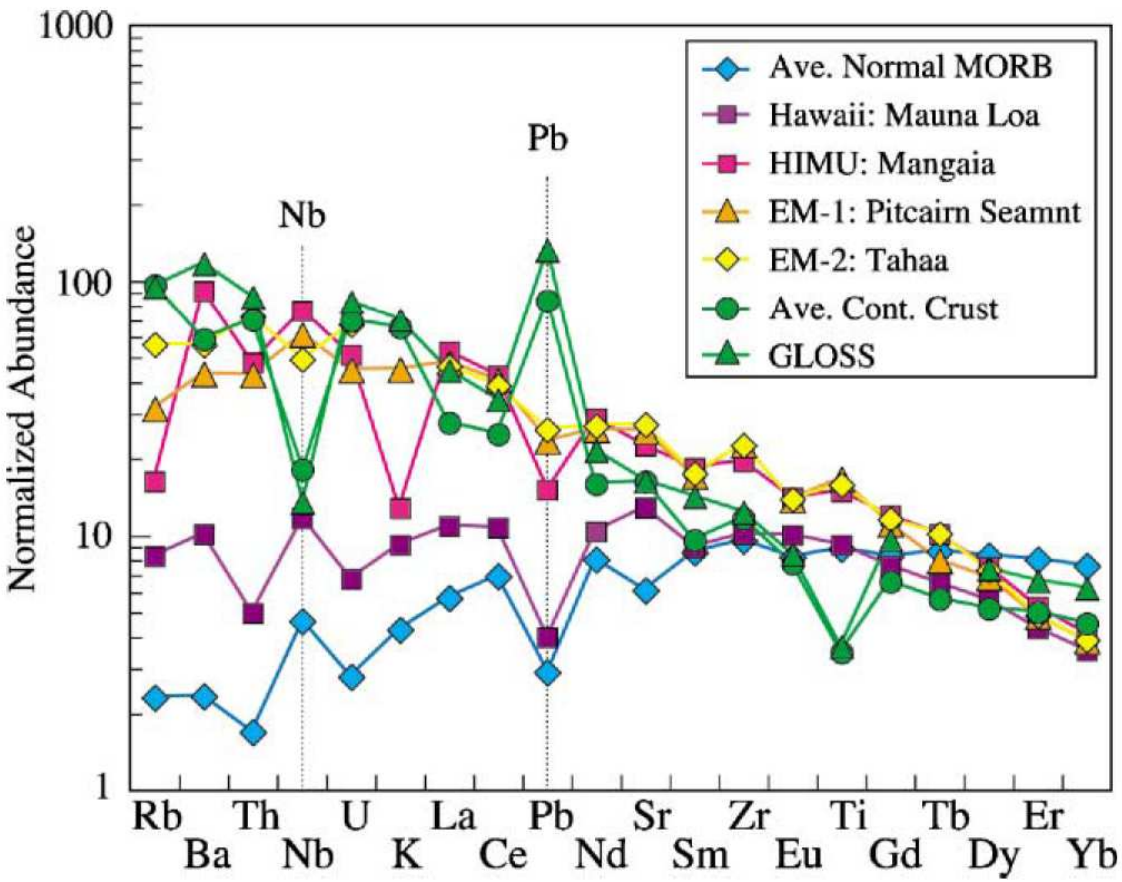

Hofmann, 2003, Treatise on Geochemistry

Averaged PRIMA normalized trace-element concentrations in OIBs from different locations.

GLOSS is the averaged composition of **gl**obally **s**ubducted **s**ediment, which is very similar to average continental crust.

Note that **Hawaii OIBs** plot most closely to MORB (but have LOWER contents of HREE than MORB)!

Composition of ocean island basalts

Trace element features

Stracke, 2012

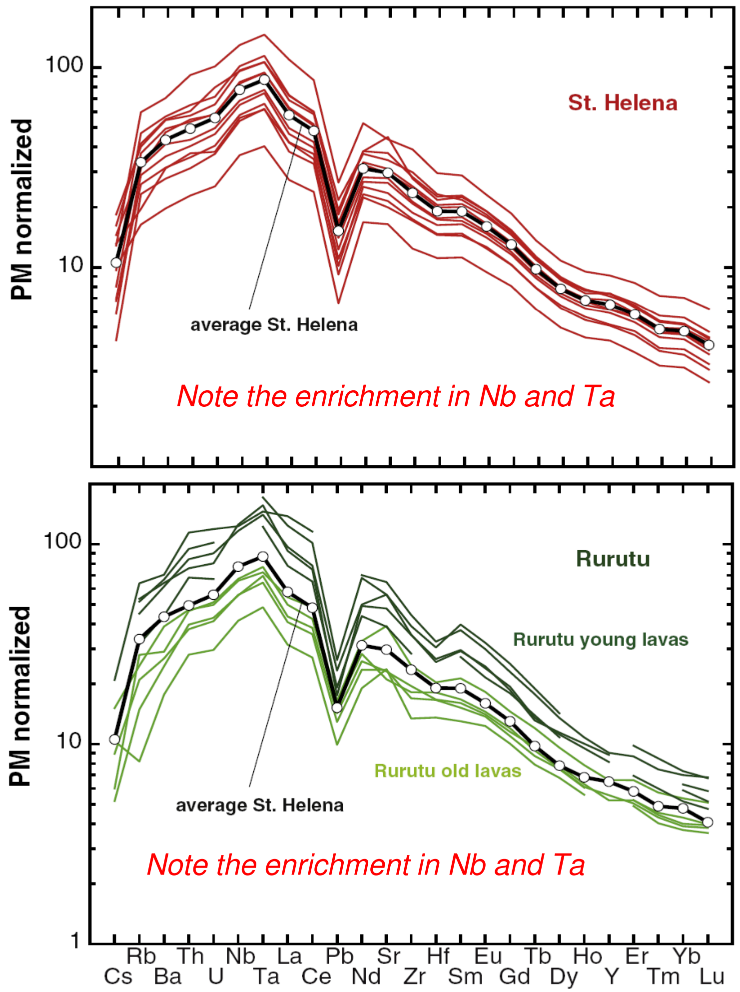

HIMU OIBs are regarded as partial melts derived from a mantle source consisting of **PREMA** + highly altered **oceanic crust/lithosphere** (high U/Pb due to hydrothermal Pb loss over U).

Also note the extreme **enrichment in Nb and Ta** over neighbouring elements (La, Th), which results from melting of Ti-phases out of the subducted slabs (now „eclogite“)!

*About **constant Nb/Ta** at **variable Zr/Hf** in OIB suggest up to **~3% rutile in the source** of (HIMU) ocean island basalts, which likely is hosted by **recycled oceanic crust** („eclogite“)*

Pfänder et al., 2007

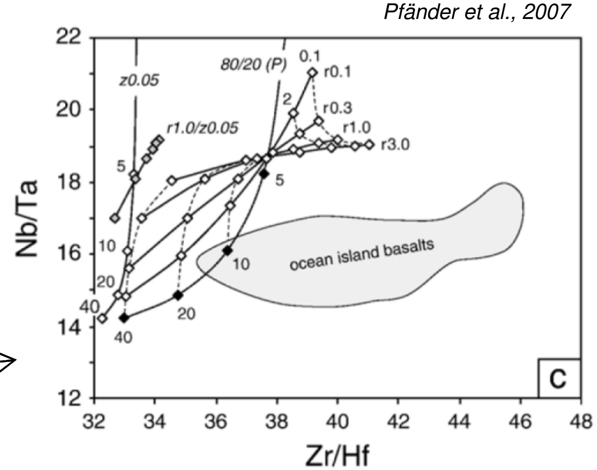

Composition of ocean island basalts

Trace element features

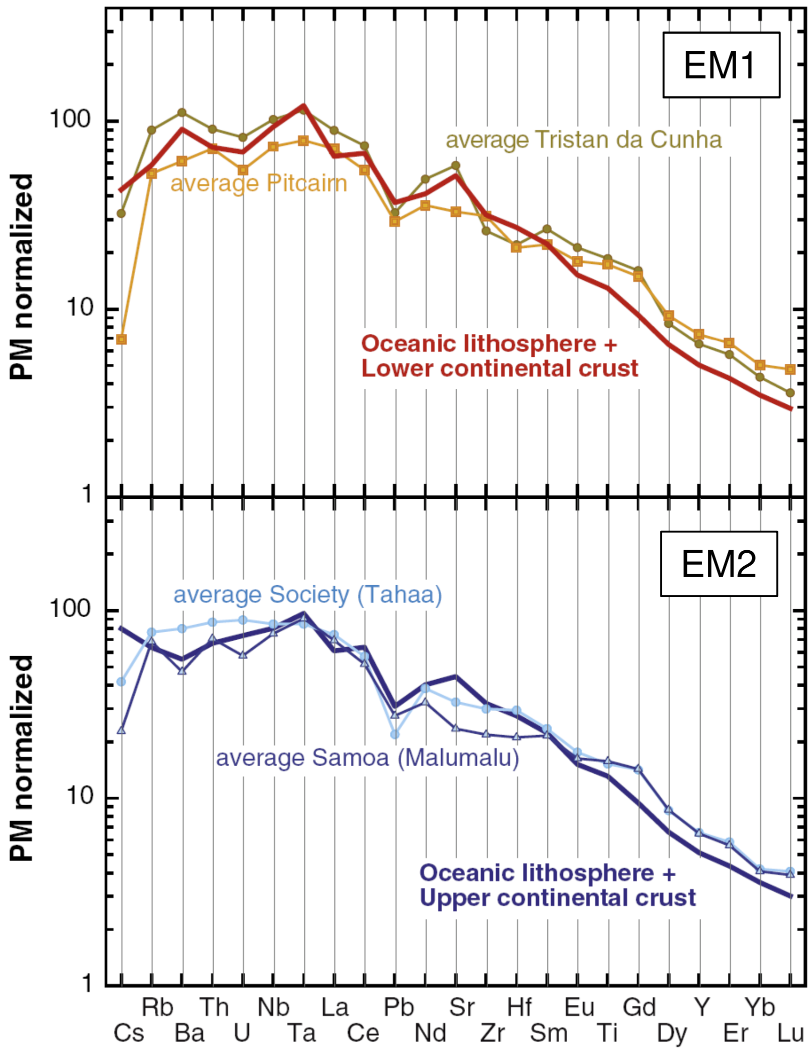

EM1 and **EM2** compositions are interpreted as reflecting partial melts of a source consisting of **PREMA** + subducted oceanic lithosphere + **lower** (EM1) and **upper** (EM2) continental crust.

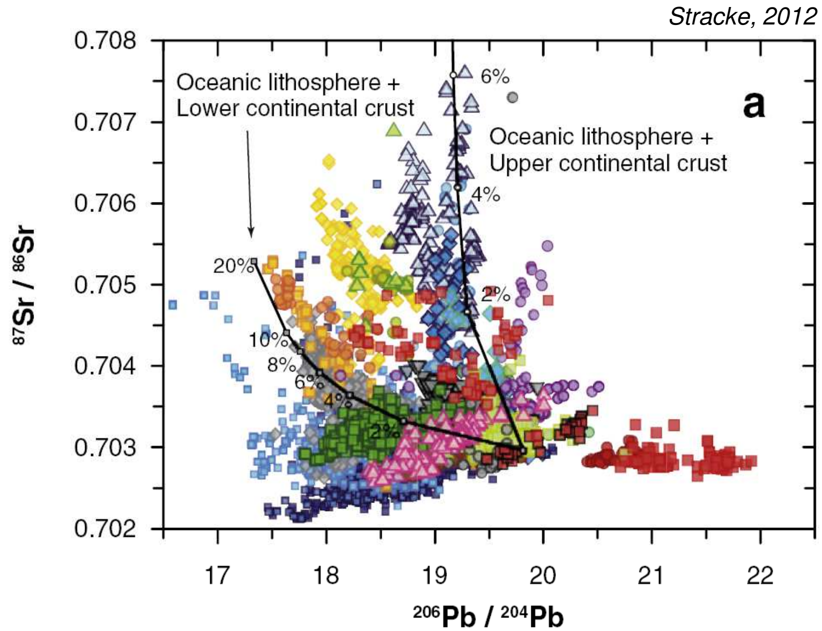

Stracke, 2012 (see also Willbold & Stracke, 2006)

Composition of ocean island basalts

Trace element features

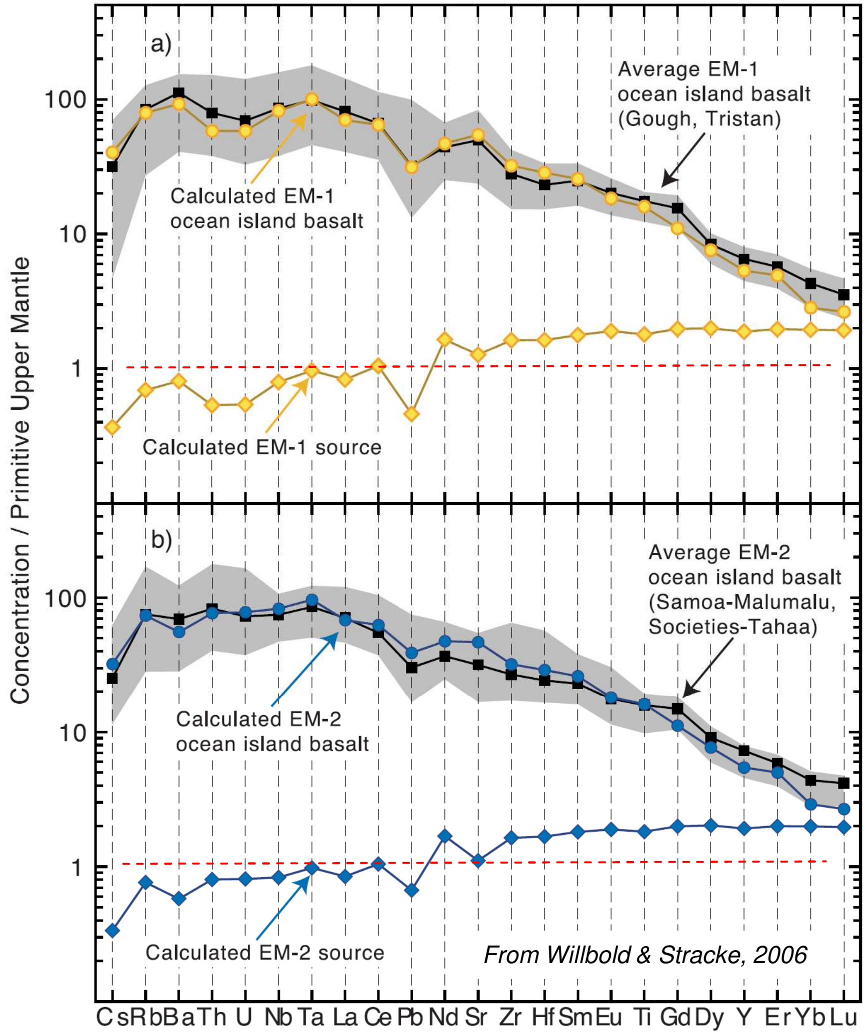

From Willbold & Stracke, 2006

EM1 and **EM2 mantle sources** as inferred from trace-element compositions of EM1 and EM2 ocean island basalts, and applying non-modal aggregate fractional melting modelling (**F=1%**, melting in the **garnet** stability field).

Note that source compositions are similar to PRIMA!

EM1 model source: 90% depleted mantle + **9% oceanic crust** + 1% **lower** continental crust

EM2 model source: 90% depleted mantle + **9.8% oceanic crust** + 0.2% **upper** continental crust

PRIMA (BSE) normalized trace-element abundances of the ***depleted mantle source*** *for comparison (from Salters & Stracke, 2004)*

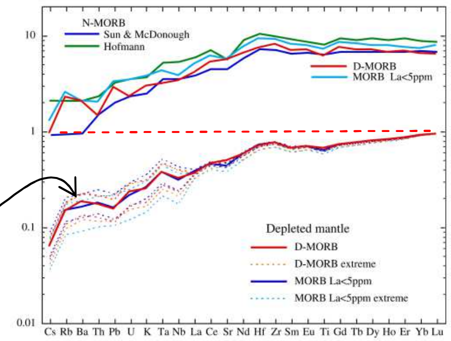

Composition of ocean island basalts

Fundamental first order conclusions

- The Earth's mantle is **heterogeneous**
- The MORB and OIB **mantle sources** have strongly **different geochemical compositions** that maintain **since the geological past** (>1 Ga)
- Unless the MORB source, the source of OIB is **enriched** in **trace-elements** and **radiogenic isotopes**
- A combination of variable proportions of primitive and/or depleted mantle **plus** subducted oceanic lithosphere **plus** upper and/or lower continental crust explains most of the observed features

Hofmann, 1994

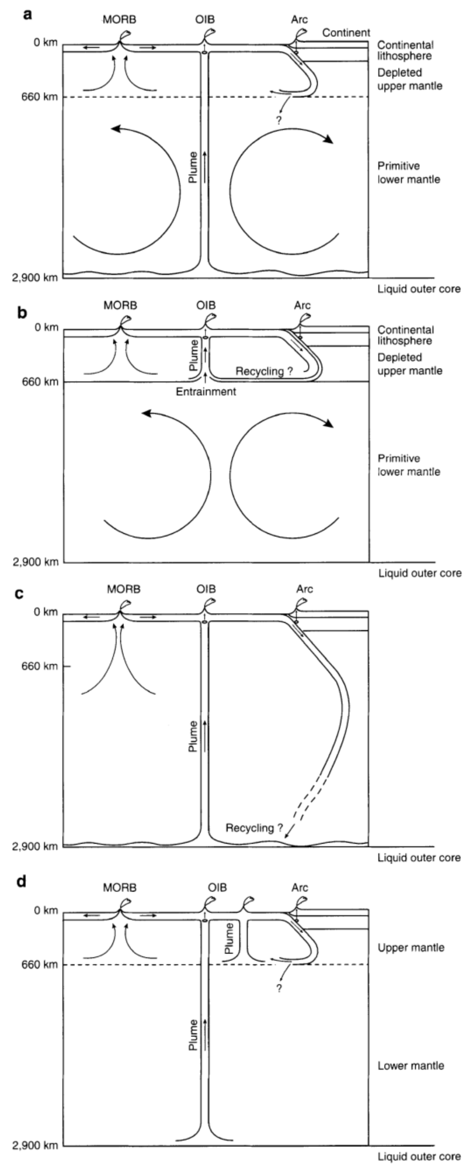

For reviews see Hofmann (1994) Nature, and Stracke (2012) Chemical Geology

Composition of ocean island basalts

Fundamental first order conclusions – implications from geophysics

Movement of Farallon Slab (Western USA, from Liu & Stegman, 2012, Nature)

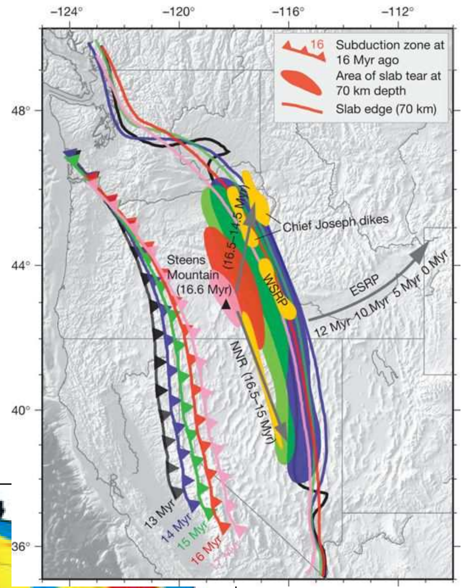

Geophysical data (mostly seismic tomography) support the **recycling hypothesis!**

Grand et al., 1997, GSA Today

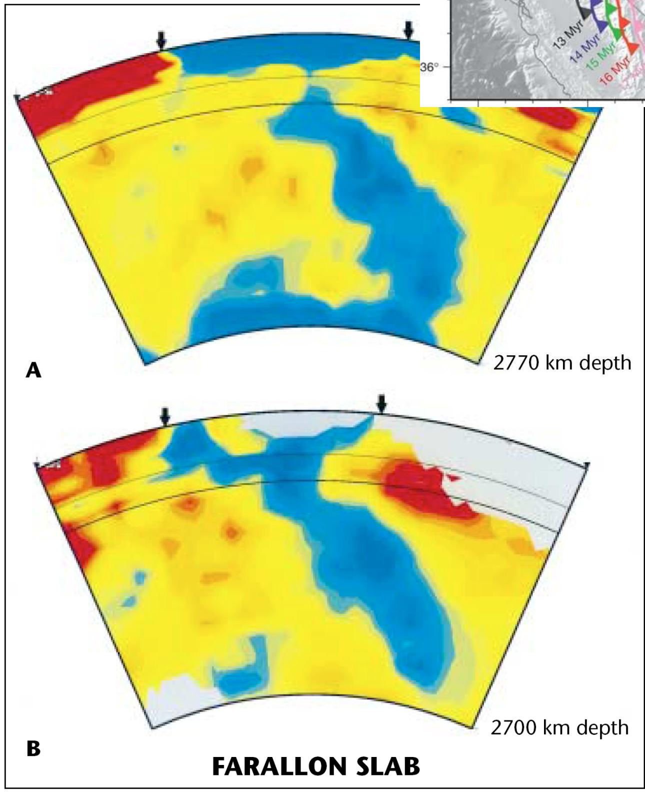

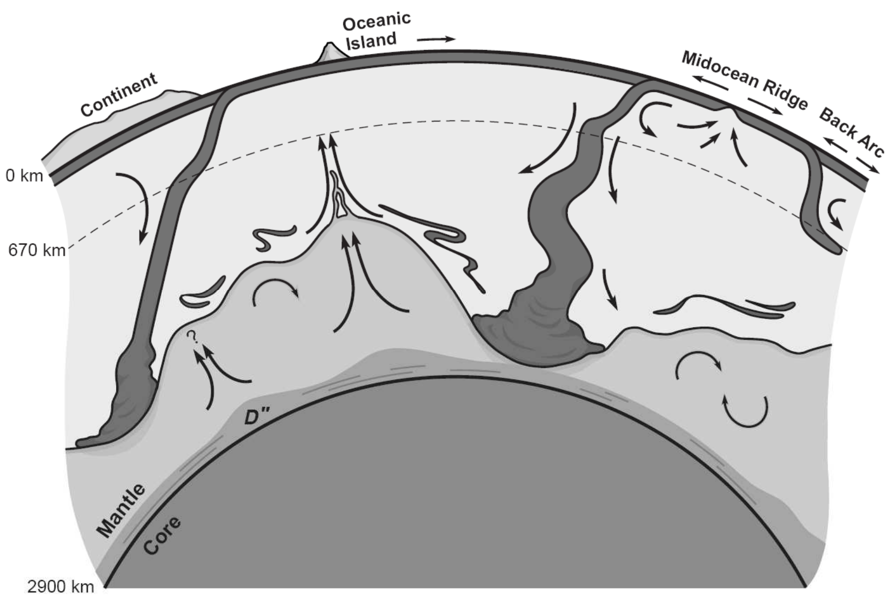

Kellogg et al., 1999, Science

Composition of ocean island basalts

... and the Cornucopia of mantle models that emerged

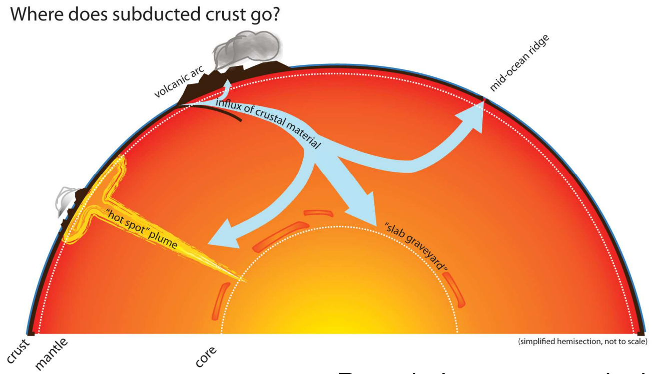

*Recycled components in the plume **and** MORB source, and storage in the D“ layer*

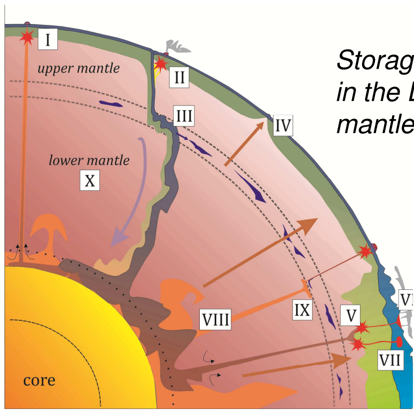

Storage of subducted lithosphere in the D“ layer, i.e. at the core – mantle boundary at ~2900 km

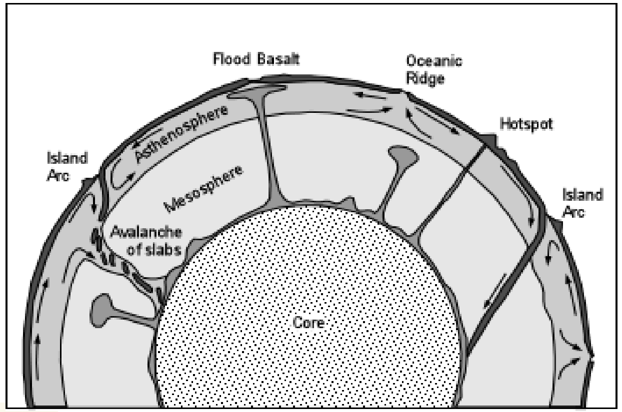

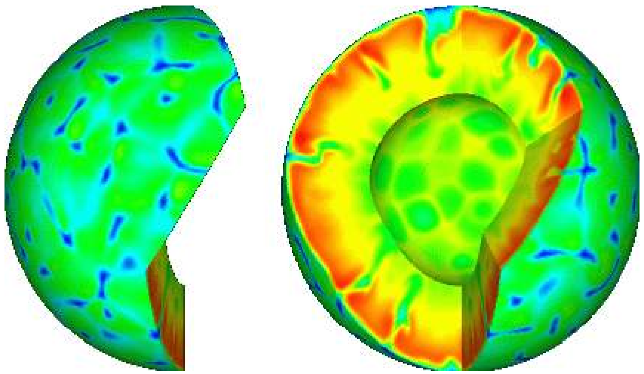

Numeric simulation of mantle convection (from Geophysics Homepage, LMU München, H.-P. Bunge)

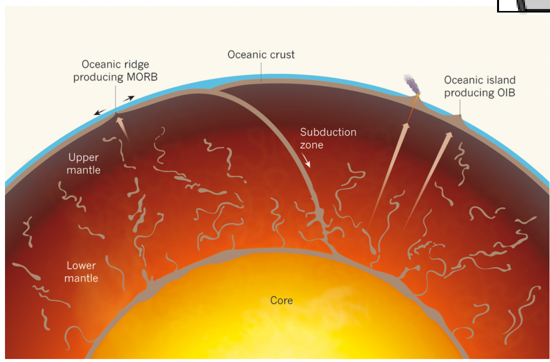

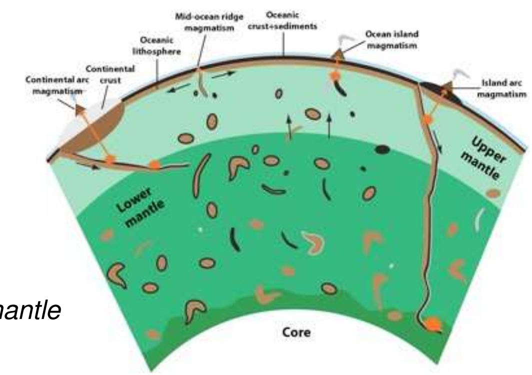

marble cake models of a multiscale heterogeneous mantle

Mantle plumes and plate tectonics

... do mantle plumes disrupt continents?

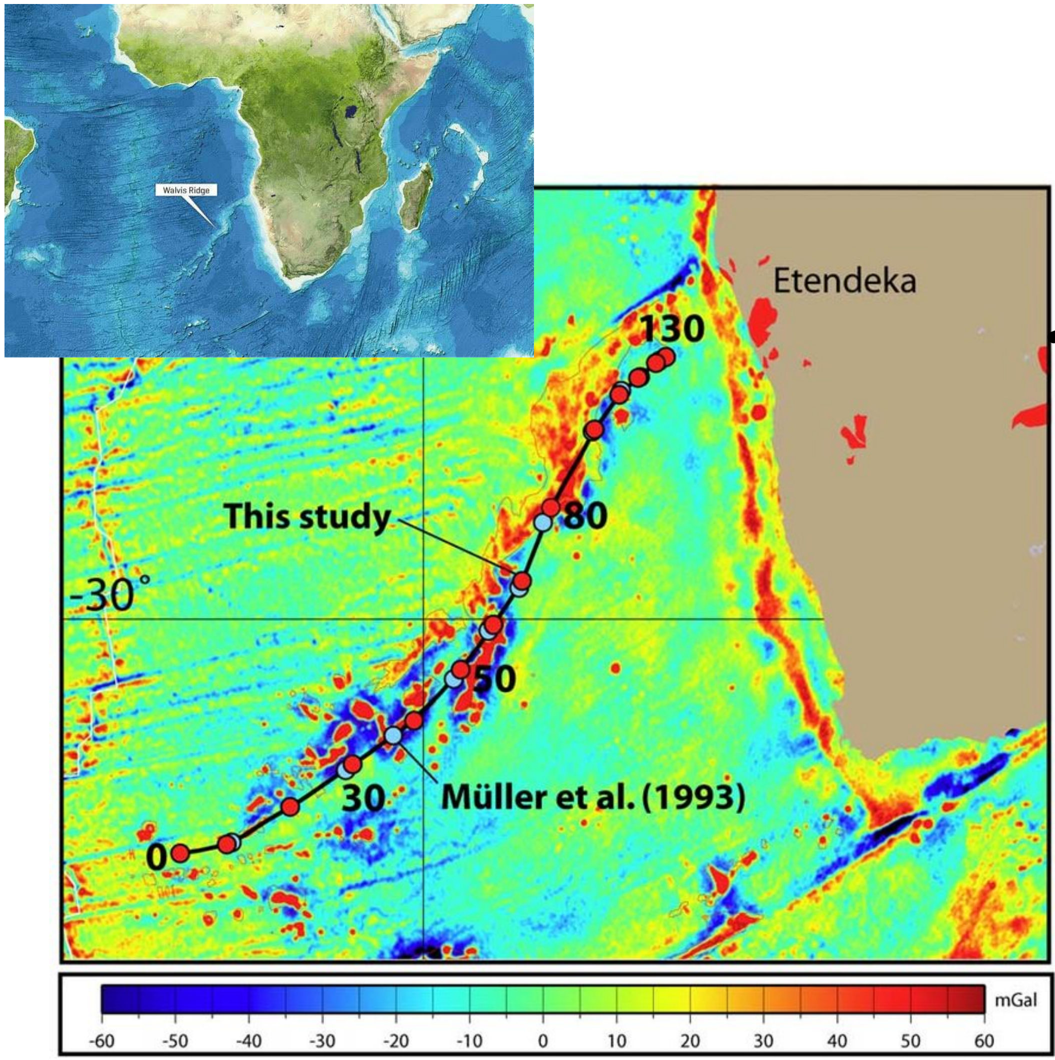

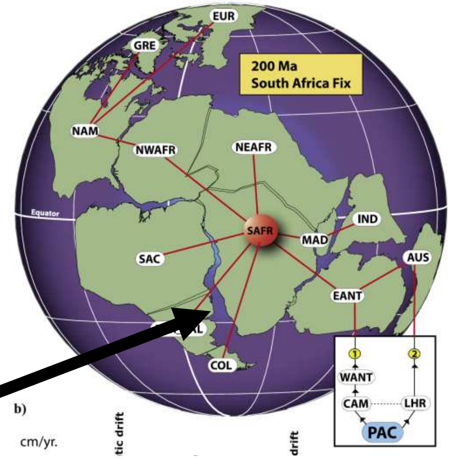

Breakup between **Africa** and **South America** as part of **Pangaea** caused by the **Tristan mantle plume**?

An age progression along the **Walvis ridge** makes this scenario very likely!

Composition of ocean island basalts

Is there a primordial signature in the OIB source mantle?

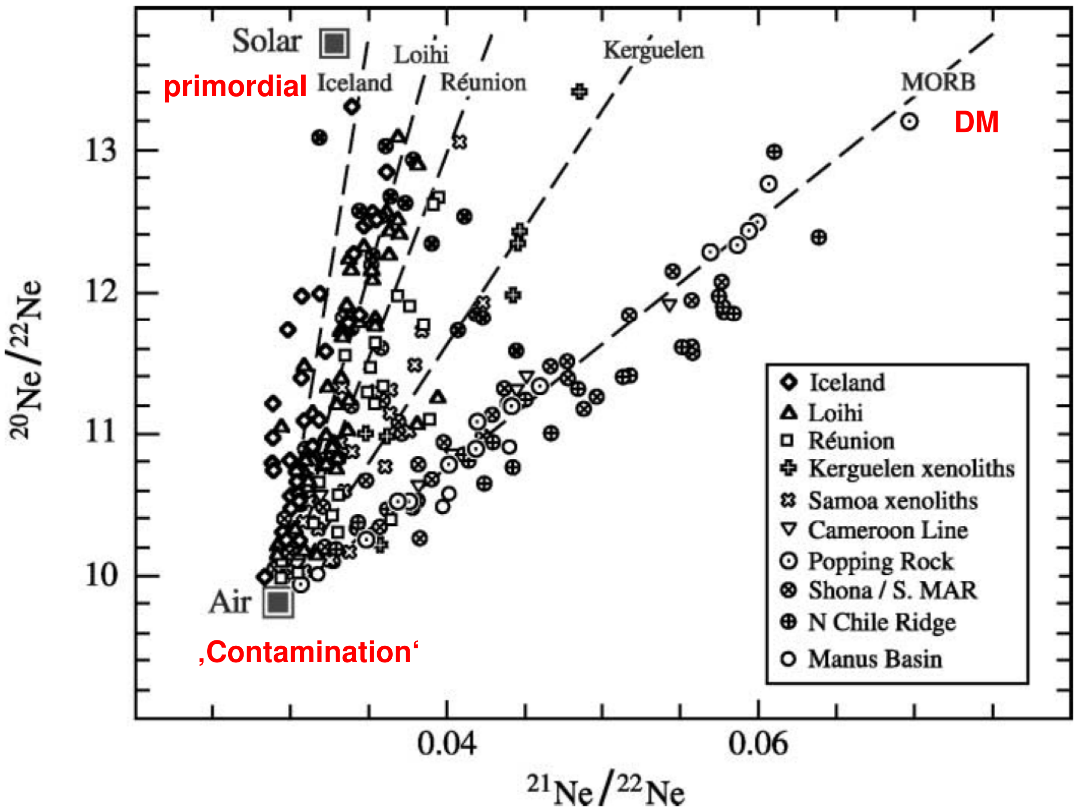

Hilton & Porcelli (2003), Treatise on Geochemistry

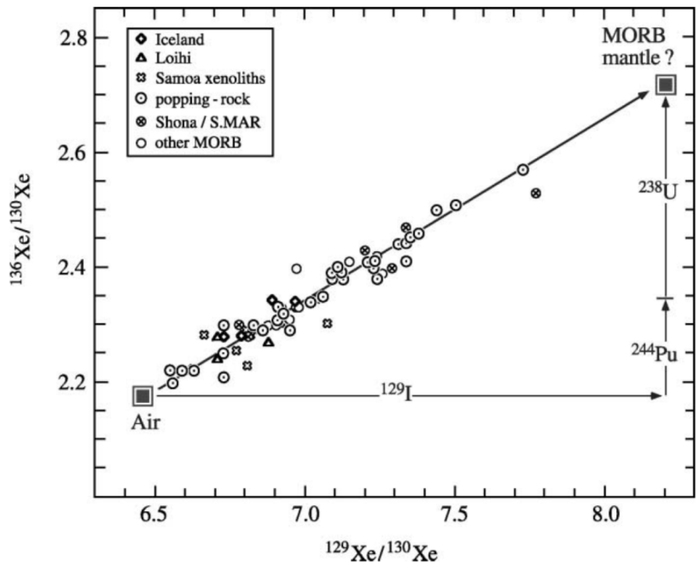

Or, what about the interaction between the OIB and the MORB source mantle? Noble gas constraints....

^{20}Ne and ^{22}Ne are primordial

$^{24,25}Mg(n,\alpha)$ **^{21}**$^{,22}Ne$

$^{18}O(\alpha,n)$**^{21}Ne**

$^{19}F(\alpha,n)^{22}Na(\beta)^{22}Ne$

Composition of ocean island basalts

Noble gas isotope features

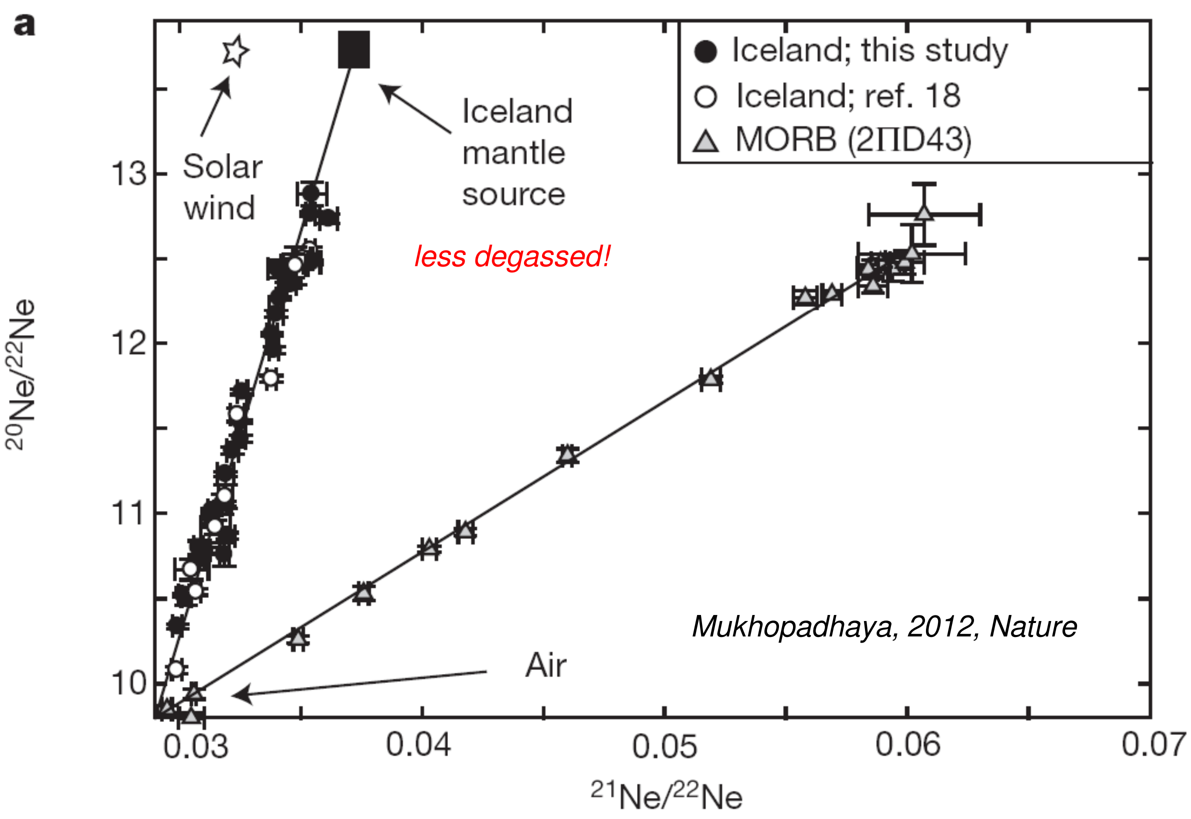

The steeper slope of the **Iceland sample** indicates a higher amount of **primordial ^{22}Ne** relative to **nucleogenic ^{21}Ne** in the Iceland mantle source than in the MORB mantle source.

This suggests a less degassed (deeper?) Iceland mantle source!

Does this mirror a heterogeneous accretion of the Earth, and subsequent restricted ‚mixing' since then?

^{20}Ne and ^{22}Ne are primordial

^{24,25}Mg(n,α) ^{21,22}Ne

^{18}O(α,n)^{21}**Ne**

^{19}F(α,n)^{22}Na(β)^{22}Ne

Composition of ocean island basalts

Noble gas isotope features

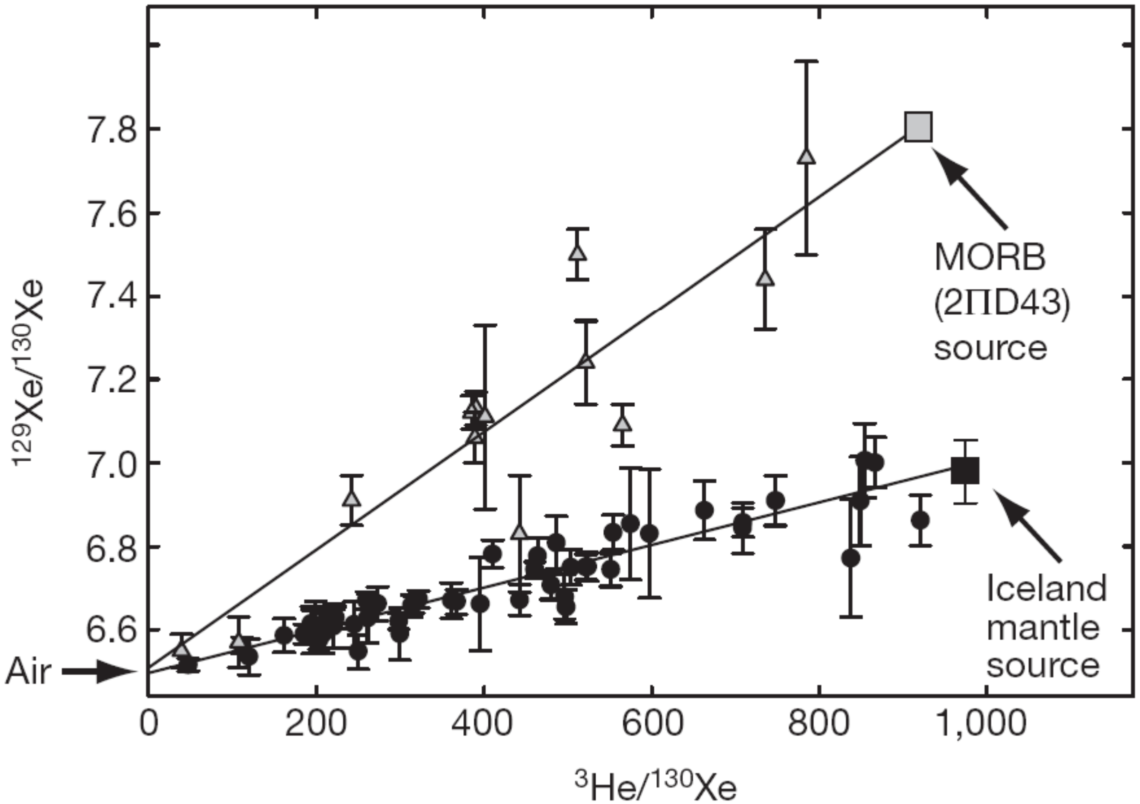

Mukhopadhyay (2012), Nature

Lower **$^{129}Xe/^{130}Xe$** in the **Iceland mantle source** than in the **MORB mantle source** indicates separation of both sources **before ~4.45 Ga**, and only **<u>very limited mixing</u>** since then!

In other words: It seems that the Earth's mantle sustained a large-scale heterogeneity since Earth formation

^{129}I (β)^{129}Xe ($T_{1/2}$ ~ 6 Ma)

^{244}Pu (^{238}U) (fission) ^{136}Xe (^{131}Xe ^{132}Xe ^{134}Xe)

Half life of ^{244}Pu: ~80 Ma

Chapter 5

Continent... matism

... or, sim ... broader sense ...

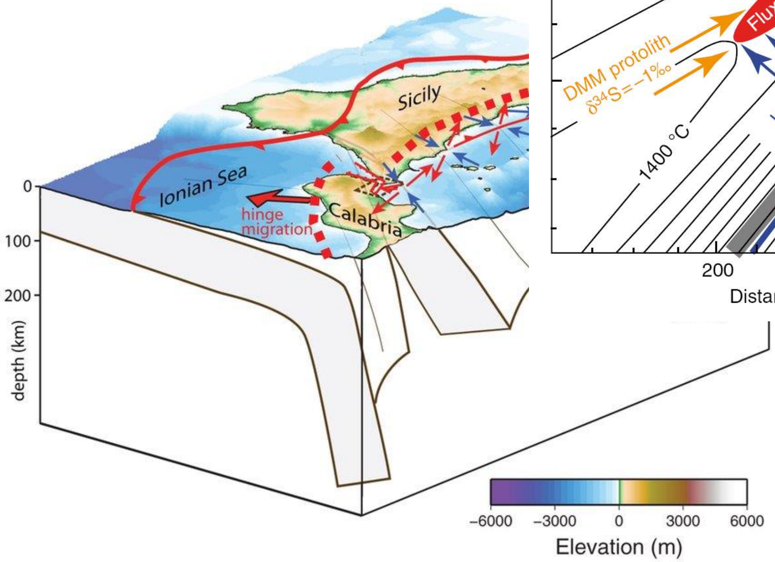

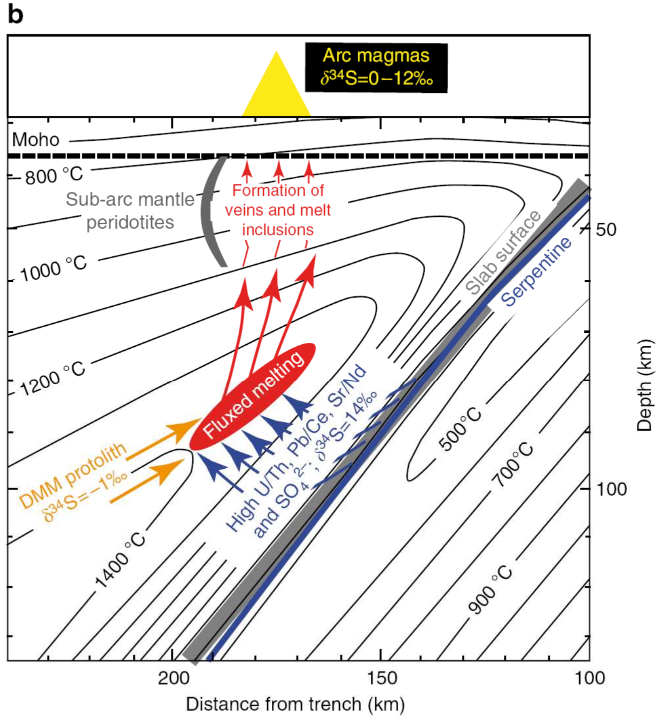

Mt. Etna (Sicily).

*...nantle source tapped ... which opened due to slab bending and subsequent **slab tear***

Bénard et al., 2017, Nature

*Note that the **Eolian Islands** north of Sicily are different in that they result from **island arc magmatism**!*

Key questions

- What is the **geodynamic framework** in which CAM occurs?
- What **rock types** emerge from continental anorogenic magmatism (CAM)?
- What is the **source** of continental (anorogenic) magmatism?

  Is it the **asthenospheric** or the **lithospheric** mantle, or both?
- What is the **degree of melting**, what is the primary magma composition?
- What is the role of **crustal assimilation** and **fractional crystallisation**?

Circum-Mediterranean (anorogenic) igneous provinces

Cenozoic volcanic provinces – tectonic setting

Lustrino & Wilson, 2007

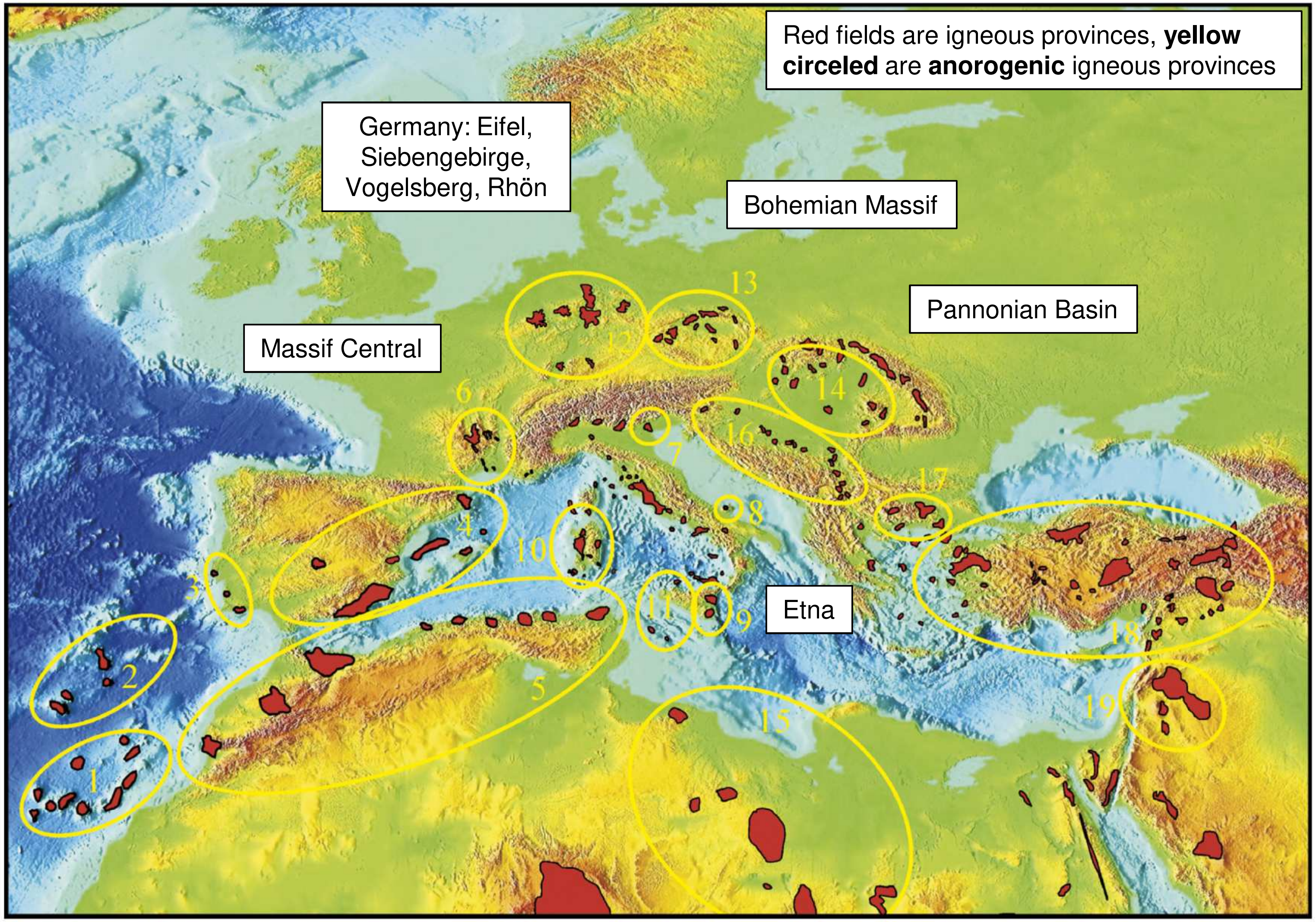

Tectonic setting of CAM

Here: Central European Volcanic Provinces – overview map

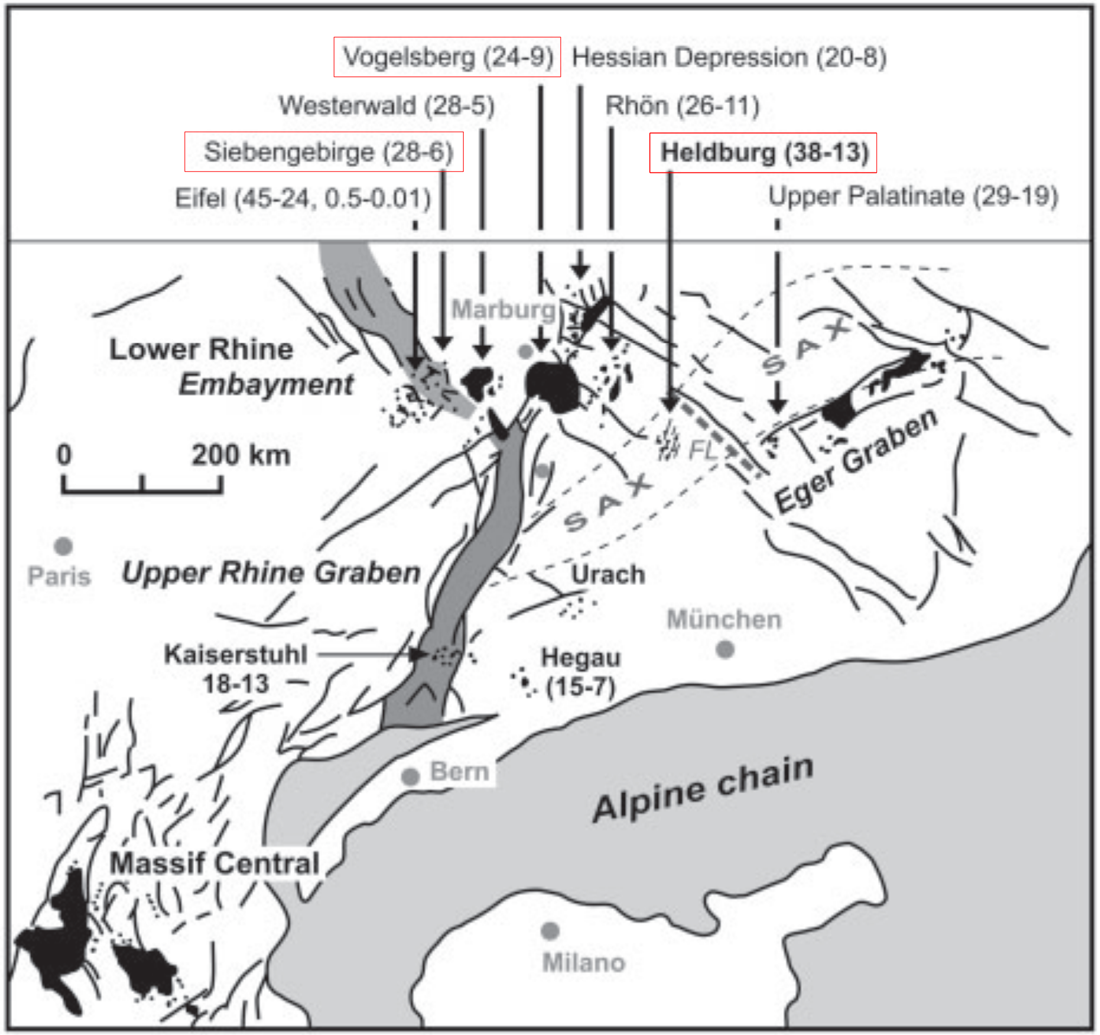

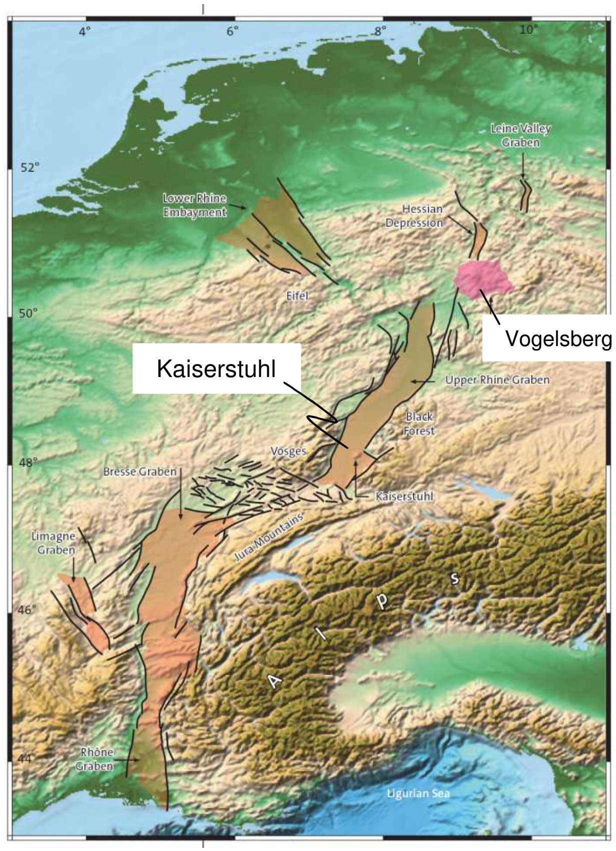

Lower Rhine graben, upper Rhine graben, Hessian depression, Vogelsberg, Bresse graben (from Frisch et al., 2010)

Tectonic setting of CAM

Magma origin – working hypothesis

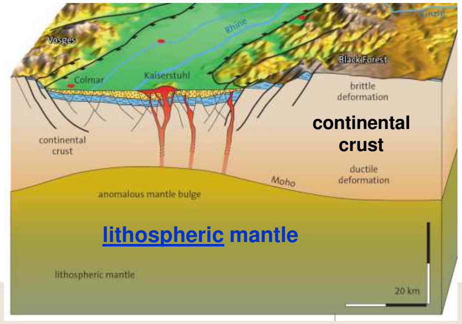

From Frisch et al., 2010

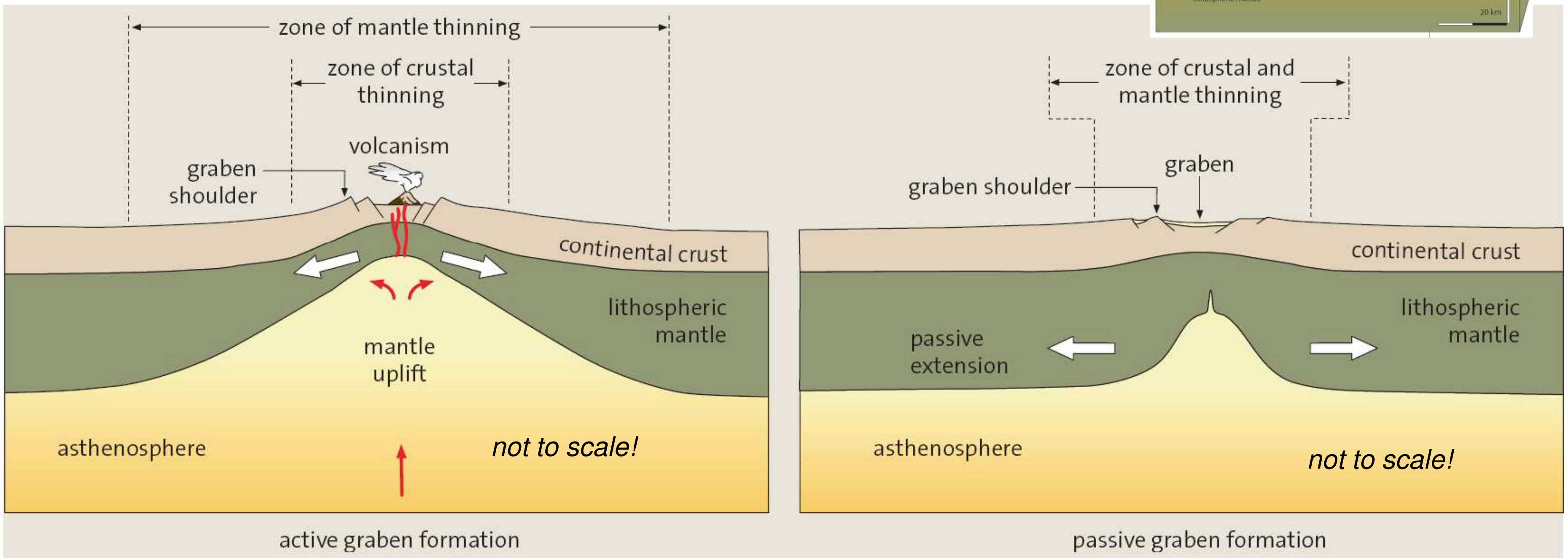

Rifting caused by mantle upwelling

Rifting caused by lithosphere extension

So, what causes melting of what, and why? Remember:

Melting the mantle?
Temperature is, what matters!

$$\left(\frac{\partial T}{\partial z}\right)_S = \frac{g\alpha_f T}{C_P}$$

Tectonic setting of CAM

Temperature distribution in the lithospheric and asthenospheric mantle beneath the Kaiserstuhl

MBL = Mechanical boundary layer

TBL = Thermal boundary layer

Conductive geotherm calculated

based on T_p = 1300°C

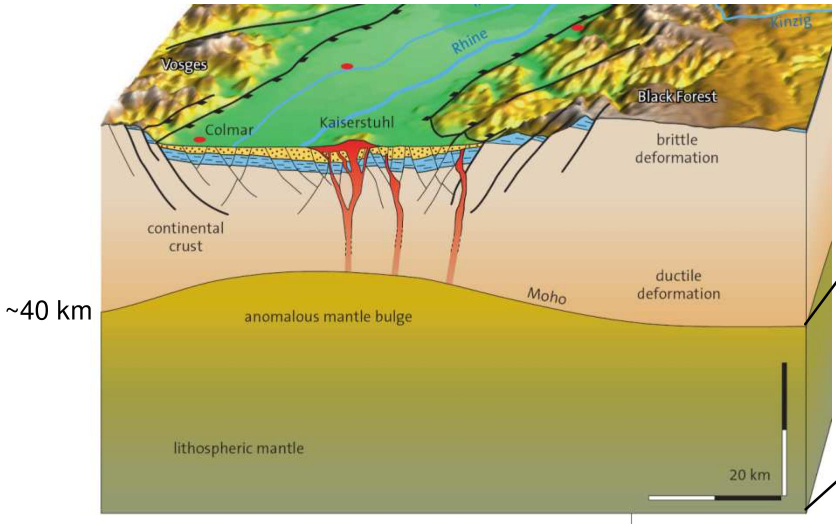

From Frisch et al., 2010

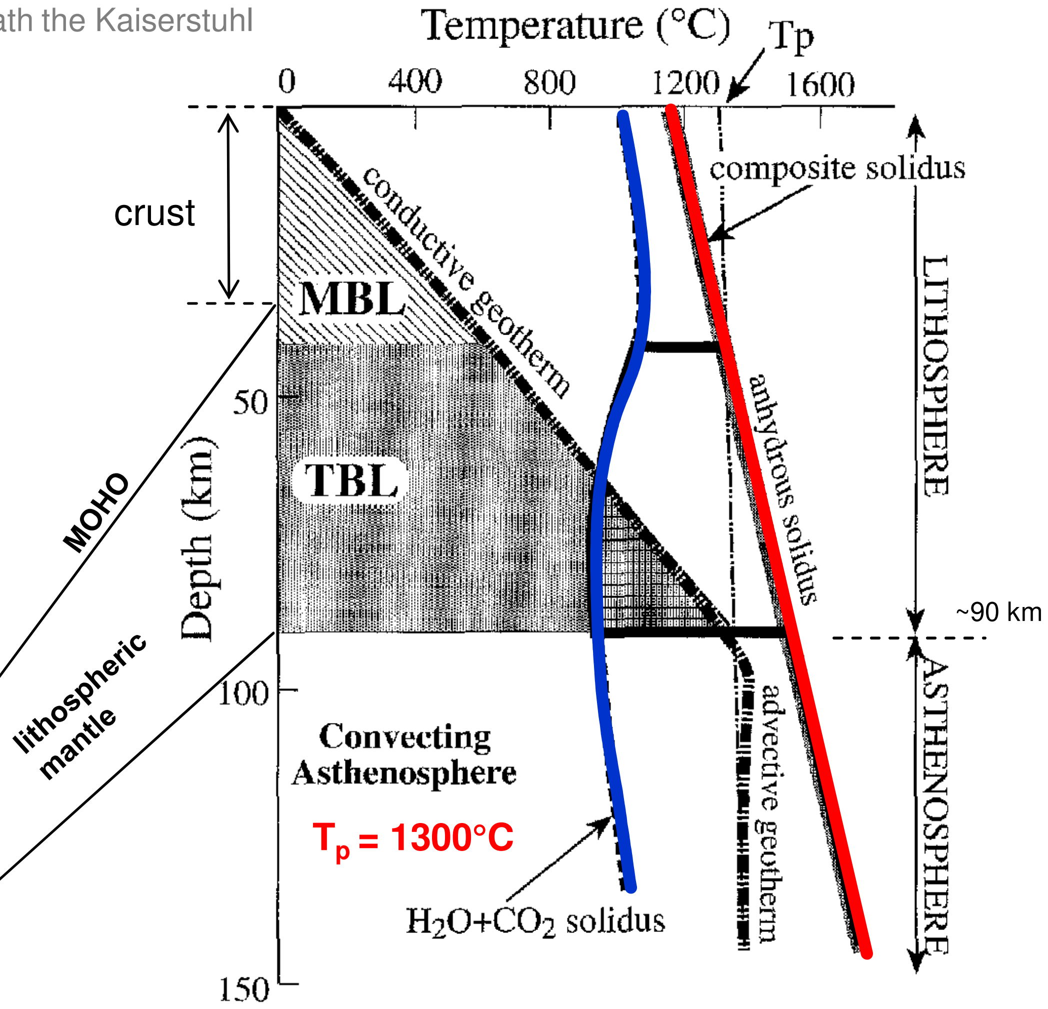

Wilson et al. (1995)

Rock types in continental magmatic settings

Siebengebirge volcanic province (Central Germany)

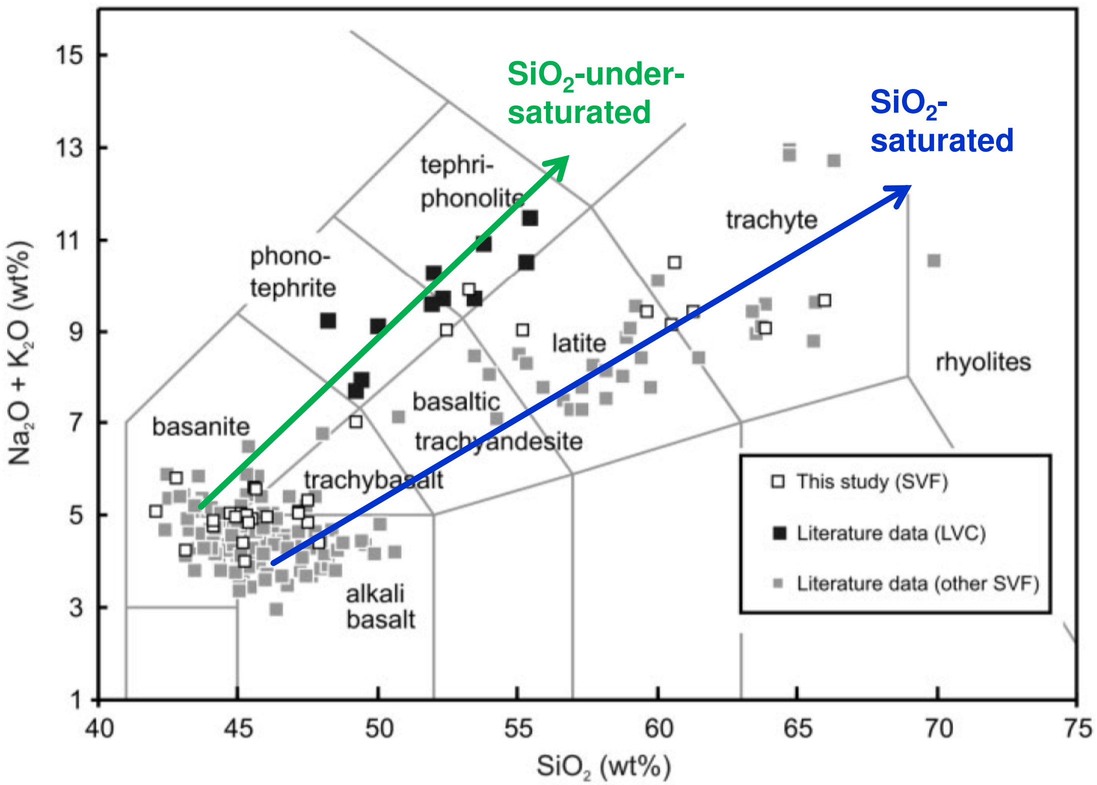

Kolb et al., 2012; Jung et al., 2012

Przybyla et al., 2017

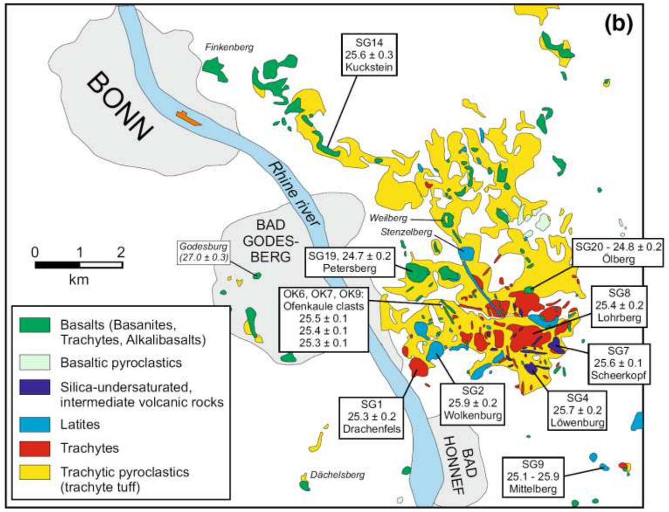

Siebengebirge volcanic province in Central Germany near Bonn (Rhein) (From Przybyla et al., 2017)

Anorogenic continental magmatism comprises both, **SiO_2-undersaturated** and **SiO_2-saturated** *alkaline* series

Rock types in continental magmatic settings

Vogelsberg volcanic province (Central Germany)

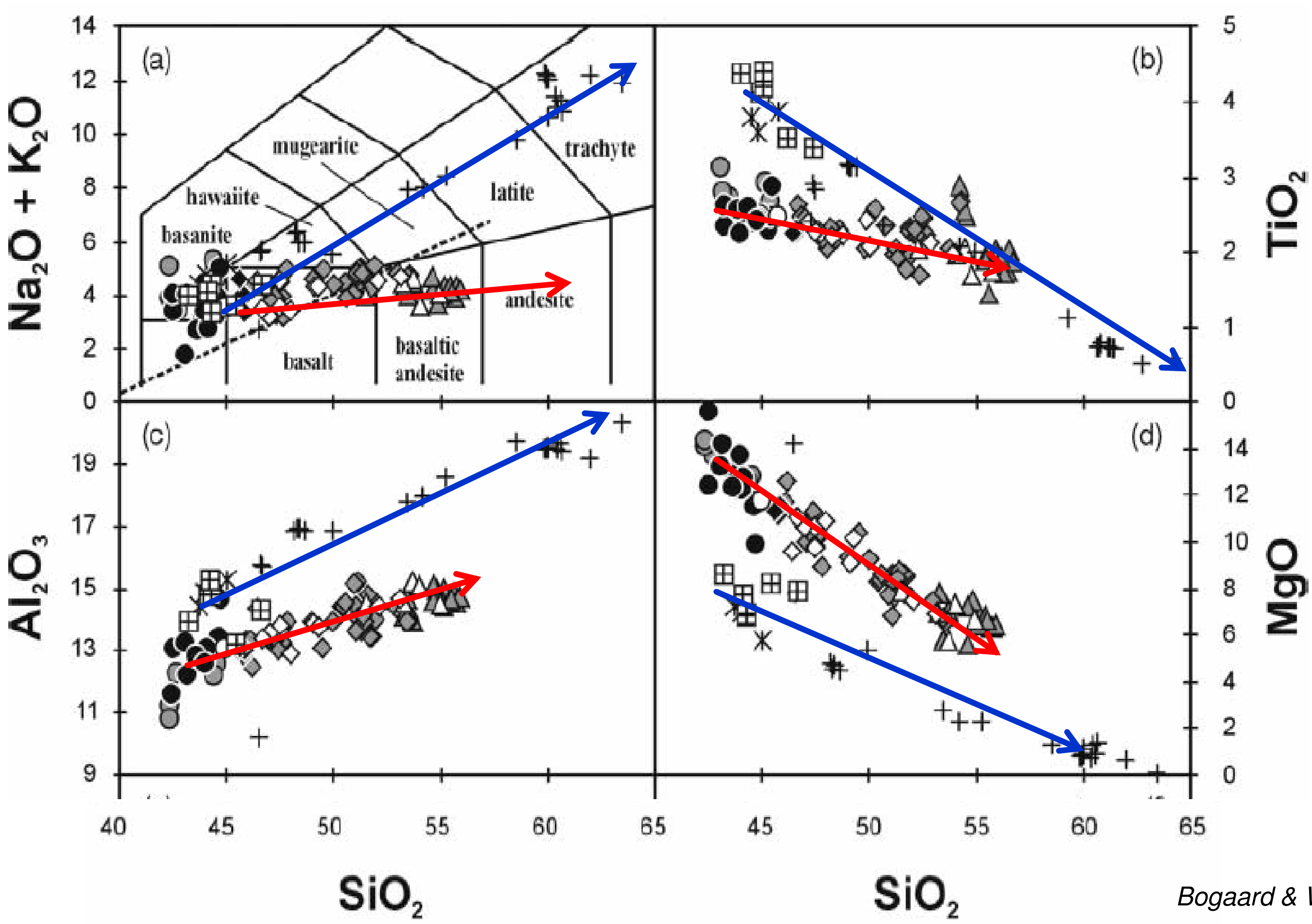

In the **Vogelsberg** volcanic province, magmatism erupted both, **alkaline series** and **tholeiite series** rocks

Bogaard & Wörner, 2003

Rock types in continental magmatic settings

Trace element and isotope characteristics

Kolb et al., 2012

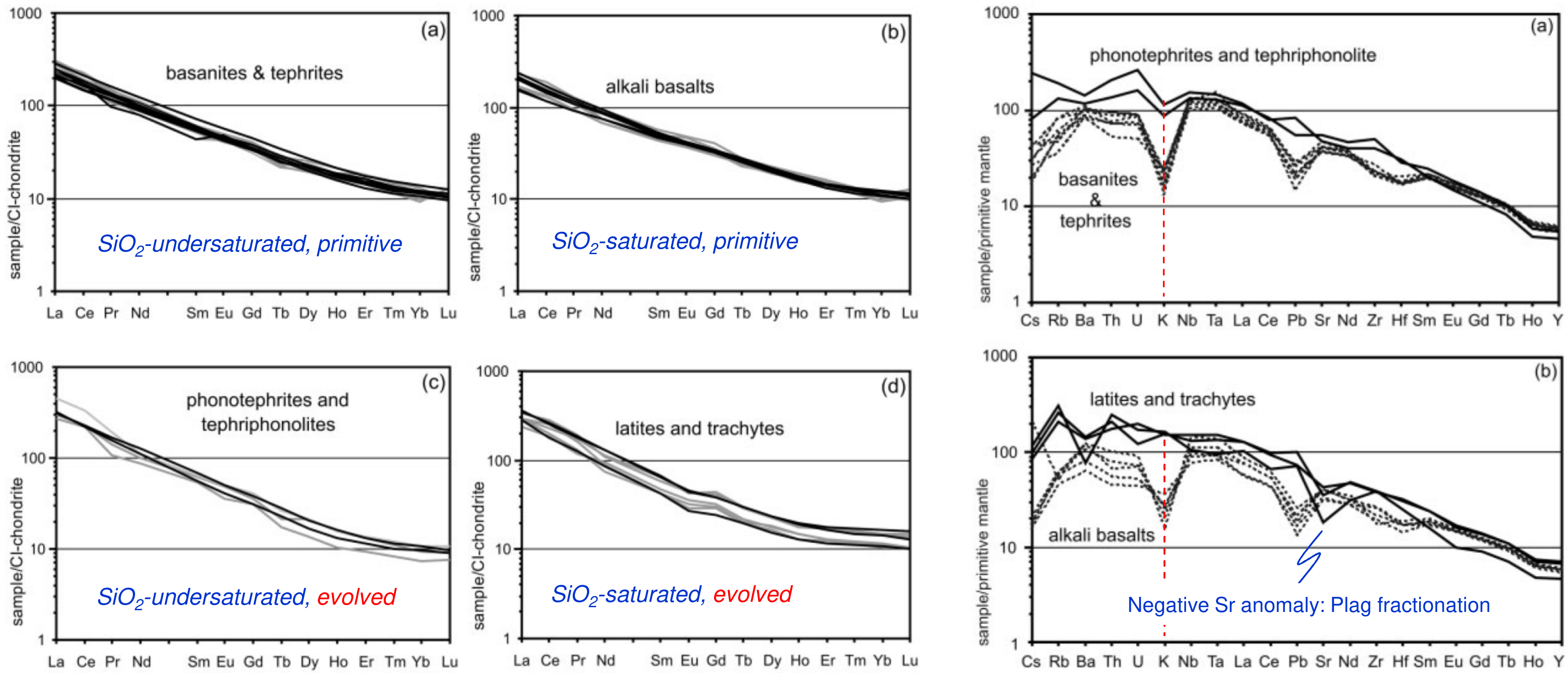

Chemical characteristics of **volcanic rocks** from the <u>**Siebengebirge**</u>. Trace element enrichment, **Nb/La ~1 (or >1)** as well as **negative (Cs, Rb), K and Pb anomalies** in the <u>basanites/tephrites</u> and <u>alkali basalts</u> are obvious. Differentiated serie have higher TE amounts.

Rock types in continental magmatic settings

Trace element and isotope characteristics

Bogaard & Wörner, 2003

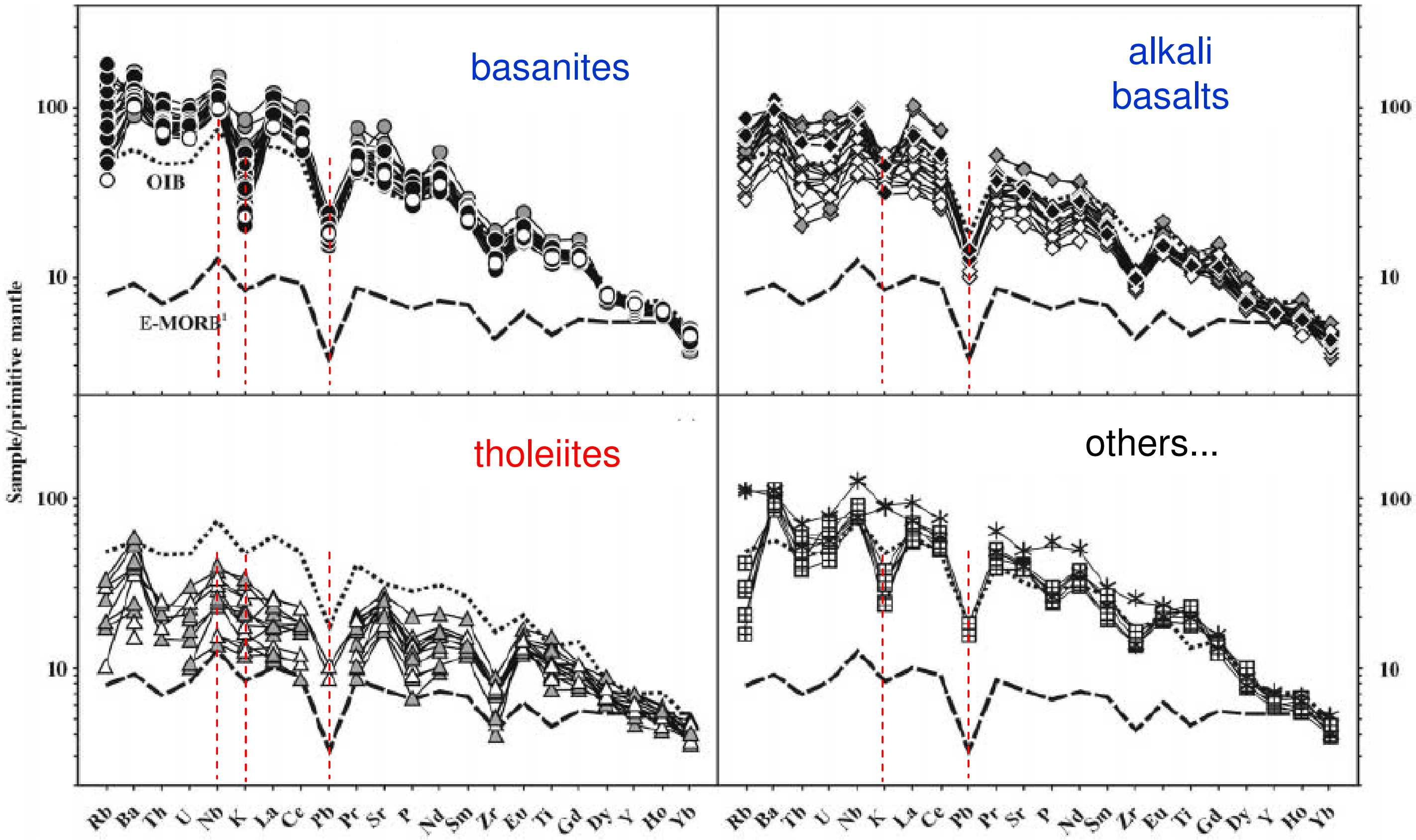

Chemical characteristics of **volcanic rocks** from the **Vogelsberg**. Note the negative K- and Pb-anomalies in the **alkaline rocks** (that strongly resemble OIBs), but the **absence of a negative K-anomaly in the tholeiites**

Rock types in continental magmatic settings

Trace element and isotope characteristics

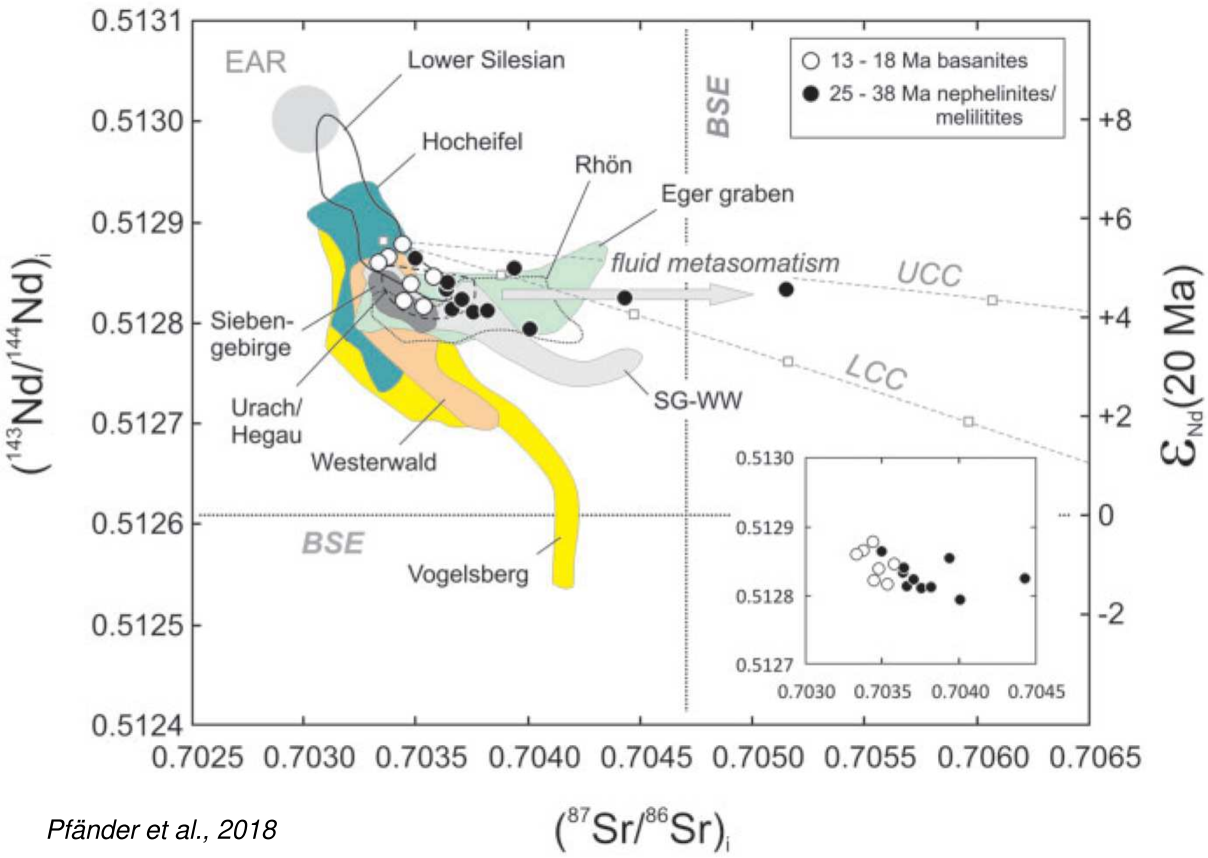

Pfänder et al., 2018

Nd-Sr isotope characteristics of **intraplate basalts** from Central to East Germany and the Silesian and Eger volcanic provinces.

Dots are **basanites and nephelinites** from the Heldburg region (N-Bavaria and S-Thuringia).

Note that the **isotope compositions** resemble – very broadly – the **PREMA composition of OIBs:** *EAR = European Asthenospheric Reservoir*

Mantle sources involved in CAM

Lithospheric vs. asthenospheric mantle source

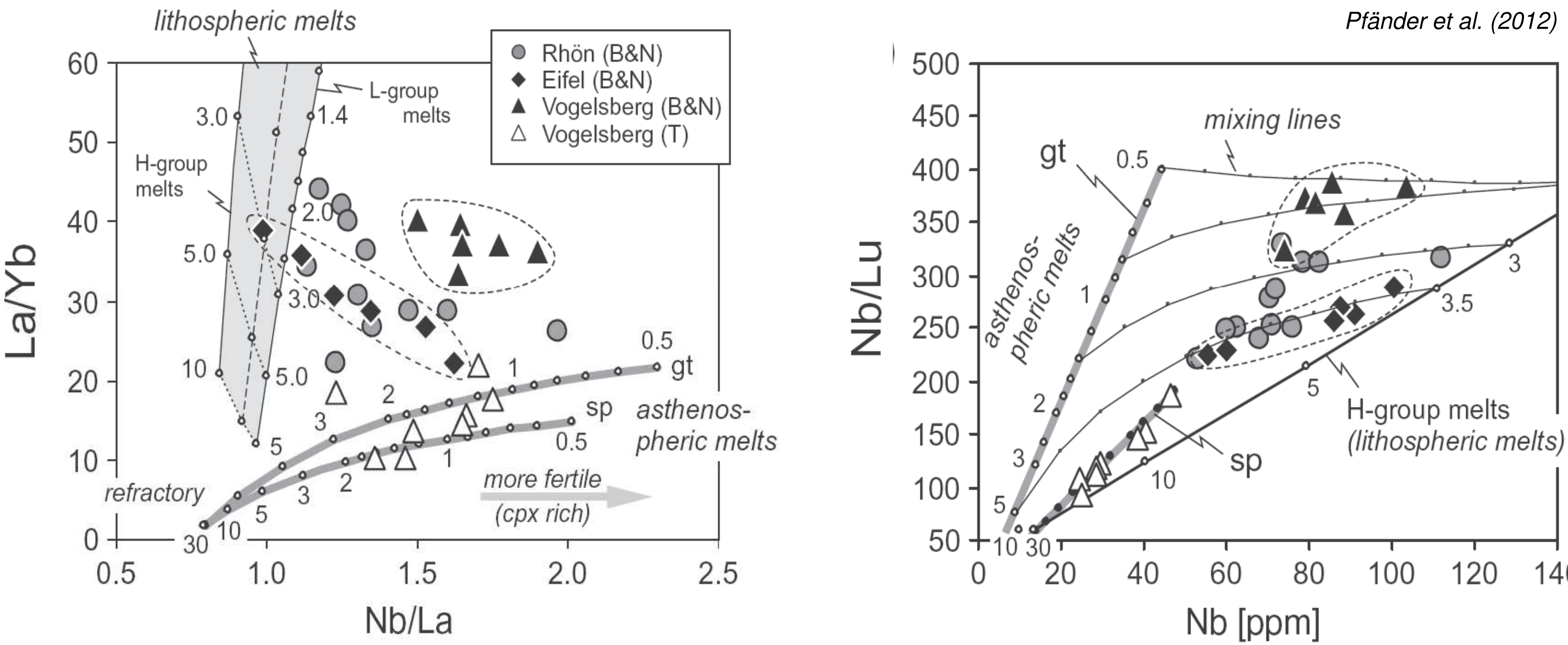

Trace-element modelling applied to **primitive mafic rocks** from the Rhön, Eifel and Vogelsberg magmatic provinces indicate the involvement of **at least three mantle source components** (primitive to slightly-depleted asthenospheric garnet- and spinel-peridotite mantle components as well as enriched spinel-peridotite lithospheric mantle)

Evolution of CAM

Regional examples and conclusions: Heldburg region

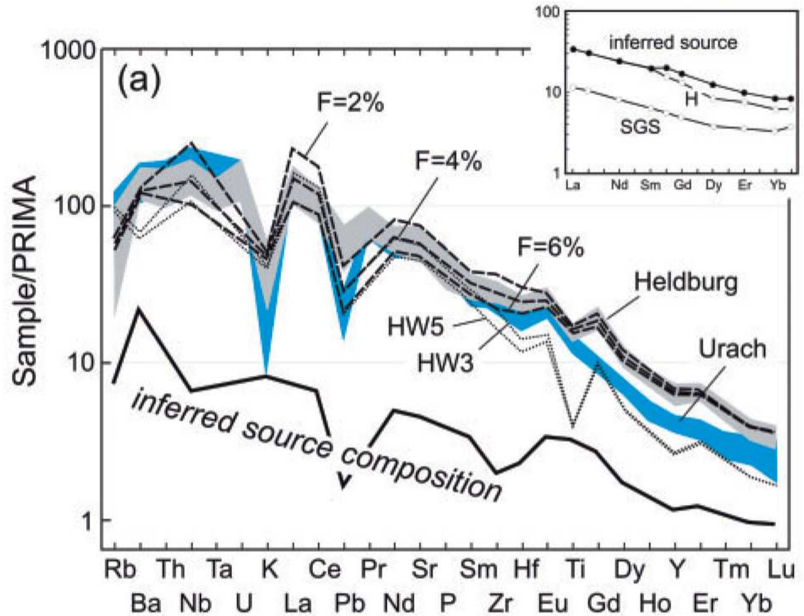

The HELDBURG region seems to be a rare example of nearly pure (low-degree) melting of a strongly metasomatised **lithospheric mantle**

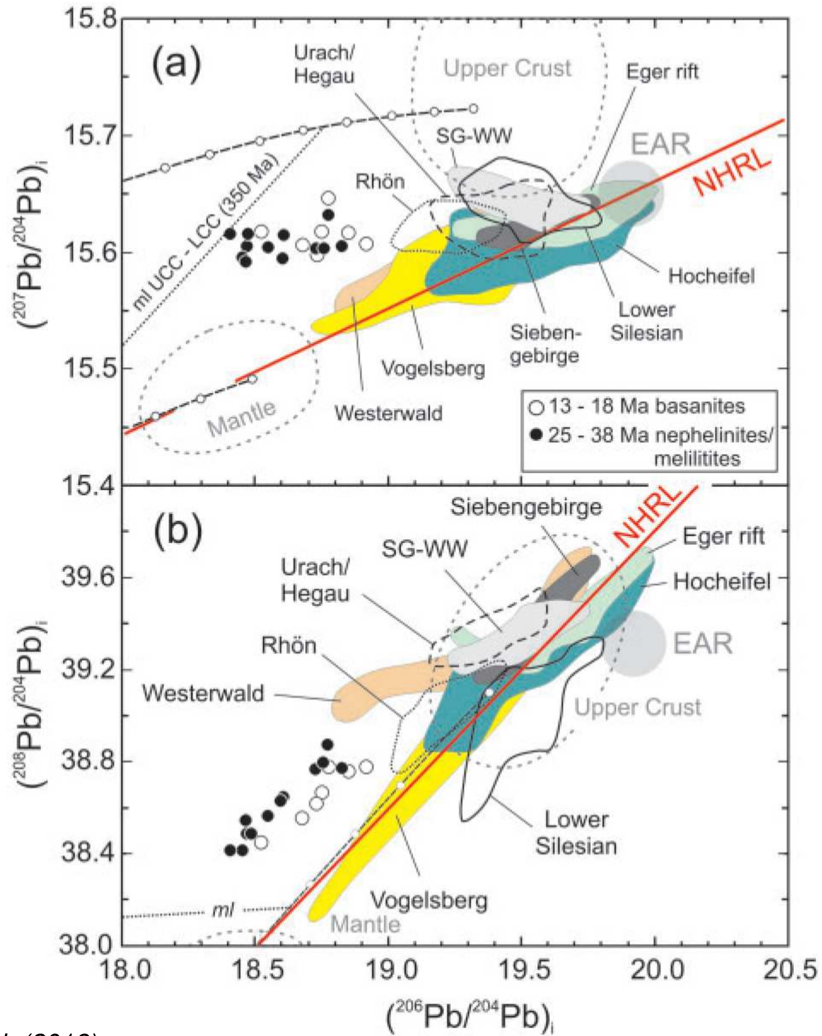

Pfänder et al. (2018)

Evolution of CAM

Regional examples and conclusions: Heldburg region

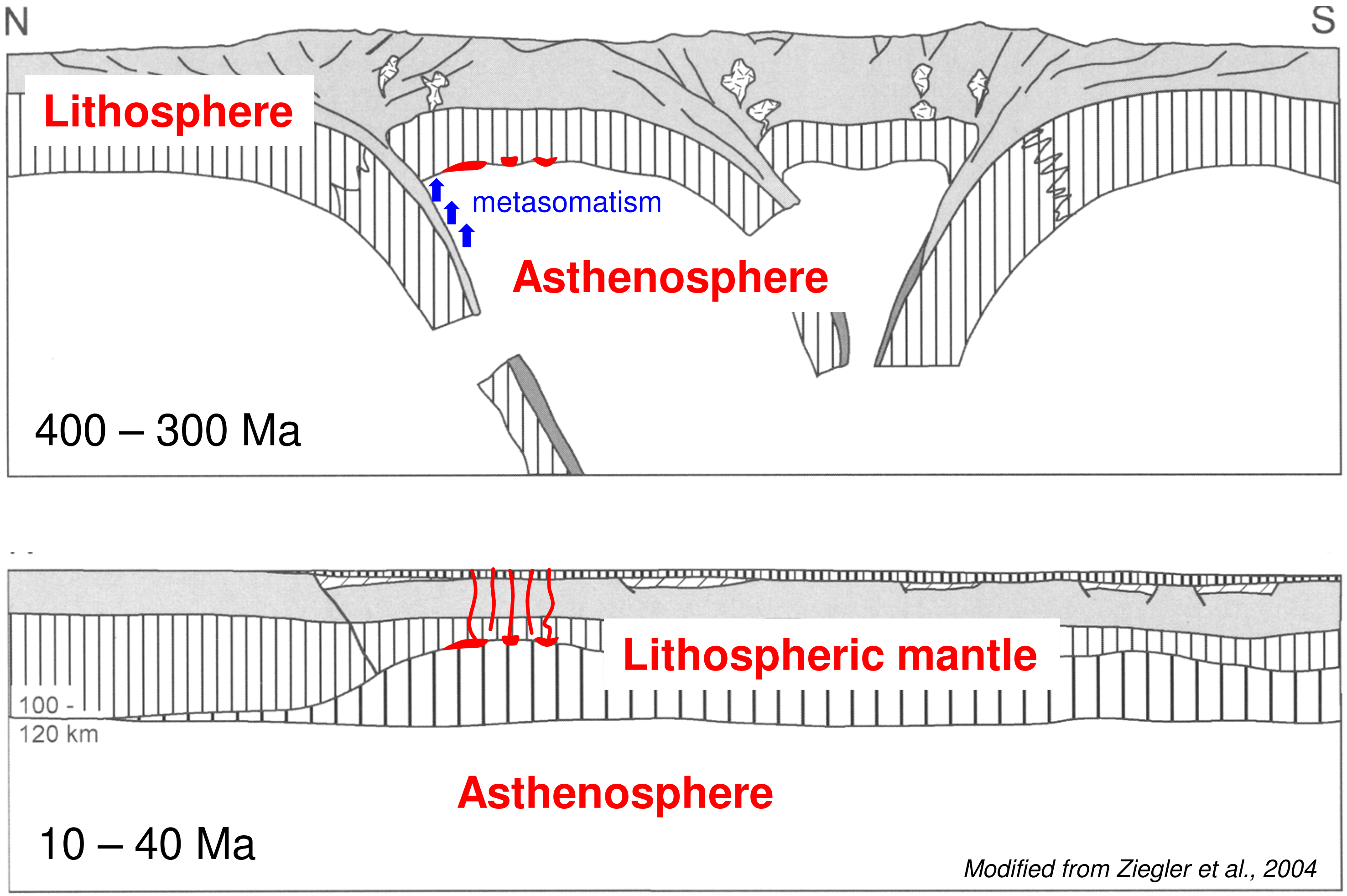

Modified from Ziegler et al., 2004

Evolution of CAM – more regional examples

Messum, Brandberg, Erongo, Paresis alkaline complexes

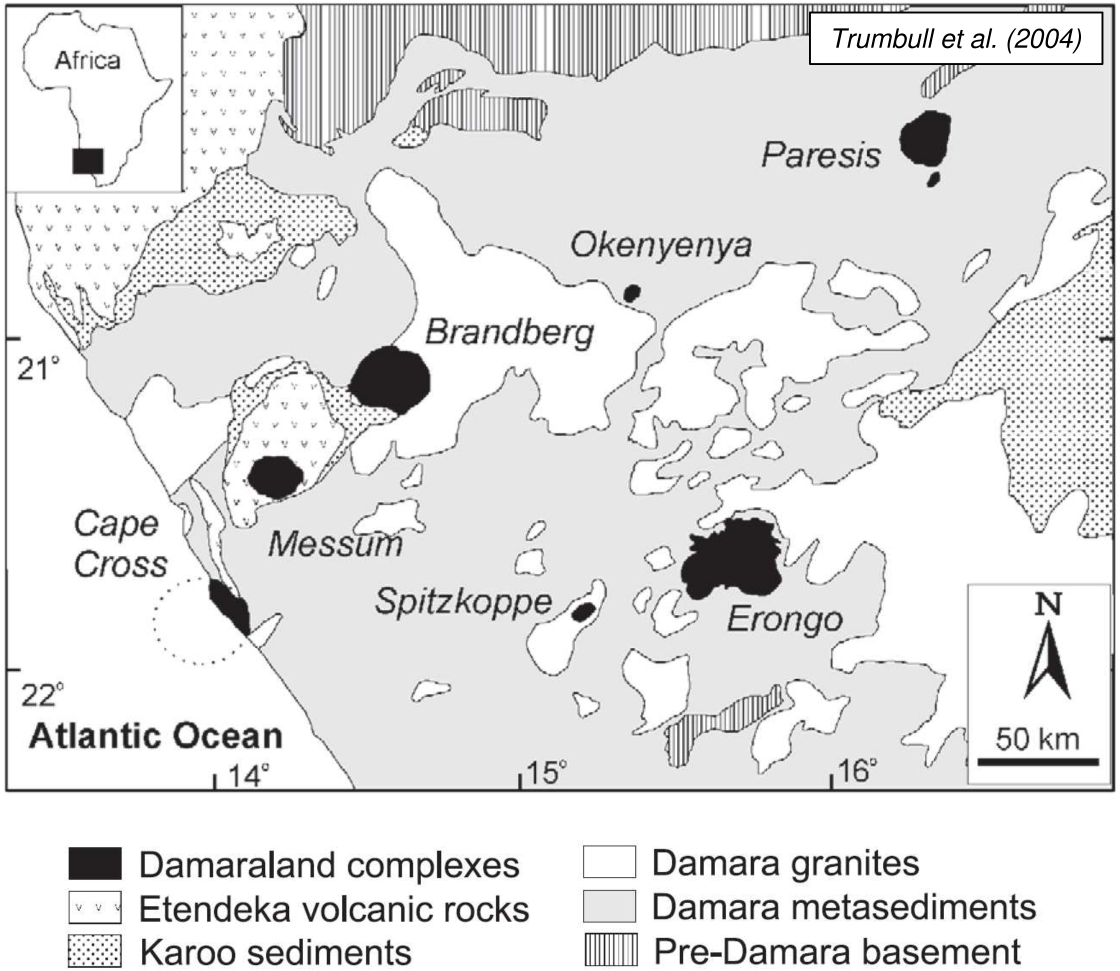

These **early Cretaceous** Complexes (137-125 Ma) comprise a broad variety of volcanic to plutonic rocks (basanites, tephrites, alkali basalts, gabbros, Qz- and Neph-syenites, alkali-granites, etc.)

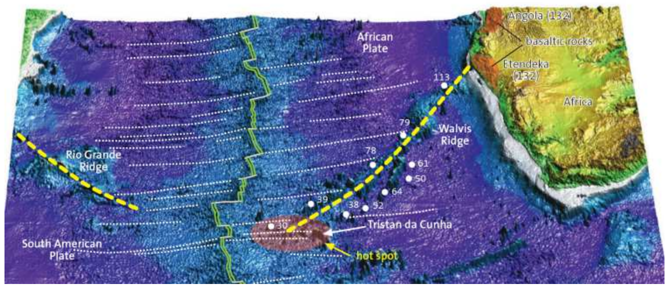

Tristan da Cunha mantle plume and ‚hot spot track' (Wlavis ridge) SW of Namibia (from Frisch et al., 2010)

Hot spot induced intraplate magmatism

Afar Hot Spot – Afar Triple Junction – Ethiopian Rift

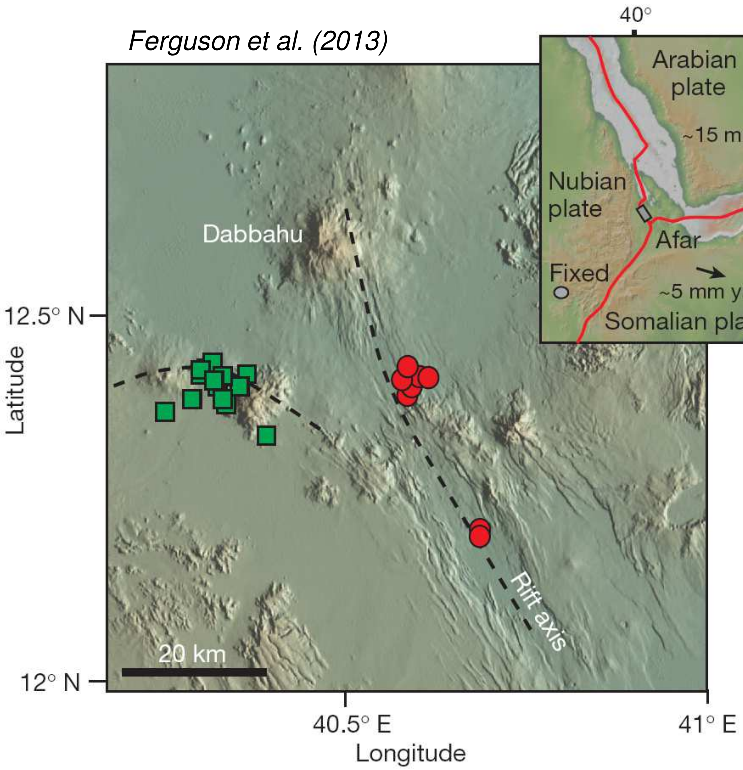

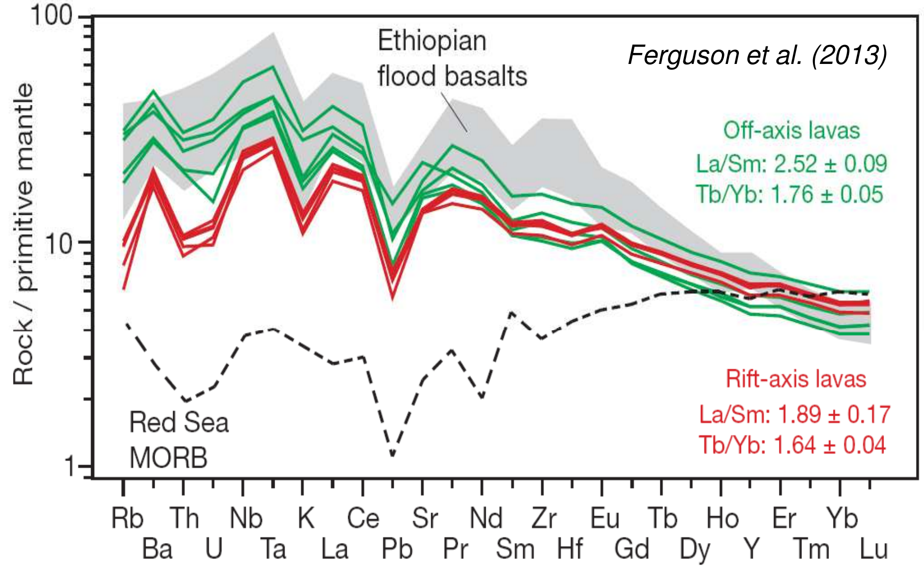

High contents of LILE, but in particular Nb and Ta indicate the plume contribution in the EFBs. Assimilation of continental crust would reduce the Pb anomaly and would lower Nb and Ta

‚Exotic‘ rock types in continental magmatic settings: Carbonatites, Kimberlites, Lamproites, Lamprophyres

Carbonatites ⟵ Lamprophyres ⟶ Lamproites

Carbonatites

Rocks from mantle derived ultra-low degree melts consisting of >50 mod.% primary Ca, Mg, Na, (K) – carbonate

Mantle source is CO_2-rich (metasomatism)

Lamprophyres

Ultramafic (often diamond bearing) rocks, intermediate between Carbonatite and Lamproite

Lamproites

Ultramafic silicic rocks derived from a H_2O-rich (but mostly CO_2-free) mantle source.

Mantle source possibly contains some CH_4

Kimberlites

Ultramafic alkaline, often diamond bearing rocks from the deepest parts of the cratonic lithosphere

Such **highly SiO_2-undersaturated** rocks typically represent **low- to ultra-low degree melts** from the interface between the **lowest parts** of the metasomatised **continental lithospheric mantle** and the **convecting asthenosphere**

‚Exotic' rock types in continental magmatic settings: Lamprophyres from Beaver Lake, Antarctica

Table 1. *Modal mineral abundances in the Beaver Lake ultramafic lamprophyre facies*

Intrusion type	Ol	Ne	Mel	Phl	Ti-Mag	Prv	Ap	Carb	Cpx	Spl	Glass	Mtc
Dyke	10–15	7–10	30–40	7–10	7–10	3–5	< 1	5–10	–	2–3	3–5	–
Plug	7–10	10–15	20–30	15–20	7–10	7–10	< 1	3–5	+ **	+	10–15	–
Sill	5–7	20–25	15–20	30–40	10–15	10–15	2–3	3–5*	–	< 1	2–3	+

* Carbonate is mainly secondary calcite; ** clinopyroxene occurs only within leucocratic globules

Foley et al., 2002

Nepheline	$Na(AlSiO_4)$ *or* $Na_3K(Al_4Si_4O_{16})$	
Melilite	$(Ca,Na)_2(Al,Mg,Fe^{2+})(Si,Al)_2O_7$	
Phlogopite	$KMg_3[(AlSi_3)O_{10}(F,OH)_2]$	
Perovskite	$CaTiO_3$	
Apatite	$(Ca,Ba,Pb,Sr,etc.)_5(PO_4,CO_3)_3(F,Cl,OH)$	

Lamprophyres *from Antarctica in a TAS diagram. Note the strongly* ***SiO_2-undersaturated*** *nature that results from* ***very low degrees of melting*** *(<2%) and a* ***great melting depth*** *(>120 km)*

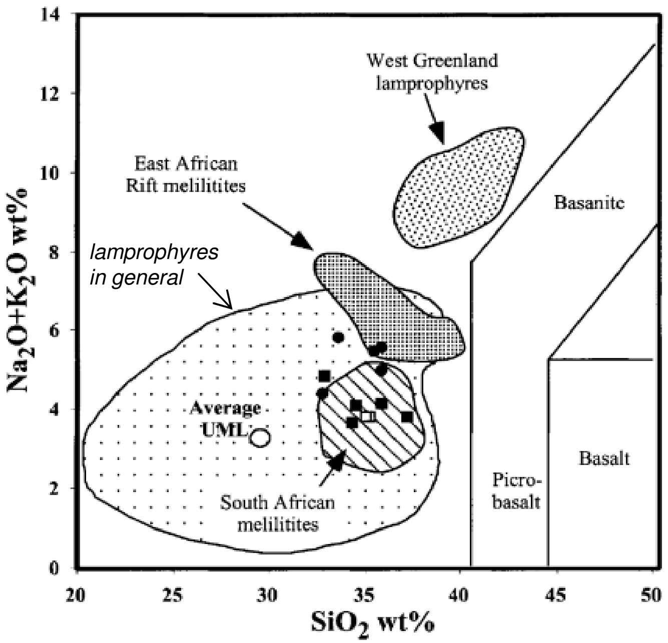

‚Exotic' rock types in continental magmatic settings: Kimberlites from Kimberley, South Africa

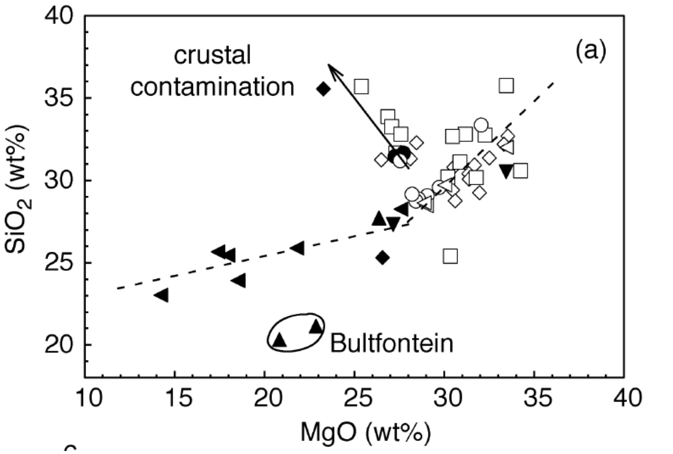

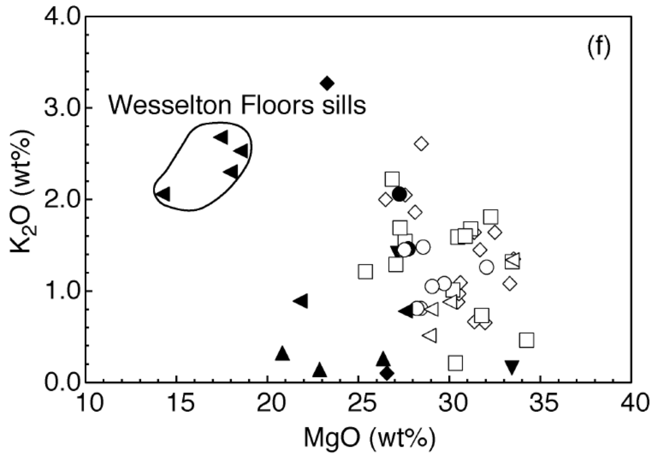

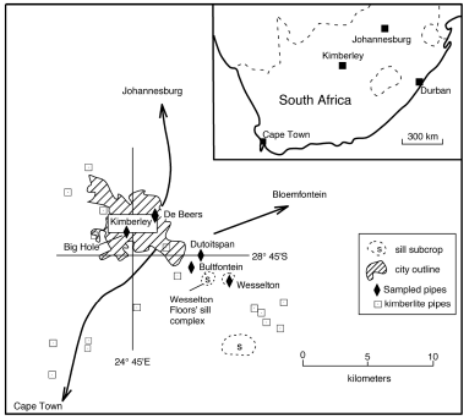

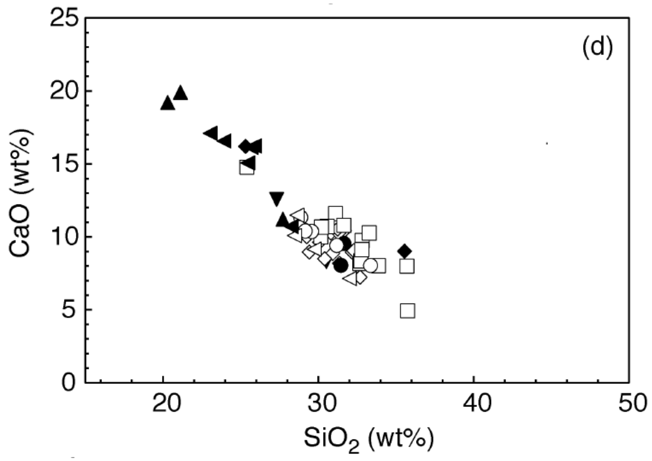

Kimberlites originate from the interface of the convecting mantle and the lowermost **cratonic continental lithosphere** – they represent the deepest known melting depths, and ultra-low degrees of melting (~1%)

Le Roex et al., 2003, Journal of Petrology

‚Exotic' rock types in continental magmatic settings: Kimberlites from Kimberley, South Africa

Le Roex et al., 2003, Journal of Petrology

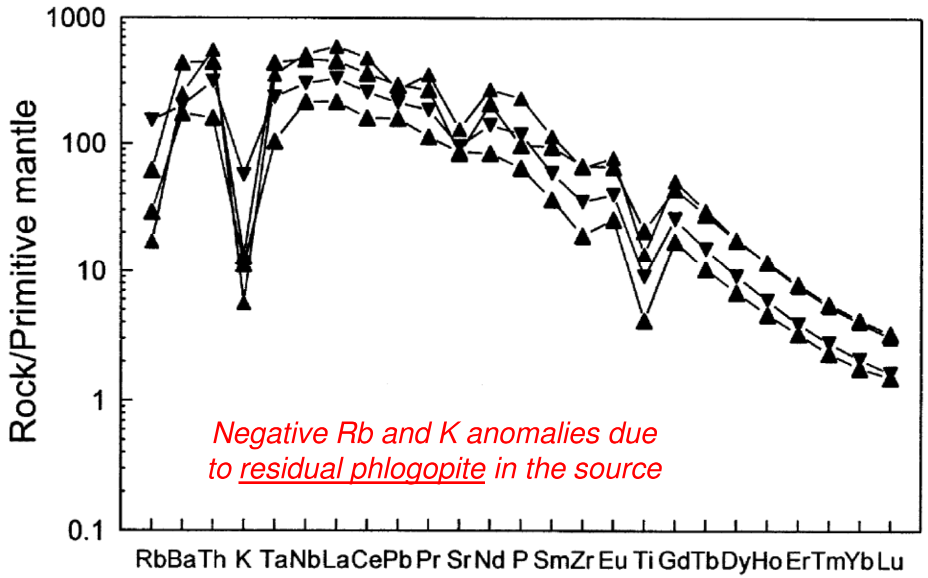

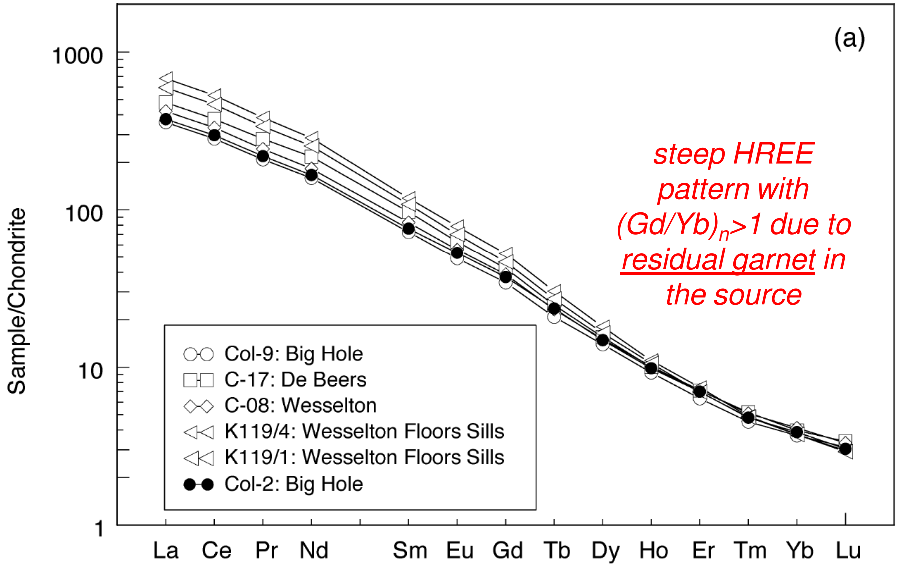

Extremely enriched trace-element patterns (very high La/Yb-ratios) due to an enriched (metasomatised), carbonate-bearing **garnet-peridotite** source (cratonic mantle) and **very low degrees of melting** (great melting depths **>160 km**)

The role of lithosphere thickness

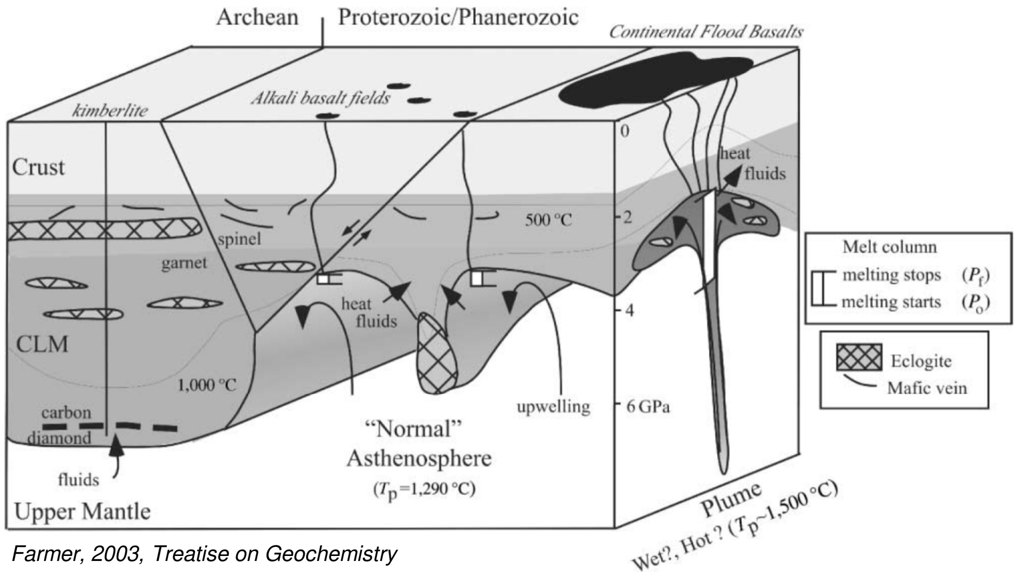

Farmer, 2003, Treatise on Geochemistry

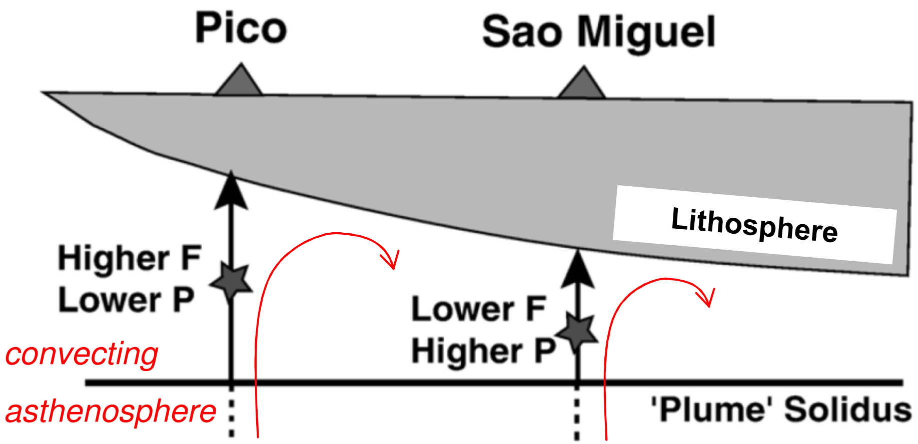

Prytulak & Elliott, 2007

Beside the potential temperature of the convecting mantle, the **degree of melting** broadly depends on the ***thickness of the lithosphere***

Geothermal gradients in Phanerozoic, Proterozoic and Archean Continental Regions estimated from heat flow measurements

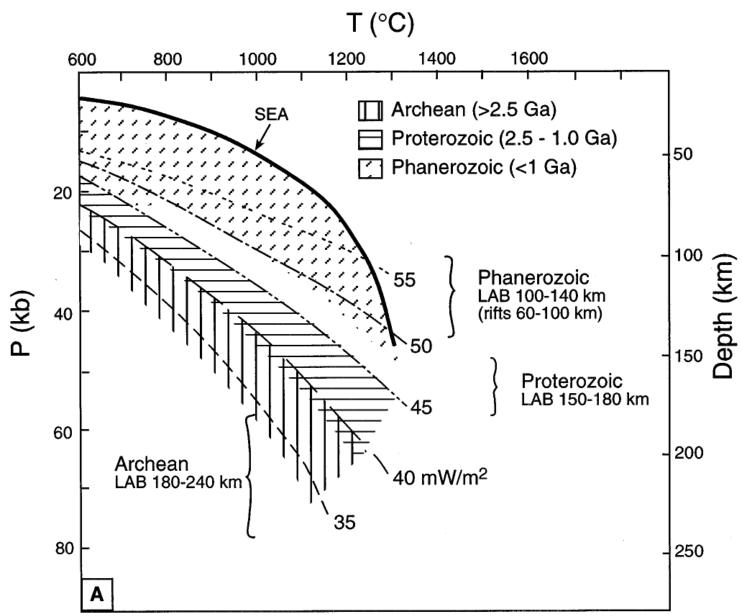

Summary I: Continental (anorogenic) magmatism

- **Rock types** are predominantly **alkaline** SiO_2-undersaturated and saturated volcanic and plutonic series (basanites, tephrites, alkali basalts, ...)
- CAM is mostly observed in **extensional geodynamic settings** where **lithosphere thinning** causes **mantle upwelling** and **decompression melting**
- During melting, **asthenospheric** and (metasomatised) **lithospheric** mantle sources are involved, leading to overall **enriched** trace-element compositions

Summary II: Continental (anorogenic) magmatism

- The degrees of melting are lower (3-7%) than in oceanic settings, dependent on mantle potential **temperature**, lithosphere **thickness** and **volatile content**
- **Crustal assimilation** and **fractional crystallisation** (AFC) play a role where primary magmas **differentiate** to more evolved series (phonolites, trachytes, ...)
- ‚Exotic' rocks such as **Carbonatites**, **Kimberlites** or **Lamprophyres** form by ultra-low degrees of melting from highly volatile-rich, **very deep** (lithospheric) mantle sources

Chapter 6

Convergent plate margins

Continental Arcs

Continental Collision Zones

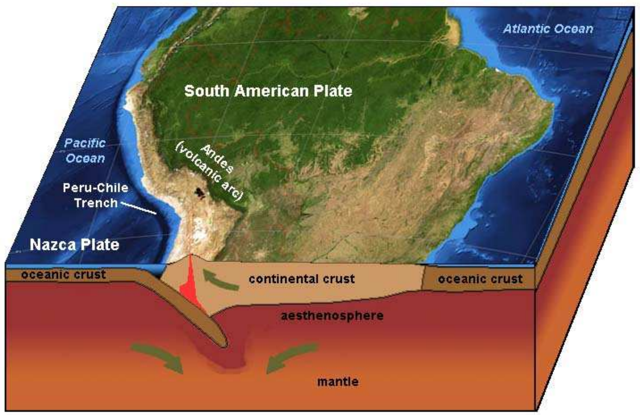

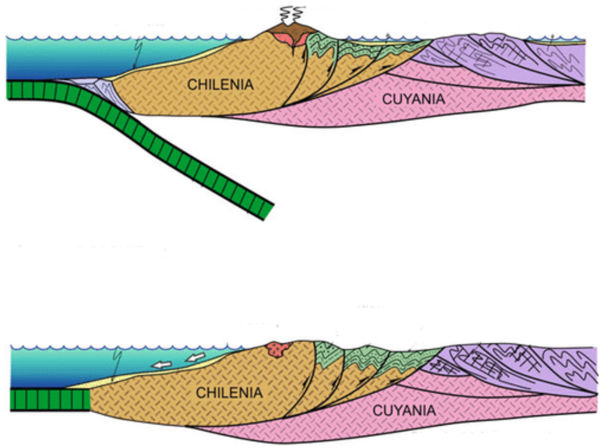

How can we generate continental crust from a mantle, whose primary melting products are basaltic?

Two aspects need to be adressed:

1) *‚Real‘ formation of juvenile continental crust from mantle melting*
2) *Remelting and internal differentiation of pre-existing (continental) crust*

What is <u>continental crust</u> from a geochemical point of view?

Estimates from Rudnick & Gao, 2003

Table 11 Comparison of the upper, middle, lower and total continental crust compositions recommended here.

Element	*Upper crust*	*Middle crust*	*Lower crust*	*Total crust*
SiO_2	66.6	63.5	53.4	60.6
TiO_2	0.64	0.69	0.82	0.72
Al_2O_3	15.4	15.0	16.9	15.9
FeO_T	5.04	6.02	8.57	6.71
MnO	0.10	0.10	0.10	0.10
MgO	2.48	3.59	7.24	4.66
CaO	3.59	5.25	9.59	6.41
Na_2O	3.27	3.39	2.65	3.07
K_2O	2.80	2.30	0.61	1.81
P_2O_5	0.15	0.15	0.10	0.13
Total	100.05	100.00	100.00	100.12
Mg#	46.7	51.5	60.1	55.3

Rudnick & Gao, 2003, Treatise on Geochemistry

What is <u>continental crust</u> from a geochemical point of view?

Estimates from Rudnick & Gao, 2003

*The continental crust comprises **0.57 %** of the BSE, but accounts for **20-70%** of incompatible and highly incompatible elements*

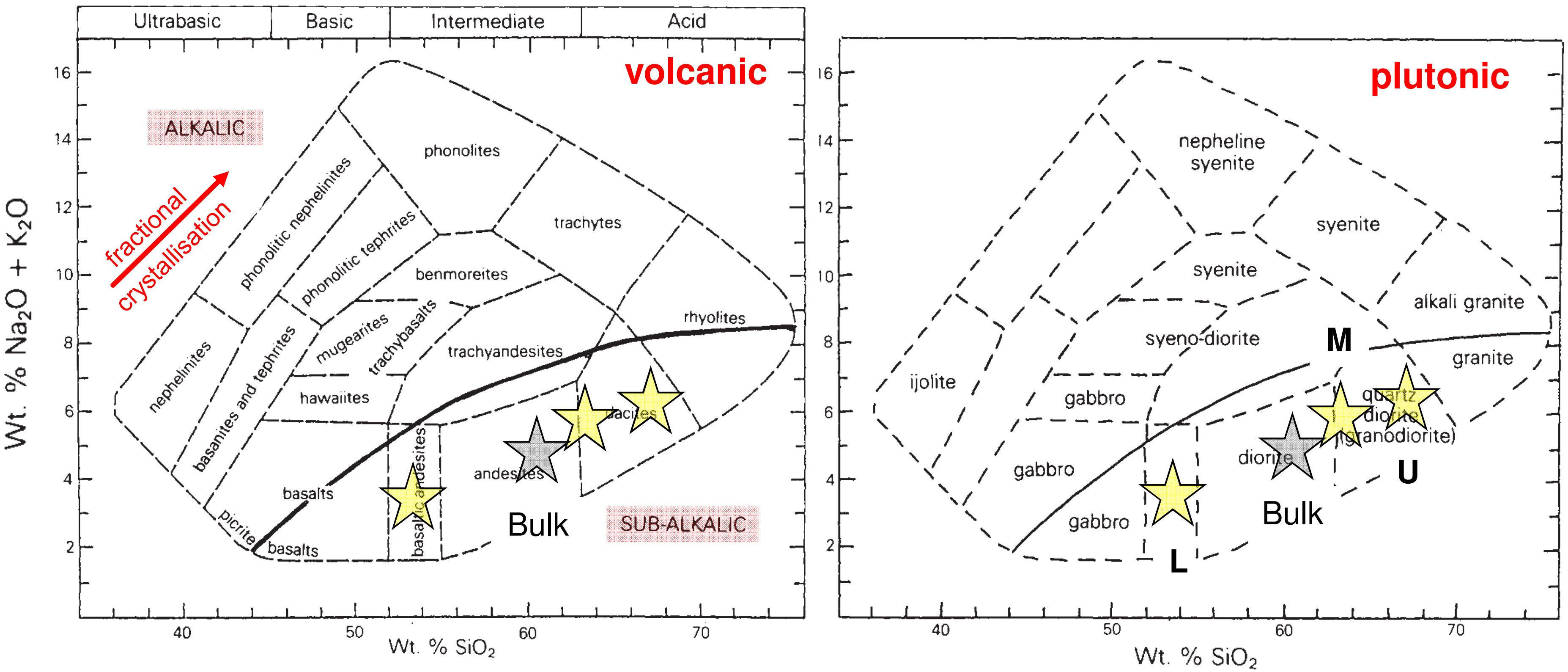

From: Wilson, M.: Igneous Petrogenesis, Springer.
Crustal estimates from Rudnick & Gao, 2003

L = lower, M = middle, U = upper, Bulk = whole continental crust

What is continental crust from a geochemical point of view?

Upper continental crust

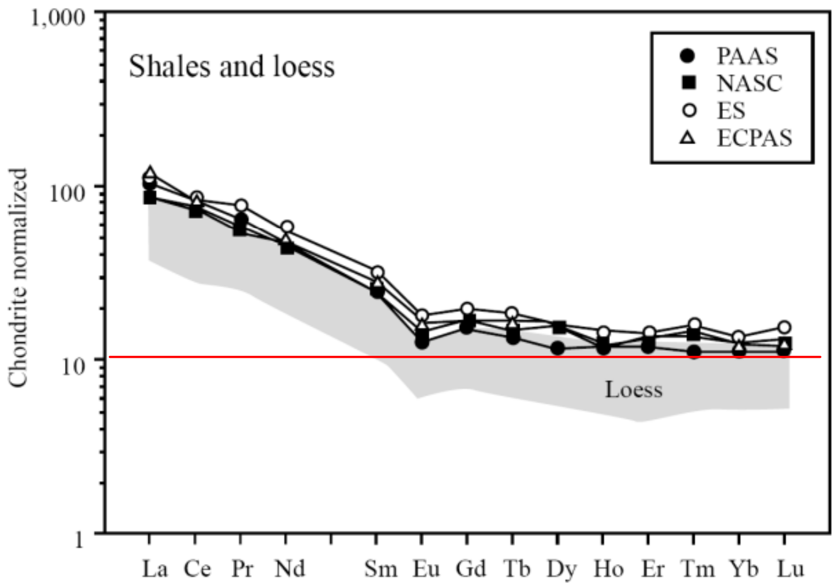

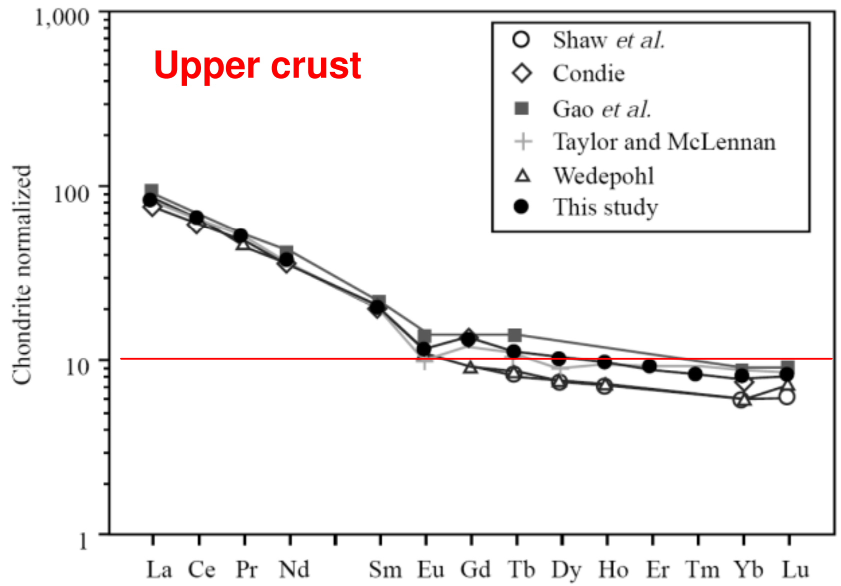

PAAS = Post Archean Australian Shale
NASC = Noth American Shale Composition
ES = European Shale Composition
ECPAS = Eastern China post-Archean Shale

Trace-element composition of the upper continental crust as estimated from shales

Rudnick & Gao, 2003, Treatise on Geochemistry

What is <u>continental crust</u> from a geochemical point of view?

Middle and lower continental crust

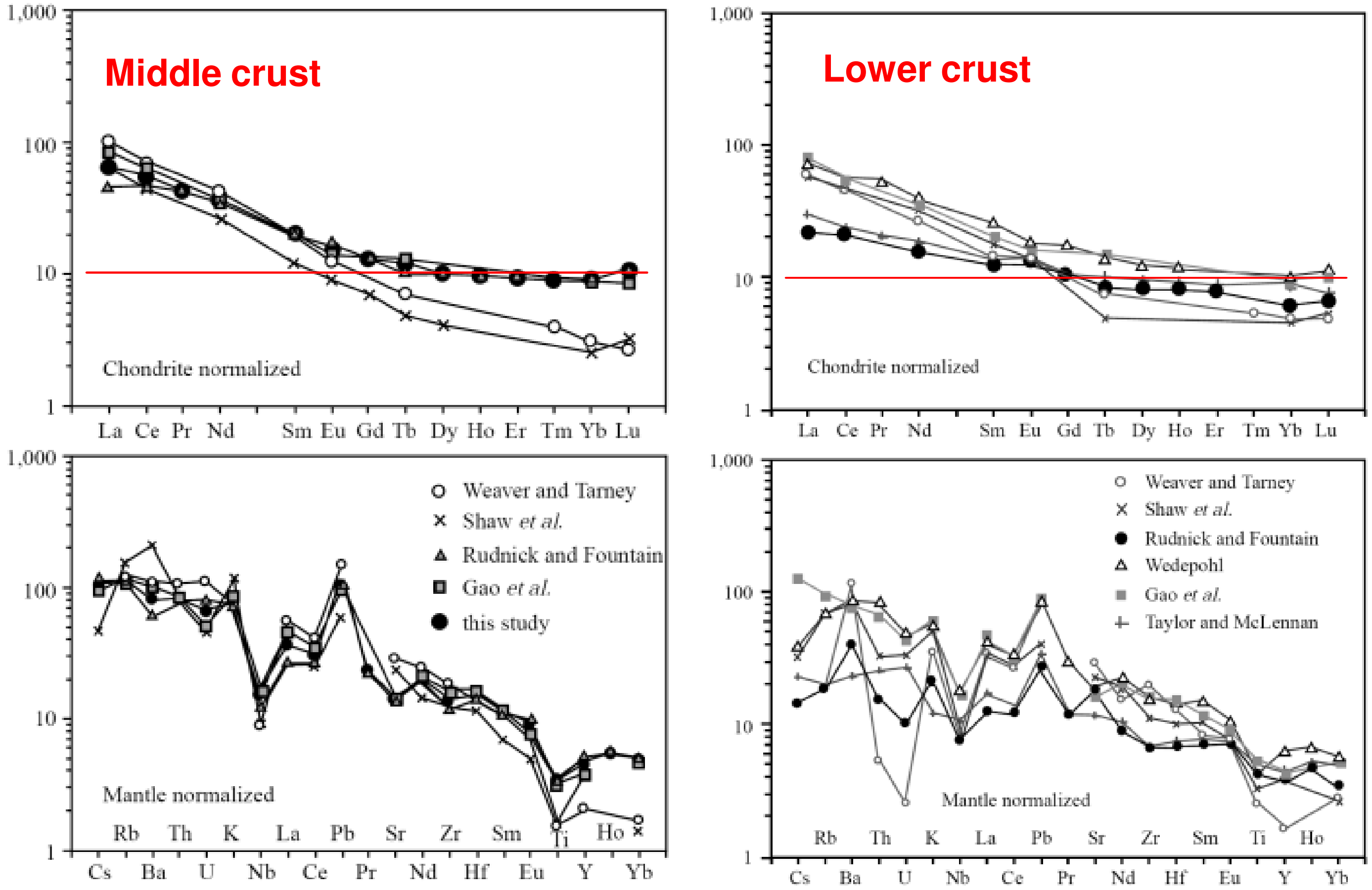

Note that different authors provide fairly **different compositions**, in particular for moderately incompatible elements (e.g. REE; **„sampling bias“**)

Rudnick & Gao, 2003, Treatise on Geochemistry

What is continental crust from a geochemical point of view?

Upper, middle and lower continental crust

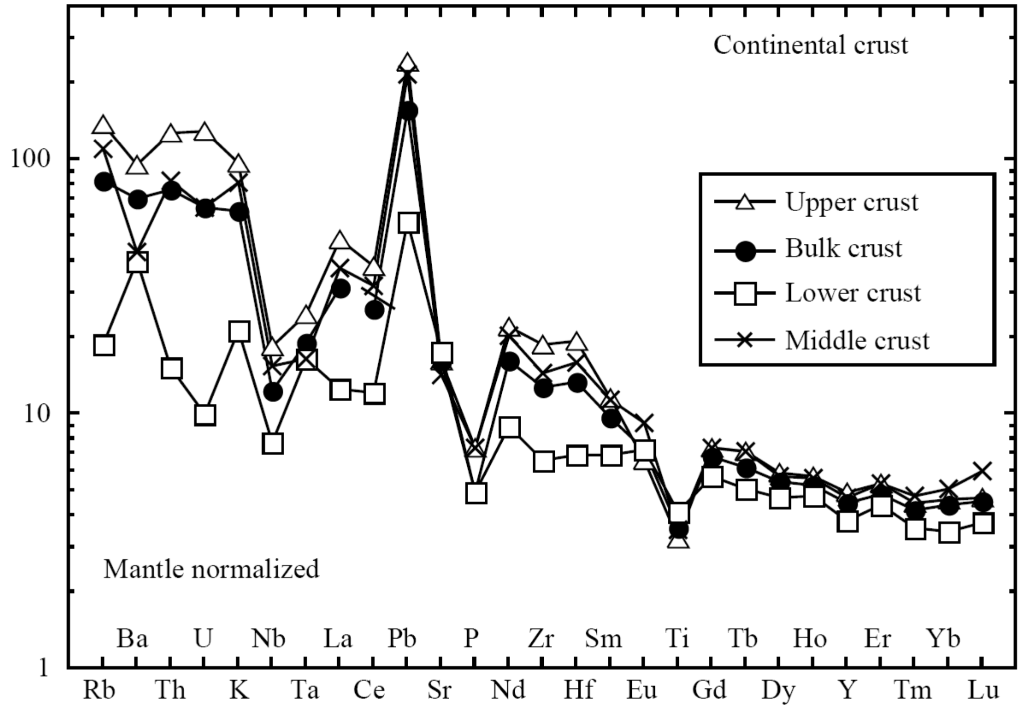

Kemp & Hawkesworth, 2003, Treatise on Geochemistry

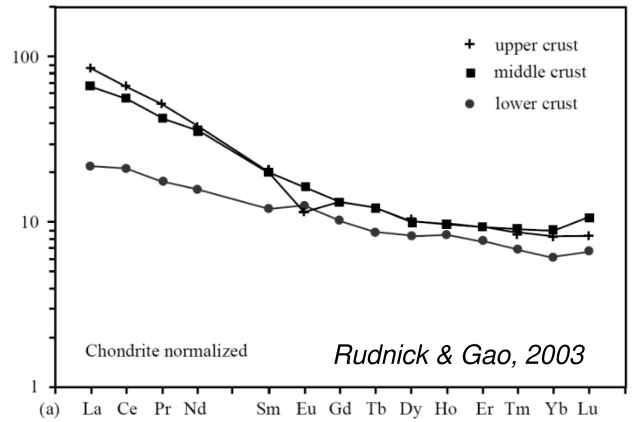

Bulk continental crust has an overall **andesitic composition**, and is **enriched** in incompatible trace-elements. Therefore, beside other **accessory phases** (monazite, apatite, xenotim), intermediate to felsic rocks contain abundant **zircon**

The earliest (continental?) crust on Earth

Zircons from Jack Hills, Australia

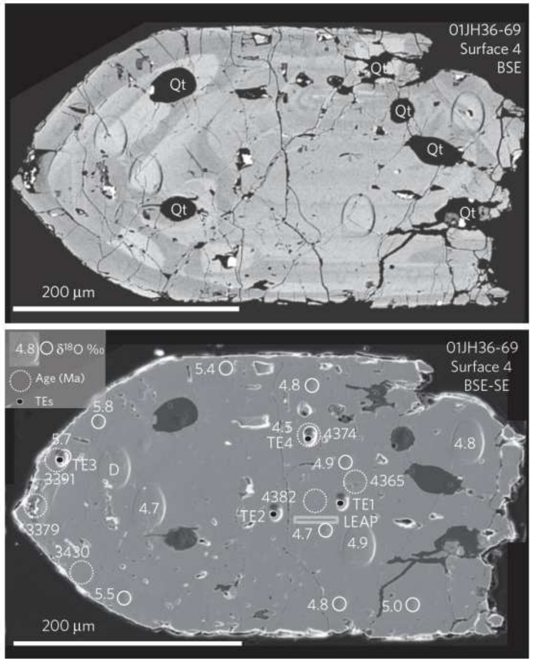

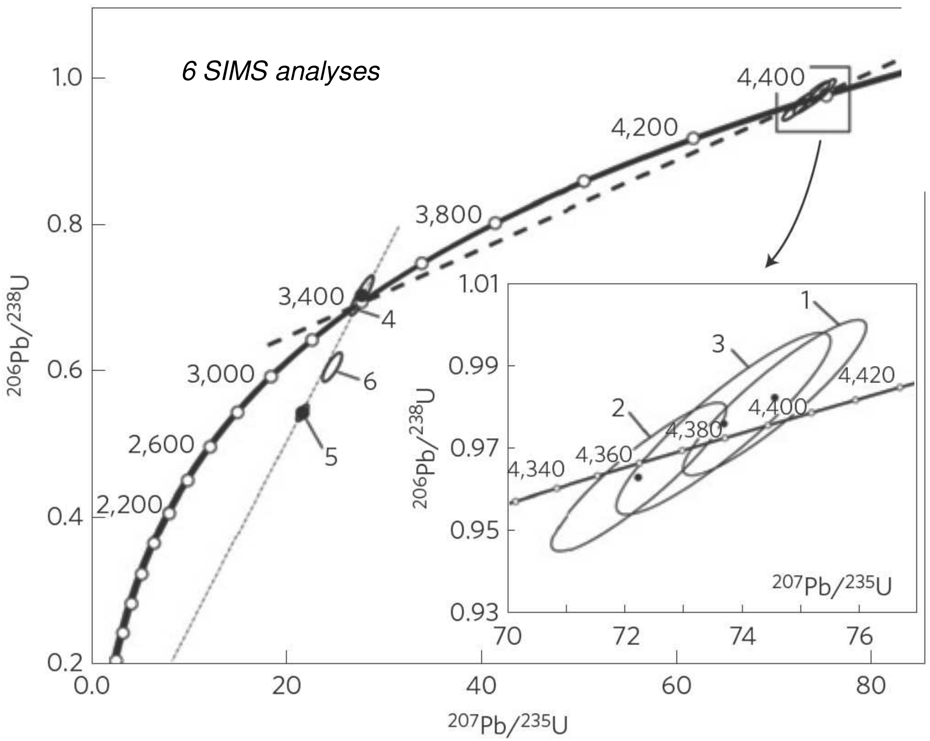

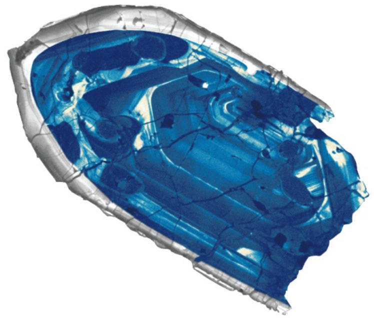

*Zircon from Jack Hills, Yilgarn Craton, Western Australia, with a **core** age of ~4.37 Ga*

Valley et al., 2014, Nature

Using SIMS and APT, Valley et al. (2014) determined a **concordant** age of **4.374 ± 0.006 Ga** for the **core of a detrital zircon** from the **Jack Hills, Western Australia**. This indiactes that **silicate differentiation** on Earth already took place less than ~200 Ma after Earth accrection

The earliest (continental?) crust on Earth

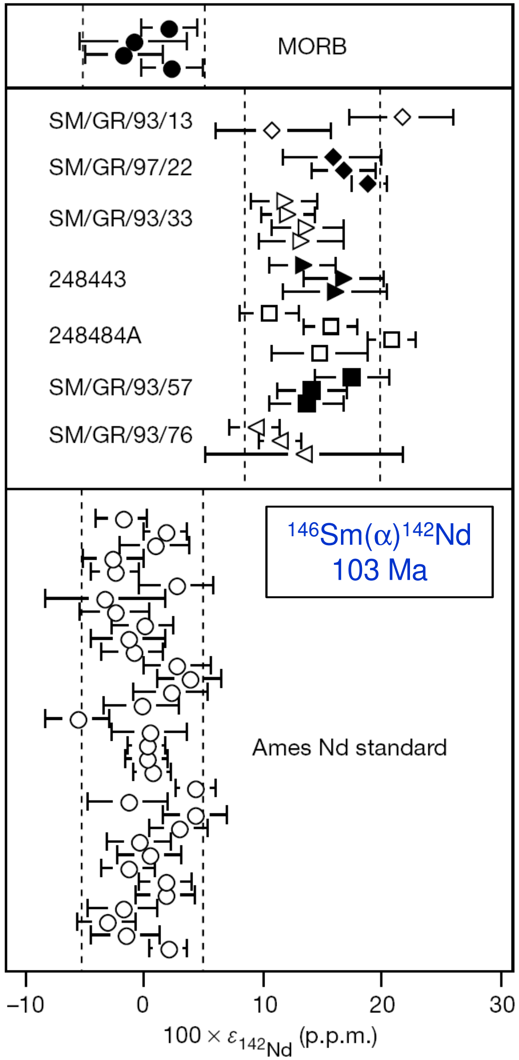

Caro et al., 2003, Nature

Positive ^{142}**Nd anomalies** (^{142}Nd excess) in meta-sediments (~3.7 – 3.8 Ga old) from the **Isua Greenstone Belt** (West Greenland) indicate very early mantle differentiation at **~4.460 Ga (± 0.115)**.

^{176}Hf/^{177}Hf anomalies (negative ε_{Hf}) in **zircons** from Jack Hills confirm very early silicate (mantle-crust) differentiation.

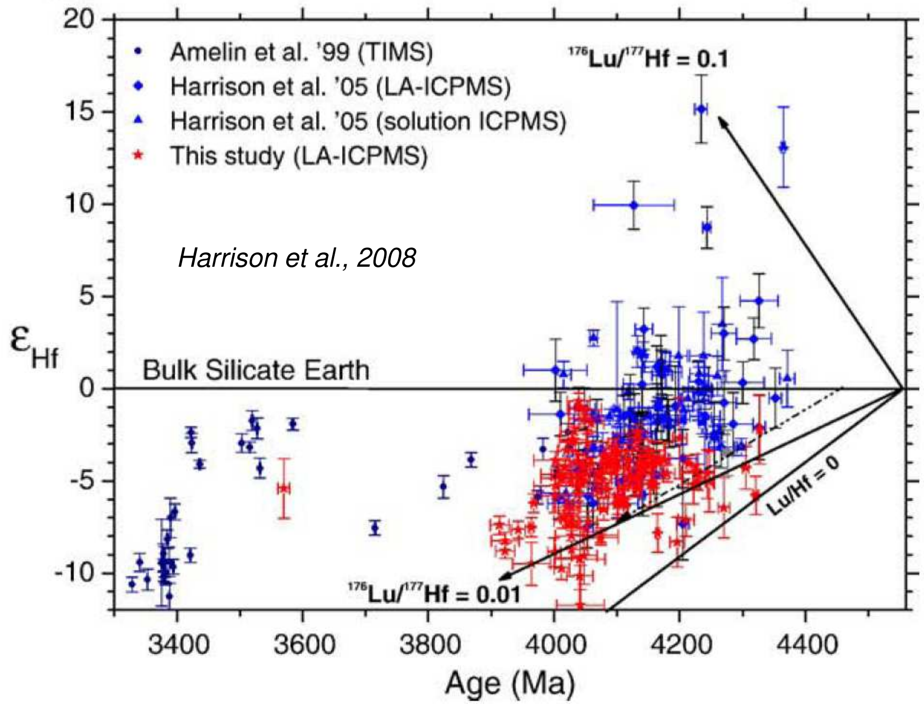

Age distribution of the continental crust

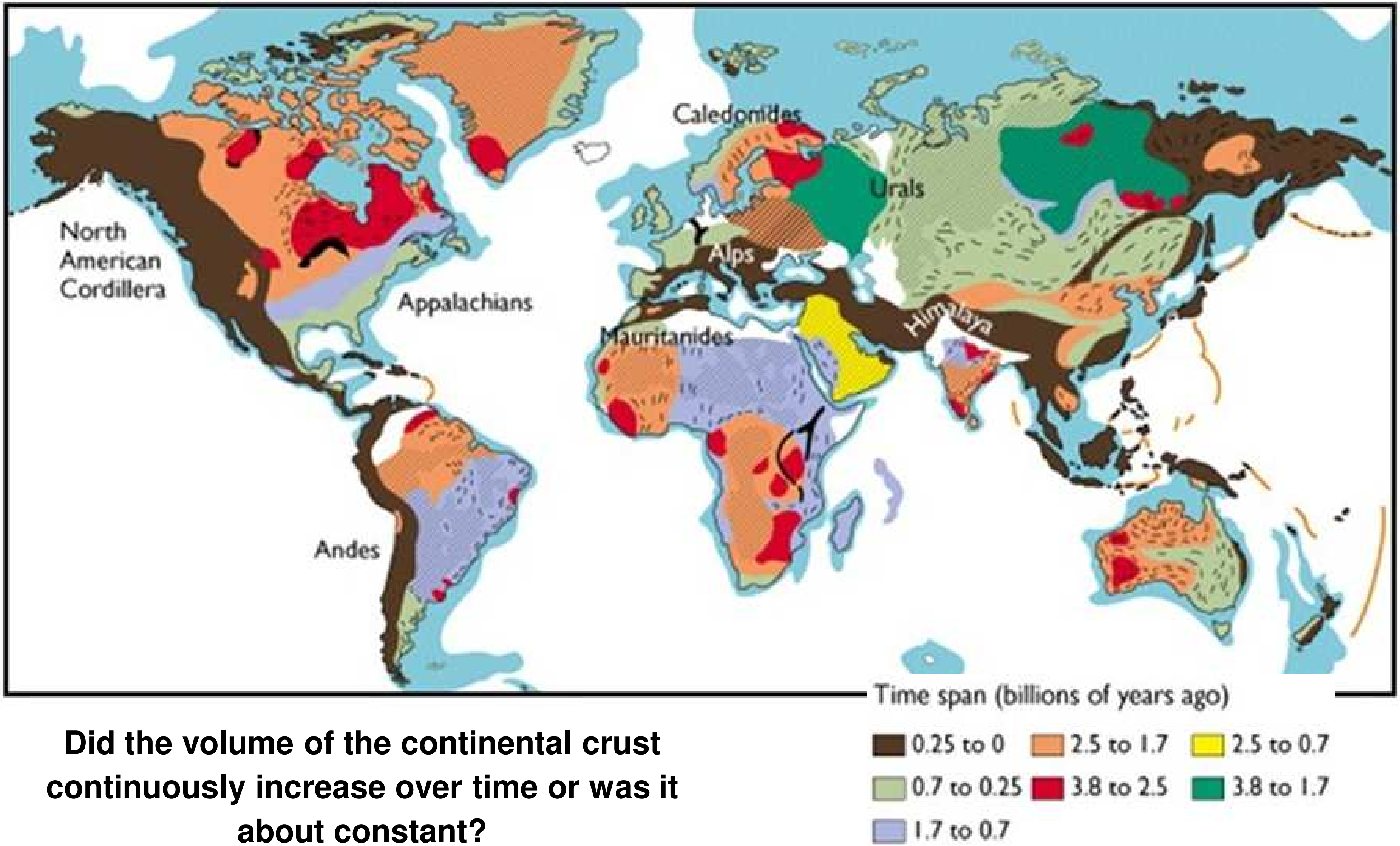

Did the volume of the continental crust continuously increase over time or was it about constant?

Growth rates of the continental crust

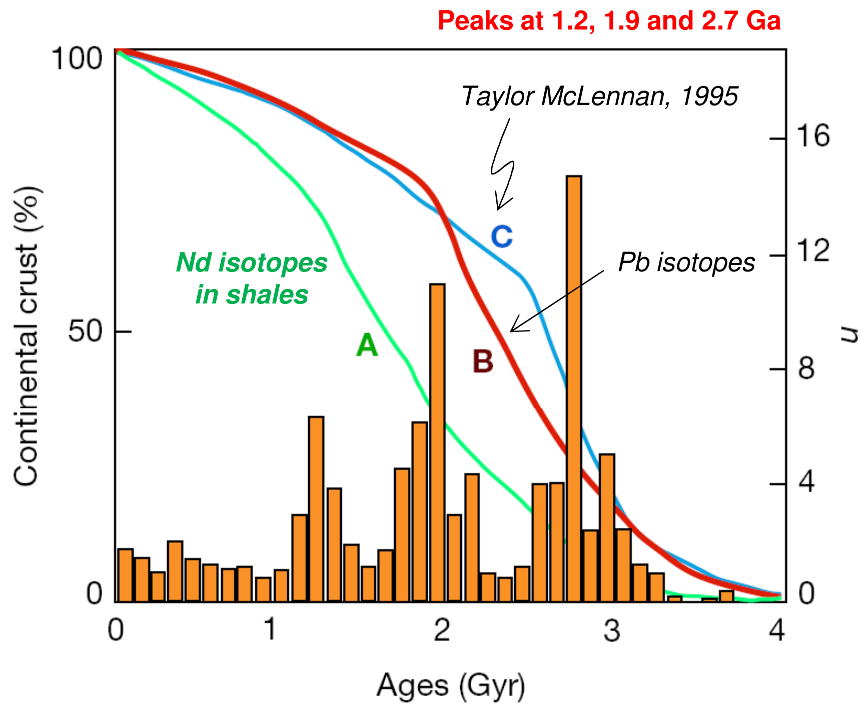

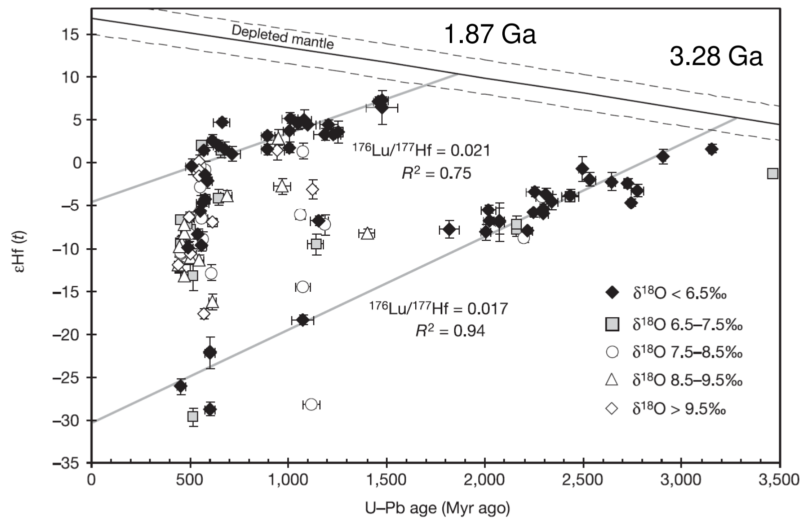

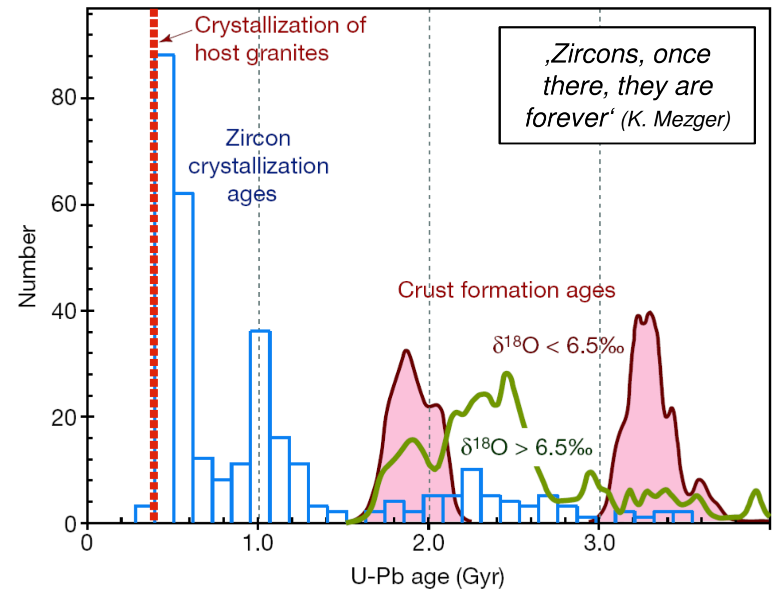

Histogram of ages of **crustal igneous rocks** with mantle-like initial isotope compositions and crustal growth curves based on different approaches

Hawkesworth & Kemp, 2006, Nature

Comparison of the composition of the bulk crust with that of island arc magmas

Crust formation in island arcs

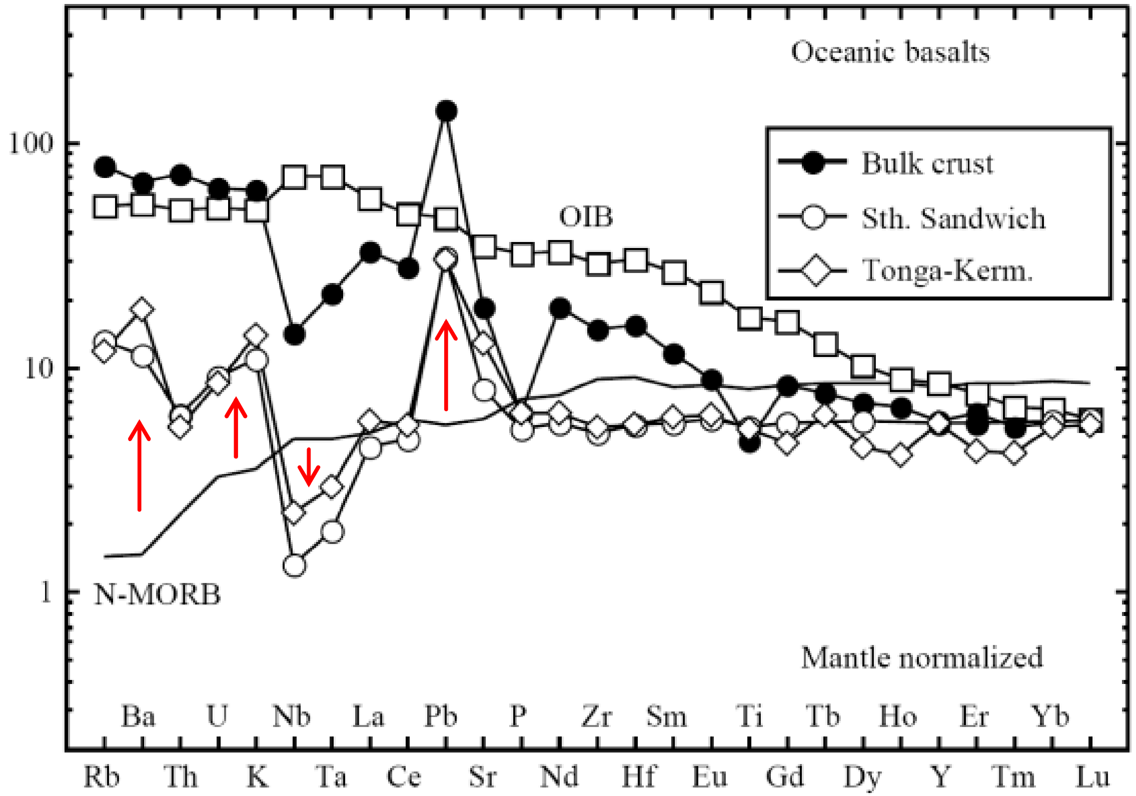

Kemp & Hawkesworth, 2003, Treatise on Geochemistry

Note the **LILE, Th, U and Pb enrichment**, but **Nb, Ta and HREE depletion** in IAB relative to MORB („slab-effct") Several features (**Nb, Ta and Pb anomalies**) are also observed in **bulk crust**, but overall concentrations of incompatible trace-elements are higher.

The precursors of new continental crust result from subduction zone magmatism

First order Formation mechanisms of continental crust

Hawkesworth & Kemp, 2006, Nature

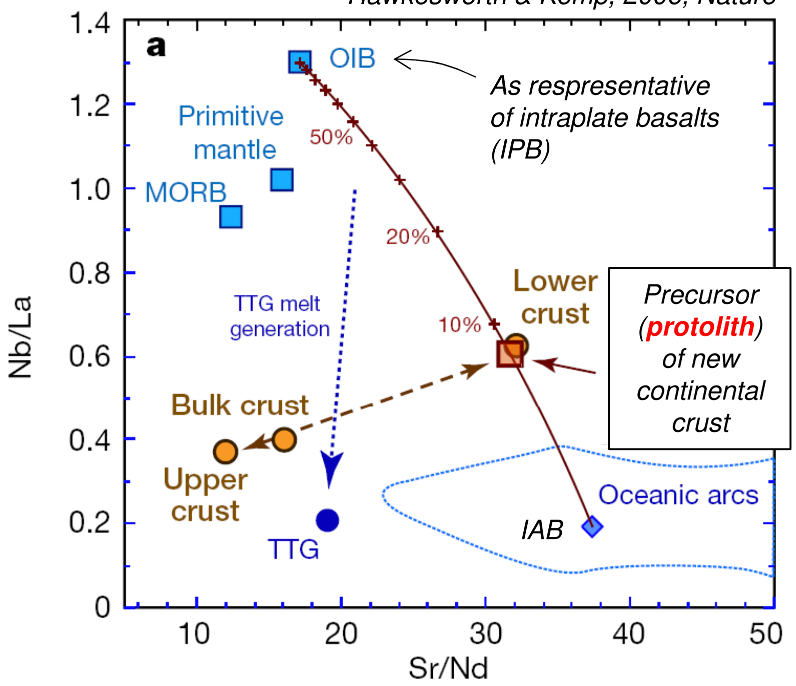

Beside island arc magmatism, **intraplate-magmatism** may contribute in some way to the formation of new continental crust

Hawkesworth & Kemp, 2006, Nature

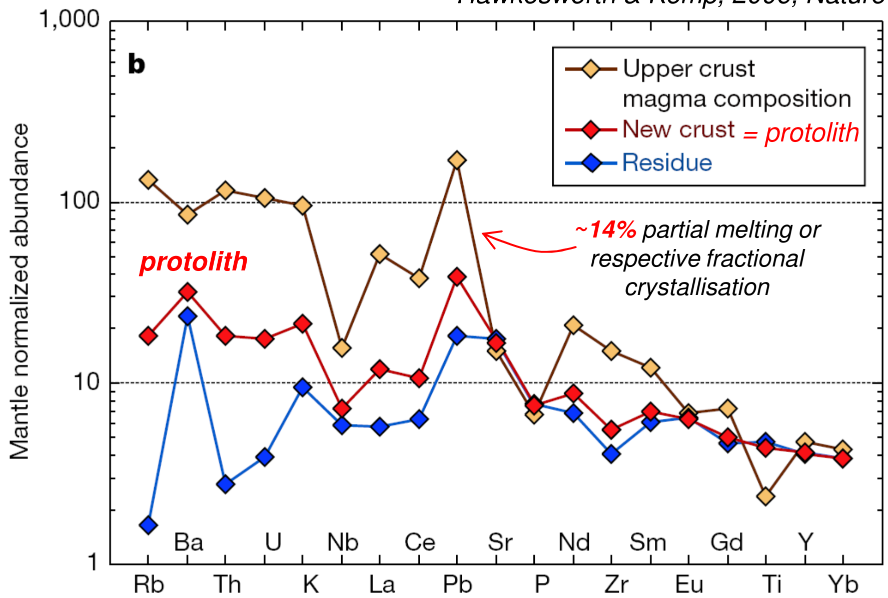

Nb/La used as a „source“ proxy, **Sr/Nd** mirrors **intracrustal differentiation** (residual plagioclase retains Sr!).

No or little garnet involved during average intracrustal differentiation! I.e., no thickened crust required ......

PROBLEM: RESIDUUM

First order Formation mechanisms of continental crust

Summary

based on Hawkesworth & Kemp, 2006, Nature

Residuum is **foundered back** into the **mantle** due to a **density inversion** caused by the formation of **high-density phases** such as garnet

Back to the mantle
(recycling)

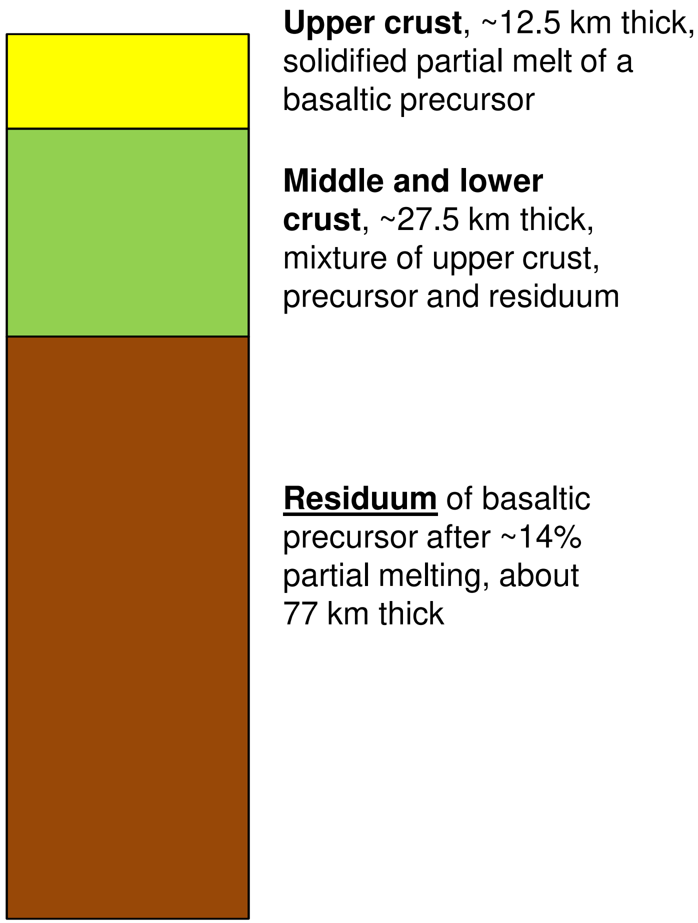

First order **Formation mechanisms of continental crust**

DELAMINATION

Delamination (foundering) of **lower crust** needs to result in (1) **rapid uplift** due to isostatic disequilibrium, and (2) intense **magmatism** if hot asthenosphere rises to fill the „gap“

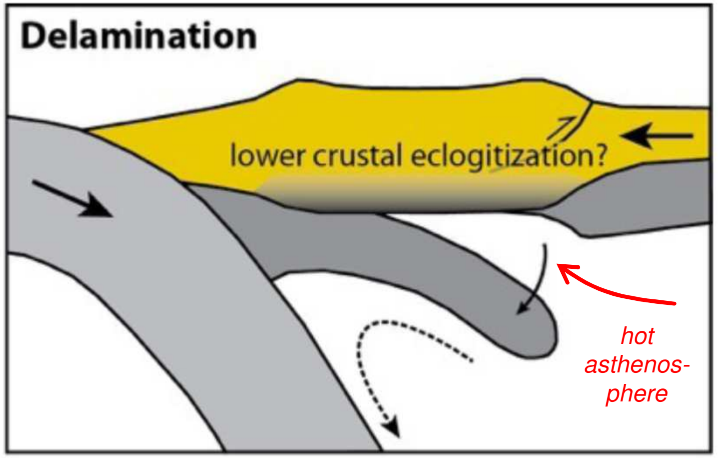

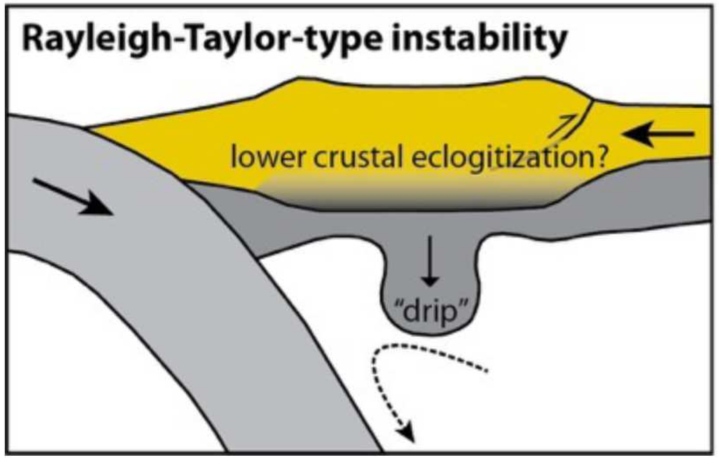

Claire Currie et al. (unknown)

First order Formation mechanisms of juvenile continental crust

*A **different scenario** derived from rocks and xenoliths from the Sierra Nevada Plutons*

Primary, mantle derived hydrous basalt or basaltic andesite

→ *high-p fractional crystallisation* →

High-MgO pyroxenites

↓

Derivative magmas → *low-p fractional crystallisation* → **Low-MgO garnet-pyroxenites**

emplacement, solidification, and remelting

Residue: Low-MgO garnet-pyroxenites

Melt: Magmas that crystallize diorites and granodiorites

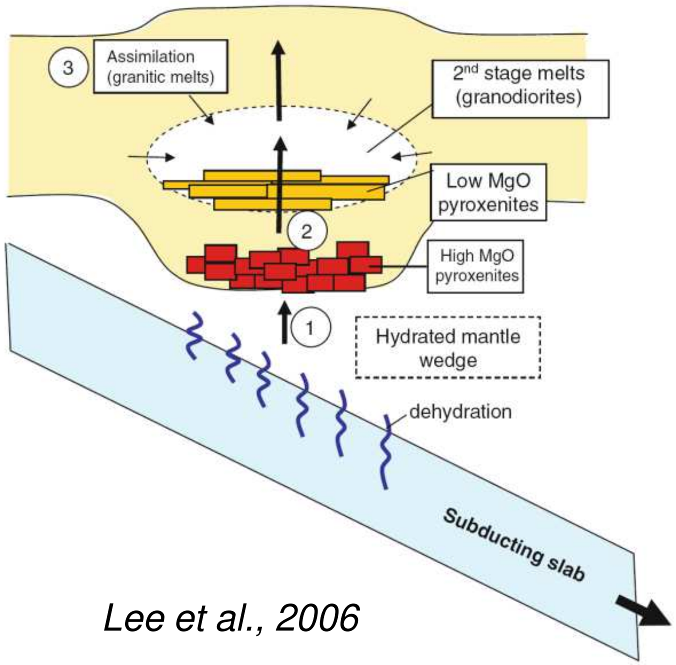

Lee et al., 2006

Problem: No amphibole is considered

First order **Formation mechanisms of <u>juvenile</u> continental crust**

Role of crustal thickness and density inversion

According to this model, only thick crust as observed in **continental arcs** enables **density inversion** and **delamination**, and recycling of ‚eclogite' (‚arclogite') back into the mantle

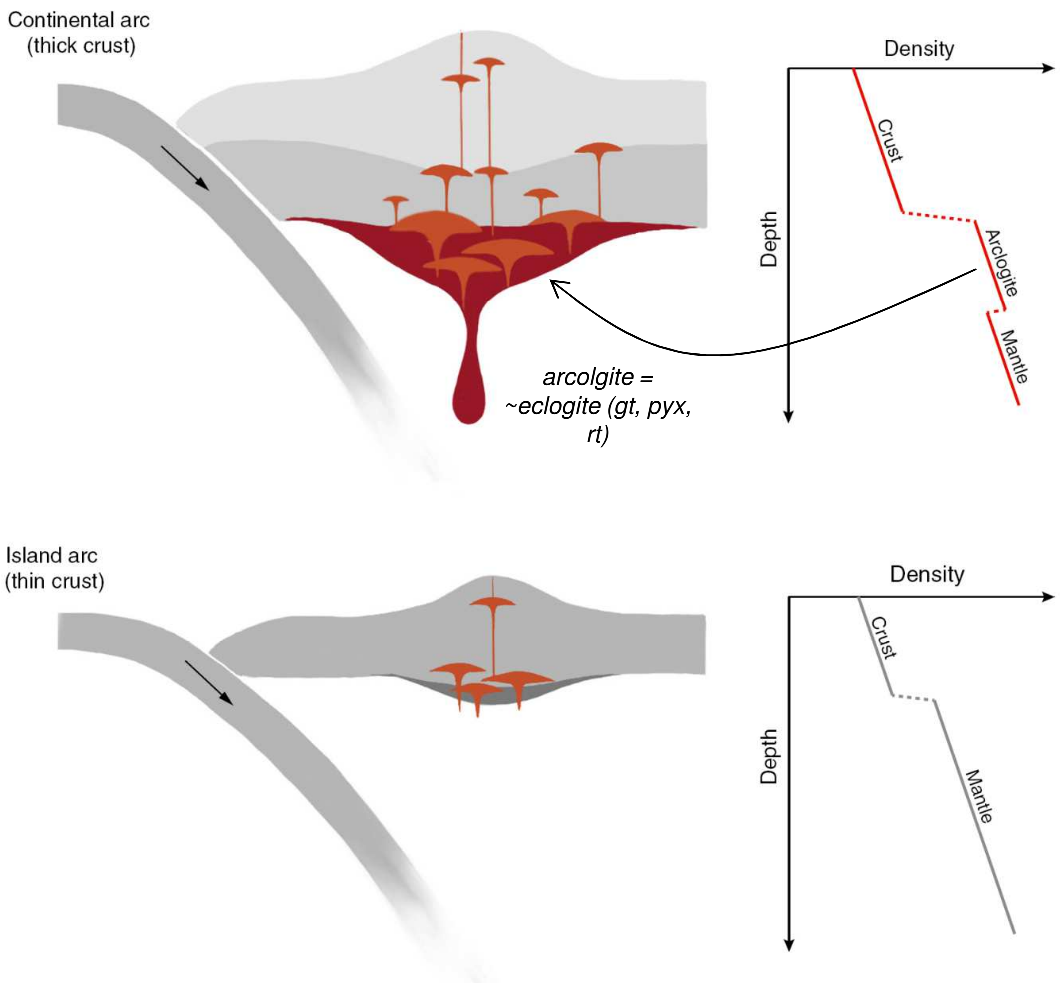

Tang et al., 2019, Nature

Magmatism in (continental) collision zones

How were crustal rocks, either primary (diorites, granodiorites)**, intermediate** (meta-igneous felsic to mafic) **or secondary** (meta-sedimentary) **processed to form more evolved lithologies** (granites, pegmatites, ...) **?**

How can we distinguish between **new** (juvenile) and **reworked** crust?

Magmatism in (continental) collision zones

Crustal reworking

Crust formation vs. **crustal remelting** ideally resolvable from **Nd-isotope** composition and **zicon age** of a rock sample.

„If the Nd-model age and the zircon age <u>coincide</u>, the rock is a piece of juvenile crust"

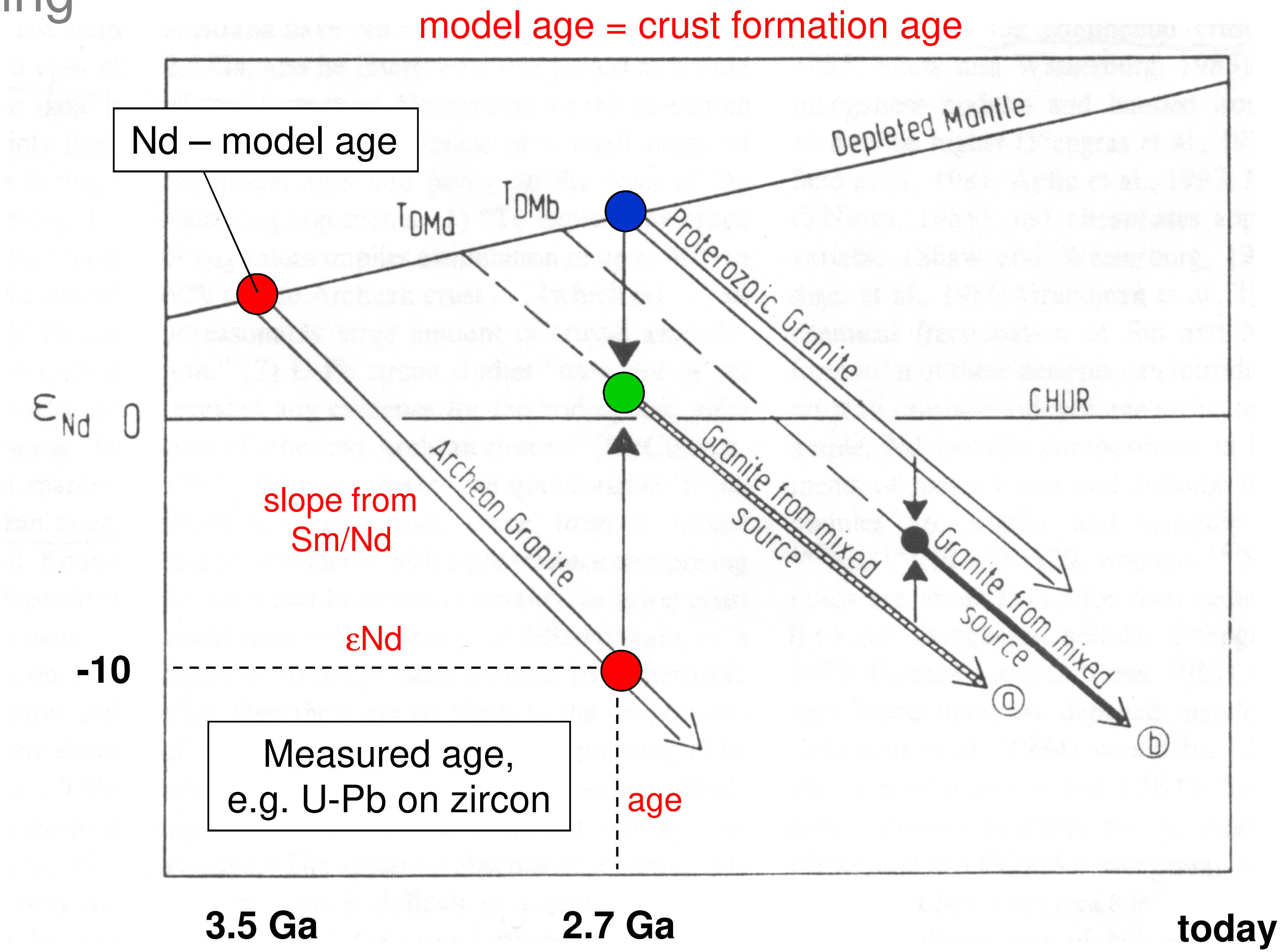

Magmatism in (continental) collision zones

Mineralogy of granite rocks

Chen & Grapes (2007)
Classification following Streckeisen

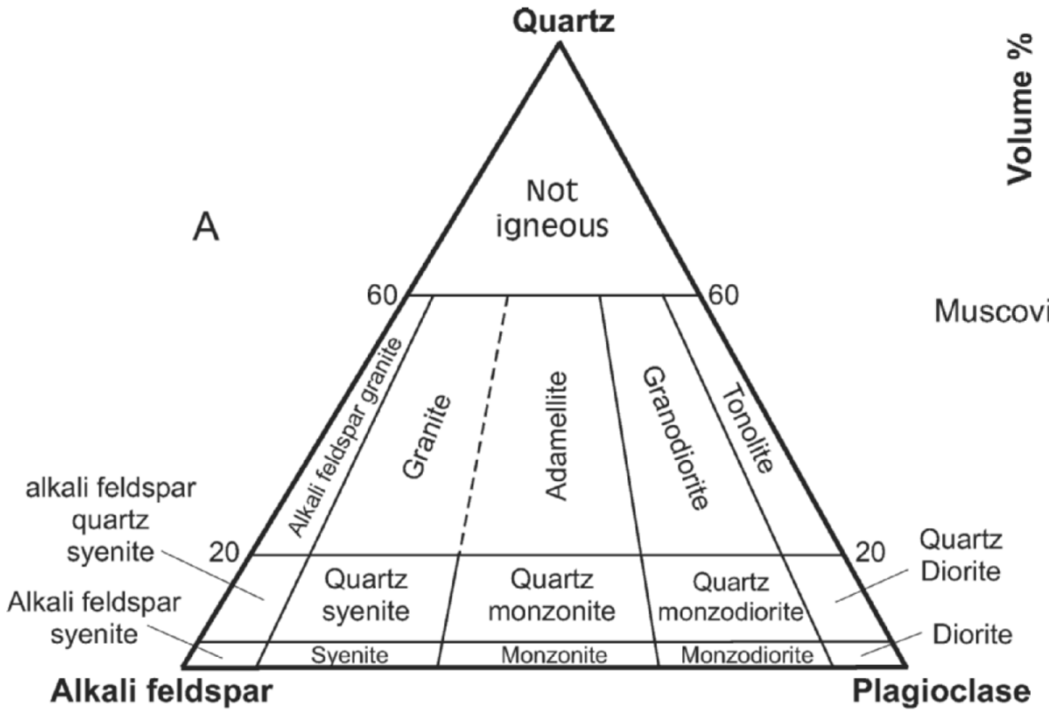

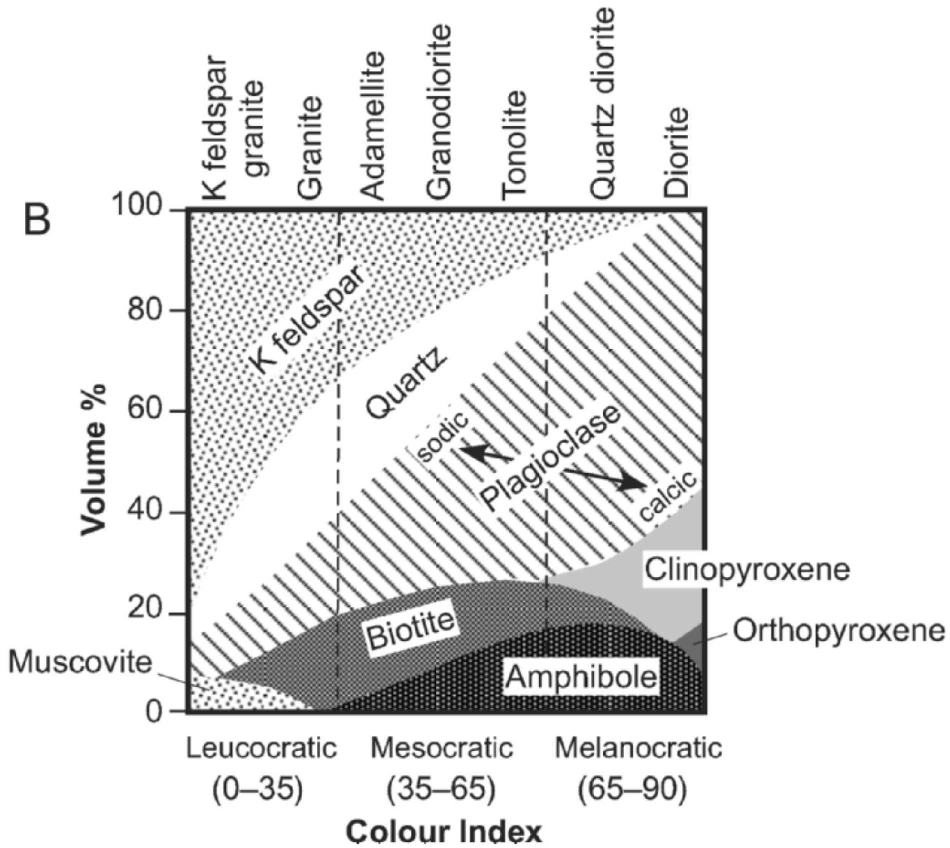

Basics!

Magmatism in (continental) collision zones

Terms used to classify granitic rocks (based on Al- and Alkali-content)

Peraluminous: Molar Al_2O_3 > Molar $CaO + K_2O + Na_2O$ [A > CKN]
(Plag + Kfs have 1:1). Bt, Ms, Cd, Sil are peraluminous minerals

Metaluminous: Molar $CaO + K_2O + Na_2O$ > Molar Al_2O_3 > Molar $K_2O + Na_2O$ [CKN > A > KN]

Subaluminous: Molar Al_2O_3 ~ Molar $K_2O + Na_2O$ [A~KN]

Peralkaline: Molar Al_2O_3 < Molar $K_2O + Na_2O$ [A<KN]

MALI (modified alkali lime Index): $Na_2O + K_2O - CaO$ (not molar!)

Magmatism in (continental) collision zones

Classification of granitic rocks (based on Al- and Alkali-content)

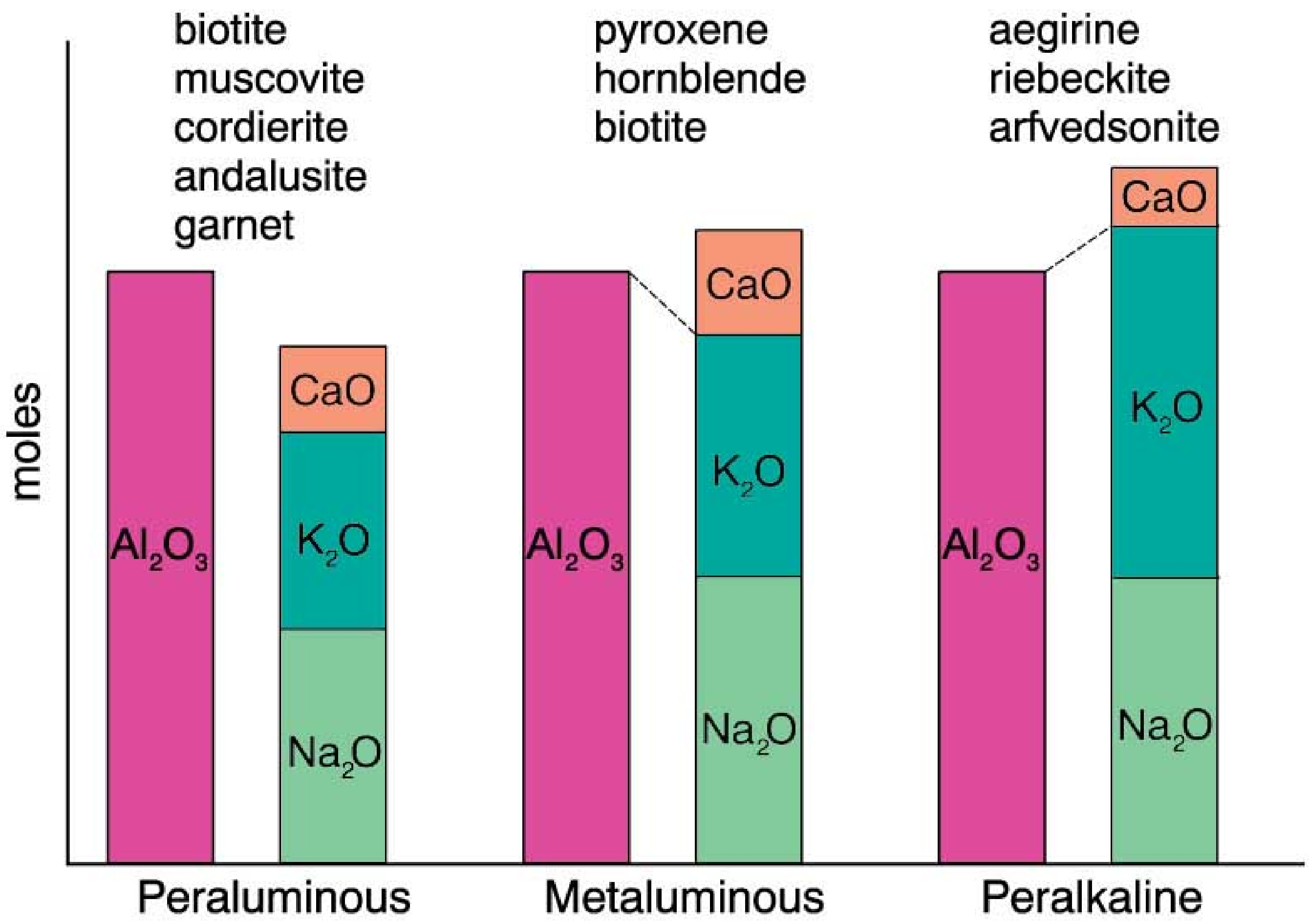

Magmatism in (continental) collision zones

High-grade metamorphic (metapelite) rocks and anatexis

Equilibrium **phase-relations** (including partial melts) in the **MnNCKFMASH** System representing a typical average (meta-) **pelite composition**.

Stable phases – dependent on p-T, are Qz, Ksp, Plag, Bt, Ms *plus* Gt, Cd, Sil and melt.

(Meta-) Pelite (~mol%): 73.6 SiO_2, 11.9 Al_2O_3, 7.2 FeO, 0.10 MnO; 3.9 MgO, 0.35 CaO; 1.4 Na_2O; 3.1 K_2O)

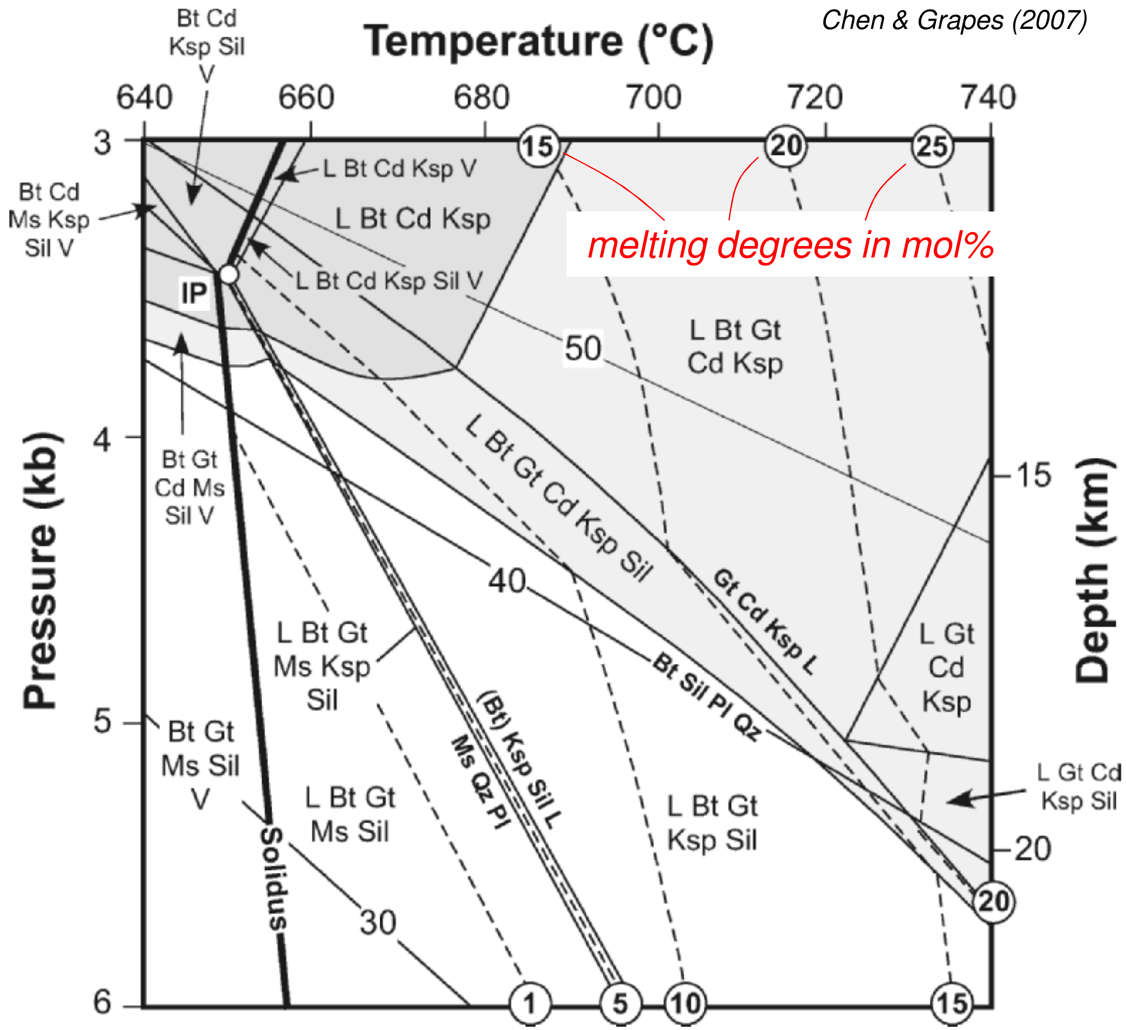

Magmatism in (continental) collision zones

High-grade metamorphic (metapelite) rocks and anatexis

Partial melting is either triggered by **free water** (~640°C at 1 GPa) or by the **breakdown of water bearing phases**. Important experimental constraints:

Muscovite breakdown melting:

Ms + Qz + Ab = Kf + AS + liquid	625 - 700°C	0.5 GPa
Ms + Qz + Ab = Kf + AS + Crd + Bt + lq	625 - 700°C	0.5 GPa

Biotite breakdown melting:

Bt + Qz + Pl ± AS = Kf + Cd + Gt + lq	690 – 820°C	0.5 GPa
Bt + Qz + Pl = Ksp + Opx ± Cd ± Gt + lq	690 – 820°C	0.5 GPa

Amphibole breakdown melting:

Hbl + Qz ± Gt = Opx + Cpx + Pl + lq	920 – 970°C	< 1 GPa
Hbl + Qz + Pl = Gt + Cpx + lq	920 – 970°C	> 1 GPa

gt + cpx = „eclogite“

Magmatism in (continental) collision zones

High-grade metamorphic rocks and migmatites

Anatexis (of meta-sedimentary or meta-igneous rocks)

and the formation of **‚granitic melts‘** is an important process of **crustal reworking** and **intracrustal differentiation** during orogeny, but may **not** produce any juvenile crust!

Magmatism in (continental) collision zones

Origin and types of granites – importance of Al-saturation

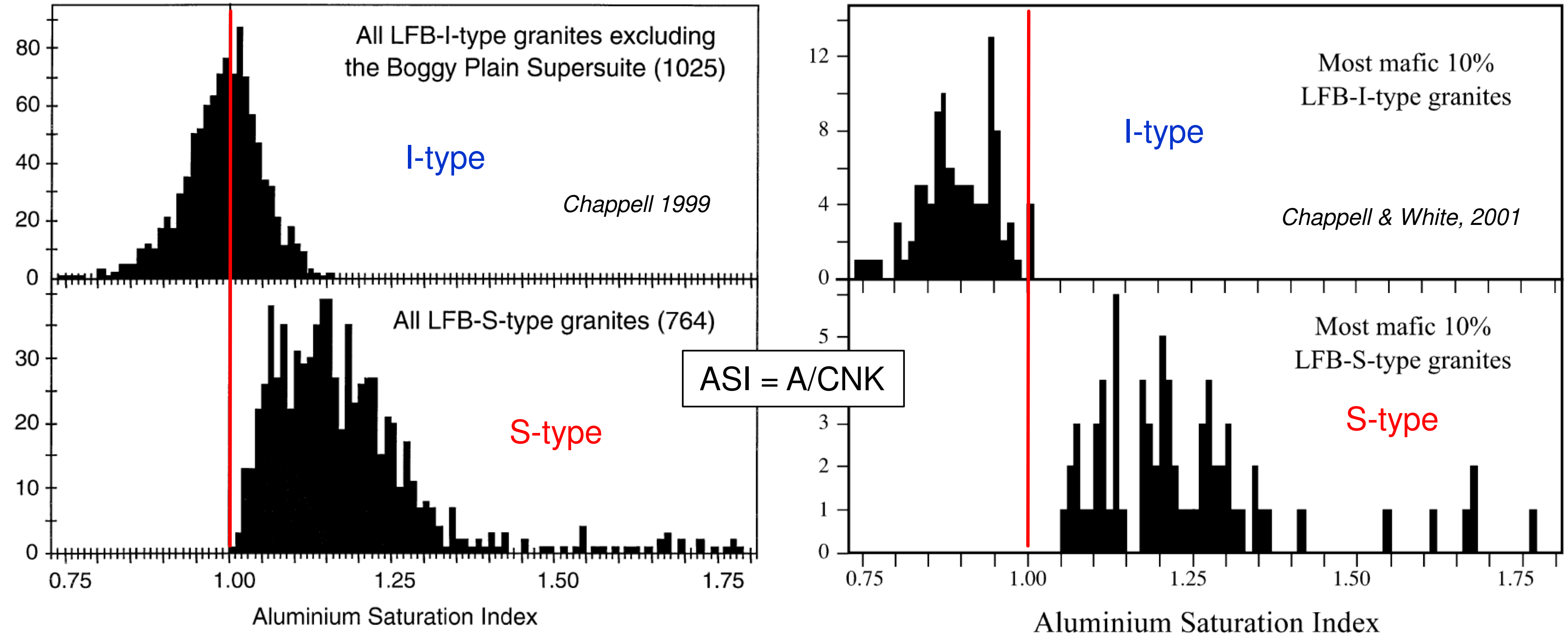

Major element characteristics based on ~2000 analyses on **granites** from the **Lachlan foldbelt**. Chappell & White (1974) first suggested predominantly meta-igenous sources for I-type and meta-sedimentary sources for S-type granites

Magmatism in (continental) collision zones

Origin and types of granites

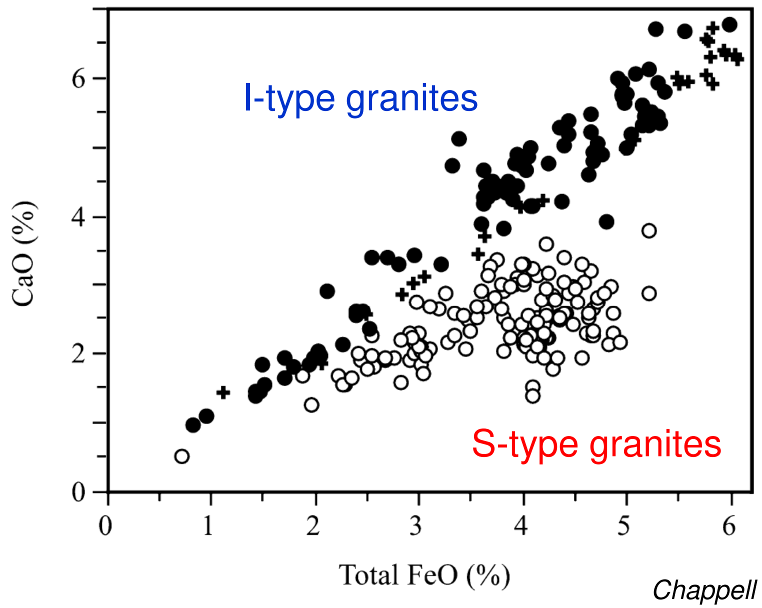

Chappell & White, 2001

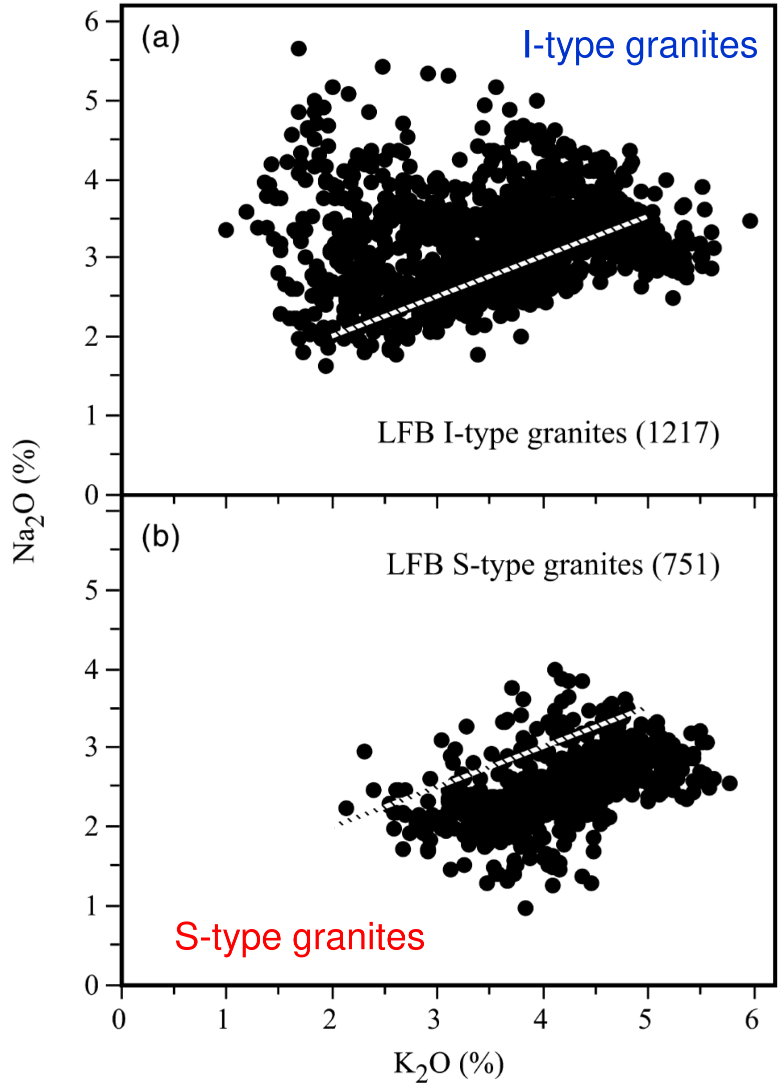

Major element characteristics of I- and S-type granites from the **Lachlan fold belt**, SE-Australia:

Trends, but no distinct differences!

Magmatism in (continental) collision zones

Origin and types of granites – experimental constraints

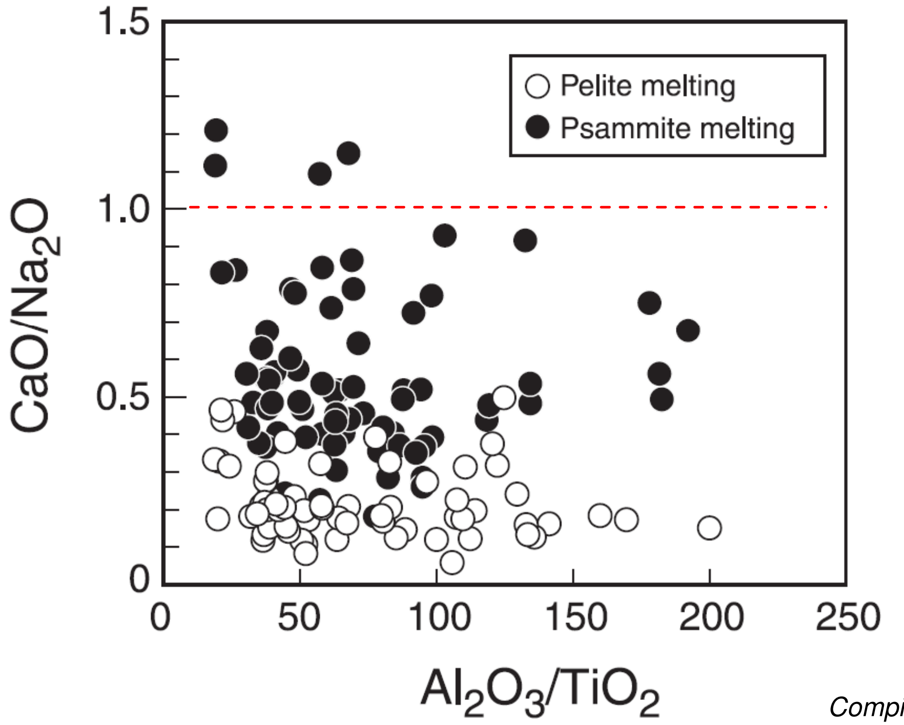

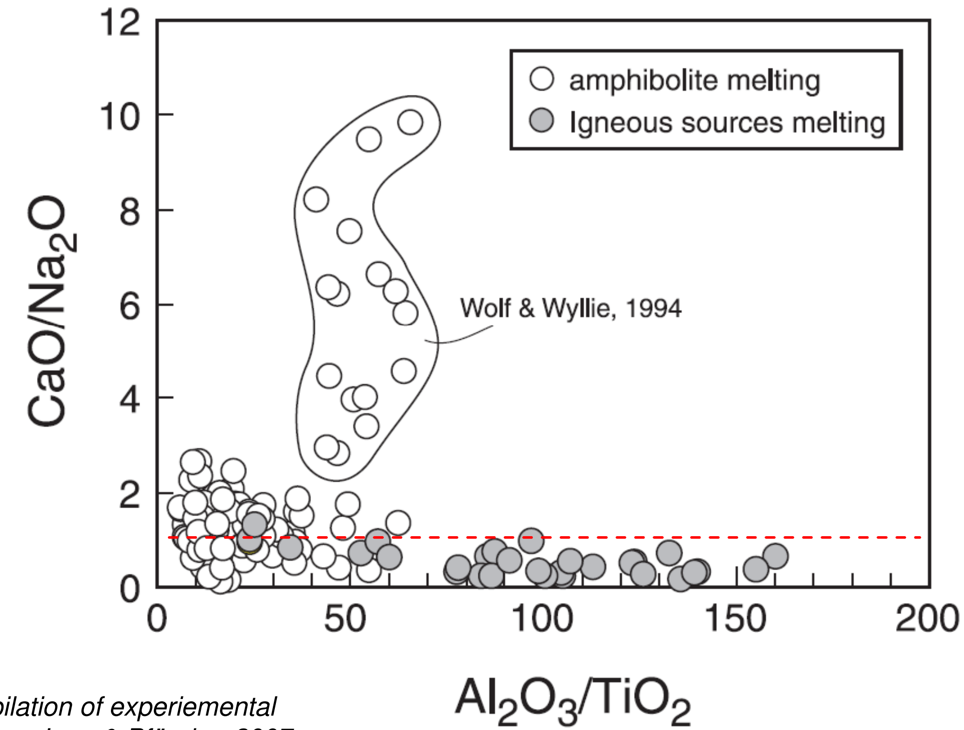

Compilation of experiemental data from Jung & Pfänder, 2007

CaO/Na_2O vs. Al_2O_3/TiO_2 of **granites** can be used as (rough!) first-order constraints on **protolith composition** and **melting temperatures**

Magmatism in (continental) collision zones

Origin and types of granites – experimental constraints

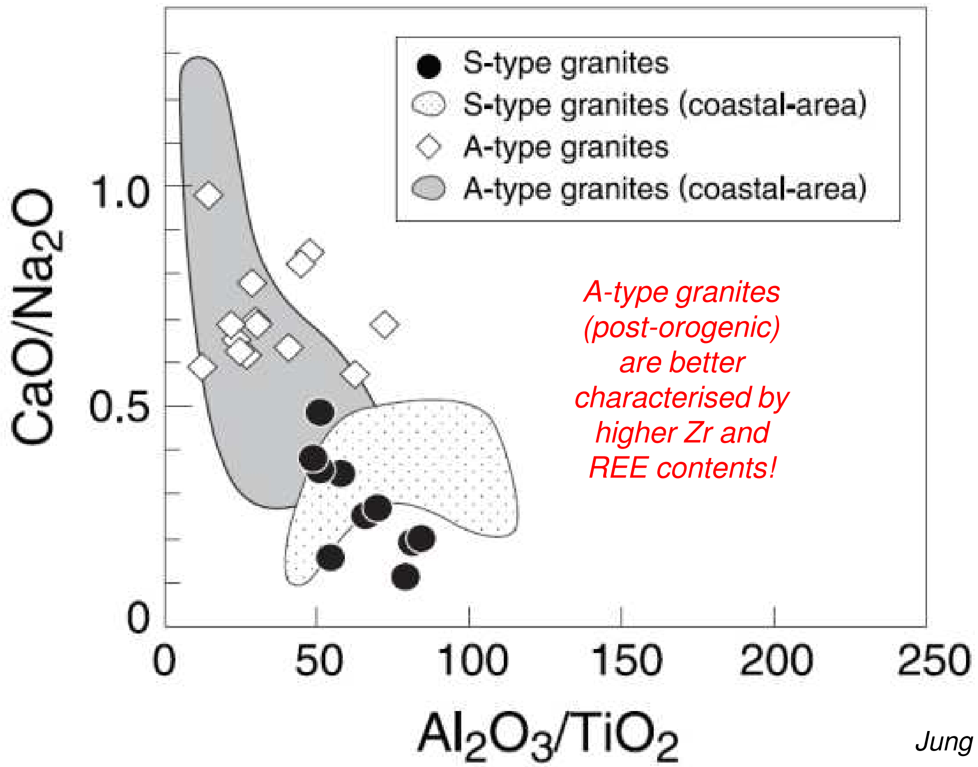

Jung & Pfänder, 2007

CaO/Na_2O vs. Al_2O_3/TiO_2 of **granites** can be used as (rough!) first-order constraints on **protolith composition** and **melting temperatures**

Magmatism in (continental) collision zones

Origin and types of granites – experimental constraints

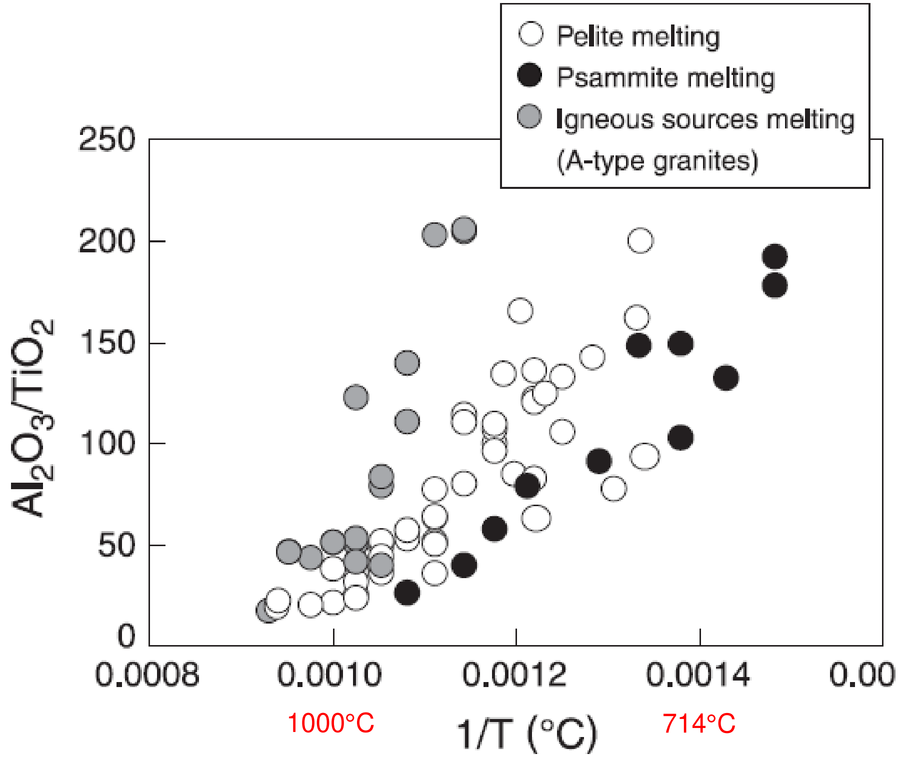

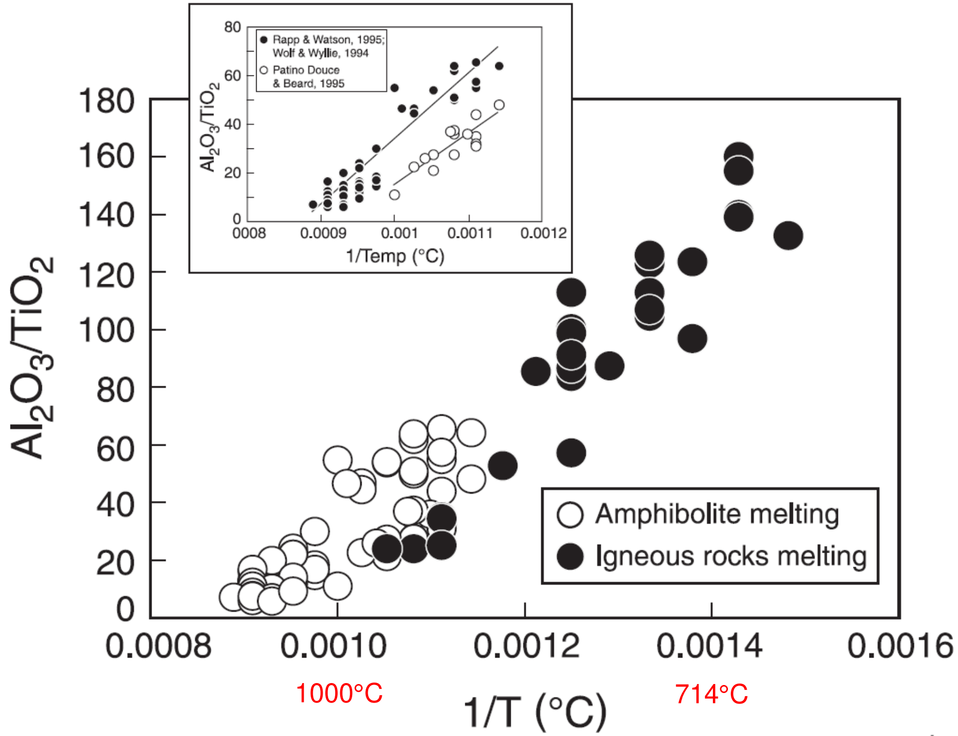

Jung & Pfänder, 2007

CaO/Na_2O vs. Al_2O_3/TiO_2 of **granites** can be used as (rough!) first-order constraints on **protolith composition** and **melting temperatures**

Magmatism in (continental) collision zones

Origin and types of granites - trace-element compositions

REE patterns of **S- and A-type granites** from the Damara orogen, Namibia.

Comparison of unfractionated, moderately and strongly fractionated S-type granites. Note that **positive Eu-anomalies** require *Kfs/Plag accumulation*

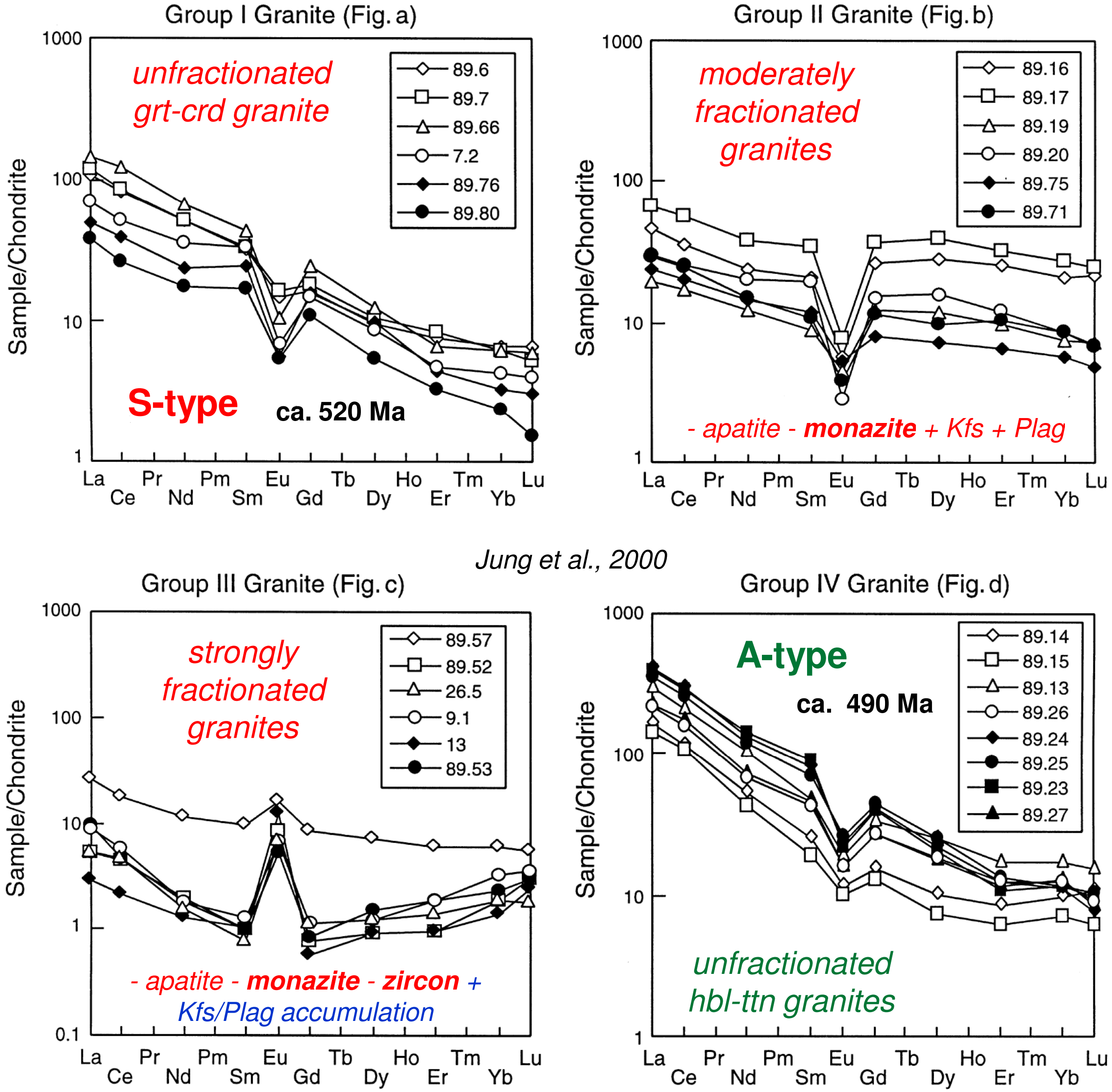

Magmatism in (continental) collision zones

Origin and types of granites – trace-element compositions

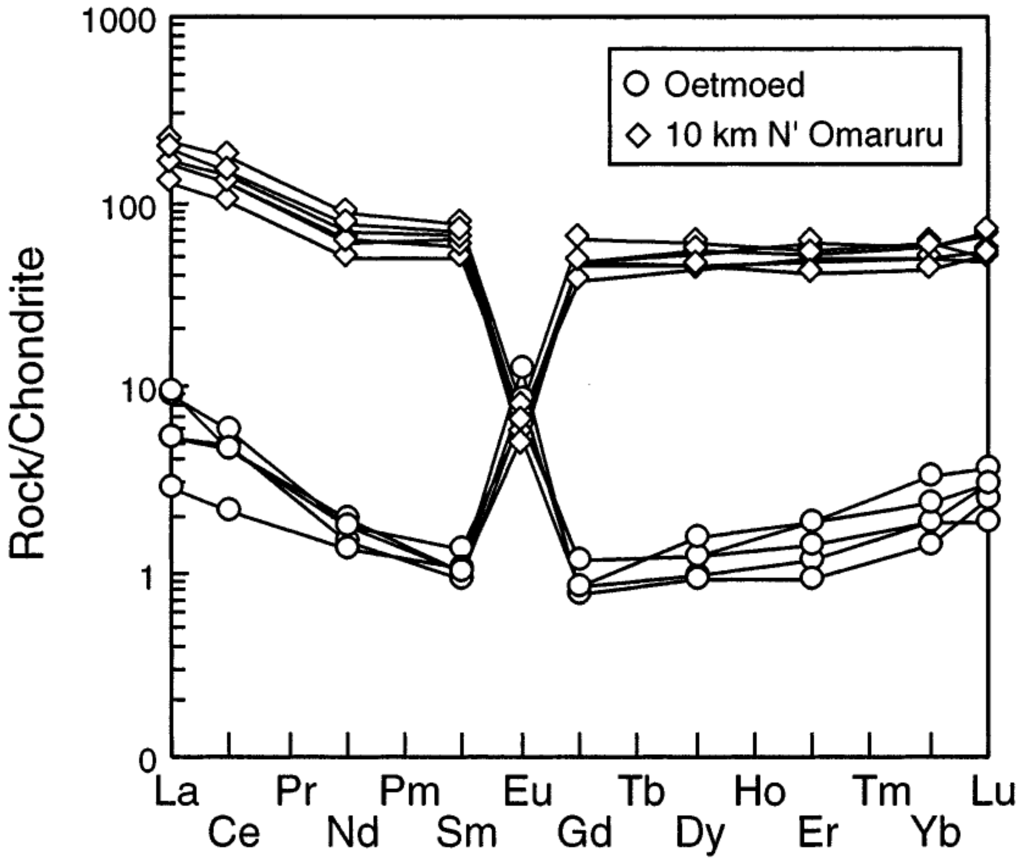

Jung et al., 2001

REE patterns of **S-type granites** from the Damara orogen, Namibia.

Flat REE patterns (upper) indicate a ‚normal' granite with **garnet** accumulation.

Low abundances and flat patterns (lower) indicate **strong fractionation** of **accessory phases** [monazite (LREE), apatite, zircon & xenotime (HREE), allanite (LREE)] along with **feldspar** accumulation.

Intracrustal differentiation

Summary

Low- to medium-grade **metamorphism**, no anatectic partial melting, but some mafic melt injection from depth. **Intrusion of anatectic magmas** (granitic ‚batholiths'), wall-rock assimilation and fractional crystallisation (AFC), contact metamorphism. →

High-grade metamorphism due to **crustal thickening** and **partial melting** due to (1) internal heating, and (2) heat addition by magma injection. →

Contribution from the **mantle** (continental arcs or mafic underplating): basaltic (alkaline, calc-alkaline, tholeiitic) magma plus **HEAT.** →

Hawkesworth & Kemp, 2006